PHENETHYLISOTHIOCYANATE: ROLE IN ENHANCING PLATINUM ACCUMULATION IN CERVICAL CANCER

By

Elizabeth Mahapatra

Department of Environmental Carcinogenesis & Toxicology
Chittaranjan National Cancer Institute, Kolkata

Thesis Submitted for the Degree of
DOCTOR OF PHILOSOPHY (SCIENCE)
Department of Life Science and Biotechnology
Jadavpur University
Index No-182/18/Life Sc./26
(2023)

CNCI
Chittaranjan National Cancer Institute
(An Autonomous Body under Ministry of Health & Family Welfare, Govt. of India)
37, S. P. Mukherjee Road, Kolkata 700 026, INDIA
Tel: 2476 5101/02/04/20/22; Fax: 91-33-2475 7606
E-mail: cncinst@gmail.com
Web site: www.cnci.ac.in

CERTIFICATE FROM THE SUPERVISOR(S)

This is to certify that the thesis entitled **"PHENETHYLISOTHIOCYANATE: ROLE IN ENHANCING PLATINUM ACCUMULATION IN CERVICAL CANCER"** Submitted by **Smt. ELIZABETH MAHAPATRA** who got her name registered on **18.09.2018** for the award of Ph. D. (Science) Degree of Jadavpur University, is absolutely based upon her own work under the supervision of **DR. SUTAPA MUKHERJEE** and that neither this thesis nor any part of it has been submitted for either any degree / diploma or any other academic award anywhere before.

Sutapa Mukherjee

DR. SUTAPA MUKHERJEE

Dr. Sutapa Mukherjee
Senior Scientific Officer (Assistant Director Grade)
Head, Department of Environmental
Carcinogenesis & Toxicology
Chittaranjan National Cancer Institute
37, S. P. Mukherjee Road
Kolkata-700 026

Dedicated to My Lovely Parents,
Mr. Sadhan Mahapatra
Mrs. Pranati Mahapatra

My Beloved Sister, Ms. Angela Mahapatra

and

To the Fond Memories of My Grandparents
Dida, Thamma and Dadu

This Thesis is a Fruit of their Blessings

THIS BELONGS TO MY FAMILY

ACKNOWLEDGEMENT

The walk of a doctoral scholar is akin to a roller coaster ride which is impossible without a generous guide and some gracious companies. In this august occasion of my thesis submission, I take a moment to thank each of these individuals who have immensely contributed in my journey. I begin with extending my heartfelt gratitude and warmest regards to my guide ***Dr. Sutapa Mukherjee****, Head and Assistant Director Grade Scientist, Department of Environmental Carcinogenesis and Toxicology (ECT), Chittaranjan National Cancer Institute (CNCI), Kolkata. My guide, Sutapa ma'am, is one of the kindest souls I have come across in these six years. I have imbibed the invaluable virtues of diligence, self-confidence, perfection, obedience, patience, sincerity and empathy from her which I shall cherish as assets all throughout my life. Her passion towards science has been the driving force of my evolution as a student of science. I am indebted to her for keeping trust in me and for being considerate of my scientific inputs in several academic aspects. I owe my independence and freedom of scientific perception to her. I personally feel, that not only me but to all her students Sutapa Ma'am is no less than a mother. Her favourite line 'WORD IS WORD' shall always remain with me as a guiding principle. I believe to have become a better person under her guidance and wish to reinstate her qualities within myself. I thank her for everything I have and for all that I will achieve in future as a researcher.*

Next up, I convey my highest regards to ***Dr. Madhumita Roy****, Former Head and Assistant Director Grade Scientist, Department of ECT, CNCI, Kolkata. I cannot thank her enough for her cooperation and amicability. Whenever I approached her, she has always been forthright in extending the much needed helping hand to me. Her grit, perfection and self-confidence in addition to her brilliant personality have helped me develop an opinionated mind. I thank her from the bottom of my heart.*

I consider myself immensely fortunate for having received help and guidance of ***Dr. Chinmay Kumar Panda****, Former Head and Assistant Director Grade Scientist, Department of Oncogene*

Regulation (ORU), CNCI, Kolkata. He helped me take up the right path at times when I was baffled with some first-hand experimental standardizations. He was extremely kind and gentle when it came to sharing academic anecdotes and opinions. He has never ever treated me differently from his own scholars. His humility and fatherly nature has been the most endearing qualities for which I shall always remain grateful.

I am thankful to ***Dr. Ugir Hossain S.K****, Senior Scientific Officer, Department of Clinical and Translational Research, CNCI, Kolkata for helping me learn some key techniques of chemistry without which my thesis would not have been complete. I shall fondly remember the sweet and bitter chit-chats which we shared on history, global politics and many more. I am definitely grateful to* ***Dr. Abhijit Rakshit****, Head, Department of Animal Care and Maintenance for sharing his valuable insights regarding mice handling.*

I also thank ***Dr. Jayanta Chakrabarti,*** *Director, CNCI for providing me with the necessary infrastructure, resources and fellowship to carry out my research in this esteemed institute. I would also like to thank* ***Central Instrument Research Facility (CRIF)*** *team and* ***CNCI support staff*** *for their cooperation and help.*

With special mention, I want to acknowledge the guidance of ***Dr. Debasish Chakraborty****, Professor, Department of Pathology, IPGMER, Kolkata. He has been very kind in meticulously teaching me the intricacies of histology and pathology. Whatever little I could master about this vast subject is only because of his kind help.*

I consider myself extremely fortunate for finding a mentor in ***Dr. Sudipta Chakraborty****, Associate Professor, Government General Degree College, Keshiary, Paschim Medinipur, West Bengal, India and my teacher in Master's Course. I owe him my entire journey as a student of science. He was the first to identify my inherent knack and aptitude of becoming a researcher early on in my formative days. His motivating words were the only reason for which I dared to take a leap into this difficult discourse of PhD. I take immense pride and express gratitude in calling myself his student.*

I would take the privilege to thank my lab seniors ***Dr. Ruma Sarkar (Rumadi), Dr. Apurba Mukherjee (Apurbadi)*** *and* ***Mr. Souvick Biswas (Souvickda)*** *for their cooperation. I cannot go without expressing my sincere gratitude to* ***Dr. Debomita Sengupta,*** *CSIR Senior Research Associate (Scientists' Pool) whom I fondly call Debomitadi. She has been my rock-solid strength in whom I confide and put my trust. She has been an elder sister while teaching me RT-PCR. She taught me to never settle for mediocrity despite challenges. Our interesting lunch-time conversations on science, society, mythology and human behaviour are the ones I hold close to my heart. I cannot thank her less for being by my side always.*

The mundaneness of PhD life can only be done away with amazing colleagues cum friends like ***Mr. Archismaan Ghosh****. In addition to being my colleague and lab mate at ECT, he has been my college classmate and a best friend since last 11 years. Right from sharing animal house chores to discussing solutions for a failed experiment, Archismaan has been my partner. His calm, pragmatic and thoughtful approach towards problems has been a life lesson for me. His work dedication and immense sense of responsibility towards his laboratory are the praiseworthy attributes which I have always looked upto. He always has my back and is my friend for this lifetime. I shall continue to be the loudest cheerleader for him always and forever. I would also like to thank my lab members* ***Ms. Salini Das*** *and* ***Mr. Debanjan Thakur (Debu)*** *for their cooperation and help. I thank our lab attendant* ***Mr. Sunit Roy*** *for his help and support.*

I acknowledge the unwavering support received from ***Dr. Mukta Basu (Muktadi), Dr. Debalina Mukhopadhyay (D2), Ms. Debopriya Roy Mahapatra (Debo), Mr. Subhabrata Guha (Subho), Ms. Nahid Sultana, Mr. Souradeep Biswas, Ms. Shalini Upadhayay*** *and* ***Mr. Saurav Bera*** *which kept me sane through this period. I could have never learnt immunohistochemistry and cryosectioning hands-on, if Muktadi was not kind enough to teach me. They have been gracious in welcoming me with widely opened arms despite being from different laboratories.*

I would like to thank the intern students whom I had the opportunity to mentor. Some of these young refreshing minds left an impact on me. I imbibed the energy and undying spirit of never giving up from ***Mr. Arka Das****. I am grateful for being able*

*to renew my focussing abilities after meeting **Ms. Disha Mitra**. Her motivation and never-ending quest to achieve the best in life has rejuvenated my spirit. I learned to be a hard-core yet passionate professional from **Mr. Arka Saha**. His meticulous and pragmatic approach towards resource use in lab is something I have adapted. I thank each one of them for enabling me to be a better researcher.*

*I cannot end without acknowledging my parents **Mr. Sadhan Mahapatra** and **Mrs. Pranati Mahapatra** who are the ultimate superheroes of my life. They have been instilling the importance of pursuing higher education within me right from childhood. They have always championed me for manifesting my education in becoming a better human being. I am indebted to them for teaching me the core humane values in life which have fuelled my journey this far. With researchers, life is not always hunky dory when it comes to finances. Yet, my parents have chosen to put with all the odds because they wanted to facilitate me in my aspirations. I hope, someday I manage to give them the comfort they deserve and fulfil all their wishes. I will have to thank my little sister **Ms. Angela Mahapatra** who has been patiently shouldering all my responsibilities at home. Despite being the youngest in my family, she has always been my greatest support. I definitely rely on her for moving ahead. With my family being the wind beneath my wings, I dare to soar higher fearlessly.*

My father says that it is not the number of penny we earn but the number of lives we manage to touch in this lifetime that counts in the end. Being a Cancer Researcher today, I take his words as beacons of hope and inspiration to make my doctoral studies count in days to come.

ELIZABETH MAHAPATRA

TABLE OF CONTENTS

❖ ABBREVIATIONS

- -SH- sulfhydryl
- 3MC- 3methylcholanthrene
- AAS- Atomic Absorption Spectroscopy
- AITC- Allyl-Isothiocyanate
- Akt- Protein Kinase B
- ALP- Alkaline Phosphatase
- ATP7A - Copper-transporting P-type adenosine triphosphate7A
- ATP7B- Copper-transporting P-type adenosine triphosphate7B
- BCIP/NBT- 5-bromo, 4-chloro, 3-indoylphosphate/ Nitro-Blue tetrazolium
- BIR- Baculoviral Repeat Domains
- BITC- Benzyl-Isothiocyanate
- BSA- Bovine Serum Albumin
- CCRT- Concurrent Chemoradiotherapy
- CDDP - cis-Diaminedichloroplatinum/Cisplatin
- ChIP- Chromatin Immunoprecipitation
- CIN-I- Cervical Intraepithelial Neoplasia-I
- CIN-II- Cervical Intraepithelial Neoplasia-II
- CIN-III- Cervical Intraepithelial Neoplasia-III
- CTR1- Copper transporter-1
- DAB- 3–3′ diaminobenzidine
- DAPI- 4′,6-diamidino-2-phenylindole
- DCF- 2', 7'-dichlorofluorescein
- DCFH-DA- 2',7'-dichlorofluorescein dihydroacetate
- DDR - DNA Damage Response

- DH- Delafield's Hematoxylin
- DLC- Differential Leukocyte Count
- DMEM- Dulbecco's Modified Essential Medium
- DNA - Deoxyribonucleic Acid
- E6AP - E6-Associated Protein
- EA50- Eosin Azure 50
- EGF- Epithelial Growth Factor
- ER- Endoplasmic Reticulum
- ERCC1- Excision Repair Cross-Complementing Gene 1
- EtBr- Ethidium Bromide
- FAAS- Flameless Atomic Absorption Spectroscopy
- FBS- Foetal Bovine Serum
- FIGO- International Federation of Gynecology and Obstetrics
- GR- Glutathione Reductase
- GSH- Glutathione
- GST- Glutathione Transferase
- HBS- HEPES-buffered saline
- HH- Harris Haematoxylin
- HPVs - Human Papilloma Viruses
- hr-HPVs - High-risk HPVs
- HSIL- High grade Squamous Intraepithelial Lesion.
- HSPs- Heat Shock Proteins
- IAPs - Inhibitor of Apoptosis Proteins
- IC- Invasive Cancer
- IF- Immunofluorescence
- IHC- Immunohistochemistry

- iNOS- Nitric Oxide Synthetase
- ITCs- Isothiocyanates
- iκB - Inhibitor of κB
- LC-MS-MS- Liquid Chromatography with Tandem Mass Spectrometry
- LCR - Long Control Region
- LI- Leukocyte Index
- lr-HPVs - Low-risk HPVs
- LSIL- Low grade Squamous Intraepithelial Lesion
- MDR1- Multi-Drug Resistance1
- MEM- Minimal Essential Medium
- MRP1- Multi-Drug Resistance-Associated Protein 1
- MRP2- Multidrug Resistance Protein2
- MTD- Maximum Tolerated Dose
- NBF- Neutral Buffered Formalin
- NCCP- National Cancer Control Program
- NER- Nucleotide Excision Repair
- NF-κB- Nuclear Factor κB
- NHEJ- Non Homologous End Joining
- NP40- Nonidet P40 (IGEPAL)
- OCT2- Organic Cation Transporter2
- OG6- Orange G6
- ORFs - Open Reading Frames
- p50- NFκB1
- p65- RelA
- PAP staining- Papanicolau staining
- PBS- Phosphate Buffered Saline

- PBST- PBS supplemented with Tween20
- PEITC - Phenethylisothiocyanate
- PET- Petroleum Ether
- Pgp1- P-glycoprotein-1
- PI3K- Phosphatidylinositol 3 Kinase
- PI3KCA- Phosphatidylinositol 3-Kinase subunit C
- PKCs- Protein Kinase C
- pRb - Retinoblastoma Protein
- PXR - Pregnane X Receptor
- Rh-123- Rhodamine
- RIPA- Radio- Immunoprecipitation Assay Lysis buffer
- RMAs- Resistance Modifying Agents
- RNS- Reactive Nitrogen Species
- ROS- Reactive Oxygen Species
- RTKs- Receptor Tyrosine Kinases
- RT-PCR- Reverse Transcriptase-Polymerase Chain Reaction
- SCGE- Single Cell Gel Electrophoresis
- Ser473- Serine473
- SFN- Sulforaphane
- SGOT- Serum Aspartate Transaminase
- SGPT- Serum Alanine Transaminase
- TAB1- TAK1 binding protein
- TAK1- TFGβ Activated protein
- TCGA- The Cancer Genome Atlas
- Thr308- Threonine308
- Thr450- Threonine450

- TME - Tumor Microenvironment
- UAB- Ubiquitin Associated Domain
- URR - Upper Regulatory Region
- WHO - World Health Organization
- XIAP- X linked Inhibitor of Apoptosis Protein

Introduction

1. Introduction

Cervical cancer is helmed as the ***fourth leading*** cause of mortality and morbidity amongst women worldwide [GLOBOCAN, 2020]. In India, cervical cancer is deemed to be the ***second most common gynaecological cancer*** affecting women after breast, uterine and ovarian cancers [Cancer Statistics, 2022; Bray et al., 2018].The global records for cervical cancer cases and deaths are enumerated to be incremental by World Health Organization (WHO) on a yearly basis [Arbyn et al., 2020]. Such an exponential rise in cervical cancer incidences and mortalities is mostly accredited to ***lack of patient awareness***, especially in the low/middle income countries alongwith the phenomenon of ***'therapy failure'*** [Wilailak et al., 2021; Srivastava et al., 2018]. As per WHO estimates, developing nations with a relatively poor socio-economic backdrop contributed in 85% of the global cervical cancer cases in 2013 [Dhillon et al., 2018]. In emergent nations, women are highly negligent of their health and generally report to the clinics only upon disease advancement. Key characteristics like ***aggravated invasiveness***, ***high metastatic potential*** and ***therapy unresponsiveness*** are intrinsic to the aggressive tumor microenvironment (TME) of such advanced cervical cancer stages [Hernandez et al., 2022; Elmore et al., 2021]. With regard to the havoc it has caused, cervical cancer is currently identified as a global epidemic which calls for the attention of clinicians as well as researchers [Zhang et al., 2021].

Human Papilloma Viruses (HPVs), a special class of oncogenic DNA viruses hailing from the ***Papillomaviridae*** family are identified as the main causative agents of cervical cancer [zur Hausen,2009a; Pincock, 2008b]. Early disease detection therefore can facilitate improved management of the scenario [Basoya and Anjankar,

2022]. As a profound measure to combat this growing health issue, National Cancer Control Program (NCCP) has initiated 'disease screening events' alongside organising 'awareness camps' for educating women about the risk factors and warning signs of cervical cancer [Bhatla et al., 2021]. Commercial availability of vaccines against high-risk strains of ***HPV*** has emerged as an effective means of disease prevention [Akhatova et al., 2022; Mishra et al., 2015]. Although, Indian women continue to remain at risk for cervical cancer owing to ignorance and resource inadequacy in family which restrain them from vaccine purchase [Bhatla et al., 2021; Kaarthigeyan, 2012]. As a result, clinicians are left with only conventional regimens to rely upon for treatment. Cervical cancer therapy mainly involves the conventional use of ***platinum-ligated chemotherapeutic drugs*** like ***Cisplatin***, ***Carboplatin***, and many more [Achkar et al., 2018;Falzone et al., 2018]. Patients with ***invasive cancer stages***, i.e., ***Stage-IIB-IVA***, are prescribed cisplatin treatment either as a ***single-agent*** or as a ***radiosensitizer*** prior to the onset of radiotherapy cycles in the popular regime of ***Concurrent Chemoradiotherapy (CCRT)*** [Gadducci and Cosio, 2020;He et al., 2022]. Popular as an active cytotoxic agent with a wide range of clinical applications, cisplatin is also employed for treating various other malignancies [Brown et al., 2019]. It is ***cost-effective*** and is known to render cellular ***cytotoxicity*** more effectively than other chemotherapeutics [Galluzzi et al., 2014]. Despite its success, ***cisplatin resistance*** is quite concerning for oncologists, cancer biologists as well as patients for it impedes therapy to result in dismal treatment outcomes [Mortensen et al., 2020]. Based on several evidences, ***'acquired cisplatin resistance'*** is rightly identified as the cardinal of therapy failure, disease relapse and recurrence [Cheng et al., 2021;Wang et al., 2021]. In this context, rationalising therapy strategies can serve as an ultimate resolve to better disease management.

Cisplatin ***(cis-Diaminedichloroplatinum; CDDP)*** begets cellular cytotoxic effects following ***intracellular hydrolytic activation*** wherein the drug transforms into a strong ***electrophile*** capable of attacking several cellular ***nucleophiles*** [da Fonseca et al., 2022; Lorusso et al., 2014; Wang et al., 2012]. These majorly includes ***Deoxyribonucleic Acid (DNA)*** and cellular antioxidants such as ***Glutathione (GSH)*** [Song et al., 2022]. Apart from DNA and GSH which are the principal drug-targets, cisplatin is also documented to pitch on the ***membrane proteins*** of subcellular organelles like mitochondria and endoplasmic reticulum (ER) [Song et al., 2022; Tchounwou et al., 2021]. Cisplatin forms intrastrand DNA crosslinks to generate bulky irreparable cisplatin-DNA adducts that trigger a milieu of cellular signalling cascades which culminate in ***programmed cell death*** or ***apoptosis*** [Hoeschele, 2016**;**.Arnesano and Natile, 2009]. However, a heterogeneous TME abundant in pleomorphic cancer cells bearing diverse genetic, epigenetic and signal transduction landscape respond differentially to the drug [He et al., 2021;Buzdin et al., 2018]. As a consequence, such neoplastic cellular variants adapt to the incoming chemotherapeutic by generating anomalous molecular crosstalk which augment cisplatin resistance in the tumor [Siddik, 2003]. The drug evasive nature of cervical cancer cells is also a manifestation of their compromised cisplatin retention abilities which is an outcome of their reprogrammed metabolic profiles [Morandi and Indraccolo, 2017]. ***Increased drug efflux*** alongwith ***reduced drug-influx*** in complementation with ***hasty drug metabolism*** and ***swift drug inactivation*** by heightened levels of antioxidants establishes a cellular chemoresistant phenotype. In fact, convenient repair of bulky drug DNA-adducts by the overexpressing ***repair enzymes*** also adds on to the cellular survival advantages [Vaidya et al., 2022]. Often dense cellular packaging of tumors retards drug diffusion into its interior thereby delimiting its accumulation and efficacy

[Bhattacharya et al., 2022]. Therefore, enhancement of cisplatin accumulation can aid in improving therapy to curtail the escalating trends in disease mortalities. To achieve this aim, holistic disease understanding is the prima facie.

Since 'metabolic reprogramming' is pivotal to the episode of acquired cisplatin resistance, its intricate association with upregulation of several prosurvival signalling cascades requires exploration [Vaidya et al., 2022]. The ***Phosphatidylinositol 3 Kinase/Protein Kinase B or Akt (PI3K/Akt)*** signaling axis is one such prosurvival cascade which confers cisplatin resistant properties upon malignant cells by transforming them metabolically to reduce their drug accumulation capacity [McCann and Kerr, 2021; Schiliro and Firestein, 2021]. Various extracellular triggers such as chemotherapeutic drug exposure activate PI3K which thereafter evokes the ***serine threonine kinase*** AKT to begin orchestration of cellular immortalization process **[**Huang et al., 2021; Iida et al., 2020]. For instance, activated phospho-Akt promotes proteasomal degradation of ***IκB*** and evokes ***Nuclear Factor κB (NF-κB)*** to allow evasion of apoptosis by triggering ***Inhibitor of Apoptosis proteins (IAPs)*** in the downstream [Dukaew et al., 2020**;**Vaidya et al., 2020**;** Rascio et al., 2021]. This prosurvival signalling nexus domineers the event of cisplatin resistance by inciting ***cisplatin exporters*** namely ***P-glycoprotein-1(Pgp1)*** and ***Multidrug Resistance Protein2 (MRP2)***[Mahapatra et al., 2022; Bourguignon, 2019]. Additionally, membrane associated high-affinity copper transporters like ***Copper transporter-1(CTR1), Copper-transporting P-type adenosine triphosphate (ATP7A/B)*** and ***Organic Cation Transporter2 (OCT2)*** are also expressed via PI3K/Akt activity [Chen et al., 2022; Su et al., 2022]. These pumps cumulatively expunge cisplatin out from the cancer cells so as to critically reduce its intracellular levels for restraining apoptosis. This lowers the cellular pharmacodynamicity and pharmacokinetics of the

drug thereby allowing cisplatin resistance to prevail [Shi et al., 2022; Wu et al., 2021; Liu et al., 2015]. In this light, comprehending these molecular underpinnings of cellular cisplatin response is essential for identification of key therapeutic targets for overcoming resistance.

Time and again, plant derived natural phytochemicals have been indiscriminately used as chemopreventive agents in cancer drug development owing to their potential to target prosurvival molecules. ***Phenethylisothiocyanate (PEITC)***, a natural isothiocyanate found in ***cruciferous vegetables*** is observed to capacitate apoptosis by restricting the activities of prosurvival molecules [Dai et al., 2016; Gupta et al., 2014; Wang et al., 2011]. Reports are also suggestive of its ability of modulating Akt for promoting caspase activation in chemoresistant cancer cells [Biswas et al., 2021;Sarkar et al., 2012]. This phytochemical also relays anti-oxidant functions through quenching of free radicals in various cancer models to augment cisplatin sensitivity [Soundararajan and Kim, 2018;Sarkar et al., 2012]. PEITC reportedly reversed cisplatin resistance by inducing apoptosis through glutathionylation-dependent degradation of Mcl-1 in biliary tract cancer cells [Li et al., 2016]. Similarly, among gastric cancer cells PEITC reverted cisplatin resistance by inhibiting mRNA and protein expressions of ***multi-drug resistance1 (MDR1), multi-drug resistance-associated protein1 (MRP1), excision repair cross-complementing gene 1 (ERCC1), survivin*** and ***Mad2,*** thereby suppressing Akt phosphorylation and transcriptional activation of NF-κB [Tang et al., 2014]. However, the influence of PEITC on the deregulated PI3K/Akt signalling milieu in the cervical cancer scenario is yet to be deciphered in details. In this regard, the present study attempts to explore the mechanism of PEITC mediated regulation of PI3K/Akt pathway for overcoming acquired cisplatin resistance in cervical cancer.

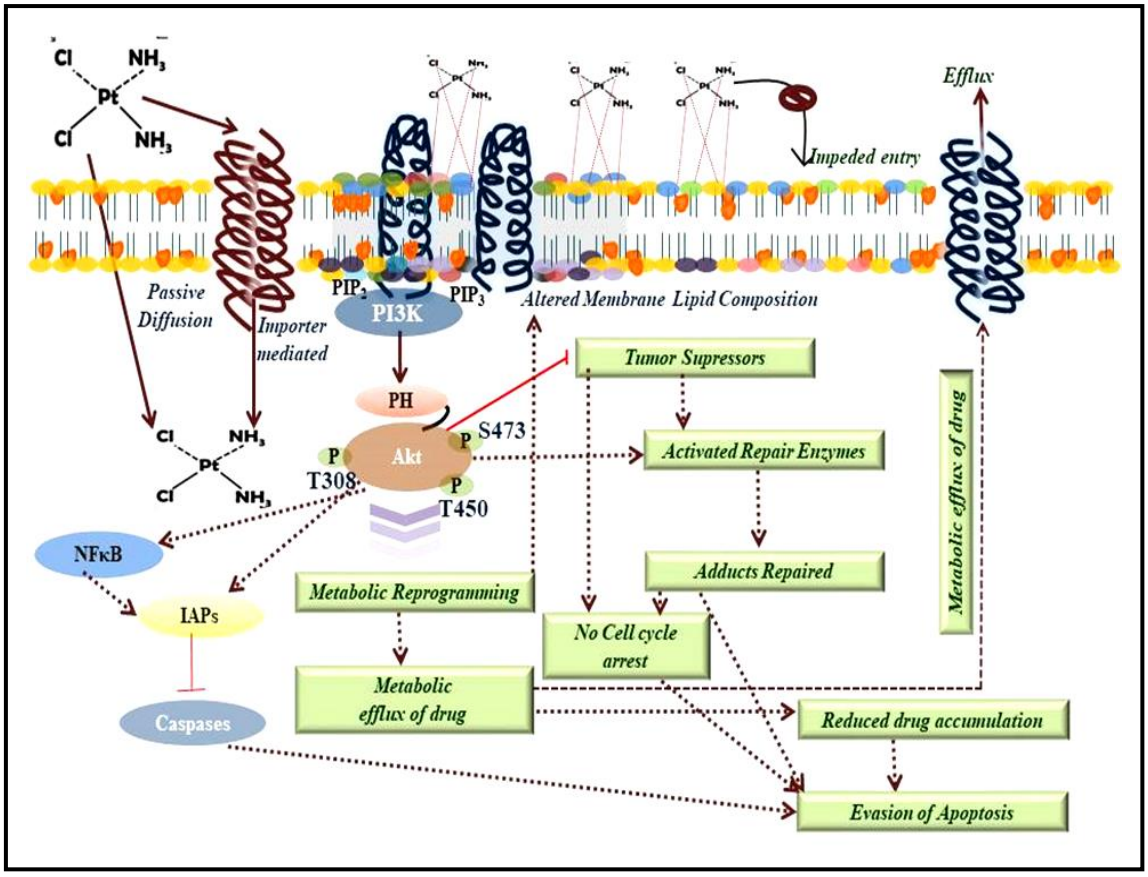

Figure 1: An Overview of PI3K/Akt Signalling Mediated Cisplatin Resistance in Cervical Cancer

Review of Literature

2. Review of Literature

2.1. Epidemiology of Cervical Cancer

As per the recent records of WHO, cervical cancer incidences are quite frequent among women across 45 countries in the world. These ***red-listed*** countries, as identified by WHO include ***Sub-Saharan Africa***, ***Asian*** nations particularly ***India*** in addition to some ***Central*** and ***South American*** countries [Jedy-Agba et al., 2020; Bobdey et al., 2016; Murillo et al., 2016]. Since 2012, cervical cancer cases have extensively risen to become an alarming problem worldwide [Zhang et al., 2021]. A clear depiction of cervical cancer incidences is presented in Figure 2.

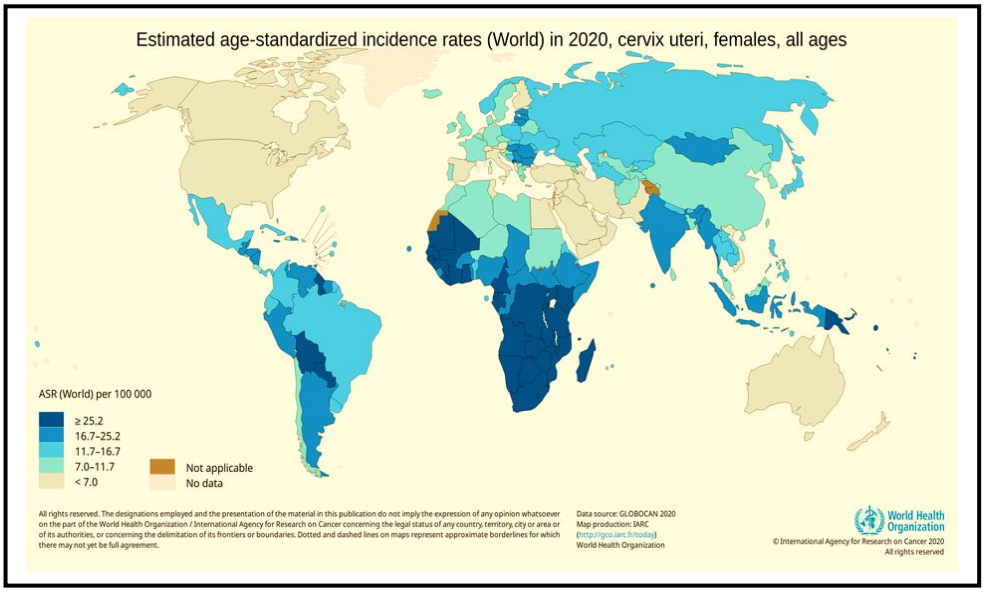

Figure 2: Worldwide Prevalence-Rates of Cervical Cancer WHO [GLOBACON,2020]

Multi-various factors such as ***socio-economic disparities***, ***geographic variations*** alongwith ***social*** and ***cultural prejudices*** that restrict the access of women to preventive measures are the key global benefactors of cervical cancer [Keetile et al., 2021; Buskwofie et al., 2020; Barrington et al., 2016]. India with

an abundance of all these contributory factors, registers paramount number of cervical cancer cases even with the support of conventional treatment strategies and the recent vaccination drives. Approximately, 1, 22,844 Indian women are diagnosed with cervical cancer each year and about 67,477 of them lose their life mid-way to therapeutic procedures [Singh et al., 2023]. India is the residence to 432.2 million women, mostly hailing from the ***15 years age group*** or older [Sreedevi et al., 2015]. Women of this age-group is attested as the cervical cancer susceptible clan [Tuncer and Tuncer, 2020; Kaarthigeyan, 2012]. Hence, cervical cancer is the second most common cancer among women of 15–44 years age group [Taneja et al., 2021]. It is therefore ranked as the highest age standardized cancer in India compared to nations like Bangladesh, Sri Lanka and Iran [Sreedevi et al., 2015]. Mortality index and prevalence rates of cervical cancer imperative of the disease being a global panacea are illustrated in Figure3.

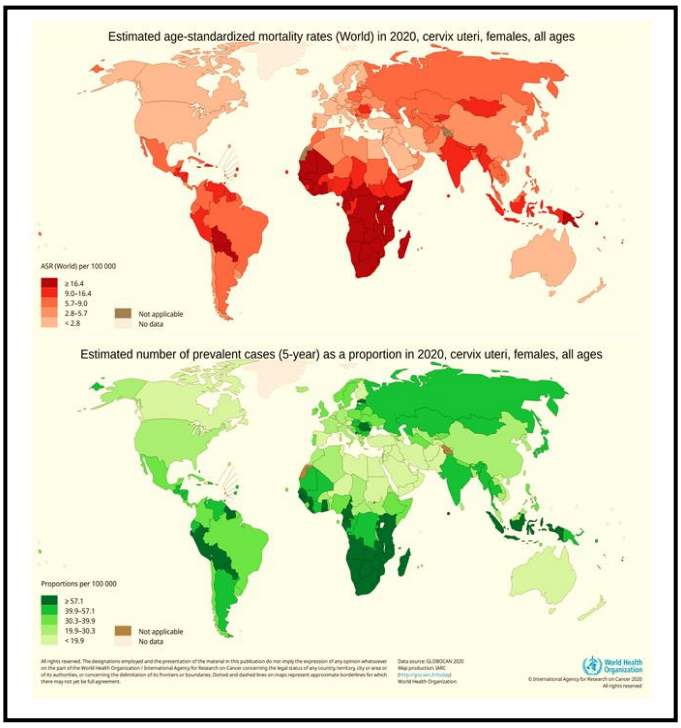

Figure 3: Worldwide Mortality and Prevalence Rates of Cervical Cancer [GLOBACON, 2020]

Current epidemiology of cervical cancer necessitates proper disease management and therapy planning which is achievable only with strategizing of cost-effective ameliorative rationales.

2.2. Aetiology of Cervical Cancer

Proper understanding of cervical cancer scenario and its aetiology is central to planning therapy and management of the disease. Infections with a special class of oncogenic DNA viruses called ***Human Papilloma Viruses (HPVs)***, hailing from the viral family ***Papillomaviridae***, are highly accredited for cervical malignancy [Day and Schelhaas, 2014]. Principally, HPVs are sexually transmitted. On the basis of its carcinogenic potentials, HPVs can be categorized as –***(i) low-risk HPVs(lr-HPVs)*** like ***HPV 6, 11, 42, 43*** and ***44***, and ***(ii) high-risk HPVs(hr-HPVs)***like ***HPV 16, 18, 31, 33, 34, 35, 39, 45, 51, 52, 56, 58, 59, 66, 68*** and ***70*** [Day and Schelhaas, 2014; De Brot et al., 2017]. Persistent and prevalent infections with hr-HPVs contribute in development of cervical cancer alongside other cancers such as the cancer of vagina, vulva, penis, anus, head and neck. HPV infections may also give rise to anogenital warts and recurrent respiratory papillomatosis [De Brot et al., 2017; Fortes et al., 2017]. Besides HPVs, several other risk factors have been implicated in the etiology of cervical cancer. These mainly include long term use of oral contraceptive [Gierisch et al., 2013], smoking [Puleo et al., 2020] and infections with *Chlamydia trachomatis* [Zhu et al., 2016].

HPVs are relatively small non-enveloped viruses with a diameter of 55 nm. It has a double stranded circular DNA genome which is 8 kb long and is enclosed within an ***icosahedral capsid*** composed of ***72 capsomers*** [Baker et al., 1991;Favre, 1975]. Functionally, the HPV genome is regionalized into-i) ***a non-coding regulatory*** region called the ***long control region (LCR)*** or the ***upper regulatory***

region (URR), ii) ***an early region*** which houses *E1, E2, E4, E5, E6* and *E7 genes*, and (iii) ***a late region*** which is made up of late expressing genes such as *L1* and *L2* [Burd, 2003]. LCR regulates the process of viral DNA replication via controlling the transcription of Open Reading Frames (ORFs). The lately transcribed proteins L1 and L2 are the structural proteins of the viral capsid. The early genes are dictators of viral replication, transcription, assembly and oncogenesis. Particularly, E6 and E7 are oncogenic and they degrade the cell cycle regulators like p53 and pRb to eventuate in cervical carcinoma [Burd, 2003]. An outline of HPV genome is represented in Figure 4.

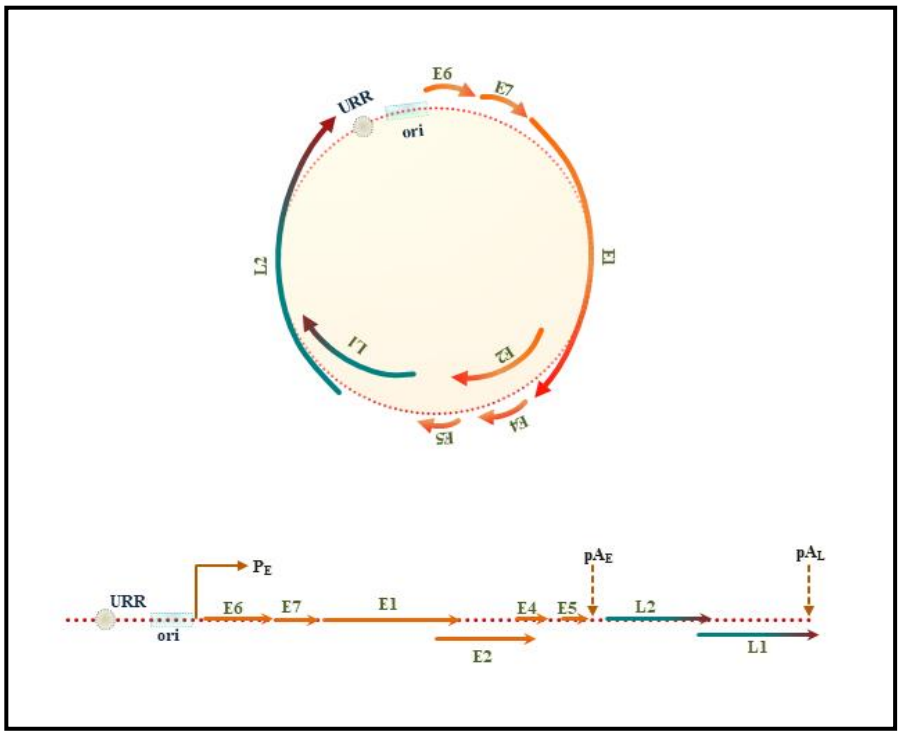

Figure 4: An outline of HPV Genome delineating the oncogenic fragments responsible for malignant transformation of cervical epithelium

These miniscule infectious agents access the cervical epithelial layer through crevices or microabrasions that generally forms due to mechanical shock or injury. Following entry, HPVs integrate their genome into that of the host to initiate

malignant transformation of the cervix. The carcinogenesis of cervical epithelium begins with the onset of viral lifecycle which initiates with viral entry into basal cell layer of the epithelium [Doorbar et al., 2015]. The basal cell layer of cervical epithelia enables multiplication and replication of the virus by providing them with a suitable microenvironment. Molecules expressed by the basal cells such as ***integrins (α6β1, α6β4), heparan sulphate*** and ***proteoglycans*** are chemoattractants for HPVs [Giroglou et al., 2001;Evander et al., 1997]. No sooner does this virus enter the basal cells, viral replication starts soon. Although, owing to poor copy number the duplication of viral DNA becomes non-reproductive. However, as the infection load spreads into the overlying parabasal and intermediate layers, which are majorly comprised of semi-differentiated cells or terminally-differentiated keratinocytes. As DNA copy number increases, productive viral replication also commences [Flores et al., 1999]. Meanwhile, the process of cervical carcinogenesis gets driven as the virus multiplies and sustains itself in the host system. This has been well-elaborated in Figure 5.

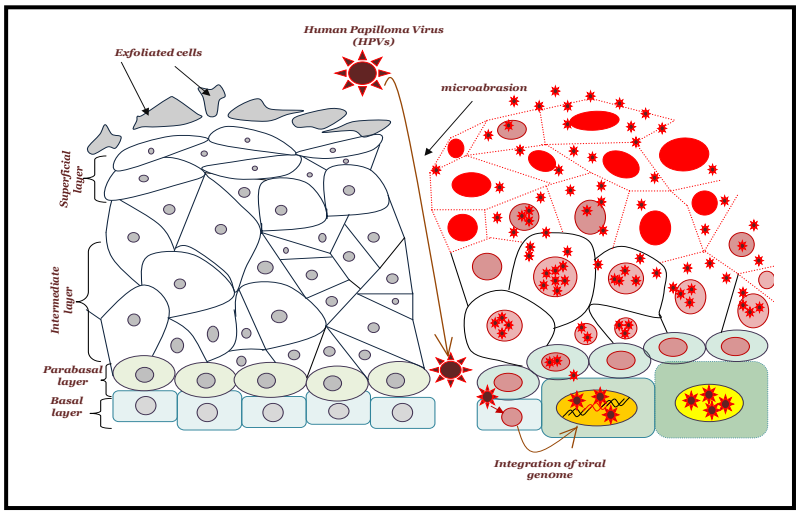

Figure 5: Host cell hijacking by HPVs elaborating the viral entry into the cervical epithelium via micro abrasions followed by integration of its genome into the DNA of basal cells to promote loss of genomic integrity for promoting cervical carcinogenesis

HPV mediated neoplastic transformation of cervix kick starts with the abridgement of tumor suppressor functions. An array of experimentations conducted in *in vitro* and *in vivo* models have successfully established the immortalizing capacities of E6 and E7 viral gene products; ensued via degradation of cell cycle controllers like p53 and pRb [Münger and Howley, 2002; Howley et al., 1991]. The guardian of the genome, p53, controls and coordinates the major genetic players involved in cell cycle arrest [Di Leonardo et al., 1994]. On top of this, p53 choreographs DNA damage repair, and apoptotic events [Smith et al., 1995]. As the episome formation is successfully accomplished by the virus, DNA damage response (DDR) is triggered. Absence of functional p53 allows the cervical cells to skip G1-arrest [Thomas et al., 1999]. These functions which are central to cell survival and death get violated in the HPV immortalized cervical cells owing to reduced p53 levels. A higher E6 level is inversely proportional to cellular p53 levels [Hwang et al., 1993]. Contrarily, the oncoprotein E7 binds with hypophosphorylated ***retinoblastoma protein (pRb)***; releasing the growth promoter E2F from the Rb-E2F complex. E2F in turn translocates to the nucleus to enable expression of genes that drive the infected cells through S-phase of the cell cycle [Syrjänen and Syrjänen, 1999]. Cumulative loss of function of both of these tumor suppressors enables the infected cells to progress through G1 and S phases even with genetic errors. Shortfall of repair processes ultimately paves a way for genomic disintegrity to prevail; mediating neoplastic growth. Recent reports suggest that E6 and E7 intervene into the tumor suppressor activity by recruiting methyl groups on their promoter region [Sen et al., 2018; Yin et al., 2017]. These oncogenic viral proteins also methylate cyclinA1 promoter and deregulate cell cycle progression to mediate tumorigenesis

[Yanatatsaneejit et al., 2011]. Schematic representation of HPV mediated molecular carcinogenesis is depicted in Figure 6.

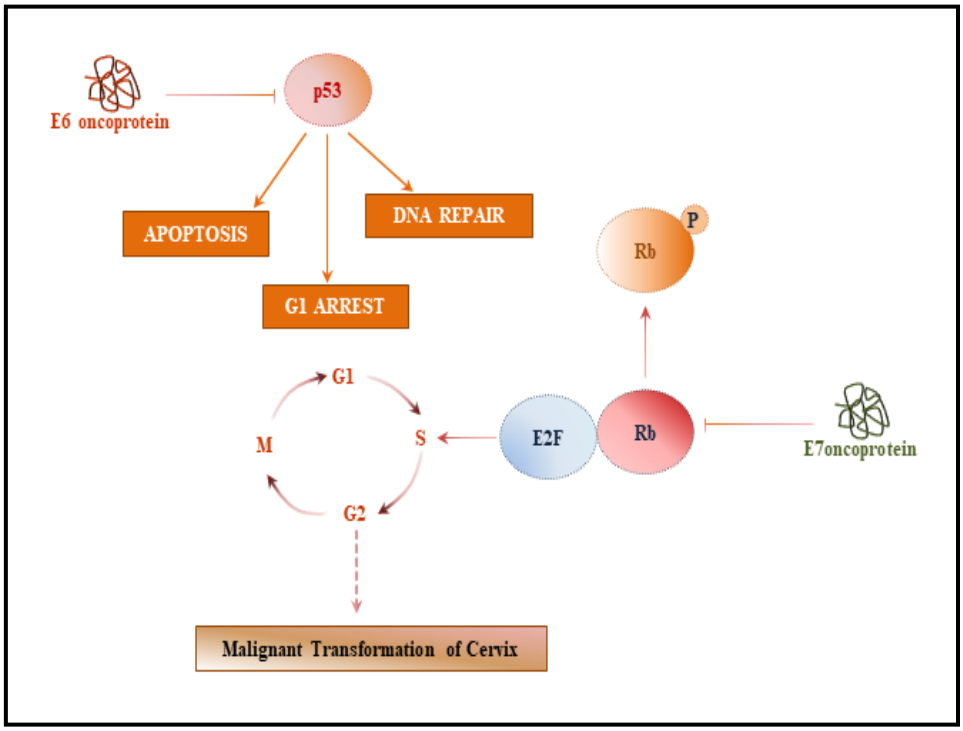

Figure 6: Mode of HPV mediated Molecular Carcinogenesis of the Cervical Epithelium

Besides HPVs, ***occupational exposure*** to ***chemical carcinogens*** in a chronic fashion can also result in similar kind of malignant transformation in the cervical epithelium. Additionally, a weak immune system, smoking habits and ageing cumulatively favours cervical carcinogenesis either due to prolonged HPV infections or by carcinogen encounters.

2.3. Characteristic Histopathological Alterations Associated with Cervical Cancer

Considering the predominance of HPV infections, it is important to understand the anatomy of cervix. Anatomically identified as the ***'neck of uterus'***, cervix is a fibromuscular organ that links the uterine cavity with vagina [Mazengenya and

Bhikha, 2020]. It is generally cylindrical in shape with the anterior and posterior walls being ordinarily apposed. Hence, the cervix occupies both an internal and an external position. The lower half or intravaginal part lies at vaginal end and is termed as ***endocervix*** whilst the upper half or ***ectocervix*** is localized above vagina in the pelvic/abdominal cavity [Mazengenya and Bhikha, 2020]. Pictorial exhibition of cervical anatomy is depicted in Figure 7.

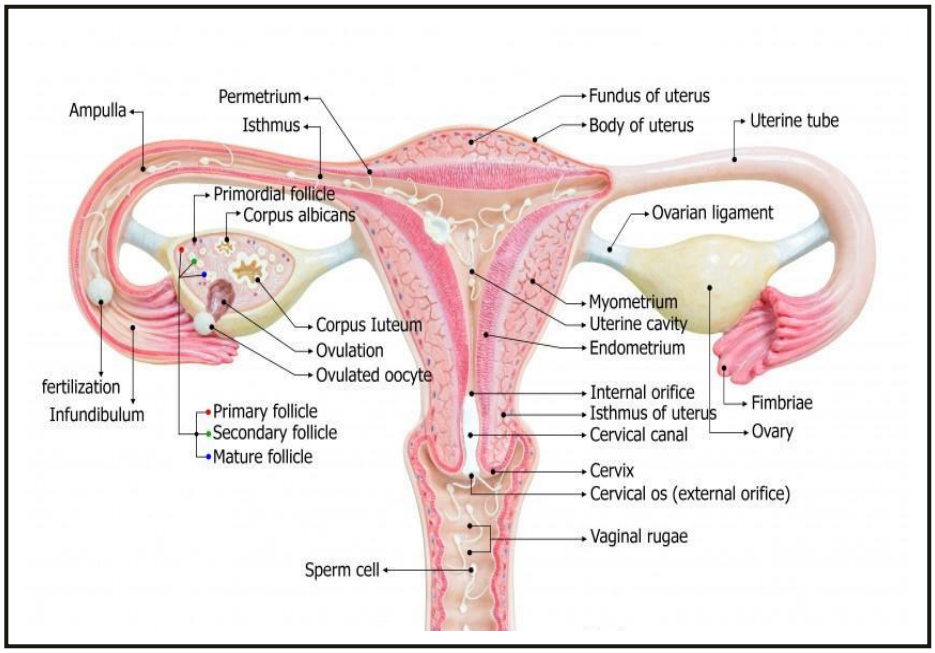

Figure 7: Anatomy of Cervix

Typically, cervix has several different epithelial linings stacked together in a ***stratified epithelium*** [Bragulla and Homberger, 2009]. The ***endocervical canal*** has ***glandular epithelial lining*** whereas the ectocervix is demarcated by ***squamous epithelium***. The cervical ***stroma*** is composed of dense fibromuscular tissue enriched with vascular, lymphatic, and nerve supplies that form a complex plexus. The lowermost cellular tier of cervical stratified epithelium is known as the ***basal layer*** or the ***basement membrane,*** separating the epithelial region from underlying stroma. This is a monolayer of round basal cells with large dark- stained nuclei and little cytoplasm which divide and functionally differentiate into the overlying ***parabasal***

layer composed of ***parabasal cells***. These cells further multiply and eventually mature into ***intermediate*** and ***superficial*** epithelial cells, comprising the overlying ***intermediate*** and ***superficial*** layers respectively. Within the endocervical interiors there lies a ***transformation zone*** which marks the transit of squamous epithelium into columnar epithelium. The thickness of cervical epithelium reduces suddenly in this zone which is also termed as the ***squamo-columnar junction***. As a result, this region is most prone to developing microabrasions or crevices which serve as 'micro gateways' for HPVs. A clear depiction of cervical histopathology and cytopathology is provided in Figure 8.

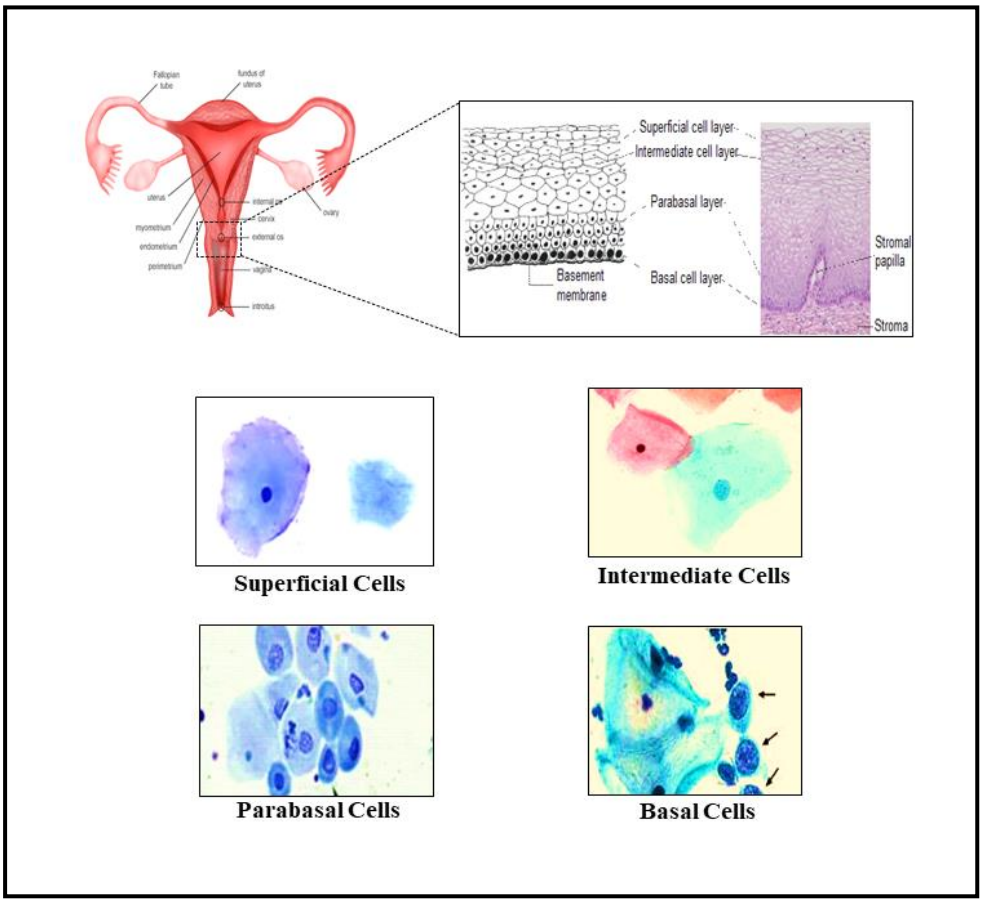

Figure 8: Histopathology and Cytopathology of Normal Cervical Epithelium

HPV mediated carcinogenesis in the cervical epithelium is manifested through abnormal tissue remodeling that progresses through ***precancerous stages*** or

precursor lesions to eventuate in ***invasive stages*** [Saunier et al., 2008; Lillo et al., 2005]. Persistent HPV infections gradually induce ***mild*** to ***moderate*** to ***severe dysplastic*** changes in the cervix, finally culminating in ***full-length dysplasia*** or ***carcinoma in situ*** stages [Saunier et al., 2008; Lillo et al., 2005]. WHO identifies the mild and moderate dysplasia as precancerous stages and collectively term them as ***Cervical Intraepithelial Neoplasia-I/II (CIN-I/CIN-II)***. Severe dysplasia, categorised as CIN-III stage is equivalent to ***invasive*** or ***microinvasive*** stages. On the other hand, Bethesda System classifies the CIN-I stage as ***Low grade Squamous Intraepithelial Lesion (LSIL)*** while CIN-II and CIN-III stages are defined as ***High grade Squamous Intraepithelial Lesion (LSIL)***. The categorisation is perfectly described in Table.1.

Medical Interventions become necessary at HSIL or carcinoma *in situ* stages. For treatment conveniences, the ***International Federation of Gynecology and Obstetrics (FIGO)*** have staged the disease on the basis of tumor size and invasiveness [Petignant and Roy, 2007]. Cervical cancer stages alongwith their aggressiveness and treatment regimen is well described in Table 2. Relative histopathological and anatomical changes are represented in Figure 9.

TABLE1: CERVICAL CANCER STAGES

TRADITIONAL CLASSIFICATION	WHO CLASSIFICATION	BETHESDA CLASSIFICTION
Mild Dysplasia	**CIN-I**	**LSIL**
Moderate Dysplasia	**CIN-II**	**HSIL**
Severe Dysplasia/ Carcinoma *in situ*	**CIN-III**	**HSIL**

TABLE2: FIGO CLASSIFICATION OF CERVICAL CANCER STAGES

STAGES			DEFINITION
I			Carcinoma strictly confined to the cervix (extension to the corpus should be disregarded)
	IA		Invasive cancer identified only microscopically; invasion limited to stromal invasion with maximum depth of 5 mm and no wider than 7 mm (the depth of invasion should not be more than 5 mm taken from the base of the epithelium, either surface or glandular, from which it originates; vascular space involvement, either venous or lymphatic, should not alter the staging)
		IA1	Measured invasion of stroma ≤3 mm in depth and ≤7 mm in width
		IA2	Measured invasion of stroma >3 mm and <5 mm in depth and ≤7 mm in width
	IB		Clinical lesions confined to the cervix or preclinical lesions greater than stage IA
		IB1	Clinical lesions no greater than 4 cm in size
		IB2	Clinical lesions greater than 4 cm in size
II			The carcinoma extends beyond the cervix but has not extended to the pelvic wall or the lower third of the vagina
	IIA		Involvement of up to the upper two thirds of the vagina, with no obvious parametrial involvement
		IIA1	Clinically visible lesion ≤4 cm
		IIA2	Clinically visible lesion >4 cm
	IIB		Obvious parametrial involvement without involvement of pelvic sidewall.
III			The carcinoma has extended to the pelvic wall; on rectal examination, there is no cancer-free space between the tumor and the pelvic wall; the tumor involves the lower third of the vagina; all cases with a hydronephrosis or nonfunctioning kidney are included unless they are known to be due to other causes
	IIIA		The carcinoma has spread to the lower third of the vagina but not to the pelvic wall
	IIIB		The carcinoma has grown into the pelvic wall, or there is hydronephrosis/non-functioning kidney
IV			The carcinoma has extended beyond the true pelvis or has clinically involved the mucosa of the bladder or rectum
	IVA		Spread to adjacent pelvic organs
	IVB		Spread to distant organs

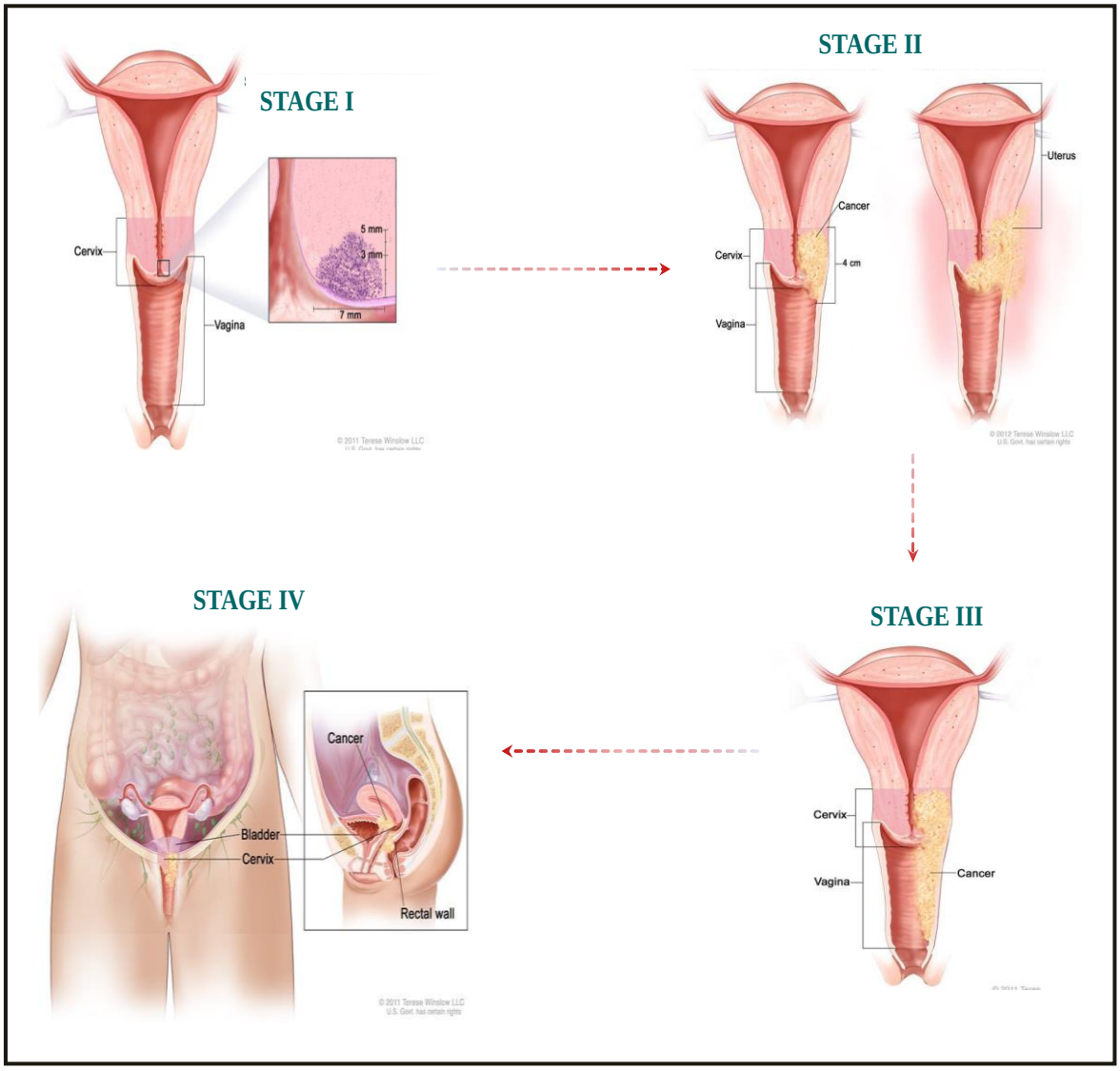

Figure 9: Anatomical Grades of Cervical Cancer as Classified by FIGO

2.4. Cervical Cancer Therapy

Cervical cancer disease is addressed by various modes which includes ***vaccination, Pap Screening Tests*** and stage-specific therapy in the form of ***Concurrent Chemoradiotherapy (CCRT)***. In recent times, vaccination awareness is on high especially with availability of commercial vaccines like ***Gardasil-9, Cervarix*** and many more [Brisson et al., 2020; Wang et al., 2020]. However, its procurement is beyond the means of many, especially in countries like India. In fact, the gold standard of Pap Smear

Test is still unheard to a major proportion of Indian women [Tiwari et al., 2011]. Cumulatively, these factors increase the risk of morbidity among women reporting late to the clinics upon disease advancement. Hence, there are two most indiscriminately employed methodology of treating cervical cancer-***chemotherapy*** and ***radiotherapy***[Burmeister et al., 2022]. As per FIGO rules, patients with invasive stages (Stage-IIB-IVA) are generally subjected to treatment with ***platinum ligated drugs*** like ***cisplatin*** either as single chemotherapeutic agents or as a ***radiosensitizer*** in CCRT. Besides these, surgery is also performed to uproot cervical tumors [Kokka et al., 2014;Maheshwari et al., 2016; Fares et al., 2020]. Figure 10 exhibits the glimpse of disease management options for cervical cancer.

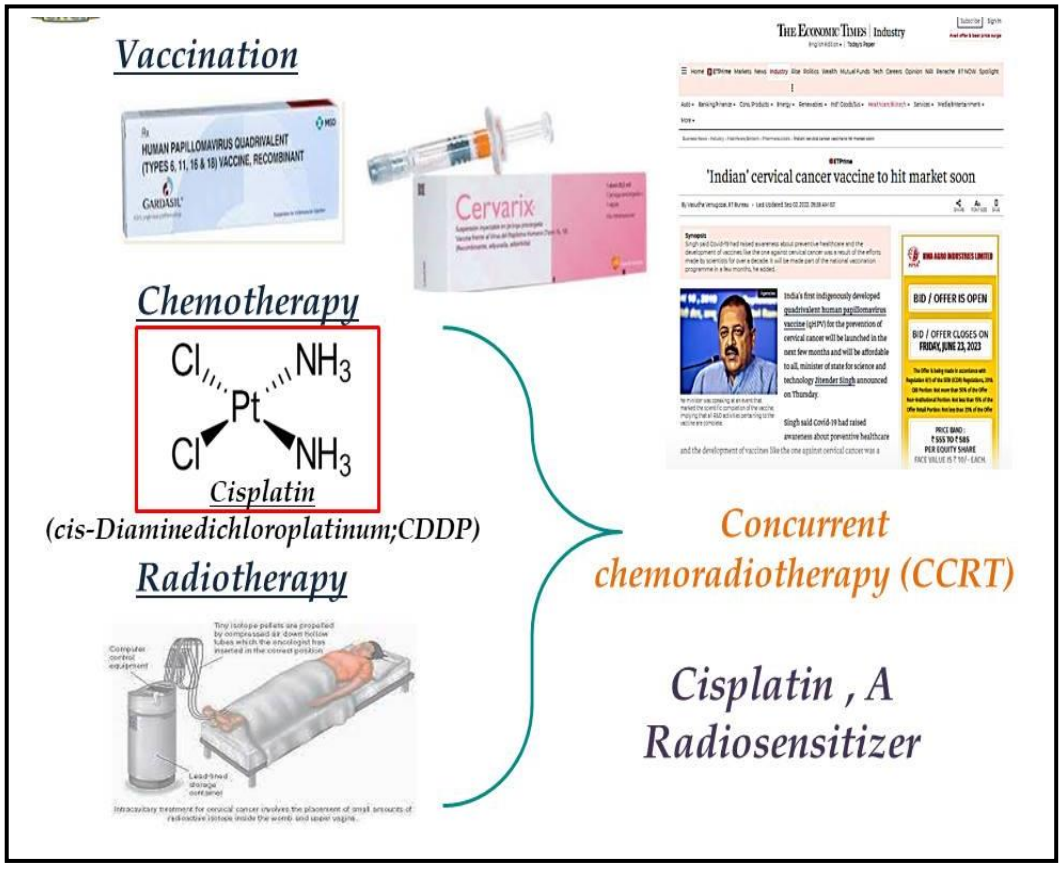

Figure 10: Therapy Options for Cervical Cancer

2.5. Cisplatin Therapy in Cervical Cancer

Chemotherapy is considered as the standard treatment for patients with advanced or recurrent cervical cancer. The chemotherapeutic agent ***cisplatin*** was identified as an anticancer agent effective for treating advanced/recurrent cervical cancer. ***Cis-Diamminedichloroplatinum (II),*** the generic name of cisplatin is suggestive of its neutral chemical nature. This drug became popular as a potential chemotherapeutic when its ability of damaging DNA was serendipitously discovered [Chattopadhyay, 2022; Hoeschele, 2016; Wiltshaw, 1979]. With a square and planar structure, this cytotoxic drug is a coordination complex of divalent platinum (Pt^{2+}) ion along with two replaceable chloride groups and two irreplaceable amine groups arranged in 'cis' configuration [Dasari and Tchounwou, 2014]. Following uptake, cisplatin undergoes intracellular biotransformation ahead of delivering cytotoxic effects within cancer cells. This process involves ***intracellular hydrolytic activation*** of cisplatin where water molecules gradually replace two of its displaceable chloride groups. This transforms the drug into a strong ***monoaqueous*** or ***diaqueous electrophilic species*** which subsequently attack cellular nucleophiles such as the DNA and the sulfhydryl groups (~SH) of thiol-containing proteins [Zia et al., 2018]. An outline of the structure of cisplatin is described in Figure 11.

Intracellular aquation of cisplatin is facilitated by lower intracellular chloride concentration of about ~4mM. Comparatively higher chloride concentration ($\sim 10^3$mM) in the blood plasma prevents its hydrolysis in the extracellular environment [Kokka et al., 2014;Maheshwari et al., 2016; Fares et al., 2020]. Cisplatin has a retention half-life of about 1.5-3.6 hours. It exhibits triphasic clearance after its administration where the distribution half-life is about 13min,

the elimination half-life is 43mins, and the terminal half-life is 5-4days. Within 24 hrs of the cisplatin administration, 90% of the drug dose gets flushed off from the body with renal clearances [Brouwers et al., 2008]. Hepatotoxicity, nephrotoxicity, cardiotoxicity, ototoxicity, gastrotoxicity, myelosuppression and anaphylaxis are some of the 'off-target' effects accompanying cisplatin treatment in patients [Ben Ayed et al., 2020]. Some of the well-known platinated chemotherapeutic drugs other than cisplatin include ***carboplatin***, ***oxaliplatin*** and ***nedaplatin***. The 'cis' configuration of cisplatin escalates its anti-tumor activity. Transplatin, a structural isomer of cisplatin, proved to be a feeble cytotoxic for it can form weaker repairable inter-strand drug-DNA crosslinks [Wang et al., 1996]. A clear depiction of intracellular activation of cisplatin is given in Figure 12.

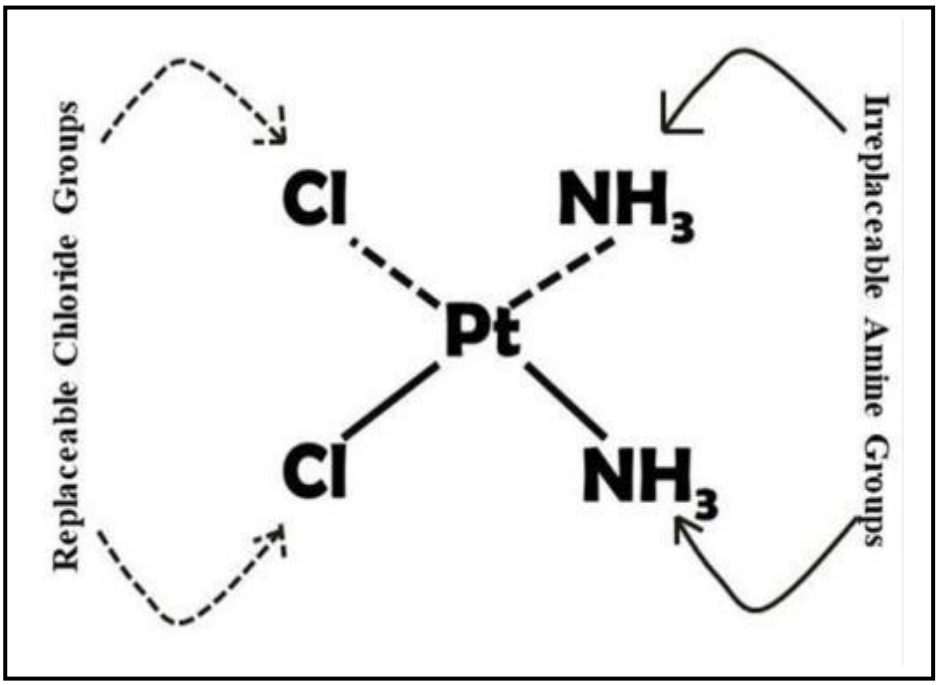

Figure 11: Structure of Cisplatin

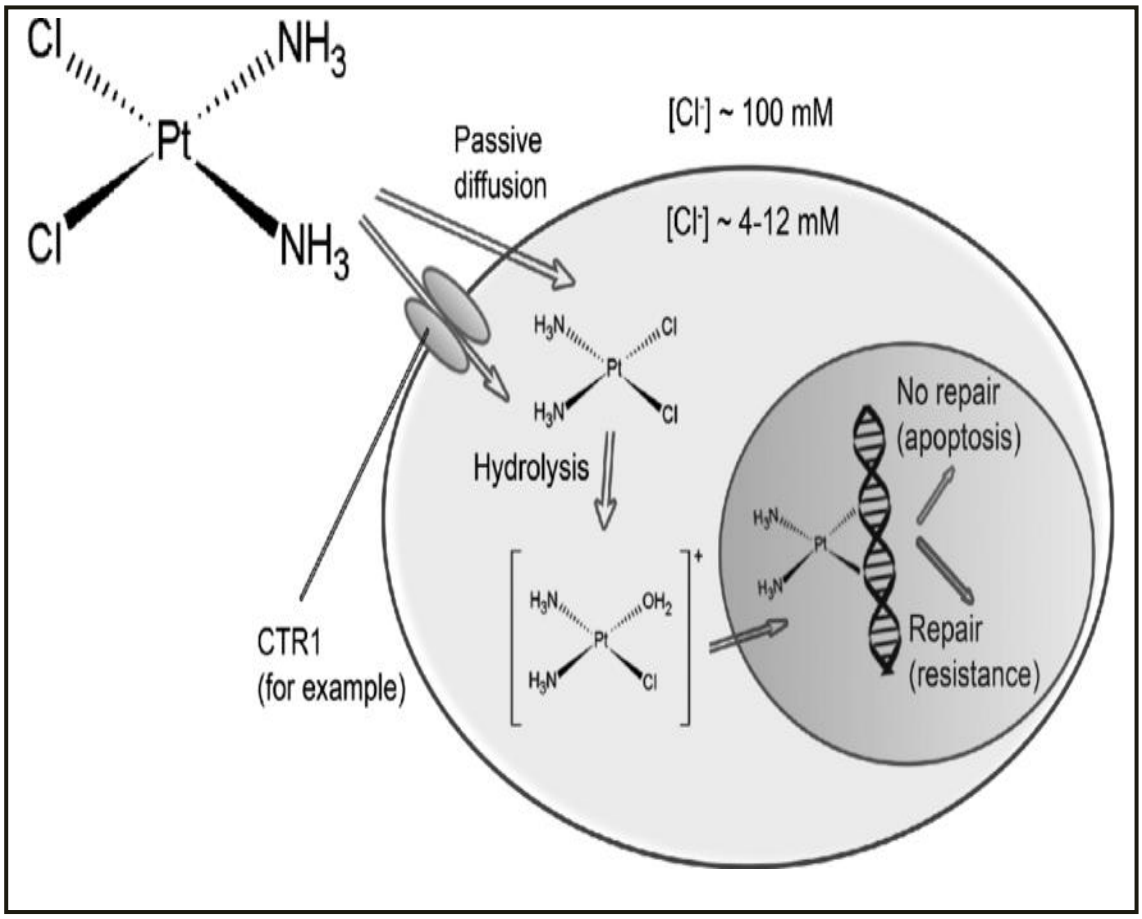

Figure 12: Intracellular Activation of Cisplatin

Following its aquation, cisplatin generates an electrophilic attack on the DNA at the *N-7 guanine* of the sugar-phosphate backbone to form complicated intra-strand crosslinks that cannot be repaired by the intracellular repair enzymes [da Silva et al., 2010]. Cancer cells with cisplatin-DNA adduct get arrested in the cell cycle phases of S, G1, or G2-M; eventually meeting up with an apoptotic fate [Lewis et al., 2009]. Thus, ***chromosomal*** or ***genomic DNA*** is obviously the **'*primary target*'** of cisplatin.

Cisplatin modulates several other ***DNA-damage independent pathways*** while rendering neoplastic cytotoxicity. Cisplatin pronouncedly executes cancer cells by

promoting *oxidative stress* and by altering ***calcium-mediated signaling modules*** alongside triggering vital ***cellular stress-associated signaling cascades*** [Podratz et al., 2011]. Cisplatin makes mitochondrial membrane leaky to incur mitochondrial DNA (mt-DNA) damage. It deregulates Electron Transport Chain (ETC) to enable respiratory burst thereby invoking the intrinsic and extrinsic apoptotic pathways [Wang et al., 1996]. In a study with ovarian cancer cell lines (OVCAR-3, OVCAR-4, and IGROV-1), sensitive to cisplatin, the drug promoted ROS overproduction through a hike in ***mitochondrial membrane potential (Ψm)***; finally mediating programmed cell death [Choi et al., 2015].

Cisplatin begets ER-stress to induce apoptosis by disrupting normal Ca2+ associated signaling cascades [Hodeify et al., 2021]. Cisplatin attacks the ***sulfhydryl group (~SH)*** of ***L-γ-glutamyl-l-cysteinyl-glycine (GSH)*** to destroy its capacities of scavenging free radicals and maintaining Ca^{2+} homeostasis [Aoki and Fujishita, 2017]. Disabling GSH activity can be a major inducer of cellular stress signaling pathways. In cisplatin-treated MCF-7, SH-SY5Y, and, HeLa-S3 cell lines, apoptotic death was induced by higher cytoplasmic Ca^{2+} levels catered by ionic-flux from the extracellular environment as well as from the intracellular calcium reservoirs like ER and mitochondria [Xia and Xu, 2015]. Conversely, excessive GSH entraps cisplatin, inactivates it, and nullifies its cytotoxic capacities [Karar and Maity, 2011]. Hydrolytically transformed cisplatin orchestrates the events of incurring cellular damage which finally ends up in activating caspases and promoting programmed cell death. An elaboration of the mechanism is provided in Figure 13.

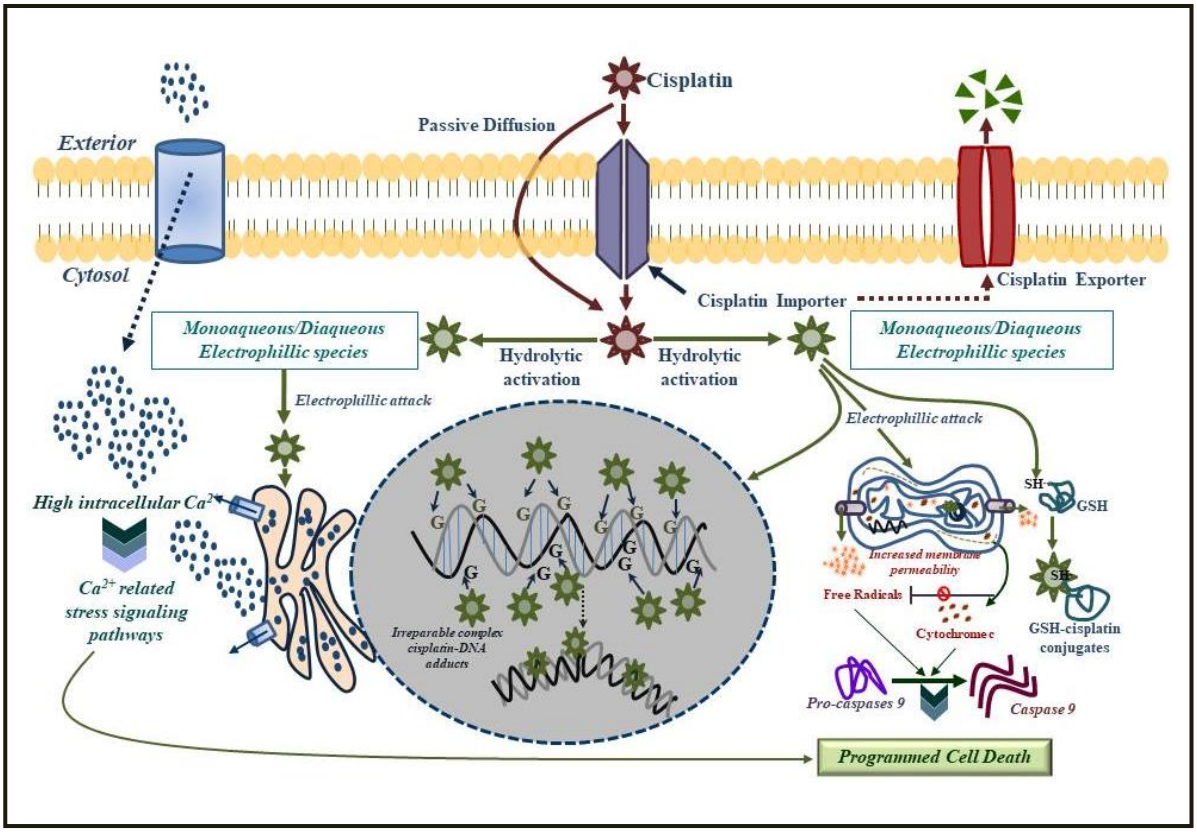

Figure 13: Mechanism of Cisplatin cytotoxicity

2.6. Cisplatin Resistance: An Adaptive Response of Tumor Microenvironment

Chemotherapy is one of the principal modes of treatment for cancer, but eventual acquirement of ***'chemoresistance'*** restrains its effectiveness. Chemoresistance can be divided into two broad categories: ***intrinsic*** or ***acquired***. Intrinsic resistance is an inherent feature of tumour rendered by its pre-existent ***resistance mediating factors*** which aid in aborting the chemotherapeutic immediately after its administration [Lippert et al., 2008;Emran et al., 2022]. On the other hand, acquired drug resistance develops during the treatment process due to induction of the similar resistance mediating factors which were initially absent in the sensitive tumors [Wiebe et al., 2012]. Such factors include ***deregulated prosurvival signalling pathways***, ***upregulated DNA damage repair pathways***, ***elevated drug efflux pumps***, ***altered drug targets***, ***reprogrammed metabolic processes*** and various microenvironmental

elements of the tumor which enables it to adapt with the incoming chemotherapeutic drug [Wang et al., 2019; Ramos et al., 2021; Mansoori et al., 2017]. Therefore, cisplatin resistance is complex and multifactorial which is identified as the 'root cause' of disease relapse and recurrence. Contribution of each of these factors in the scenario of cisplatin resistance is elaborated as follows:

i.Upregulation of PI3K/Akt Signalling- Being the primordial prosurvival signalling pathway, PI3K/Akt cascade helms the processes of cellular survival, growth and proliferation in response to extracellular cues including growth factors, hormones as well as chemotherapeutic drugs like cisplatin. Initial stimulation by these agents causes activation of membrane associated ***Receptor Tyrosine Kinases (RTKs)***; switching on a phosphorylation cascade made up of ***serine threonine kinase*** enzymes [Lemmon and Schlessinger, 2010]. Signalling onsets with activatory phosphorylation of PI3K and Akt at several Threonine (Thr308, Thr450) and Serine (Ser473) residues [Chen et al., 2001; Manning and Toker, 2017]. Multiple malignancies are linked to an unusual exacerbation of PI3K/Akt effectors [Zhang et al., 2015; Ghoneum and Said, 2019; Sanaei et al., 2022; Dong et al., 2021]. With HPV onslaughts in effect, cervical cancers often present a constitutive deregulation in their PI3K/Akt signalling [Zhang et al., 2015]. The oncogenic viral early gene products initiate cervical carcinogenesis by interacting with these prosurvival molecules of the host cell [Keysar et al., 2013]. Besides abrogating p53 and pRb functions, HPVs opportunistically modulate the Phosphatidylinositol 3-Kinase subunit C (PI3KCA) gene which is the second messenger activating Akt kinases [Lechner et al., 2013;Wu et al., 2014]. Binding of E6 oncoprotein to the RTKs such as epidermal growth factor receptor (EGFR), insulin receptor beta and insulin-like growth factor receptor beta (IGFRβ) evokes

PI3K to activate Akt; resulting in series of alterations and activation of a cascade of in the downstream targets [Lee et al., 2006;S. K. Choi et al., 2015]. In a positive feedback loop, Akt potentiates E6 interaction with 14–3-3σ, an important protein required for carcinogenic progression [Spangle and Munger, 2013; Mole et al., 2020]. In a clinical study, 39 out of 46 cervical cancer specimens evinced phosphorylation of Akt at serine 473 as a result 48% of stage Ib-IIb cervical cancers are accompanied by Akt activation [Menges et al., 2006;Veldman et al., 2003]. With such a signalling prelude, cisplatin fails to relay cytotoxic actions. Hence, cisplatin resistant cervical cancers mostly report PI3K/Akt signalling dysregulations [Mu et al., 2021;Bhattacharjee et al., 2022].

ii. Activation of NFκB- Nuclear Factor κB (NFκB) is the immediate downstream effector of PI3K/Akt pathway which is the ultimate determinant of cellular survival fates [Kuang et al., 2017]. It comprises of a family of transcription factors critically regulating expression of genes involved in immune and inflammatory responses, as well as cell growth, survival, metabolism, differentiation and death [Bai et al., 2009]. Therefore, NFκB aids in cellular adaptation to stressors such as chemotherapeutic exposure. In fact, cisplatin resistance among malignancies are positively related with NFκB upregulation [Zhang et al., 2015; Ghoneum and Said, 2019; Sanaei et al., 2022; Dong et al., 2021]. Cisplatin espouses ***Epithelial Growth Factor (EGF)*** like activity for which its cellular encounter leads to activation of EGFR; resulting in NFκB inductions through PI3K/Akt pathway [Crowley et al., 2005]. The regulatory subunits making up NFκB include- ***p50 (NFκB1)*** and ***p65 (RelA)*** which generally remains in inactive form upon binding to ***Inhibitor of κB (IκB)*** in the cytoplasm [Yu et al., 2009]. With extracellular

triggers like cisplatin, IκB dissociates away from p50 and p65 following inhibitory phosphorylation and proteasomal degradation. Thereafter, p50 and p65 translocates to the nucleus wherein it binds to the response elements of ***inflammatory mediators (IL6, IL8, GMCSF-1, COX2)***, ***prosurvival effectors (HIF-1α, Ki67, PCNA, TNFα, VEGF), nuclear orphan receptors (PXR)*** and ***xenobiotic detoxifiers*** like ***DNA-damage repair enzymes (Ku70), antioxidant enzymes (catalase, peroxidase, GSH)*** as well as ***drug exporters(MRP2, ATP7A, ATP7B)*** alongwith ***epigenetic regulators (HDACs)*** [Oeckinghaus and Ghosh, 2009]. However, this multivarious regulation of NFκB is highly dependent upon the cellular context. In the pretext of chemotherapy adaptation, NFκB sequesters factors related to drug detoxification and epigenetic regulation in succession with those involved in metabolism and cellular growth [Ponnusamy et al., 2019]. As a stress response, p65subunit of NFκB binds with ***Pregnane X Receptor (PXR)*** instead of p50 to form a heterodimer that get recruited in the nucleus for transcriptional activation of Ku70, MRP2, HDACs, GSH and etc [Okamura et al., 2020; Shizu et al., 2016]. Following drug detoxification, p50 partners with p65 after PXR removal and this heterodimer facilitates cancer cells to resume abnormal proliferation being supported by a reprogrammed metabolism[Chen et al., 2020]. In this regard, NFκB is very crucial regulator of cisplatin resistance.

iii. Induction of IAPs- The PI3K/Akt/NFκB axis induces the expression of ***Inhibitor of Apoptosis Proteins (IAPs)*** which provide a direct escape route to cisplatin by preventing apoptosis [Peng et al., 2022]. Two of the IAPs namely ***X linked Inhibitor of Apoptosis Protein (XIAP)*** and ***survivin*** are identified to be intricately associated with cisplatin resistance [Devi et al., 2021; Chaudhary et al., 2016]. With a molecular weight of 56.7 kDa, XIAP protein is 479 amino acid long

having 3 Baculoviral Repeat Domains (BIR1/ BIR2/ BIR3), 1 Ubiquitin Associated Domain (UAB) and 1 RING domain [Chaudhary et al., 2016]. In order to protect cancer cells from cisplatin encounter, XIAP binds to caspases with their BIR3 domain and degrades it by means of E3 Ubiquitin Ligase Activity. Despite apoptotic triggers after cisplatin chemotherapy, XIAP activation culls apoptosis by preventing apoptosome formation. Higher levels of XIAP inhibit both intrinsic and extrinsic apoptosis pathways. Apart from binding caspases, it also promotes tumor metastasis by enhancing the expression of NFκB by binding to ***TAK1 binding protein (TAB1)*** and ***TFGβ Activated protein (TAK1)*** [Obexer and Ausserlechner, 2014]. Conversely, survivin which is the smallest IAP with a single BIR domain is also implicated in the scenario of cisplatin resistance [Albadari and Li, 2023]. In addition to inhibiting apoptosis, the central role of survivin is to control cell cycle especially at G1 and G2-M transits. Survivin works synergistically with XIAP for degrading caspases. Upregulation of both these proteins underlies cisplatin resistance in multiple malignancies. Hence, XIAP and survivin are potential targets considerable for treating cisplatin resistant cancers.

iv. Accelerated DNA Repair Machinery- To overcome cisplatin efficacy, modification of drug targets is essential. In this case, cisplatin cytotoxicity results from formation of bulky irreparable intrastrand drug-DNA adduct [Rocha et al., 2018]. For HPV infected cervical cancers, repair machinery is highly proficient in the tumors owing to the transformative actions of E1 and E2. HPVs, while attempting to integrate its genome into the host cell's DNA, incurs DNA damage that eventually evokes ***DNA Damage Response (DDR)*** [Machida et al., 2010]. Such a constitutively upregulated activity of DNA damage repair enzymes

empower cervical cancer cells to quickly repair the cisplatin-DNA adducts. Primarily, ***Non Homologous End Joining (NHEJ)*** and ***Nucleotide Excision Repair (NER)*** pathways are implicated in cisplatin resistance [Reinson et al., 2013]. Over 20 proteins hailing from the excision repair cross-complementation group 1 (ERCC1) partake in the process of clearing away the cisplatin-DNA conjugates [Reinson et al., 2013]. Enzymes like Ku70 are overtly expressed among locally advanced cervical cancers espousing poor cisplatin response [Kiss et al., 2021]. Therefore, an escalation of repair machineries in the cell is the hallmark of cisplatin resistance in neoplasia.

v. Expression of Cisplatin Exporters- Several members of the ***ATP-binding cassette (ABC)*** transporter superfamily play a significant role in conferring drug resistance in both clinical and tumor cell models. PI3K/Akt/NFκB axis in the upstream eventuates in gradual expression of such multidrug resistance proteins in the membrane for expunging the incumbent chemotherapeutic drug. For cisplatin, ***MRP2*** in addition with ***copper transporter pumps*** like ***ATP7A, ATP7B*** and ***S1A009*** are specifically responsible for quick drug efflux [Oeckinghaus and Ghosh, 2009]. As mentioned already, NFκB in conjugation with PXR leads to transcriptional activation of these drug exporters [Okamura et al., 2020; Shizu et al., 2016]. Translated MRP proteins primarily reside in the trans-Golgi network which translocates to the membrane vide vesicular transport wherein they perform drug export. In various instances, antiport pumps namely ATP7A, ATP7B and S1A009 uptake copper ions within the cell in bargain of effluxing cisplatin. To meet up the rising metabolic demands of cancer cells, often multiple membrane associated amino acid transporters get expressed which aid in rerouting metabolites in lieu of denouncing cisplatin [Shi et al., 2022; Wu et al., 2021; Liu

et al., 2015]. As a result, upregulation of such solute carrier proteins alters/affects cisplatin pharmacodynamicity by reducing intracellular drug accumulation critically. All these pumps are highly drug specific in action and therefore can be regarded as predictive markers of resistance for malignancies. Entire molecular crosstalk contributing to the scenario of cisplatin resistance is explained in Figure 14.

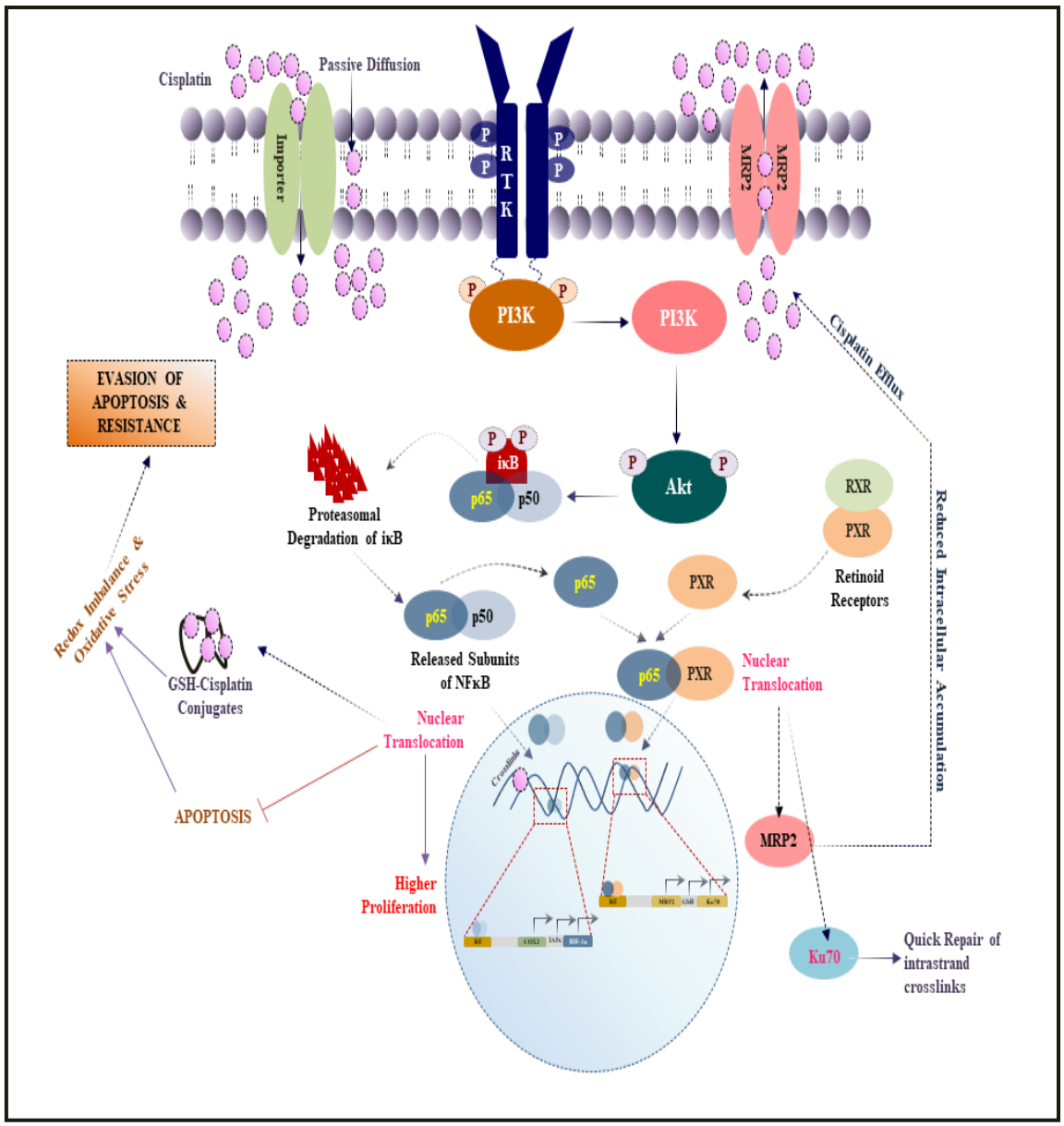

Figure 14: Molecular Basis of Cisplatin Resistance

2.7. Heterogeneous Tumor Microenvironment: An Escape Route to Cisplatin Cytotoxicity

Interplay of PI3K/Akt effectors in a heterogeneous tumor microenvironment is an important mechanism contributing to drug resistance and has been observed in many types of cancer. Prosurvival molecules such as Akt /p-Akt^{Thr308}, COX2, HIF-1α, VEGF in addition with NFκB orchestrate oncogenic PI3K/Akt signaling cascade which significantly drives carcinogenesis [Wu et al., 2021]. The PI3K/Akt pathway operates in a positive feedback loop involving COX2 and NFκB which ultimately activates genes contributing in cell proliferation and angiogenesis [Jiang and Liu, 2009]. Understanding the intricate network associating these prosurvival molecules might provide valuable insight for the identification of novel therapeutic targets for drug resistance.

For neoplasms, which are dynamically evolving, such kind of dysregulated signalling gives rise to heterogeneous cellular clones that espouse pleomorphic phenotypes [McGranahan and Swanton, 2017]. These clones are akin to individual entities that are behaviourally, genetically, epigenetically and phenotypically isolated from each other. Hence, they tend to behave differentially to chemotherapeutics like cisplatin. As a result, with chemotherapy these clones are subjected to a 'selection pressure' owing to which some survive while the rest get eliminated [Ibragimova et al., 2017]. Cells undergoing swift chemotherapeutic execution are termed as 'chemosensitive' clones while the survivors are identified as either 'intrinsically resistant' or 'acquired resistant' clones [Fittall and Van Loo, 2019]. Intrinsically resistant clones follow a Darwinian process of somatic selection where they compete for space and resources within their microenvironments. They acquire mutations over time that improves their fitness to withstand successive chemo encounters thereby

accounting them for possible disease relapse and recurrence. Conversely, the ‘acquired resistant’ clones participate in 'evolutionary arms race' upon drug treatment wherein they eventually accumulate mutations to diversify genetically for developing therapy resistance [Venkatesan and Swanton, 2016]. Unlike intrinsic clones, acquired resistant cells initially develop a transient ‘chemotolerant phenotype’ which transforms into a permanent ‘chemoresistant phenotype’. Tolerance is always transcriptionally induced which paves a way for ‘clonal evolution’; contributing in therapy failure. In this context, comprehending the evolutionary principles of dynamic neoplasms can definitely aid in strategizing treatment rationales with ‘chemosensitisers’ or ‘chemoenhancers’. Considering the role of PI3K/Akt pathway, therapeutic regimes with resistant modifying agents could be planned by identifying some of its effectors as ‘targets’ in days to come. A pictorial description of clonal evolution of tumors is displayed in Figure 15.

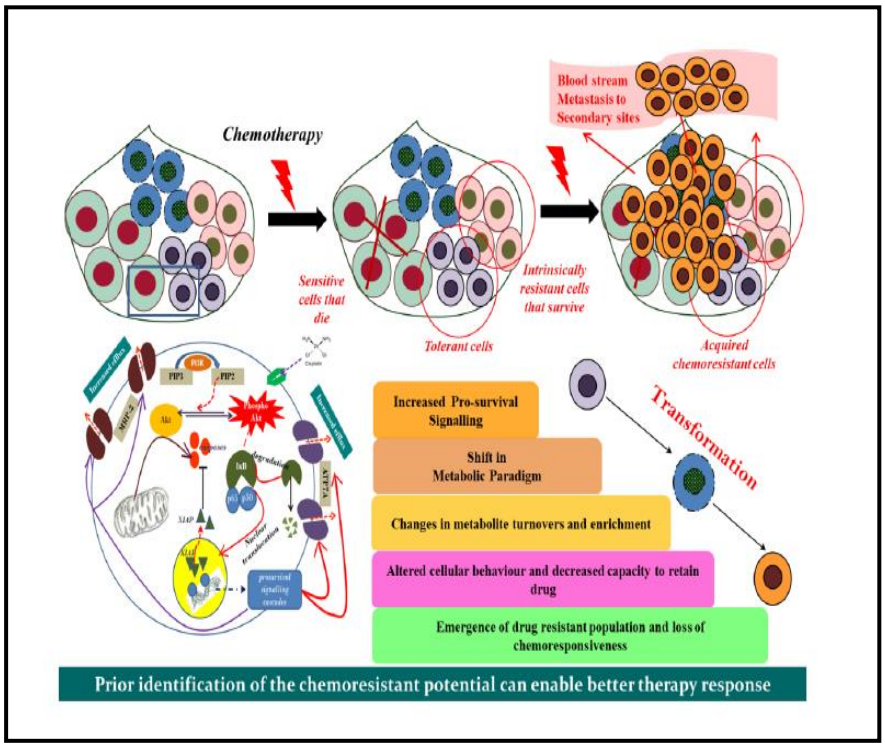

Figure 15: Clonal Evolution of Tumors

2.8. Resistance Modifying Agents: A Solution to Cisplatin Resistance

Compounds or substances that increase the sensitivity of cancer cells to conventional therapeutic agents are referred to as ***Resistance Modifying Agents (RMAs)***. These compounds are resistance reversal agents which act either as ***chemosensitizers*** or as ***chemoenhancers.*** In this regard, several synthetic chemical agents alongwith natural phytochemicals have been widely employed [Pisa and Kapoor, 2020;Housman et al., 2014]. As already described, resistance to chemotherapy emerges as a cellular adaptive response [Lei et al., 2023; Mansoori et al., 2017], RMAs may help in this context by concocting the mechanisms of resistance. Some of them are-

- ***Blocking Efflux Pumps:*** RMAs can directly inhibit or block these efflux pumps thereby preventing the removal of drugs from the cells. This allows the therapeutic agents to accumulate at effective levels within the cells for relaying cytotoxicity.

- ***Interfering with Cellular Defense Mechanisms:*** Some resistance mechanisms involve the activation of cellular defense mechanisms such as secretion of cytokines which enable cellular detoxification of chemotherapeutics. RMAs interfere with these defenses; making the cells vulnerable to treatment.

- ***Enhancing Drug Uptake:*** RMAs also facilitate cellular uptake of drugs by increasing its penetration so as to improve its retention.

- ***Overcoming DNA Repair Mechanisms:*** RMAs also interfere with DNA repair mechanisms, making it more difficult for cancer cells to repair the damage caused by DNA intercalating agents like cisplatin.

Use of natural phytochemicals as RMAs has already been proved to be a non-toxic way out to overcome the problem of cisplatin resistance. Figure 16 enlists some natural phytochemicals with proven properties of being a RMA in different cancer scenarios.

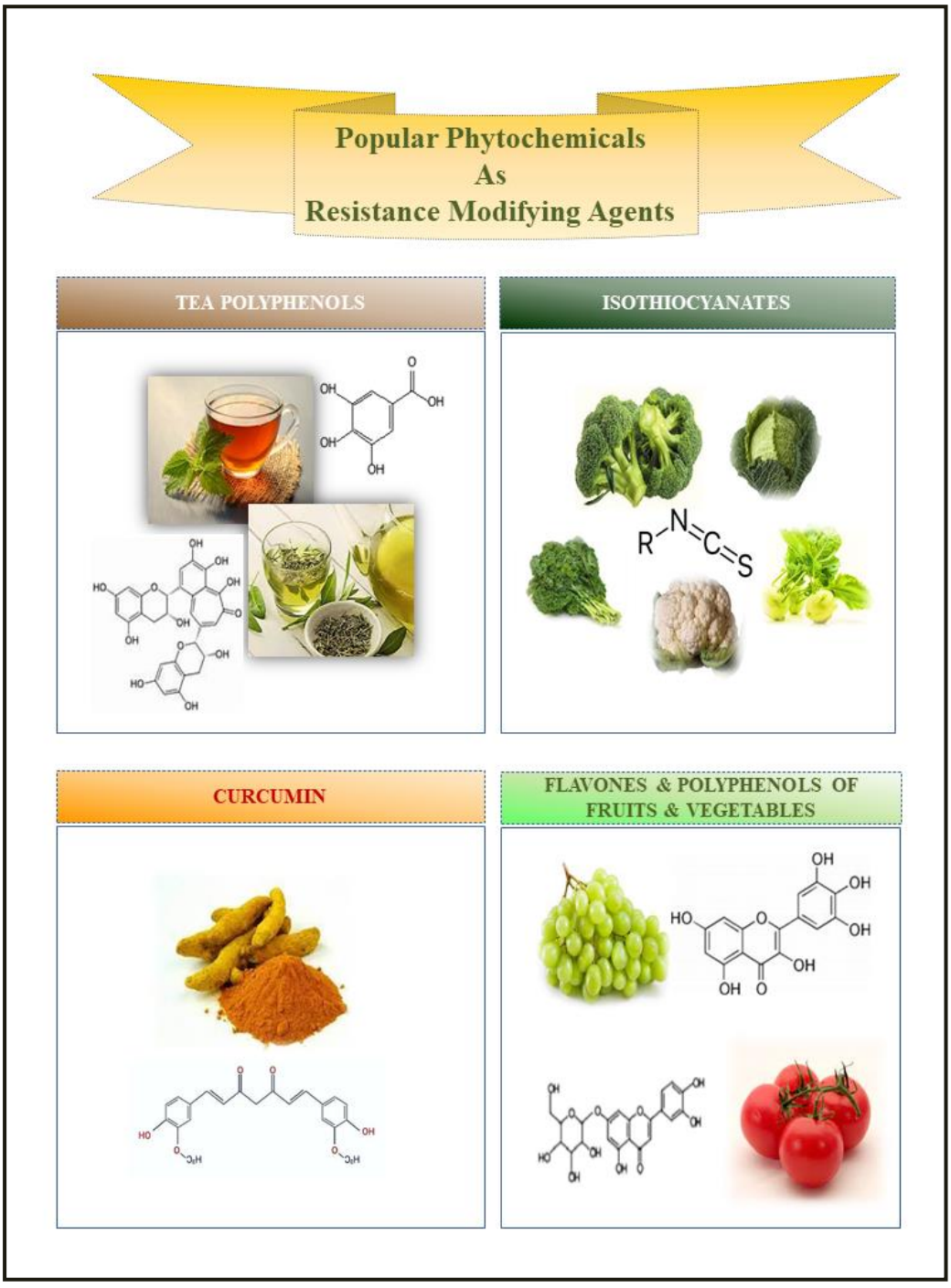

Figure 16: Natural Phytochemicals as Resistance Modifying Agents

2.9. Phenethylisothicyanate: A Potential Cisplatin Resistance Modifying Agents

Among plant derived phytochemicals, ***Isothiocyanates (ITCs)*** derived from ***Brassicaceae*** family plants bearing ***cruciferous vegetables*** like ***Brassica vegetables*** are ***broccoli, cauliflower, Brussel sprouts, cabbage, mustard, kale, watercress, turnip*** and ***radish showed promising effects in reversing resistance*** [Dayalan Naidu et al., 2018]. All these vegetables are enriched in ***Glucosinolates (GL)*** which is the precursor of all the biologically active ITCs namely ***Sulforaphane (SFN), Phenethyl-Isothiocyanates (PEITC), Benzyl-Isothiocyanates (BITC),*** and ***Allyl-Isothiocyanates(AITC)*** [Shakour et al., 2022]. Plenty of experimental excerpts are indicative of the chemosensitizing potentials of these ITCs [Wang et al., 2011;Dai et al., 2016; Gupta et al., 2014; Biswas et al., 2021;Sarkar et al., 2012]. PEITC, being one such isothiocyanate is one of the most encouraging ITCs because of its easy availability and affordability [Biswas et al., 2021;Sarkar et al., 2012]. Its efficacy as chemopreventive agents is well known from epidemiological studies which showed that dietary intake of PEITCs is associated with reduced risk of certain human cancers [Gupta et al., 2014; Wang et al., 2011]. In fact, the efficacy of PEITC has been observed to vary among different malignancies with genetic polymorphisms in their Glutathione Transferase (GST) enzymes [Wang et al., 2011]. Mostly natural phytochemicals are preferably repurposed in the treatment of malignancies for their properties as anti-oxidants. PEITC, owing to the presence of a ***sulfhydryl (-SH)*** group tends to conjugate with GSH thereby making it unavailable for scavenging free radicals [Biswas et al., 2021;Sarkar et al., 2012]. Multiple reports suggested that PEITC is proficient in bonding covalently with cysteine which is a key component of the ***catalytic centres*** or ***metal-binding domains*** of several cellular enzymes. Modifications of cysteine

residues are directly linked with ***oxidation***, ***glutathiolation***, ***nitrosylation*** and ***disulfide formation*** of proteins which affects signaling transduction [Wu et al., 2023; Esteve, 2020]. Therefore, PEITC definitely has a potential to support the actions of a chemotherapeutic drug as a 'pro-oxidant' in an unresponsive cellular backdrop. Chemopreventive studies with PEITCs have been rampant in the treatment of various types of carcinomas. Mukherjee et al, in their laboratory, have identified PEITC as a chemosensitizer of cervical cancer cells [Mukherjee et al., 2015]. Herein, PEITC modulated Protein Kinase C (PKCs) and telomerase activities for chemosensitizing cervical cancer cells. It was examined that HeLa cells pre-treated with PEITC and SFN, underwent apoptosis in higher frequency after treatment with adriamycin or etoposide. PEITCs also regulated Heat Shock Proteins (HSPs) for guiding breast cancer cells and leukemia cells into cell cycle arrest and apoptosis [Sarkar et al., 2012]. Of late, PEITC was studied to reverse paclitaxel resistance in MCF-7 breast cancer cells by regulating Aurora Kinases [Biswas et al., 2022]. Implications of SFN and PEITC in modulating Akt are also well examined by several other researchers as well [Biswas et al., 2021;Sarkar et al., 2012]. A summary of PEITC's effectiveness as a chemosensitizer is elucidated in Figure 17. Based on all these evidences, investigation of the potential of PEITC as RMAs is of utmost importance for amelioration of chemoresistant cervical cancers.

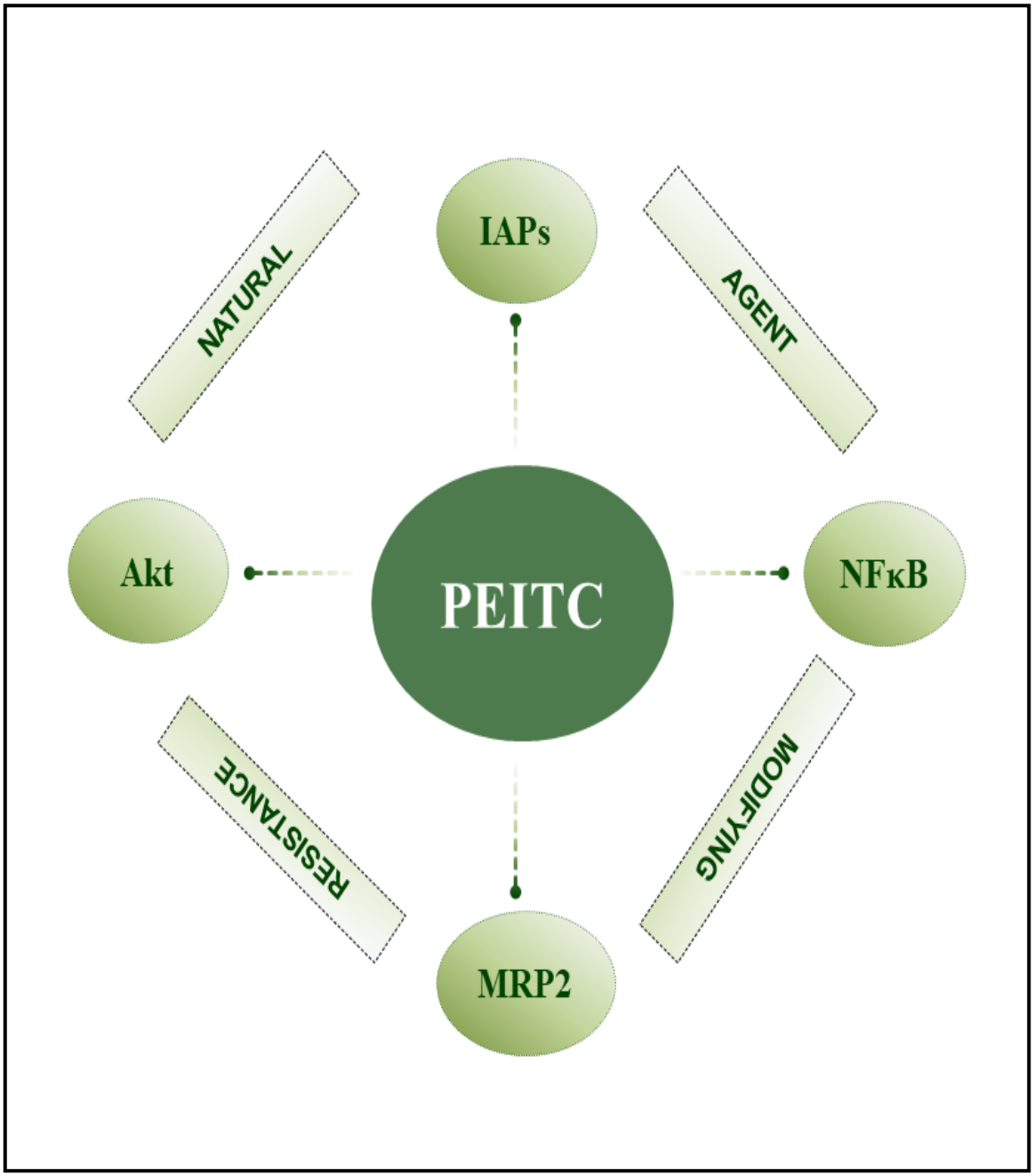

Figure 17: Phenethylisothicyanate as a Resistance Modifying Agent

Aim & Objectives

3. AIM OF WORK

The present work aims to unravel the probable mechanism in which a ***deregulated PI3K/AKT signalling cascade*** imparts ***cisplatin resistance*** among ***cervical cancer cells***. This study attempts to establish few noteworthy PI3K/AKT pathway effectors namely ***Akt, MRP2, NFκB, XIAP*** and ***survivin*** as ***'prime targets'*** of ***Phenethylisothiocyanate (PEITC)***, a natural isothiocyanate for reversal of cisplatin resistance.

Overall, the present study highlights the reversal effect of PEITC on PI3K/Akt signalling mediated cisplatin resistance in cervical cancer by improvement of cellular drug retention capacities.

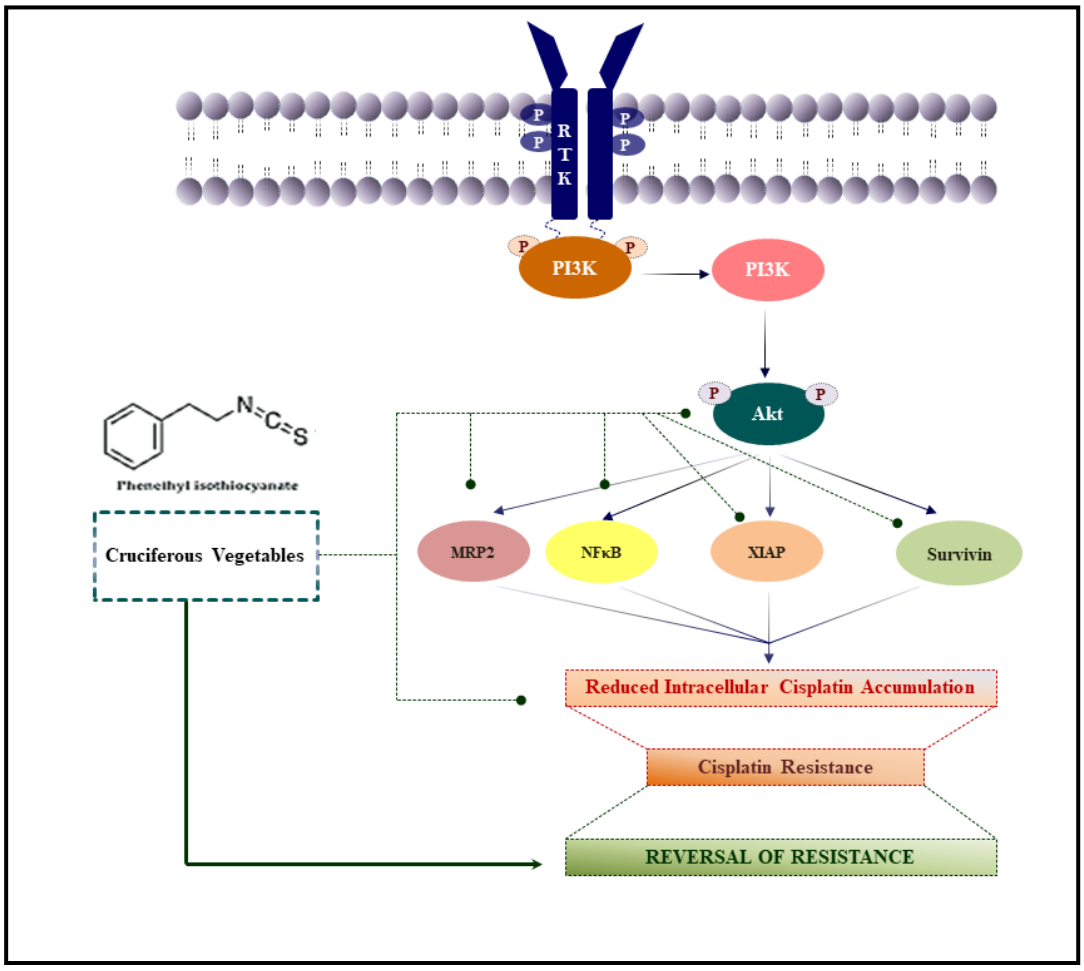

Figure 18: Schematically Represented Aim of Work Highlighting Study Focuses

4. OBJECTIVES OF WORK

The aim of work had been achieved through the following objectives:

i. **Objective 1:** Development of a cisplatin resistant subline ($SiHa^R$) as an *in vitro model*, from parental SiHa (HPV16 positive human cervical squamous cell carcinoma cell line) and a 3methylcholanthrene (3MC, a chemical carcinogen) induced *in vivo* cervical cancer model in Swiss Albino Mice (*Mus musculus*).

ii. **Objective 2:** Identification of the invasive carcinoma stages while monitoring cervical carcinogenesis in the *in vivo* cervical cancer model for periodic cisplatin intervention study.

iii. **Objective 3:** Characterization of the *in vivo* (Swiss Albino Mice) and *in vitro* ($SiHa/SiHa^R$) models for their presumptive cisplatin-resistant phenotype based upon the expression profiles of PI3K/Akt pathway effectors(Akt, XIAP, Survivin, NFκB).

iv. **Objective 4:** Assessment of the impact of a deregulated PI3K/Akt pathway on the status of cisplatin exporters (MRP2, ATP7A/7B) and intracellular cisplatin accumulation capacities in *in vitro* and *in vivo* models.

v. **Objective 5:** Investigation of the combinatorial efficacy of Phenethylisothiocyanate (PEITC) and cisplatin in regulating the PI3K/Akt pathway effectors for reversal of acquired cisplatin resistance in *in vitro* and *in vivo* models.

vi. **Objective 6:** Estimation of chemosensitizing potential of PEITC in relation to enhancing intracellular cisplatin accumulation, GSH depletion and ROS generation.

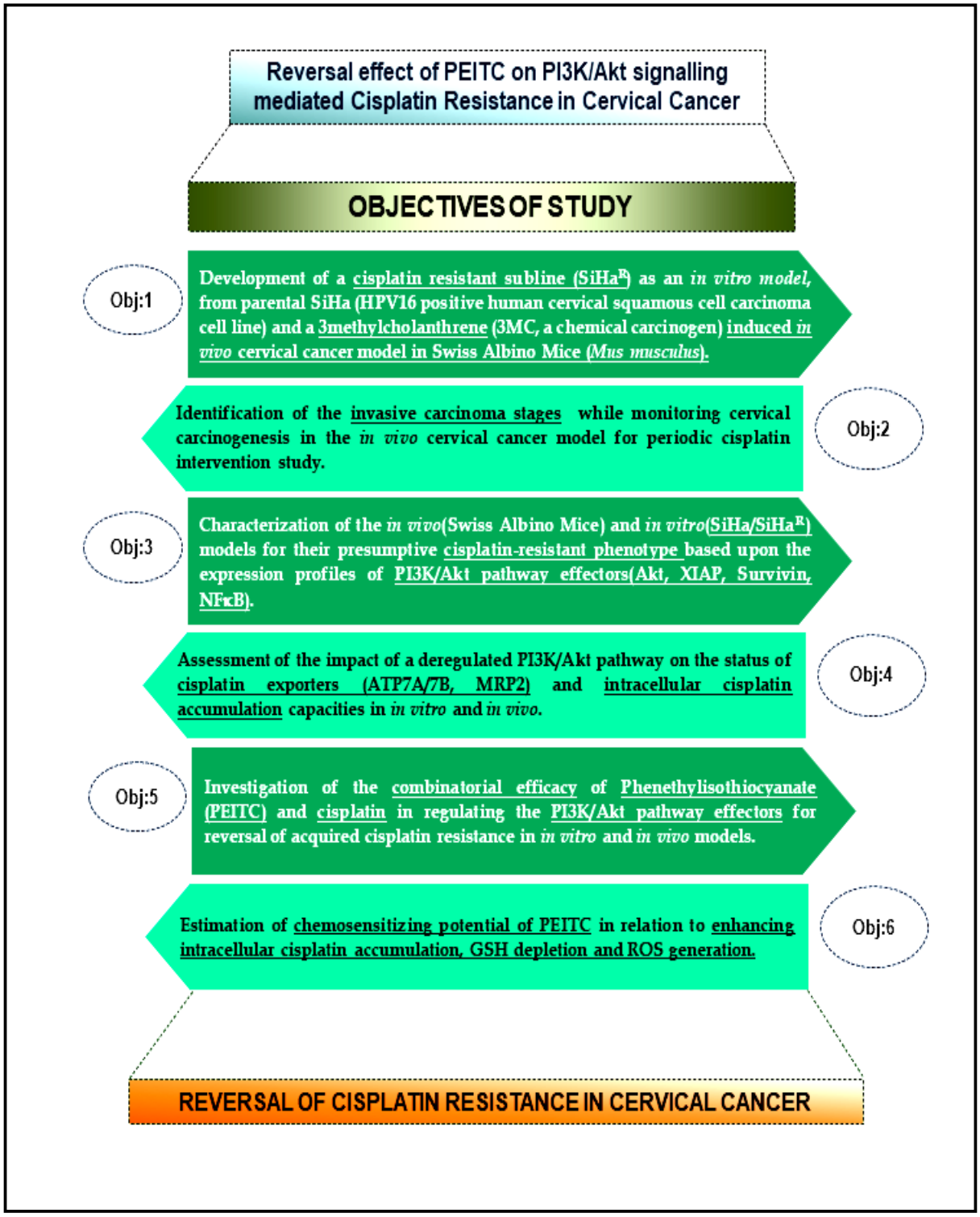

Figure 19: Pictorially Described Objectives of Work

Chapter 4

Materials & Methodologies

5. MODEL SYSTEMS

This study was conducted using *in vitro* and *in vivo* models.

5.1 *In vitro* models

SiHa, a HPV-16 positive cervical squamous carcinoma cell line was used in this study. A cisplatin (CDDP) resistant subline ***SiHa^R*** was developed by the process of "pulse treatment". SiHa and SiHa^R were comparatively studied for the regulation of PI3K/Akt pathway in conferring cisplatin resistance.

C33A, a HPV negative cell line was further used for validating the findings of *in vivo* model.

HaCaT, a normal squamous keratinocyte cell line was additionally used for confirmation of the experimental findings obtained in both *in vitro* and *in vivo* set ups.

5.2 *In vivo* model

5-6 weeks old virgin female Swiss Albino mice (*Mus musculus*) was used for development of an *in vivo* cervical cancer model. ***3methylcholanthrene (3MC),*** a ***Polycyclic Aromatic Hydrocarbon (PAHs)*** which is also a well known ***carcinogen*** was used for this purpose.

A solution of 3MC prepared in ***Petroleum Ether (PET)*** was used for ***'cervical painting'*** to induce carcinogenesis. Herein, 3MC solution of concentration (0.6mg/ml) was pipette-flushed over the murine cervix for 30 weeks in a chronic fashion. The administration dose of carcinogen was selected following proper dosimetry.

A vivid representation of the model systems is displayed in Figure 20.

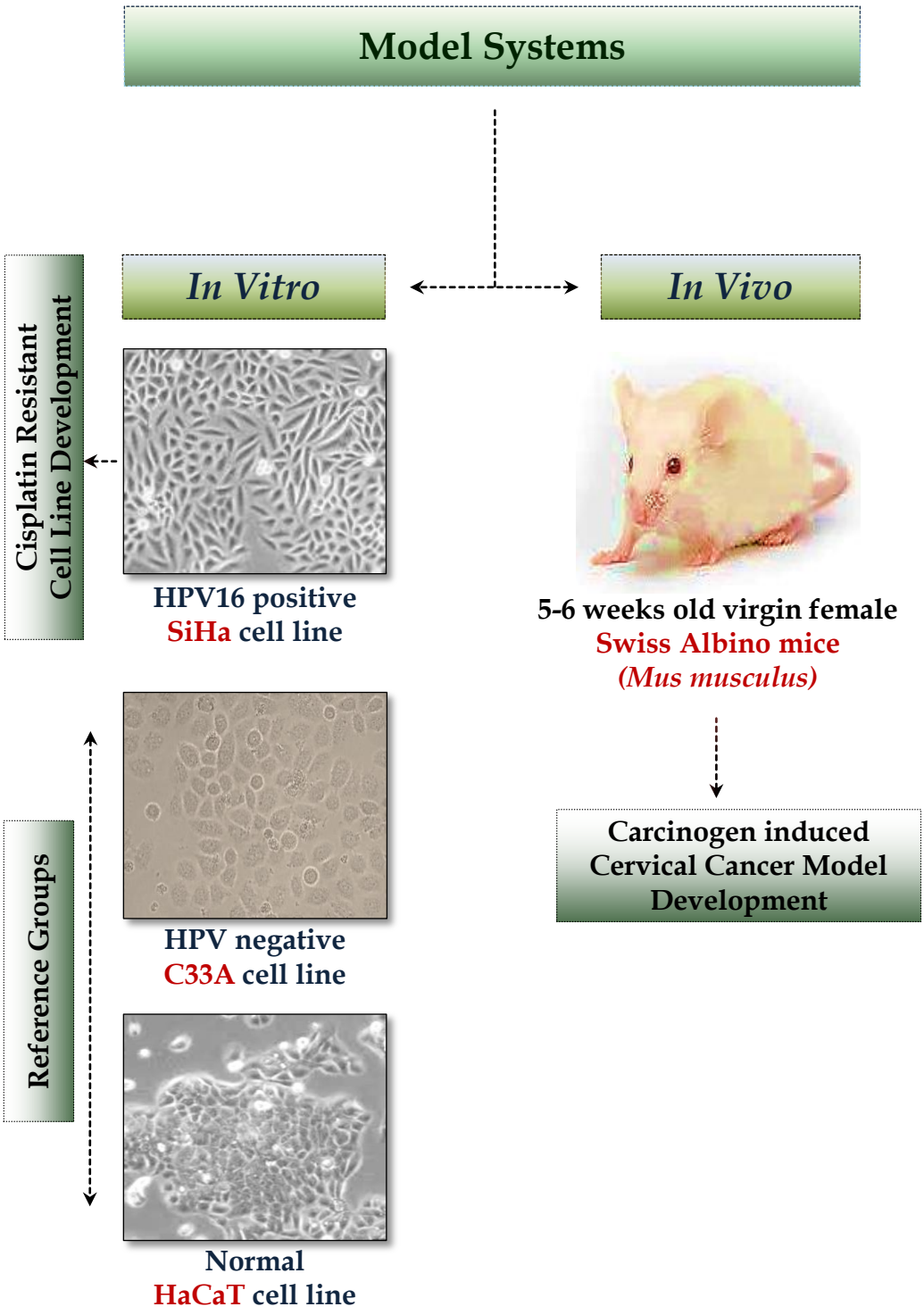

Figure 20. Model Systems Used in the study: Schematic Representations of the *in vitro* and *in vivo* models used in the study. SiHa, an HPV16 positive cervical cancer cell line was used for developing a cisplatin resistant subline. A HPV negative cell line C33A was used as an *in vitro* reference against carcinogen induced *in vivo* cervical cancer model developed in Swiss Albino mice *(Mus musculus)*. A normal squamous epithelial cell line HaCaT was used for overall validation of experimental observations.

6. MATERIALS AND METHODS

6.1. MATERIALS

❖ ***Chemicals and Reagents***

Cell lines (NCCS, Pune), MEM (Himedia), DMEM (Himedia), Foetal Bovine Serum (FBS; Gibco), gentamycin (SIGMA), penicillin (SRL), streptomycin (SIGMA), 3MC (MP Biomedicals), PET (Petroleum Ether), CDDP (Cipla), PEITC (SIGMA), MTT (SRL), DMSO (SRL), Harris Haematoxylin (Merck Millipore), Orange G6 (Merck Millipore), Eosin Azure (Merck Millipore), Molecular Grade Alcohol (Merck Millipore), Delafield's Hematoxylin (SRL), 2% Eosin (Himedia), Paraffin Wax (Merck), Poly L-lysine (SIGMA), DPX (SIGMA), Acetone (SRL), Primary Antibodies (GenTex, abcam), Secondary Antibodies(GenTex), Sheath Fluid (BD Biosciences), Bradford's Reagent (Himedia), SDS (SRL), Glycine (SRL), Methanol (SRL), PVDF membranes (Invitrogen), BSA (SIGMA), BCIP/NBT (SIGMA), AP-tagged secondary antibodies (GeneTex), anti β-actin antibody (Santa Cruz), Platinum Standard Solutions (SIGMA), RNase-A (SIGMA), Propidium Iodide (SRL), anti cisplatin modified DNA antibody (abcam), RetroScript Kit (Ambion/Applied Biosystem), Primers (IDT), Agarose (Lonza), EtBr (SRL), TRIzol Reagent (Invitrogen), Rhodamine (Rh-123) (SIGMA), JC-1 Mitochondrial Membrane Potential Assay Kit (Cayman), DCFHDA (SIGMA), Glutathione Assay Kit (Cayman), Opti-MEM (Gibco), Lipofectamine (Thermo Fischer Scientific), IL6 Activity Assay Kit (Invitrogen), IL8 Activity Assay Kit (Invitrogen), Aspartate Transaminase Assay Kit (AUTOSPAN), Alanine Transaminase Assay Kit (AUTOSPAN), Alkaline Phosphatase Enzyme Activity Kit (AUTOSPAN), Creatinine Estimation Assay Kit (AUTOSPAN), Antioxidant Assay Kit (Cayman),

NOS activity Assay Kit (Cayman), Low Melting Agarose (SIGMA), DAB (Santa Cruz), bFGF (Invitrogen), hEGF (Invitrogen), B-27 (Invitrogen), Collagenase IA (Himedia).

❖ ***Equipments***

CO_2 Incubator (Thermo), Inverted Light Microscope (Olympus), Cold Centrifuge (SIGMA 3K10), ELISA Plate Reader (TECAN), Bright Field Microscope (Zeiss), Flow Cytometer (LSR Fortesa), Sonicator (REMI), Western Blot Apparatus (BioRad), Semi-dry Transfer Apparatus (BioRad), fluorescent microscope (OLYMPUS), Atomic Absorption Spectrometer (VARIAN), Haemocytometer, Thermal Cycler (BioRad), Gel Documentation System (BioRad), Spectrofluorometer (VARIAN), Nanodrop Spectrophotometer (GENE), Liquid Chromatography with Tandem Mass Spectrometry (LC-MS-MS; WATERS), Rocker, pH meter, Tube Rotator.

6.1. Methodologies

❖ ***Cell Culture***

SiHa, C33A and HaCaT cells were respectively maintained in MEM and DMEM supplemented with 10% FBS and antibiotics (gentamycin 40 μg, penicillin 100 units, and streptomycin 10 μg/ml) at 37^0C in a humidified CO_2(~ 5%) incubator. Cells were observed for visible morphological changes under an inverted light microscope.

❖ ***Animal Maintenance***

As per the approval of Institutional Animal Ethical Committee, virgin female Swiss Albino mice (n=140) were randomized into seven broad groups on basis of their body weight after estrous synchrony [Mcclintock, 1971]. Each group was further classified into subgroups separated in two batches of 10 animals [No of mice (n) = 5 /cage. (x2)

for each subgroup]. ***Group I*** was kept as an ***'untreated'*** control group where mice did not receive any treatment. ***Group III*** (subgroups 6–10) comprised of mice which had their cervix chronically painted with 3MC solution prepared in PET for respective intervals of 6, 12, 16, 24 and 30 weeks. It was specifically designated as ***'3MC treatment'*** group for studying cervical carcinogenesis along these time spans. To rule out any carcinogenic effect of the solvent (if any), ***Group II*** (subgroups 1–5) was assigned as a ***'vehicle control'*** batch with mice being solely treated with PET. A snippet of cervical painting is given in Figure 21

From Group III animals, those bearing ***Invasive cancer*** mice (IC) were further randomized into ***'no intervention' (Group IV)***, ***'cisplatin treatment' (Group V), 'PEITC treatment' (Group VI)*** and ***'combination treatment' (Group VII)*** groups for studying the effect of CDDP as well as PEITC either singly or in combination. Herein, Group IV mice did not receive any intervention. Group V (subgroups 11&12), Group VI (subgroups 13&14) and Group VII (subgroups 15&16) mice received intraperitoneal injection of CDDP **(3 mg/kg body weight)** and PEITC **(2.5 mg/kg body weight)** for two consecutive weeks. Admissible doses of 3MC, CDDP and PEITC were selected only after proper dosimetry. An overview of animal batch separation is given in Table 3. All throughout experimental period, mice were maintained in clean cages under standard laboratory conditions (room temperature: 25 ± 2^0C; 12-h light/dark cycles) and periodically monitored for any visible health abnormalities and deaths. Food and water was provided *ad libitum*.

❖ ***Pulse Treatment for development of CDDP resistant subline***

SiHa cells were subjected to treatment with logarithmic range of CDDP doses varying between 0.1µM-200µM. MTT assay was performed to identify the IC_{20}, IC_{30}, IC_{50}

and IC_{70} doses of the drug for this cell line. Parental chemosensitive SiHa cells transformed gradually through a transient ***'chemotolerant'*** phenotype to a permanent ***'chemoresistant'*** phenotype following exposure to three consecutive pulses of specific CDDP concentration in ***'pulse treatment'***. Thereafter, these cells were maintained in drug free conditions for a 14 days ***'drug holiday'*** period. Once again, the surviving cells were challenged for verification of its chemoresistant phenotype. Pulse treatment was initiated by treatment of SiHa with 0.5µM CDDP followed by escalated concentrations (1µM, 1.5µM, 2µM, 2.5µM and 3µM) of the same. One shot of CDDP was administered once every week. Finally, a CDDP resistant subline of SiHa named ***SiHa^R*** was developed over a period of 18months. $SiHa^R$ was calculated to be 2.75 fold CDDP resistant and was therefore a clinically relevant *in vitro* model for studying chemoresistance. Detailed description of the protocol is given in Figure21.

❖ ***MTT Assay***

MTT assay was performed to identify the growth inhibitory concentrations (ICs) of CDDP and PEITC separately for SiHa and $SiHa^R$ cells. In order to identify CDDP doses prior to initiating 'pulse treatment', SiHa cells were seeded within 96-well plates in a density of 10,000cells/well for each points in triplicate followed by maintenance at 37^0C for 24h, 48h and 72h respectively. Excepting untreated control set, others were treated with CDDP doses ranging between 0.1µM to 200µM for the mentioned time points and eventually incubated with MTT (6mg/5 ml) reagent for 4h. In due course, 170µl of MTT containing supernatant was discarded after centrifugation at 1000rpm for 10 min at 4^0C followed by DMSO addition and mild shaking for another 10min. The blue coloured formazan product formed was detected at 570 nm in an ELISA plate reader. Thereafter, cell viability of $SiHa^R$ in the parental

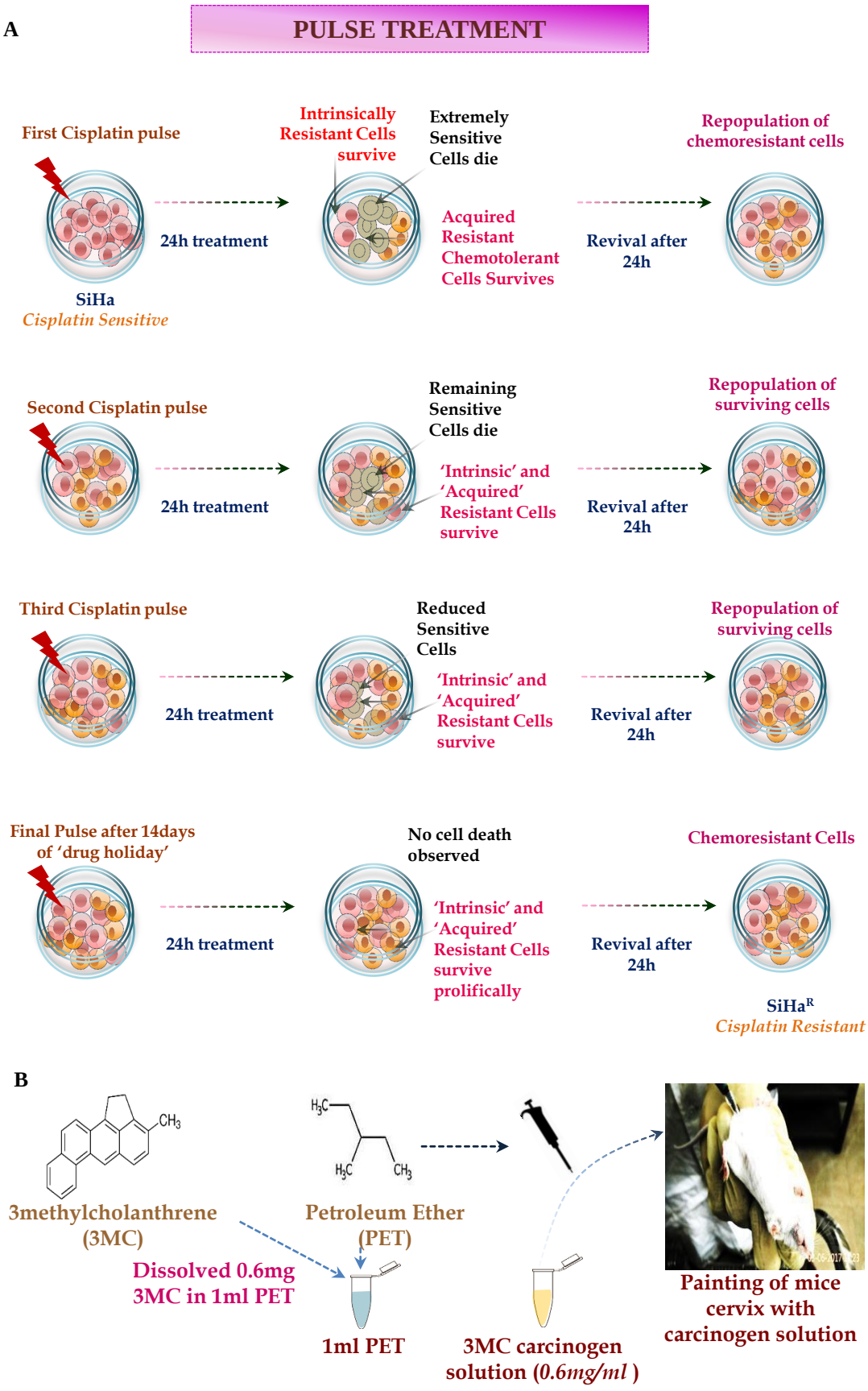

Figure 21: Model Development Protocol- (A) Pulse treatment protocol for developing SiHa^{R}, a CDDP resistant subline of SiHa. (B) Cervical Painting for developing a 3MC induced cervical cancer *in vivo* model in Swiss Albino mice.

TABLE3: ANIMAL BATCH SEPARATION

Animal Batches	Group Name	Treatment Type				
		PET	3MC	CDDP	PEITC	PEITC +CDDP
UNTREATED CONTROL	GROUP I					
VEHICLE CONTROL	GROUP II					
	subgroup1 (6 weeks)					
	subgroup2 (12 weeks)					
	subgroup3 (16 weeks)					
	subgroup4 (24 weeks)					
	subgroup5 (30 weeks)					
3MC TREATMENT	GROUP III					
	subgroup6 (6 weeks)					
	subgroup7 (12 weeks)					
	subgroup8 (16 weeks)					
	subgroup9 (24 weeks)					
	subgroup10 (30 weeks)					

Animal Batches	Group Name	Treatment Type				
		PET	3MC	CDDP	PEITC	PEITC +CDDP
INVASIVE CANCER (IC)	GROUP IV					
	GROUP V					
	subgroup11 (1week)					
	subgroup12 (2weeks)					
	GROUP VI					
	subgroup13 (1week)					
	subgroup14 (2weeks)					
	GROUP VII					
	subgroup15 (1week)					
	subgroup16 (2weeks)					

IC_{20}, IC_{30}, IC_{50} and IC_{70} doses were accordingly studied for 24, 48 and 72h respectively.

Similar protocol was also followed for identifying the optimum dose of PEITC. To achieve this, SiHa and $SiHa^R$ sublines were subjected to varied concentrations (0.5, 1, 2, 3 μM) of the phytochemical for 3h. Absorbances were recorded at 570 nm for enumerating the optimum ICs of CDDP in combination with PEITC. All results were represented as percentage (%) of surviving cells with respect to the specific doses for respective treatment agents.

❖ ***Calculation of doubling-time for SiHa and $SiHa^R$***

SiHa and $SiHa^R$ were seeded in densities of $1*10^5$ cells/well within 6 well plates. Herein, they were allowed to grow for the time periods of 12, 16, 20, 24, 28, 32, 36 and 40h respectively. At respective time points, cells from the allocated wells were trypsinized and enumerated using a haemocytometer under inverted microscope. For every time instant, cell counts were recorded and the doubling time was accordingly ascertained. This experiment was performed in triplicates. All results were represented as Mean ±S.D.

❖ ***Record of mice body weight and tumor incidences***

Weekly body weight alterations in mice were recorded to assess the periodic impact of 3MC, PET, CDDP and PEITC treatments on their physiology. An orderly record of cervical tumor incidences along with the gradually acquired cervical dysplastic stages was also maintained for the 3MC treated mice batches.

❖ ***Cytopathological study***

Pap Smear Tests were undertaken to monitor cervical carcinogenesis among mice during treatment. Phosphate Buffered Saline (PBS, pH-7.4) were dropped on a clean grease free glass slide on which cervical exfoliated cells were smeared into thin conventional layers after collection. Cervical smears were stained as per the polychromatic Papanicolaou staining (Pap staining) process. The cell smears were fixed in 100% ethyl alcohol followed by subsequent staining with Harris Haematoxylin (HH), Orange G6 (OG6) and Eosin Azure (EA50) for 5-6 mins respectively. Excess haematoxylin stain was removed by rinsing the slides in tap water whereas excess of OG6 and EA50 was respectively washed in 70% and 90% alcohols followed by clearance in 100% ethyl alcohol and xylene. Thereafter the slides were dried, mounted and observed under light microscope. Over 50 fields were scanned for the visible and significant cytopathological changes.

❖ ***Enumeration of Leukocyte Index and Differential Leukocyte Count***

A leukocyte index was prepared by calculating the ratio of the number of leukocytes observed to the total number of cervical exfoliated cells present in a particular field of the Pap smears obtained from each treatment batch. More than 50 fields were examined for each slide and data were recorded to enumerate the leukocyte index (LI) using the following formula:

$$\mathbf{LI=} \frac{\textbf{(Number of Leukocytes Observed)}}{\textbf{(Total Number of Cervical Exfoliated Cells)}}$$

Study of differential subpopulations of leukocytes infiltrating the cervical region during treatment course was also performed. A numerical count of the microscopically identified leukocyte subpopulations was quantitatively estimated as 'Differential Leukocyte Count' (DLC). Over 50 fields of Pap stained slides were randomly scanned for calculating DLC. For each field, DLC was enumerated as a percentage (%) of specific number of leukocyte subpopulation (eosinophils, neutrophils and monocytes) observed among the total number of leukocytes as per the following formula:

$$\text{DLC} = \frac{\text{(Number of specific type of leukocytes* 100)}}{\text{(Total number of leukocytes)}}$$

❖ ***Histopathology***

Freshly dissected out cervical samples were washed in ice cold PBS (pH-7.4) and fixed in Neutral Buffered Formalin (NBF) for 72h. Dehydration and fat-removal of fixed tissues were carried out in alcohol upgrades (50%, 70%, 90%, 100%), Acetone, Acetone: Xylene (1:1; v/v) and Xylene followed by paraffin embedding for overnight at room temperature. Paraffin blocks containing embedded tissue were prepared with the aid of "L-block casts" and stored at 4^0C in the following day. Microtome-sectioned tissues (~5µm thickness) were drawn out and stretched over PolyL-lysine pre-coated slides which were further stained with Delafield's Hematoxylin (DH) for 4min after deparaffinization over a hot-plate, rehydration in alcohol downgrades (100%, 90%, 70%, 50%), bluing and excess stain removal in tap water. Thereafter, priming of these tissues for Eosin staining was undertaken by subsequent immersion in 70% and 90% alcohols respectively. Eventually, 1% Eosin was used for

counterstaining the cytoplasm. Stained slides were thereafter dipped in xylene and mounted with DPX for microscopic analysis. For every experimental cohort, over 20 fields of these slides were scanned for observable histopathological changes under Brightfield light microscope.

❖ ***Antigen Staining by flow cytometry***

SiHa and $SiHa^R$ cells harvested in PBS supplemented with 10% FBS from 55mm plates after trypsinization were pelleted down following centrifugation at 1500 rpm for 6min. Thereafter, 200µl of chilled acetone was added to these pellets and incubated at -20^0C for fixation and permeabilization. Acetone removal was undertaken by washing and centrifugation of the fixed cells in PBS at 1500 rpm for 6min. Non-specific antigen blocking was further carried out in 10%FBS at 4^0C for 45 min following which they were centrifuged for excess FBS removal. Cells pellets were thereafter resuspended in PBS supplemented with respective primary antibodies (1:1000) and kept under constant shaking at 4^0C overnight. In the following day, cell tubes were taken up for antigen staining by incubation with respective fluorophore tagged secondary antibodies at room temperature after removal of excess primary antibodies. Likewise, excess secondary antibodies were also washed off by centrifugation after 2h. The resulting pellets were lastly resuspended in equal volumes of PBS and sheath fluid. These cell suspensions were transferred into FACS tubes and loaded onto the flow cytometer for detection of results. All experiments were recorded in triple biological replicates and results were represented as scatter plots as well as in terms of graphs delineating percentage of positively stained cells (%) for each study points.

❖ ***Cell cycle analysis of Ku70 positive cells by flow cytometry***

SiHa and $SiHa^R$ cells harvested in PBS supplemented with 10% FBS from 55mm plates after trypsinization were pelleted down after centrifugation at 1500 rpm for 6min. 200µl of chilled acetone was added to these pellets and incubated at -20^0C for fixation and permeabilization. Acetone removal was thereafter undertaken by washing and centrifugation in PBS at 1500 rpm for 6min. Fixed cells were blocked in 10%FBS at 4^0C for 45min following which they were centrifuged and for excess FBS removal. Cells pellets were resuspended in PBS supplemented with anti-Ku70 primary antibody (1:1000) and kept under constant shaking at 4^0C overnight. In the following day, these cell tubes were taken up for incubation with FITC-tagged secondary antibody at room temperature after removal of excess primary antibodies. Following removal of excess secondary antibody, these cells were processed for cell cycle analysis wherein they were treated with RNase-A at 37^0C for 30 min after which Propidium Iodide Stain was added to each of them for flow cytometry analysis using FITC and PE filters. All experiments were performed in three biological replicates. Distribution of Ku70 positive cells among all the cells of different cell cycle phases were represented as overlay histogram curves. Percentage of Ku70 positive cells were additionally plotted as bar graphs for better interpretation of results.

❖ ***STRING Database Analysis***

Existent protein level interaction of the selected the PI3K/Akt pathway effectors levels were determined using STRING database analysis.

❖ ***Preparation of cell and tissue lysates***

Trypsinized SiHa and $SiHa^R$ cells were harvested in PBS followed by centrifugation at 1500 rpm for 6min. Resulting pellets were further resuspended in NP40-Lysis Buffer(pH-8; 5M NaCl, 0.5M EDTA,1M Tris, NP-40) and ice-incubated for 20 mins. Similarly, Cervix tissues along with the adjoining tumor regions were dissected out, washed, and pooled separately from the mice batches. Tissue and tumor parts were dried, weighed and homogenized in Radio- Immunoprecipitation Assay Lysis buffer (RIPA; pH-8; 5M NaCl, 0.5M EDTA,1M Tris, NP-40,10% Sodiumdeoxycholate,10% SDS). The extracts were kept in ice for 30 min followed by sonication. Both the cell and tissue lysates were centrifuged at 10,000g for 20 min at 4^0C. The resulting supernatants were stored in chilled vials at -20^0C until protein estimation.

❖ ***Estimation of total protein***

Total protein content of the cell and tissue extracts was spectrophotometrically estimated using 1X Bradford's reagent against a standard curve of BSA. Absorbance was recorded at 595 nm with the experiment being repeated for 5 times.

❖ ***Western Blot Analysis***

The expression statuses of all the study markers in cell and tissue proteins were comparatively studied by western blotting. Equitable amounts of tissue protein (~30µg) were respectively loaded into each well of SDS-polyacrylamide gels, electrophoretically separated using electrophoresis buffer (25mM Tris, 192mM glycine, 10% SDS) and electro-transferred to chilled methanol charged PVDF membranes with the aid of a transfer buffer (250mM Tris, 192mM glycine, 10% Methanol) in semi-dry condition. These membranes were blocked with 5% (w/v)

BSA solution, washed with Tris Buffered Saline (TBS; pH-7.5; 25 mM Tris.HCl, 150 mM NaCl) and incubated overnight with primary antibodies at 4^0C under constant shaking. Blots were thereafter washed with TBS thrice and TBST Buffer solution (TBS; tween 20) for 4 times. Subsequently, these membranes were incubated with alkaline phosphatase conjugated secondary antibodies (1:500dilutions) at 4^0C for 2h, followed by TBST washing (4times) and incubation with the chromogenic substrate 5-bromo, 4-chloro, 3-indoylphosphate/ Nitro-Blue tetrazolium (BCIP/NBT) for visualizing protein expressions in the form of bands. β-actin was used as a loading control. Experiments were performed in triplicate and the respective band intensities were calculated after normalization with the loading control using ImageJ software.

- ***Immunofluorescence (IF)***

Equal numbers of SiHa and $SiHa^R$ cells were seeded (2.5×10^5cells/well) onto coverslips placed within 6-well plates for performing immunocytochemistry. PEITC and CDDP-treatments were ensued at respective time-points in this setup following which the medium was discarded from each well. Thereafter, medium remnants were washed away using PBS (3 washes/5 mins) and the adherent cells were fixed in chilled acetone for 15-20 mins. Furthermore, 5% saponin was added after methanol removal for permeabilization. Again, these cells were subjected to 3 PBS washes for 5 mins followed by BSA blocking and overnight incubation with primary antibodies (1:1000) in a cold room within a humid chamber. Next day, excess of primary antibodies were washed off in PBS supplemented with Tween20 (PBST solution). Thereafter, these cells were incubated with respective fluorophore-tagged secondary antibodies (1:1000) at room temperature. Likewise, excess secondary antibodies were removed in 3 PBST washes followed by counterstaining with the fluorescent dye 4′,6-diamidino-2-phenylindole (DAPI) for 2 min. After a

single methanol wash, each of these coverslips bearing immunostained cells were mounted over clean grease-free slides and observed under fluorescent microscope. Slides were scanned for 50 fields for recording significant observations. All experimental steps were performed in complete darkness following addition of secondary antibody and DAPI.

❖ ***Flameless Atomic Absorption Spectroscopy***

Equal densities of CDDP treated SiHa and $SiHa^R$ cells were trypsinized, harvested, acetone-fixed and pelleted down by centrifugation at 1500 rpm for 6 mins. Following the removal of supernatant, all cell pellets were stored in -20^0C until use. These frozen cell pellets of SiHa and $SiHa^R$ were later brought to room temperature, lysed in RIPA and acid-digested in concentrated nitric acid at 60^0C for 2 h. All samples were quantitated for platinum levels at an absorbance of 265.9 nm in an inert argon gas chamber supplied with a platinum lamp being operated at 10 mA current in an Atomic Absorption Spectrometer (AAS). The measurements were recorded against varied concentrations (0.1nM-25 μM) of platinum standard solutions. Results were represented as fold change trend curves for proper interpretation. All experiments were recorded in triplicate with evaluated results being expressed as Mean±S.D.

❖ ***Retention of Pt-DNA adducts in vitro***

Cisplatin treated $SiHa^R$ cells were harvested and pelleted down by centrifugation at 1500 rpm for 5min followed by acetone fixation at -20^0C for 20 min. After acetone removal by centrifugation, fixed cells were incubated with antibody specific to Pt-modified DNA for overnight at 4^0C. Thereafter, excess antibodies were washed away by centrifugation at 1500 rpm for 5 min followed by incubation with FITC

conjugated secondary antibodies for 2h at room temperature prior to flow cytometric detection. Results were represented as histograms. Experiments were repeated thrice with values expressed as Mean±S.D.

❖ ***Reverse Transcriptase PCR***

Isolation of total cellular RNA was performed using TRIzol Reagent. cDNA was synthesized from 2 μg of total RNA using RetroScript kit which was amplified by PCR using the following forward and reverse primer sequences:

The primer sequences used for generating RT-PCR results are as follows:

Akt 1:

Forward primer CAGGAGGTTTTTGGGCTTG

Reverse primer TGAGGAAGACAGGACCAGGA

Akt 2:

Forward primer AAAGAAGGCTGGCTCCACAA

Reverse primer GTCGCTCTTCAGCAGGAAGT

XIAP:

Forward primer ACTTCGGGTTTCACGACTCC

Reverse primer CCGAGCCCCAATCTGGAAAT

Survivin:

Forward primer CCCTCACTGCTGAAGGACAC

Reverse primer GACAGCCCTCACTCCCTAGA

β-actin:

Forward primer GACAGTCAGCCGCATCTTCT

Reverse primer GCGCCCAATACGACCAAATC

PCR product was analyzed by electrophoresis in ethidium bromide (EtBr) containing 2% agarose gel and visualized under Gel Documentation System.

- ***JC1 Staining***

SiHa and $SiHa^R$ cells were comparatively assessed for their mitochondrial transmembrane potential by staining of with JC-1 mitochondrial stain. As per requisite, SiHa and $SiHa^R$ cells were seeded ($5x10^5$) over coverslips placed in 6-well plates and incubated with JC-1 staining solution (100µl stain /ml of culture medium) provided in the kit at 37^0C for 30 mins. Thereafter, these plates were centrifuged at 400g and the supernatant was discarded. Assay Buffer of 2 ml was added to each well and again centrifuged at 400g. Following aspiration of the supernatant, excess stain was removed by final washing in 1ml Assay Buffer. Coverslips were thereafter mounted over DPX loaded grease free clean slides and scanned (~20 fields) thoroughly under the fluorescent microscope.

- ***Rhodamine 123 Assay***

PEITC and CDDP treated SiHa and $SiHa^R$ cells, seeded in densities of 2.5×10^5 cells/well in 6-well plates were stained with 5 µg/ml of Rhodamine (Rh-123) and incubated at 37^0C for 30 min. Spectrofluorimetric analysis at excitation and emission wavelengths of 488 nm and 525 nm were undertaken. Results were graphically expressed as fold change of the fluorescent intensities. Experiments were performed in triplicate and results were represented as Mean ±S.D.

❖ ***Chromatin Immunoprecipitation (ChIP)***

To the genomic DNA isolated from cervical tissue, protease inhibitors and p65 antibodies (2 μg/100-200μg of protein) was added and kept for cold incubation at 4^0C in tube rotator overnight for enabling Immunoprecipitation of protein complex. This was transferred to a column containing filter coated with Protein-A Sepharose beads and further kept at 4^0C overnight over a flat shaker. On the following day, non-specific proteins were washed off using 1X and 0.1X IP Buffer respectively by cold-centrifugation at 12000g for 1mins. Thereafter, reverse crosslinking was done for separation of the probable chromatin sections from bound protein. Again, the chromatin sections were purified and eluted out with aid of an IP Elution Buffer followed by PCR based analysis.

❖ ***Quantitative and Qualitative Estimation of Reactive Oxygen Species (ROS) in vitro***

Intracellular ROS was quantitatively measured by flow cytometry. Equal numbers of SiHa and $SiHa^R$ were seeded in 55mm plates (2.5×10^6 cells) and over cover slips in 6-well plates (2.5×10^5 cells) and incubated for 24h. After respective time points, plates were trypsinized and stained with 10 μM 2',7'-dichlorofluorescein dihydroacetate (DCFH-DA) for 45 min followed by flow cytometric analysis at FL1-H filter. Scatter plots and histograms were generated using Cell Quest software. DCFH-DA passively diffuses within cells to transform into a diol moiety, which is further oxidized into a fluorescent compound, 2', 7'-dichlorofluorescein (DCF), by intracellular ROS. DCF was quantitated spectrofluorimetrically (VARIAN; Excitation: 485 nm and Emission: 530 nm). Respective coverslips from the

corresponding 6-well plates were scanned for over 50 fields for qualitative analysis of generated ROS using FITC filter under fluorescent microscope.

❖ ***Estimation of systemic ROS levels in isolated blood leukocytes of mice***

One volume of mouse blood collected aseptically from heart was mixed with three volumes of Solution A (pH-7.2; 0.87% NH_4Cl in 10 mM Tris HCl), incubated on ice for 20 min and centrifuged at 400 g for 20 min at 0^0C. The supernatant was discarded and the pellets were again resuspended in Solution A followed by centrifugation at 400 g for another 20min at 0^0C. The resulting pellets were suspended in Solution B (pH-7.2; 0.25 M mesoinositol, 10 mM Na_2SO_4, 1 mM $MgCl_2$), cold centrifuged at 1500 rpm for 5 min at 4^0C, and resuspended in HEPES-buffered saline (HBS; pH 7.4; 140 mM NaCl, 5 mM KCl, 10 mM HEPES, 1 mM $CaCl_2$, 1 mM $MgCl_2$, 10 mM glucose). Cell numbers were adjusted to 10^6 cells/ml/point in HBS and incubated with DCFH-DA for 45 min at room temperature in complete darkness. DCF generation was quantitated spectrofluorimetrically (VARIAN; Excitation: 485 nm and Emission: 530 nm). For each point, readings were recorded approximately in five technical replicates in triplicate attempts of the experiment. Results were expressed as Mean ±S.D.

❖ ***Estimation of free GSH level***

Glutathione reductase (GSH) [E.C1.8.1.7] depletion rates were spectrophotometrically assessed by following the protocol of Glutathione Assay Kit. To 50µl of cervical tissue and cell lysates in the 96well strips, 150µl of Assay Cocktail was added. These strips were incubated at 37^0C by constant shaking followed by kinetic recording of absorbances at 414nm for 30min. GSH was quantified by plotting the absorbances against a standard curve. Results were

graphically plotted as relative fold change of values. All experiments were repeated thrice.

❖ ***Quantitative Estimation of RNS generation***

Equal volumes of peritoneal macrophage suspension (10^6cells/ml) in PBS and Griess reagent (1% sulphanilamide, 0.1% naphthyl ethylenediamine hydrochloride and 5% orthophosphoric acid) was incubated at 37^0C for 30 min in a humidified chamber for quantifying Reactive Nitrogen Species (RNS) levels. Absorbance was recorded at 550 nm with a spectrophotometer against a standard blank. NO levels were enumerated against a standard curve of sodium nitrite generated by using varied concentrations of Sodium nitroprusside. Readings for each point were taken for about five times in triplicate attempts.

❖ ***Quantitative Estimation of Nitric Oxide Synthetase Activity***

Indirect assessment of Nitric Oxide synthetase (iNOS) enzyme (E.C1.14.13.39) activity was done using a spectrophotometer by calculating the percentage of L-citrulline catalytically produced from L-arginine by means of NOS activity Assay Kit. The assay principle is based on the Griess reaction, which involves the conversion of nitrite to a deep purple azo-compound which was spectrophotometrically detected at 540 nm. Experiments were repeated thrice and results were represented as relative fold change graph.

❖ ***Total Antioxidant Enzyme Assay***

Free Radical quenching capacity of the antioxidant scavengers present in the blood serum isolated using serum separating vials, was assessed with the help of Antioxidant Assay Kit. Incubation of blood serum samples with the provided assay buffer at 37^0C

in humidified conditions under constant shaking was undertaken followed by spectrophotometric recording of absorbances in kinetic cycles at an absorbance range of 405-750nm. Enzyme activity was calculated in IU/L with reference to a standard curve. Results were represented as Relative Fold Change.

❖ ***Preparation of Single cell suspension from cervical tissues and tumors***

Cervical tissues and tumor samples were transferred in chilled PBS immediately after collection. These were washed well in sterile conditions within Laminar Airflow Hood. Tissue samples were processed and minced well using sterile fine-forceps and scalpel in chilled PBS followed by their transfer in microcentrifuge tubes containing Type-I Collagenase prepared in DMEM-F12 medium supplemented mildly with ~4% FBS. All this while, surgical instruments were washed well in 70% ethanol and heat-sterilized in spirit-lamp flame after absolute drying. Tissue fragments were thereafter subjected to a controlled slow digestion process for 3 hrs at 37^0C in a humidified CO_2 (~5%) incubator with interim shaking for dislodging digested cells. Thereafter, single cells were collected by centrifuging these tubes at 3000 rpm for 6 min at room temperature. After discarding the supernatant, the pellets were washed once in PBS by centrifugation at 1500 rpm for 5 min. Resulting pellets were resuspended in PBS and used for quantification of ROS, RNS, iNOS and GSH levels.

❖ ***Estimation of Serum Alanine Transaminase (SGPT) and Aspartate Transaminase Activity (SGOT)***

The hepatic toxicity induced as a result of chronic carcinogen treatment was assessed by estimating the kinetics of serum aspartate transaminase or serum glutamic-oxaloacetic transaminase (SGOT; E.C 2.6.1.1) and serum alanine transaminase or serum glutamic-pyruvic transaminase (SGPT; E.C 2.6.1.2). The serum samples were

isolated from blood and collected aseptically from the heart using serum separating vials. These were used to analyse the enzyme activities using colorimetric kinetic assay kits respectively. In this process, 200µl of serum samples were incubated with 20µl of assay reagent for 1minute at 37^0C. Assay reagent was prepared by addition of reaction buffer and reagent (1:4; v/v). Analysis of optical density of the final reaction mixtures was made using a spectrophotometer at 340nm. All optical densities were evaluated against a standard blank. The quantitated serum kinetics of alanine transaminase and aspartate transaminase was expressed in IU/L. The experiment was repeated thrice.

- ***Estimation of Alkaline Phosphatase Activity***

  The serum isolated from blood was also used for determining alkaline phosphatase enzyme (ALP; E.C 3.1.3.1) activity. This study was performed using ALP kinetic assay kit. In accordance with the kit protocol, 20µl of serum samples were incubated with 1000µl of working solution for 30seconds at 37^0C. Working solution was constituted by 2-Amino-2-Methyl-1 Propanol buffer and the substrate p-Nitrophenyl Phosphate (1:1; v/v). As soon as the reaction initiates, the reaction mixture turns yellow. Absorbance of these mixtures was spectrophotometrically recorded at 405 nm against standard blanks. The kinetics of generation of p-Nitrophenol and phosphate by the activity of ALP present in the serum samples is expressed in IU/L. The experiment was repeated thrice.

- ***Estimation of Serum Creatinine Level***

  Creatinine levels were quantitated in the serum obtained from mice of both treated and untreated groups by following the convention of Jaffe's method. The results

were expressed in terms of fold increase in creatinine levels so that a comparative study can be made. All the experiments were repeated thrice.

❖ ***Single cell gel electrophoresis (SCGE or Comet assay)***

Genotoxic effect of 3MC on DNA was assessed following the standard laboratory protocol. Concisely, a suspension of 0.6% (w/v) low melting agarose (LMA) and isolated leukocytes ($1x10^4$cells) was smeared over a frosted microscopic glass slide which was priorly coated with the fixative 0.75% (w/v) normal melting agarose (NMA). Following solidification at 4^0C, cell and nuclear membranes were lysed in lysis buffer (pH-10; 2.5 M NaCl, 0.1 M Na_2EDTA, 10 mM Tris, 0.3 M NaOH, 1%Triton X-100, and 10%DMSO). Exposed DNA from the lysed out leukocytes were unwound in a highly alkaline electrophoresis buffer (pH >13.0; 300 mM NaOH, I mM Na_2EDTA) prior to electrophoresis for 20min (300mA, 20 V). Slides were washed in neutralizing buffer (Tris 0.4 M, pH 7.5) thrice, stained with EtBr (final concentration 40 µg/ml) and examined under a fluorescence microscope. Image analysis, head DNA quantification, comet tail DNA length estimation and comet tail moment calculation were performed using Komet Software.

❖ ***Immunohistochemistry(IHC)***

To determine the tissue distribution of antigens of interest, IHC was performed. Cervical tissue sections (~5µm thick) were stained with respective primary antibodies of proteins for locating them within tissues [Basu et al., 2020]. Paraffin from stretched tissue sections was removed by heating the slides at 65^0C for 20 min followed by xylene treatment and rehydration through 100%, 90 %, 70 % and 50 % alcohol downgrades. After washing these sections serially in PBS for 10min,

'antigen-retrieval' was carried out using pre-heated citrate buffer [pH-6; comprising of $C_6H_80_7.H_2O$ and $(CH_2COONa)_2.2H_2O$] at 85^0C for 1 h following which they were incubated with the respective primary antibodies diluted in 1 % BSA solution within a humid chamber overnight at 4^0C. Excess primary antibodies were washed in 1XPBS. Slides were further incubated with HRP conjugated secondary antibodies (1:500) in 1% BSA solution for 2h at 37^0C followed by immunostaining with the chromogenic substrate 3–3′ diaminobenzidine (DAB) and counterstaining with DH. These slides were dehydrated through successive alcohol grades and xylene. Finally, they were mounted in DPX for observation under light microscope. About ten fields were scanned in order to score for the positive staining intensities. Staining intensities (1 = weak, 2 = moderate, 3 = strong) were enumerated as per the percentage of positively stained cells (< 1 = 0, 1–20 = 1, 20–50 = 2, 50–80 = 3 and > 80 = 4). Final evaluation of the tissue specific protein expressions was made as very low (Score 1), low (Score 2), intermediate (Score 3) and high (Score 4-5) levels.

- ***Sphere Formation Assay***

To ascertain the sphere forming capacity of C33A, $1x10^5$ cells were seeded in 55mm low-attachment plates containing Sphere Formation Medium (DMEM 96.97ml, Penicillin and Streptomycin 1ml, B-27 2ml, bFGF 20µl, hEGF 10µl).Cells were allowed to form sphere over a period of 5days. Intermittently, the conditioned medium was collected for characterization of its contents. The collected soup was thereafter purified for its protein content using a dialysis tube concentrator followed by estimation of the protein by Bradford Assay and ELISA. Meanwhile, sphere enrichment was checked by FACS and the sphere formation was tracked microscopically over the period of 5days.

❖ ***Transfection studies***

HaCaT cells in an approximate density of $5x10^3$ were seeded into 6well plates and allowed to grow in DMEM supplemented with 10% FBS until 60% confluence was achieved. Thereafter, DMEM was replaced by Opti-MEM supplemented with Lipofectamine containing Akt cloned plasmids (~414.7ng/µl). After 48hrs, cells were trypsinized and harvested for flow cytometry analysis.

❖ ***Estimation of TNFα, IL10, IL6 and IL8 activity in cervix tissue lysate***

TNFα, IL10, IL6 and IL8 cytokine activity was recorded using the cervical tissue lysates and conditioned medium with the help of IL6 and IL8 activity estimation kits. The kits employed the principle of sandwitch ELISA, where the tissue lysates were incubated in pre-coated 96 well plates with IL6 and IL8 primary antibodies respectively. Biotinylated secondary antibodies were added to these wells followed by addition of the chromogenic substrate. The optical density of the coloured solution was measured using ELISA reader (TECAN) at 450 nm. The results were recorded against standard blank. The experiment was repeated thrice.

❖ ***Cyclocondensation Assay***

Enumeration of the 'optimum period' and quantitation of intracellular PEITC in SiHa and $SiHa^R$ following 1h, 2h, 3h, 4h, 5h and 6h of its administration was undertaken by cyclocondensation assay (Zhang and Talalay, 1998). SiHa and $SiHa^R$ cells were treated with 2µM of PEITC (Maximum Tolerated Dose or MTD). PEITC concentrations were determined by spectrophotometry against a standard curve. This methodology involved quantification of intracellular PEITC levels in terms of 1, 3Benzodithiole-2-thione which is the PEITC-intermediate

formed during cyclocondensation reaction. Generated intermediate is quantified spectrophotometrically at 365nm. The accumulation levels of the specific concentrations of the intermediate with a molecular weight of 184.30g were also additionally verified by mass spectroscopy in terms of the detectable mass-peaks within the cell-lysates harvested at specific time points. Spectrophotometric absorbances were plotted against a standard curve for calculating PEITC levels in µM/ µg of protein. Intracellular presence of respective concentrations of PEITC was validated by Liquid Chromatography with tandem mass spectrometry (LC-MS-MS; WATERS). Each experiment was undertaken in triplicate and results were expressed as Mean ±S.D.

❖ ***In silico*** **studies**

Molecular docking was applied to see the various interactions of PEITC (PubChem ID: 16741) with all the molecules AKT (PDB ID: 1H10), AKT1 (3OCB), AKT2 (1MRY), MRP2 (2GIA), NFκB-p65 (4Q3J), XIAP (3CLX) and Survivin (1F3H). Each protein structure was prepared by the removal of water molecules and co-crystalized ligands and subsequent addition of polar hydrogen atoms. Similarly the compound PEITC was also prepared by addition of 7.5 hydrogen atoms using Avogadro tool. AutoDock Vina software was utilized in all the docking experiments, with the optimized protein models as the docking target. For each target protein, individual runs were performed. Ranking of the resultant docking poses were screened using a built-in scoring functions. By utilizing the AutoDock tools, different size grid box were employed with center of the grid box being placed around the active site of each protein for docking using AutoDock Vina. The screened poses were analyzed using BIOVIA Discovery Studio Visualizer and PyMOL.

❖ ***Statistical Analysis***

The mean values of the PEITC, CDDP and PEITC+CDDP treated experimental points were compared by factorial Analysis of Variance (ANOVA). The relationship between the studied parameters was analysed by calculating Pearson's correlation coefficient using CORREL function of Microsoft Excel. Data were expressed as mean± standard deviation (S.D.) A p value <0.0001 was considered as statistically significant.

Work Plan

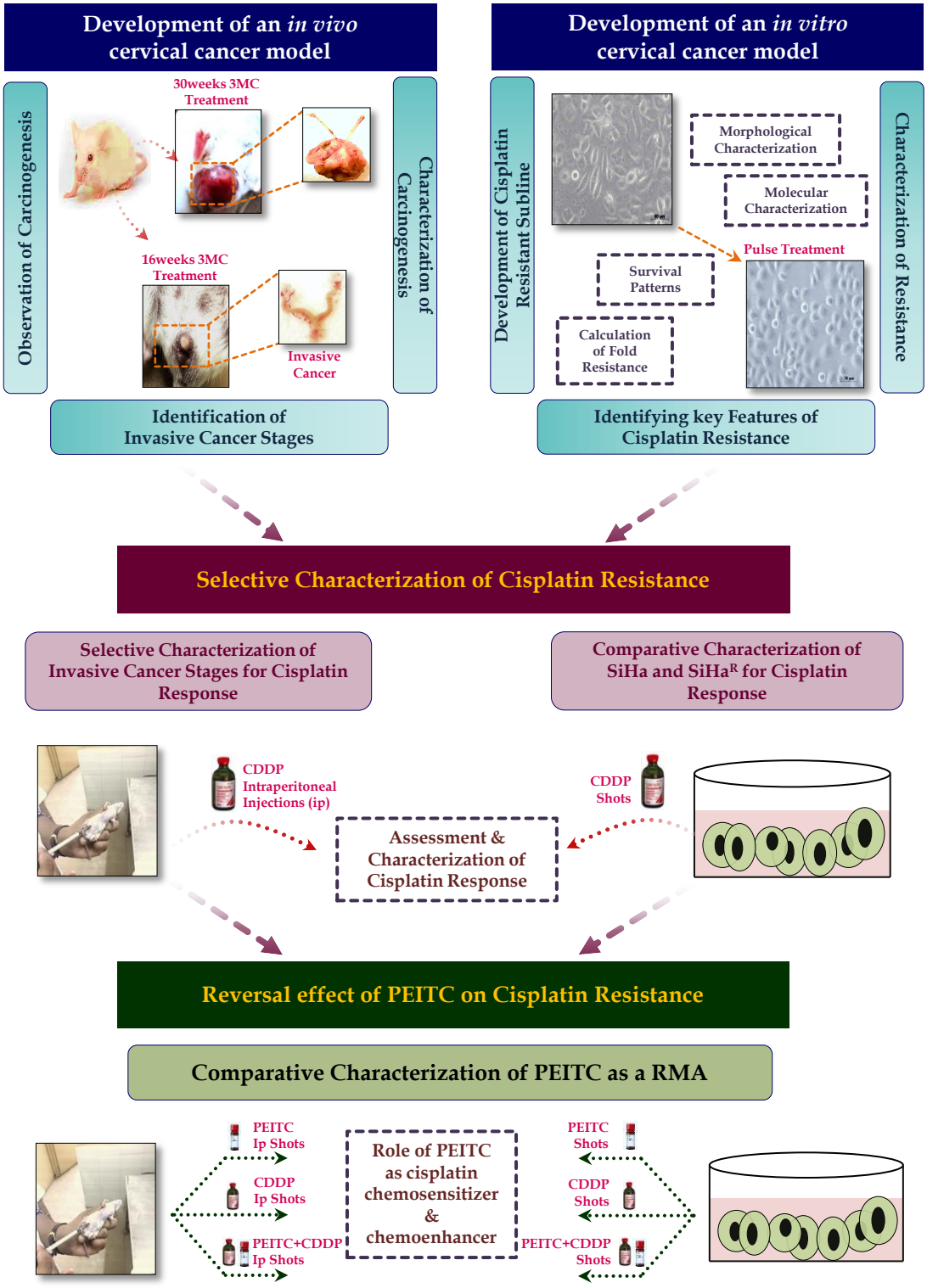

Figure 22: Overall Plan of Work

Results

In vivo findings

7. RESULTS

7.1. *In vivo* Findings

- **Study Design for Development of a Carcinogen Induced *In vivo* Cervical Cancer Model**

  Figure 23 showcases the overall work plan designed for development of a carcinogen induced *in vivo* cervical cancer model. For this purpose, a 3MC carcinogen solution of concentration 0.6mg/ml was prepared in PET. This was identified as the optimum carcinogen concentration ($<LC_{50}$) for safe administration among 5-6 weeks old virgin female Swiss Albino mice (*Mus musculus*) with synchronised estrous cycles. Chronic 'cervical painting' was undertaken by flushing 50µl of 3MC solution (0.6mg/ml) over mice cervix through a period of 30 weeks. Experimental mice batches were monitored at the respective interval of 6, 12, 16, 24 and 30 weeks for any visible changes in appearance of their external orifices. Detections of 3MC or PET induced alterations in mice body weight alongwith their cervical cytopathology were regularly recorded and compared with the same from untreated control group. Mice from each treatment groups were sacrificed at an intermittence of 6^{th}, 12^{th}, 16^{th}, 24^{th} and 30^{th} week followed by isolation of their cervical tissues, cervical tumours, blood as well as other vital organs namely spleen and liver. A thorough scrutiny of the carcinogenic progression was performed with these collected samples time dependently by histopathological, biochemical and molecular characterization.

- **Body weight fluctuations, Orifice deformations and Cervical Cytopathology alterations accompanied chronic 3MC treatment in mice**

  Prior to sacrifice, the experimental mice were preliminarily monitored for alterations in their body weight patterns, appearance of external orifice and cervical

cytopathology (Figure 24 & 25). As denoted from Figure 24A, the body weight of mice from control and vehicle control batches were comparably stable whilst those from 3MC treatment group exhibited fluctuating trends. Herein, a gradual loss in mice bodyweight after 6 weeks (24.303±0.331gm) and 12 weeks (23.632±0.513gm) of 3MC treatment was evidenced. However, the mice body weight envisaged an increasing trend (30.342±0.273gm) when the treatment span was extended to 16 weeks. This rising pattern was consistent upto 24^{th} (31.312±0.289gm) and 30^{th} week (32.525±0.289gm) of 3MC administration. Mice orifice appearances were simultaneously tracked for any abnormalities. As depicted in Figure 24B, the mice orifice assumed deformations with gradual increase in 3MC exposure. Mildly swelled orifices were vivid amongst 3MC treated mice in the 16^{th} week. Furthermore, extension of the carcinogen treatment duration upto 24^{th} and 30^{th} weeks led to an explicit enlargement of the lower abdominal area. Conspicuous and palpable outgrowths were especially apparent at 30^{th} week. No remarkable changes were observed among the control and vehicle control groups.

In order to ascertain the direct impact of chronic 3MC administration on murine cervix, cytopathological changes were closely investigated by Pap Staining. Accordingly, cervical swabs were collected from the three experimental mice batches at respective treatment time-points and stained for microscopic study. Pap smear micrographs as shown in Figure 25 exclusively portray cytopathological features indicative of cervical carcinogenic progression among 3MC treatment group only. Hyper-keratinized cervical squamous epithelial cells with ‘nuclear holes’ frequented the mice cervix in 12th week of 3MC treatment. At and after 16^{th} week, leukocytes such as eosinophils, neutrophils and monocytes were identified as persistent infiltrators of 3MC treated mice cervix. In the 24^{th} and 30^{th} weeks, murine cervical

exfoliates appeared as ‘bizarre’-structured cells exhibiting ‘hyperchromatic nuclei’ alongwith ‘perinuclear halo’ as signs of ‘severe dysplasia’ and ‘vacuolation’. Such cellular distortions were absent in PET treated groups and were therefore, comparable with untreated control mice batch.

❖ **Chronic 3MC treatment rendered persistent cervical inflammation**

Pap smear findings were suggestive of chronic cervical inflammation and malignancy associated changes. In this regard, confirmation of 3MC induced inflammation driven cervical carcinogenesis was necessary. Micrographic snippets in Figure 26A clearly showed that chronic 3MC treatment of mice resulted in infiltrations of eosinophil, neutrophil and monocyte multitudes alongwith scanty macrophages in the cervical region. A comparative leukocyte index (LI) was also calculated for untreated control, vehicle control and 3MC treatment groups for re-validation. As represented graphically in Figure 26B, 3MC treatment up to 6 weeks was accompanied by sparse drainage of eosinophils (LI value: 4±0.2) in the mice cervix which were at par with the untreated control and vehicle control groups. As the treatment duration reached 12 weeks, neutrophils appeared in excessive numbers with a significantly high LI value of 8.5±0.176 in comparison to other two mice batches. Monocytes joined the milieu of infiltrating cervical leukocytes when the carcinogen treatment reached successive periods of 24 and 30 weeks. The LI value during 24^{th} week of 3MC treatment was calculated to be as high as 10.2±0.340 which remained unchanged with an insignificant rise (11.8±0.18) during the 30^{th} week. In relation to untreated control and vehicle control groups, these LI values for both 24^{th} and 30^{th} weeks of 3MC treatment were extremely high. The LI value of vehicle control group presented no significant difference with that of untreated control batch thereby negating any contribution of PET in inflammogenesis of cervical neoplasia *in vivo*.

A characteristic uprise of neutrophils over other leukocyte subpopulations was noticed. Particularly, neutrophils of diverse morphologies were observed to populate the cervical region (Figure 27A). As a result, Differential Leukocyte Count (DLC) for untreated control, vehicle control and 3MC treatment mice were comparatively enumerated. Results in Figure 27D, confirms cervical neutrophil dominance as a typical attribute of 3MC treated mice as opposed to untreated control (Figure 27B) as well as vehicle control (Figure 27C) batches. Once again, eosinophils in the 6^{th} week and 12^{th} week of 3MC treatment came up with DLC values of 25.11± 0.58% and 35.01 ± 0.58% respectively. This underwent a little negative deviation by about 32.30 ± 0.58% in the succeeding 16^{th} week. Conversely, neutrophils of diverse morphologies (Figure 27A) with relatively higher DLC values (16^{th} week: 52.13± 1.00%; 24^{th} week: 66.33±1.00%; 30^{th} week: 78.01± 0.58%) gradually replaced the eosinophilic milieu within the mice cervix. Subsequently, with increasing treatment duration monocytes furthermore collaborated with the cervical neutrophils to intensify inflammation. Macrophages, although sparsely noted, was also obtained in the cervical infiltrates of these mice. An anecdote of cervical leukocyte infiltration trends among 3MC treated mice is very well-depicted in Figure 27D. In vehicle control mice, transient and insignificant neutrophil infiltration was apparent only at 16^{th} week of PET treatment (Figure 27C). Their DLC patterns were comparable with that of untreated control mice (Figure 27B). Corroborating trends of LI and DLC results asserted that 3MC triggered continual inflammatory changes in the murine cervix to facilitate carcinogenesis.

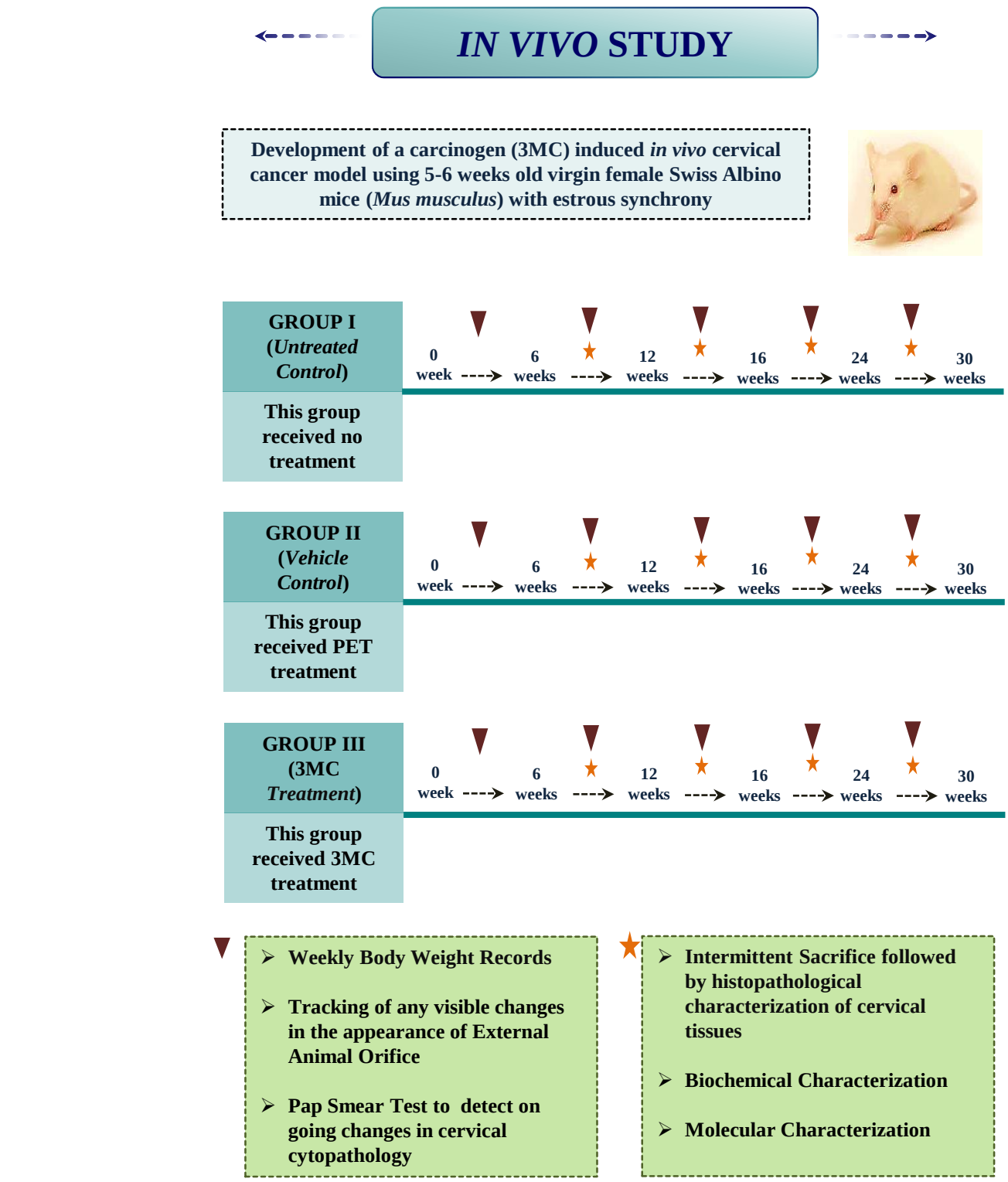

Figure 23: Plan of Work for *in vivo* study: An Overview of the Discourse followed for Development and Characterization of Carcinogen Induced *in vivo* cervical cancer model.

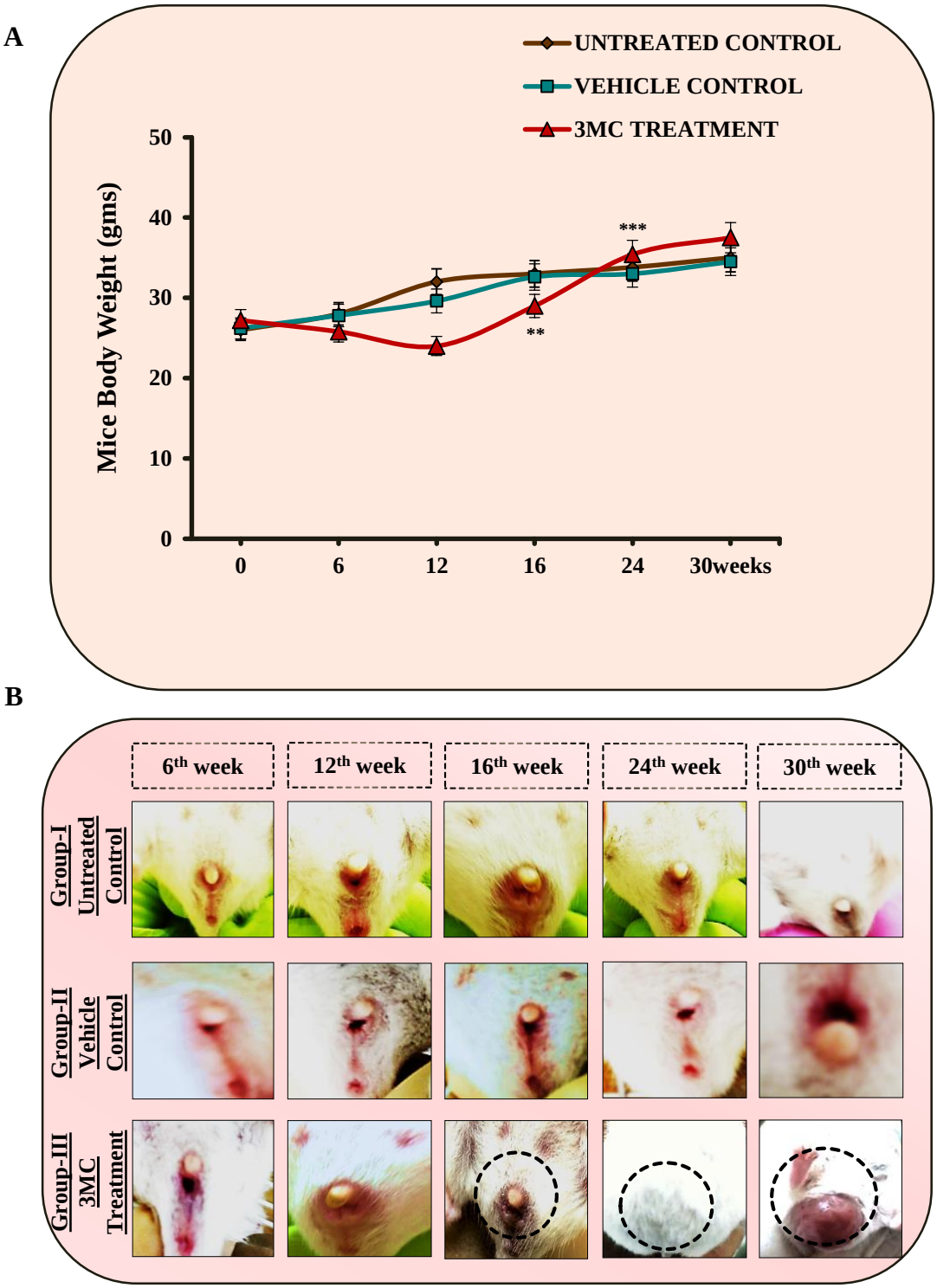

Figure 24: Appearance of External Orifice and Body weight changes: (A) Trends in alterations of body weight of Group I, II and III mice. Values are represented as Mean ± S.D (***p<0.0001; **p<0.05). (B) Glimpses of mice orifice depicting 3MC treatment induced deformations in comparison with untreated control and vehicle control groups.

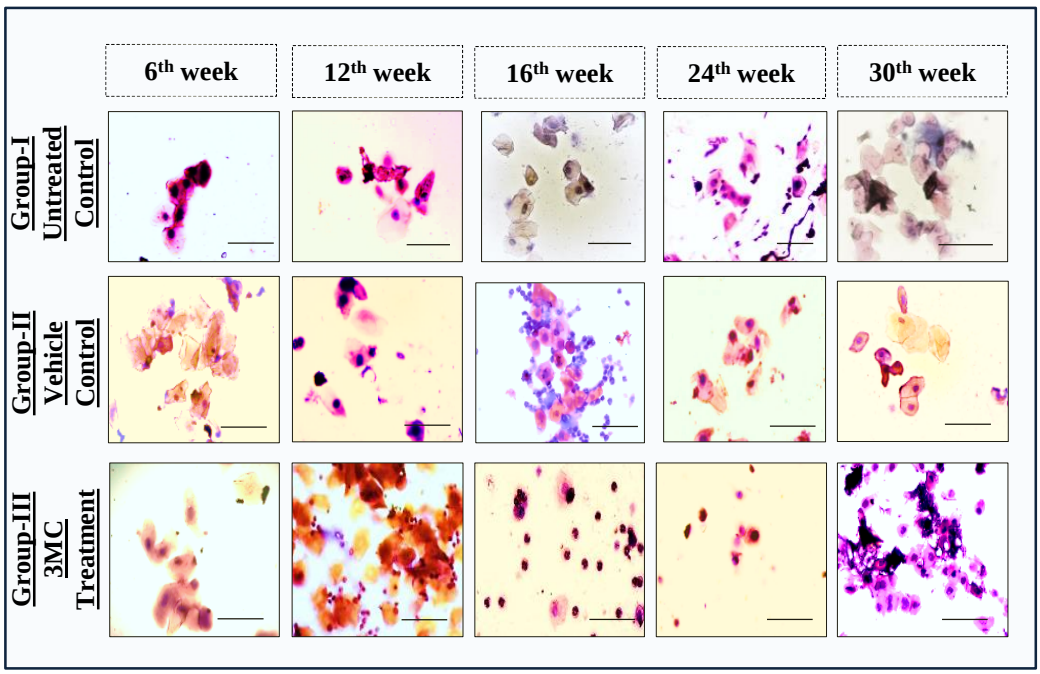

Figure 25: Cervical Cytopathology and Leukocyte Index: Representative micrographs of Pap Smears depicting comparative cytopathological changes in cervical exfoliated cells of Group I, II and III mice[Magnification: 200X; Scale bar: 20µm

A

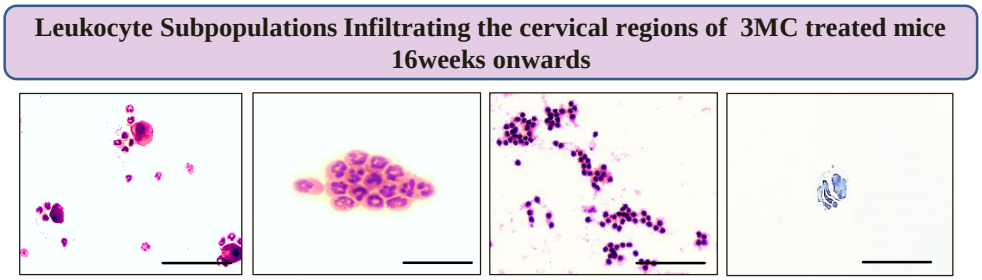

B

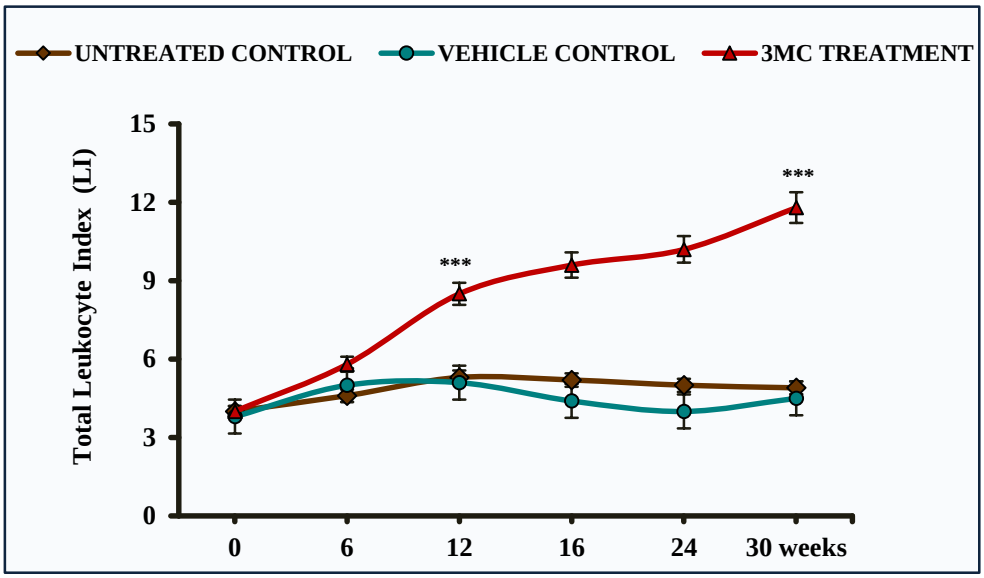

Figure 26: Account of chronic cervical inflammation: (A) Abundance and Distribution of diverse subtypes of leukocytes infiltrating the cervix of 3MC treated mice [Magnification: 200X; Scale bar: 20µm]. (B) Graphical excerpt of Leukocyte Index (LI) calculated from Pap Smear results confirming 3MC induced flux of inflammatory cells among Group III mice only. Values are represented as Mean ±S.D ($^{***}p<0.0001$).

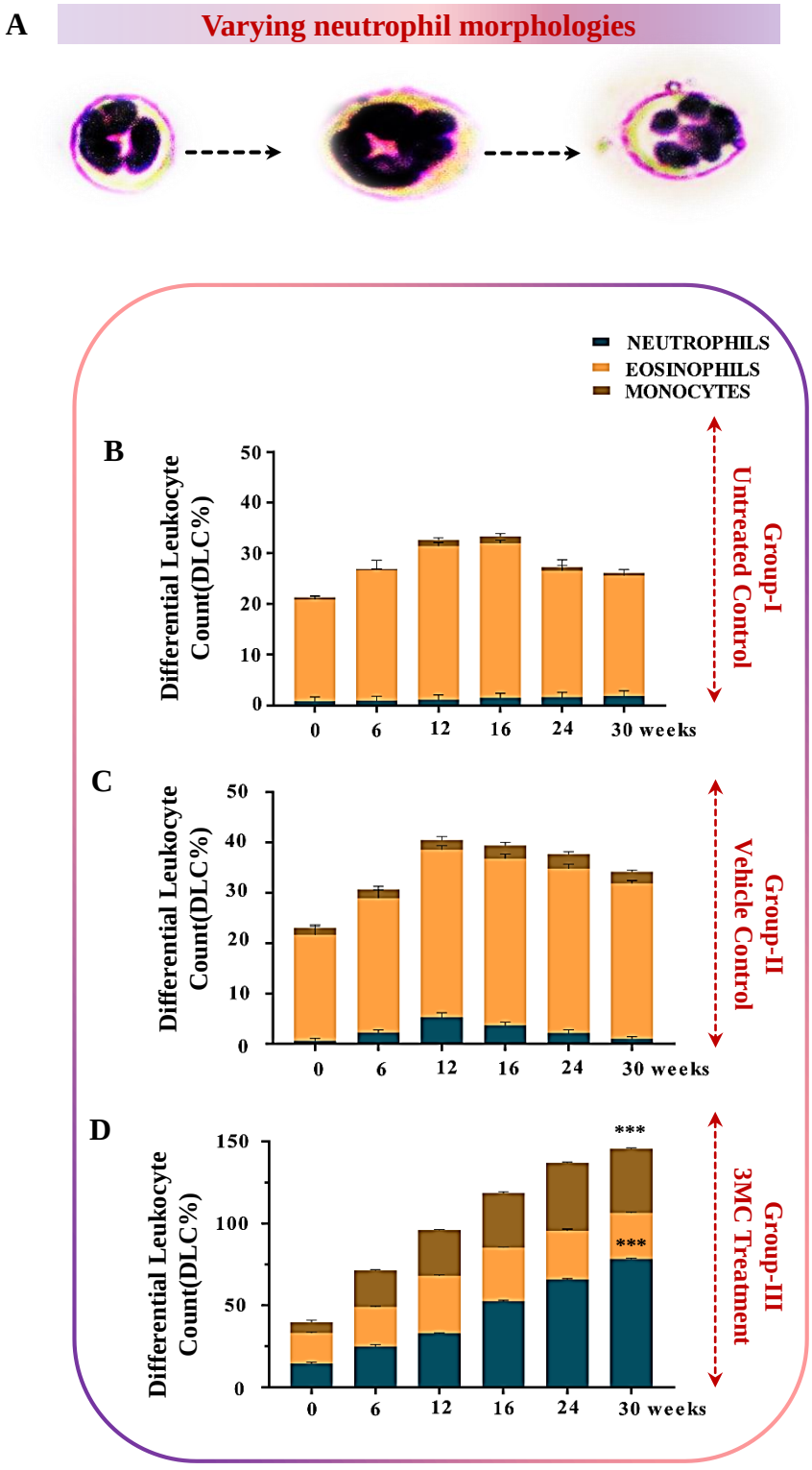

Figure 27: Differential Leukocyte Count (DLC): (A) Neutrophils of different morphologies as obtained in cervical Pap smears. (B-D) Comparative DLC of Group-I, II and III mice citing the prevalence of inflammation in the cervix of 3MC treated mice. Values are represented as Mean ±S.D ($^{***}p<0.0001$)

❖ **Chronic 3MC treatment remodelled cervical histology to promote generation of anaplastic tumors**

Altered cervical cytopathology necessitated an exploration of its underlying histology for surveillance of cervical carcinogenesis and identification of invasive cancer stage. In treatment intermittence, mice from control, vehicle control and 3MC treatment groups were sacrificed for isolation of their reproductive system followed by decapitation of cervical tissues. Concomitant changes in the anatomy of murine reproductive organs and cervical histopathologies are serially exhibited in Figure 28 (A-C). As depicted in Figure 28 (A & B), untreated control and vehicle control mice continued to harbour normal anatomy for their reproductive organs even at the end of 30 weeks. Herein, cervical tissues showed no signs of dysplasia. Conversely, remodelled anatomy and cervical histopathologies were evident among 3MC treated mice (Figure 28C). Reproductive organs dissected out from mice receiving 12 weeks of 3MC treatment appeared to be mildly thickened with moderately dysplastic cervical tissues. At 16^{th} week of 3MC treatment, highly thickened mice reproductive organs developed new blood vasculatures. Decapitated cervical tissues from these organs presented invasive carcinoma wherein intricate epithelial invaginations could be observed within the stroma. Further extension of 3MC treatment beyond 24 weeks resulted in growth of palpable tumors at the cervical region. Therefore, the relative cervical histopathology appeared to be poorly differentiated with absolute disorientation of cervical epithelial layers.

For better characterization of the cervical tumors, region wise histopathological analysis was performed. Cervix associated tumors were categorically separated into ‘cortical’, ‘cortico-medullary’ and ‘medullary’ regions. Histopathological exhibits of tumor cortex (Figure 29, upper panel) displayed large

keratin pearls thereby hinting towards malignancy associated tissue remodelling. In the cortico-medullary region, squamous epithelial cells abnormally transformed into ‘giant tumor cells’ with aggregations of nuclei in their centre (Figure 29, lower left panel). A glimpse of the medullary tumor core (Figure 29, lower right panel) furthermore unravelled the invasion of epithelial regions into the stroma from the overlying tissue tier. These histopathological annotations indicated the development of an aggressive and poorly differentiated ‘anaplastic squamous cell carcinoma’ in the mice cervix.

Figure 30A upholds a graphical record of the tumor incidences across untreated control, vehicle control and 3MC treatment groups. On this basis, vehicle control mice mostly had normal cervix with mild dysplasia being barely present among few of them. On the other hand, 3MC treatment groups emerged with either moderate dysplasia or invasive carcinoma or anaplastic tumors. Box and violin curve of Figure 30B further shows that majority of mice receiving 6 weeks of 3MC treatment developed only mild or moderate cervical dysplasia. Again, frequency of mice bearing moderate cervical dysplasia or carcinoma *in situ* was relatively high in 12 weeks 3MC treatment batch. Abundance of invasive cancers became more pronounced from 16^{th} week onwards. These stages were consistently present among minor proportions of mice receiving 24 and 30 weeks of 3MC treatment as majority of them had developed anaplastic cervical tumors. Untreated control mice were devoid of any such malignant or pre-malignant cervical lesions. All these findings cumulatively affirmed that chronic 3MC treatment paved a way for cervical carcinogenesis *in vivo*.

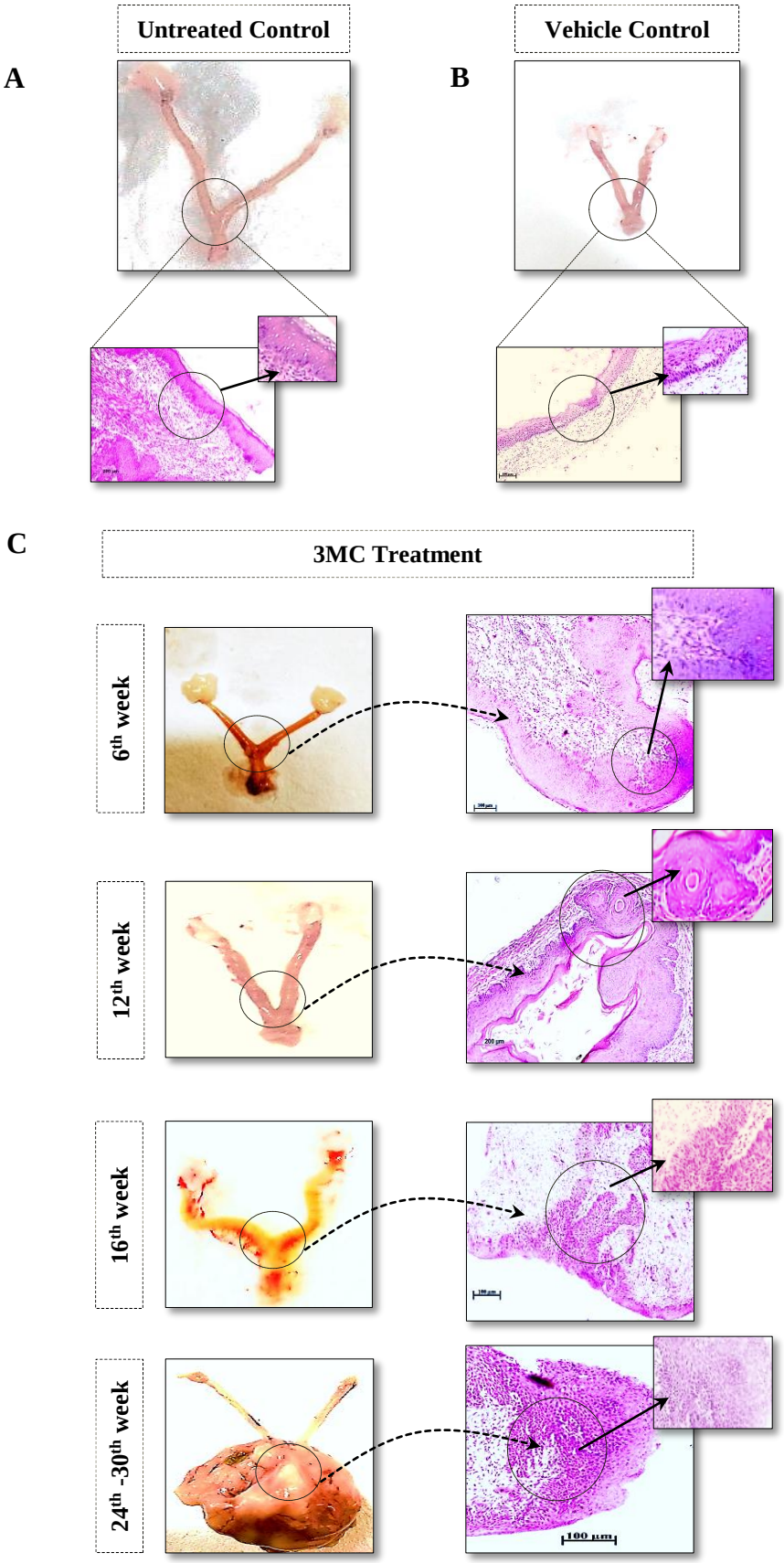

Figure 28: Histopathological (H&E) Characterization: (A-C) Gross Anatomical appearance of mice reproductive organs in addition with their relative cervical histology for -(A) untreated control, (B) vehicle control and (C) 3MC treatment batches [Magnification: 200X; Scale bar: 100µm].

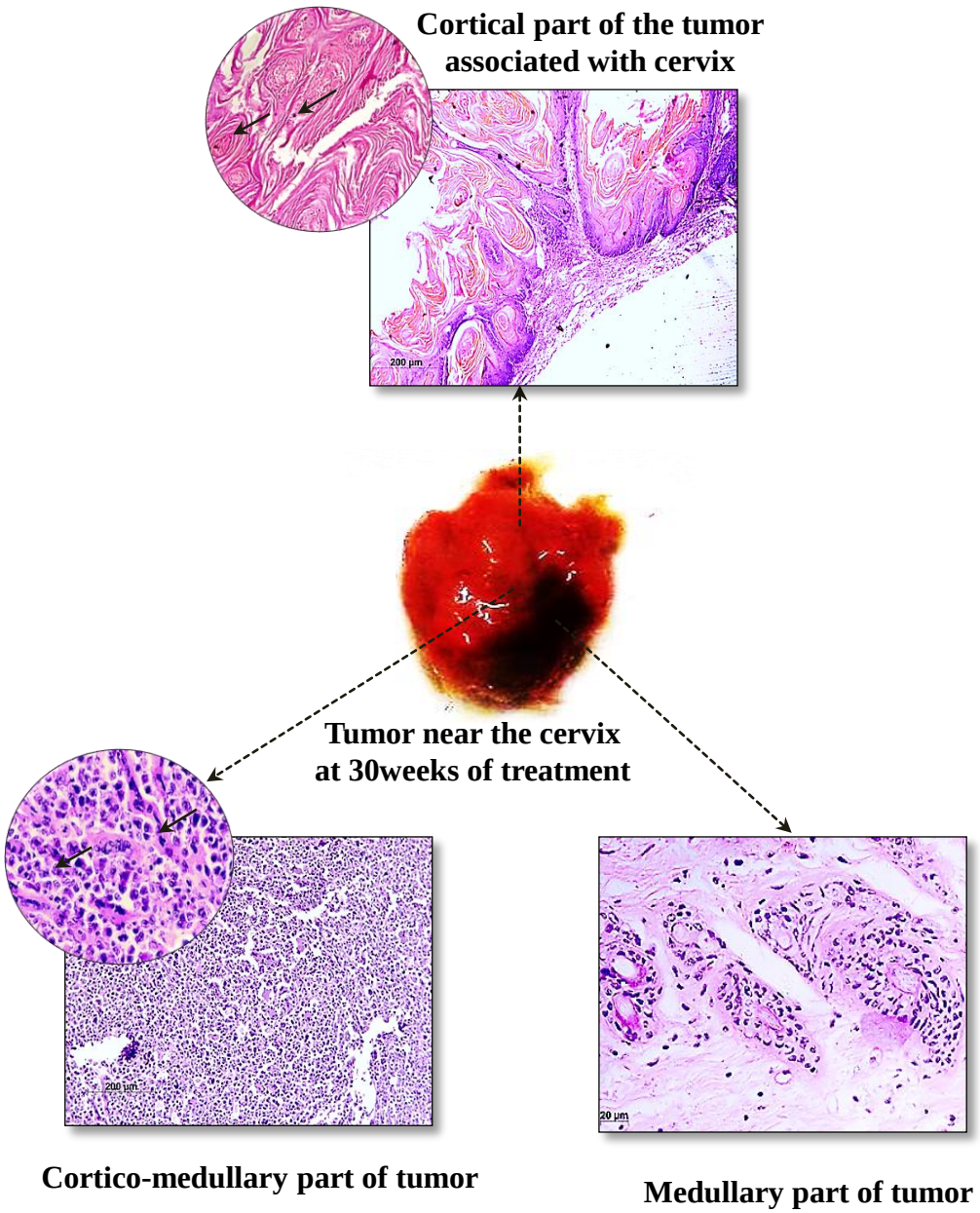

Figure 29: Histopathological Characterization (H&E Staining) of cervical tumor: Region wise histological features of the 3MC induced anaplastic tumor depicting the presence of large keratin pearls (upper panel), giant tumor cells (lower left) and invasive patterns (lower right).

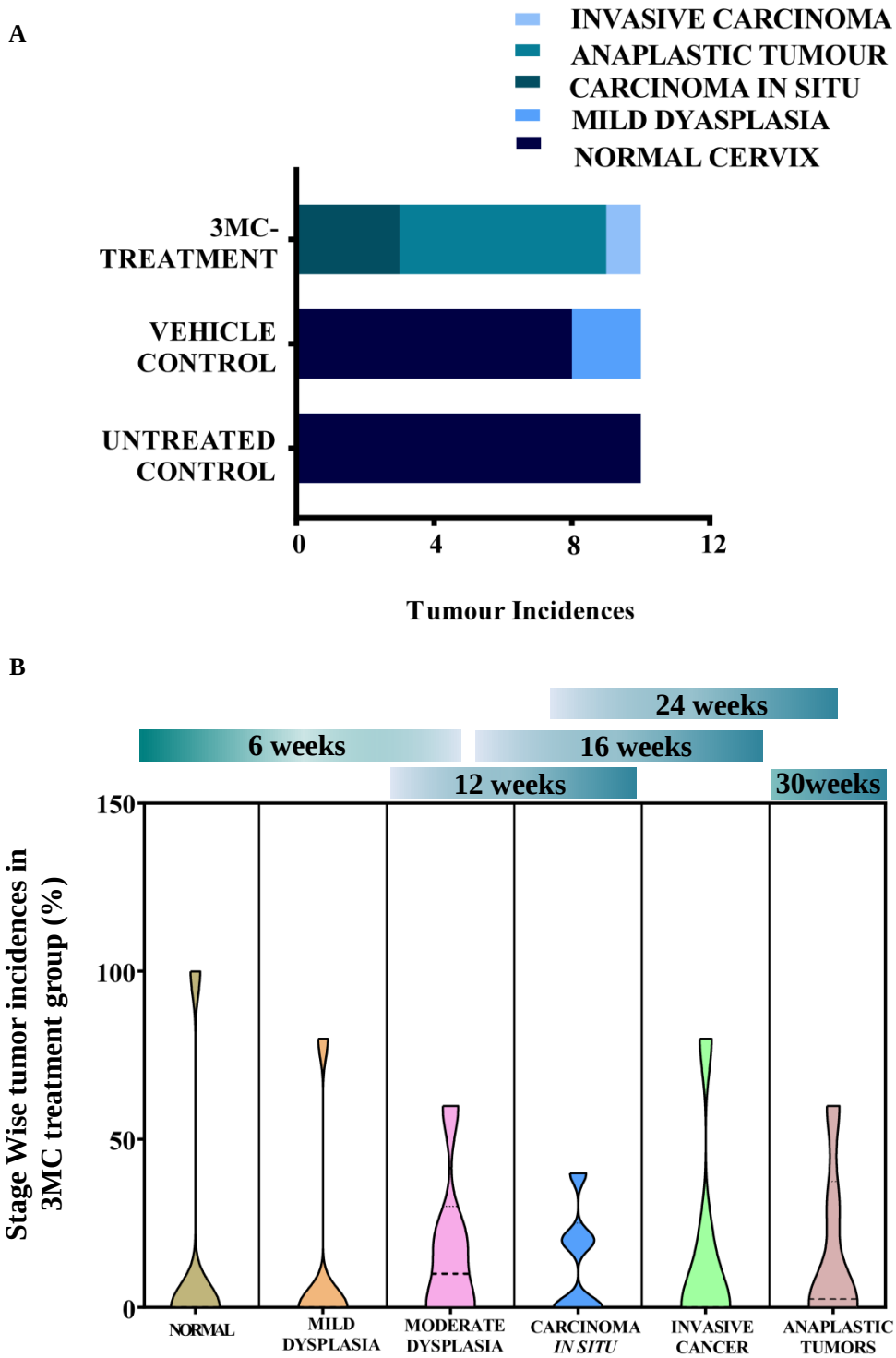

Figure 30: Records of tumor incidences: (A) Different stages of cervical carcinoma observed within the three groups of mice. (B) Stage wise tumor incidences recorded at 6, 12, 16, 24 and 30 weeks of 3MC treated mice of Group-III.

❖ **Systemic changes in mice accompanied chronic 3MC treatment**

Additional changes in systemic organs such as spleen and liver was noticed among mice receiving 3MC treatment chronically upto 16^{th} week and more. Comparative overview of the splenic anatomy and histology as portrayed in Figure 31A upholds detection of splenomegaly among 3MC treated mice at 16^{th} week which was absent in untreated control and vehicle control mice groups. As a confirmation of Pap smear delineations, splenic histology was thoroughly studied further for its potential in being a systemic source of leukocytes augmenting cervical inflammation. 3MC treated spleens exhibited profuse eosinophil infiltrations along with increased number of 'germinal centres' with intense eosin stained peripheries (indicated by arrows) as opposed to those from vehicle control and untreated control mice. This envisages the impact of the systemic stress induced by carcinogen treatment.

Coherent alterations in hepatic histology were also noted in these 3MC treated mice (Figure 31B). Presence of mononuclear infiltrates, necrotic hepatocytes alongside damaged portal tract bearing bile duct proliferation and marked atypia were well noted in their liver histological sections. Contrarily, an absolutely normal hepatic histology showing normal central veins with no evidence of hepatocyte injury, fibrosis or dysplasia and malignancy was found among untreated and vehicle control mice. These cumulative findings indicated that 3MC incited systemic organs to foster chronic inflammation in the cervix for promoting cervical carcinogenesis.

❖ **Dysregulated *in vivo* toxicity parameters intricately associated with 3MC mediated abnormal splenic and hepatic histologies**

In order to ascertain if remodelled splenic and hepatic histologies catered to overall loss in physiological hormesis, liver function and kidney function tests were

carried out. Biochemical assays like estimation of serum SGPT, SGOT and ALP activities were undertaken in addition with measurement of serum creatinine levels. Relative trends in alterations of these *in vivo* toxicity parameters are demonstrated in Figure 32 (A-D). For SGPT and SGOT enzymes, an uprising trend in their respective activities was observed after 4 to 5weeks of 3MC treatment. These surged significantly (SGPT: 12.3±0.261; SGOT: 20.62±0.759) by 6^{th} week of 3MC treatment with respect to untreated and vehicle controls (Figure 32A & B). This escalation of enzymatic activities exhilarated further with progression of 3MC treatment through 12^{th} -16^{th} week. By 24^{th} to 30^{th} weeks, an eventual stasis was achieved. A similar increasing pattern in activities of serum ALP was also observed (Figure 32C). No change in serum enzyme activity was documented during the initial 6weeks of 3MC treatment. However, with treatment duration reaching 12 weeks, the serum ALP kinetics were recorded as 3.4±1.032 IU/L. This was extremely higher when compared to untreated control or vehicle control mice batches. Significant increase in enzyme activity was apparent when treatment progressed to 16 weeks and more. Once again, ALP activity of vehicle control mice was comparable with untreated control batches. High SGPT, SGOT and ALP activities therefore coherently associated with hepatic histopathological alterations in 3MC treated animals specifically.

Consistently elevated serum creatinine levels were maintained in 3MC treated groups between 12 to 30 weeks which was initially missing in the 6^{th} week (Figure 32D). Creatinine titres in the serum varied gradually to significantly peak (2.4 ±0.072 folds) by 12^{th} week onwards. These changes were not attained in vehicle control or untreated control batches. Hence, an abysmal profile of *in vivo* toxicity parameters was suggestive of a systemic physiological fall out among 3MC treated mice.

❖ **Chronic 3MC treatment promoted systemic inflammation by mediating free radical outburst and genotoxicity**

Free radical generation also characterizes the maintenance of inflammatory states. Therefore, impact of 3MC mediated splenic, hepatic and renal impairment upon systemic inflammation profiles was further ascertained in terms of quantifying ROS, RNS and iNOS activity among the blood leukocytes and peritoneal macrophages. Figure 33 (A-C) elaborates relative interpretations of these findings with reference to untreated control and vehicle control mice. In 3MC treated mice, a significant appraisal in ROS levels were noted from 16^{th} week onwards (Figure 33A). ROS levels kept on rising thereafter and peaked at 24^{th} week. These observations allied with the escalating trends of RNS levels in the mice peritoneal macrophages (Figure 33B). Nitrite generation was also documented to rise from 16^{th} week (3.813± 0.00686µM/10^6cells/min) which reached highest levels by 30 weeks. Both of these findings corroborated with the activity trends of iNOS as shown in Figure 33C. In the 16^{th} week, the optimum iNOS activity produced citrulline at rates of 11.89± 0.15311% which increased manifold in the 24^{th} and 30^{th} weeks.

To ascertain whether inflammation imposes systemic genotoxic stress, single cell gel electrophoresis assay or comet assay was performed with the leukocytes isolated from mice blood of all the three groups. Figure 34A displays the distribution patterns of damaged DNA among 3MC treated mice. Results revealed distinct DNA-tails among 3MC treated groups with incremental time period of carcinogen administration. Among vehicle control mice, presence of such damage was absent. Figure 34B reaffirmed a concomitant rise in comet tail moment among 3MC treated mice. All these findings were suggestive of free radical outburst and eventual genotoxic stress being the originators of systemic stress.

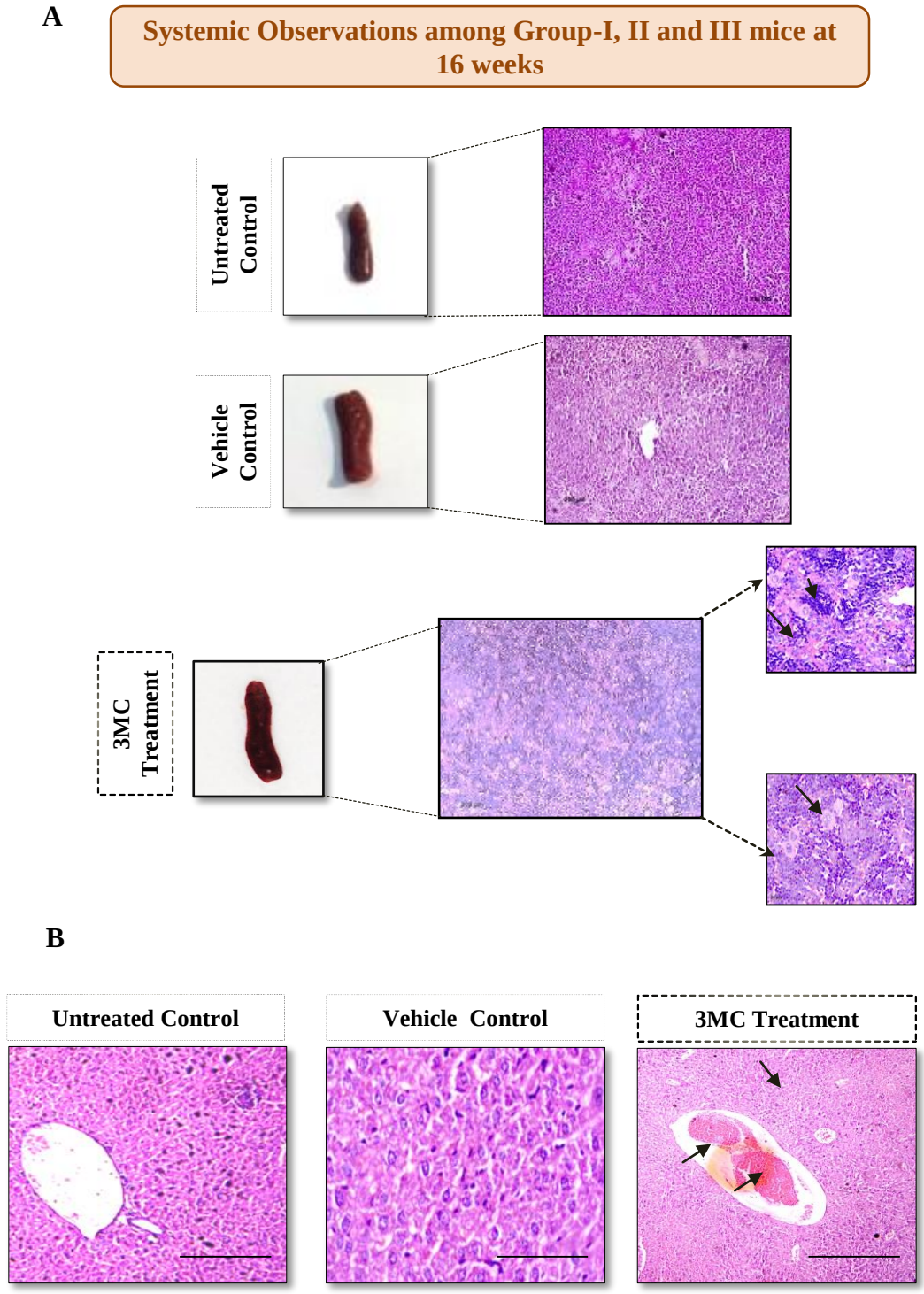

Figure 31: Splenic and Hepatic Histopathological Abnormalities: (A) Representative anatomy of spleen alongwith their relative histology from Group-I, II and III mice. (B) Murine Hepatic histopathology (H&E) displaying characteristic pathological marks in Group III mice evidential for development of invasive carcinoma [Magnification: 400X; Scale bar: 20µm].

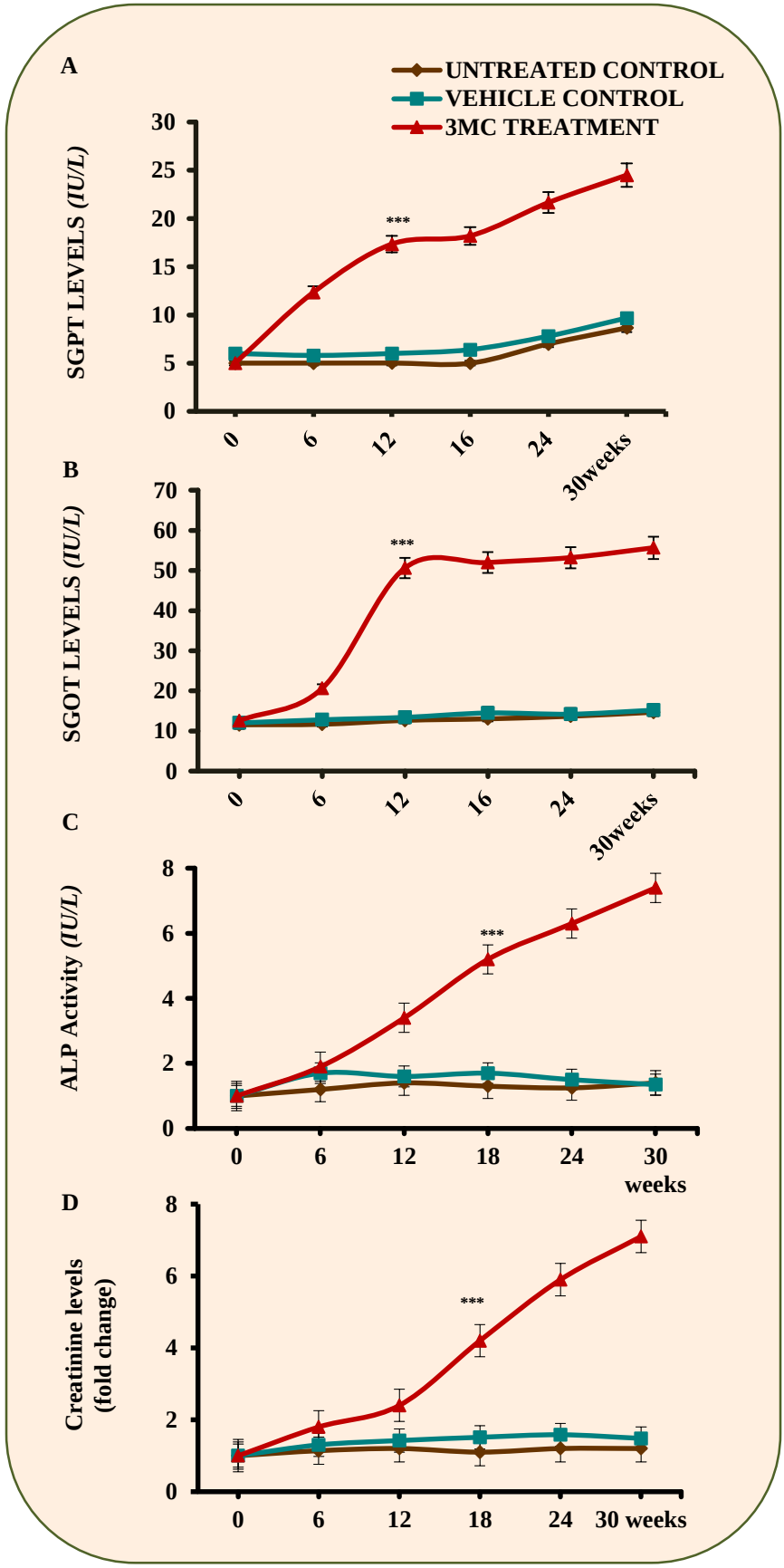

Figure 32: *In vivo* (Systemic) toxicity parameters: Comparative levels of Serum (A) SGPT (B) SGOT (C) ALP activity and (D) Creatinine the of Group I, II and III mice. Values are represented as Mean ±S.D ($^{***}p<0.0001$)

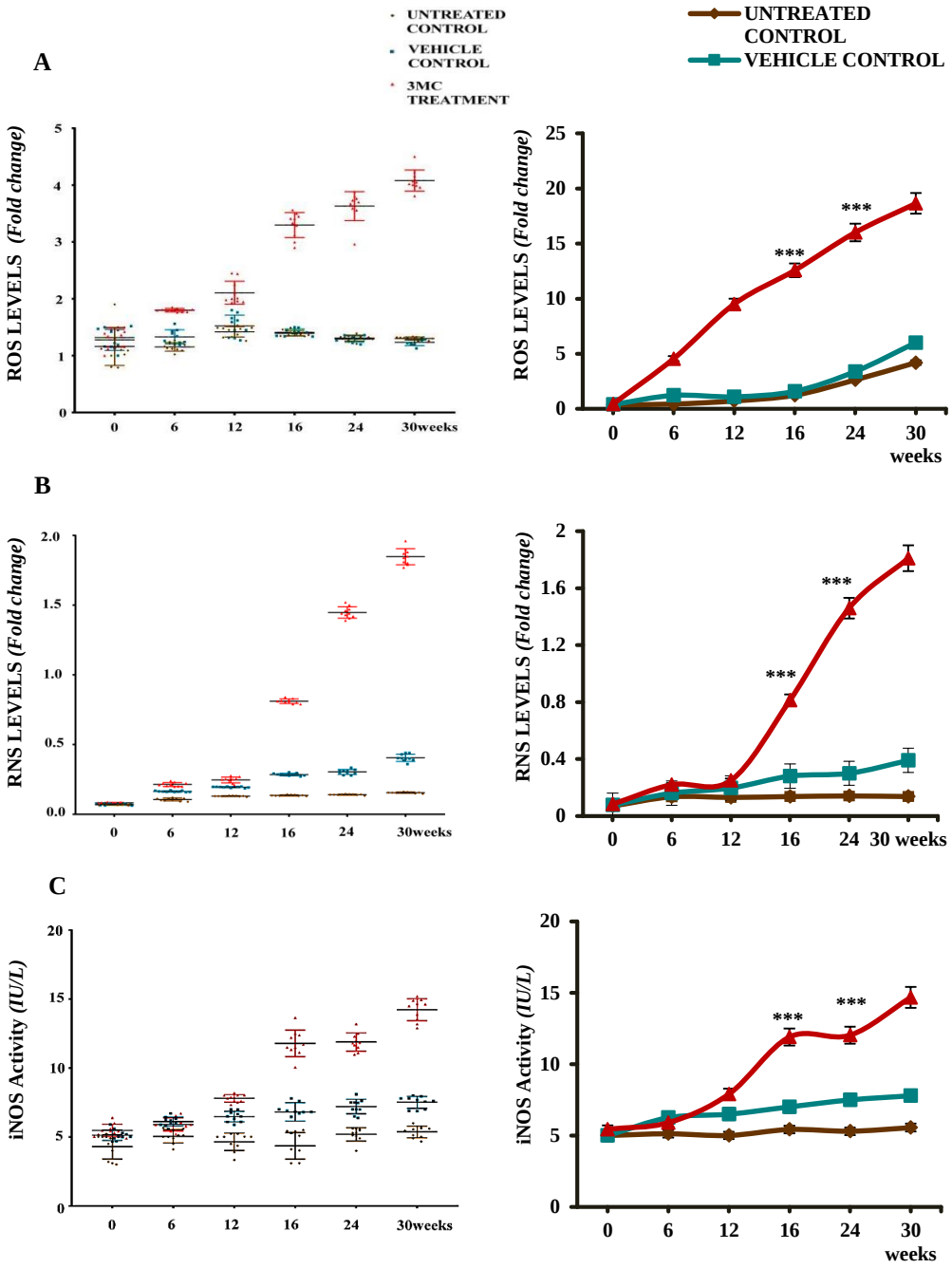

Figure 33: Systemic Biochemical Parameters: Comparative levels of (A) Systemic ROS (B) Systemic RNS and (C) Systemic iNOS activity in the blood of Group I, II and III mice. Values are represented as Mean ±S.D ($^{***}p<0.0001$)

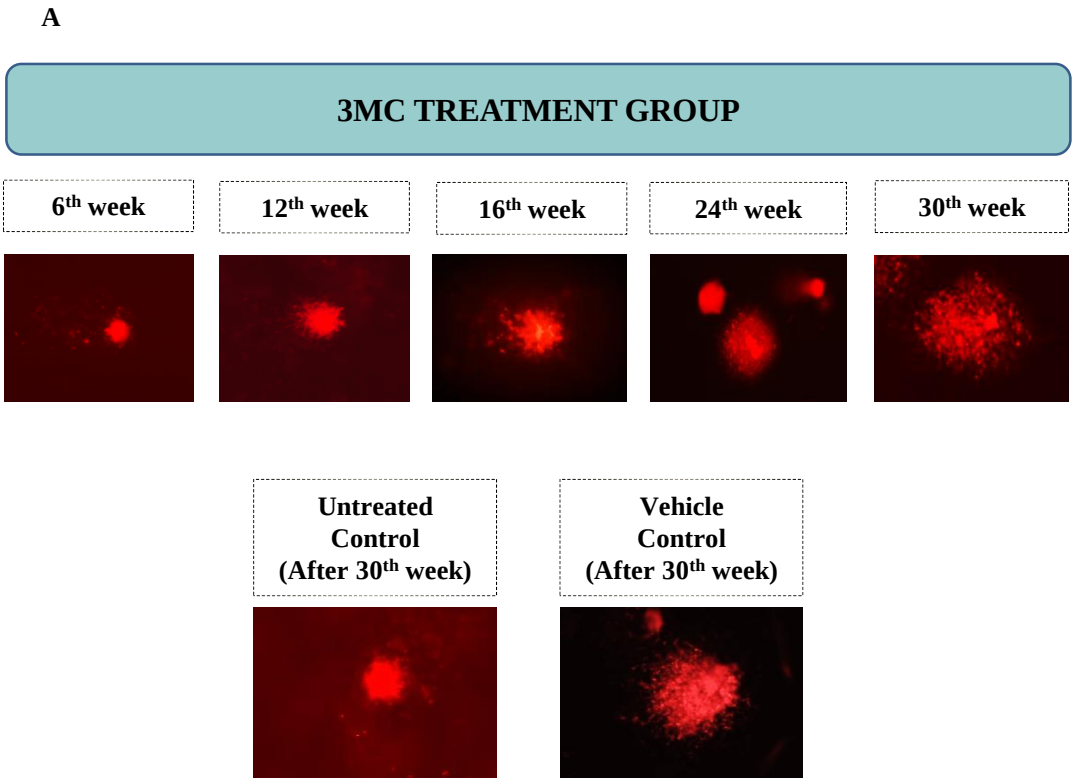

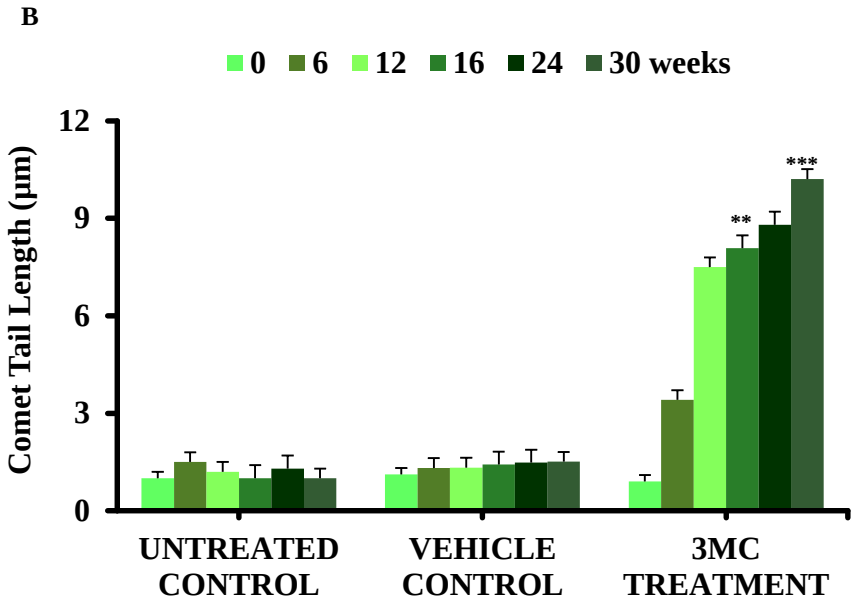

Figure 34: Carcinogenesis associated Genotoxicity Assessment (Comet Assay): (A) Fluorescent micrographs depicting 3MC induced progressive changes in DNA damage of leukocytes isolated from Group-III mice in relation to untreated control (Group-I) and vehicle control or Group-II. (B) Calculated Comet Tail moment plotted graphically for deduction of treatment time dependent DNA damage trends among the three groups. Values are represented as Mean ±S.D ($^{***}p<0.0001$; $^{**}p<0.05$)

❖ **Chronic Systemic Inflammation Reinforced Inflammogenesis of Cervical Cancer upon 3MC treatment for 30weeks**

Time dependent biochemical and molecular characterization of isolated samples was carried out to unveil the direct impact of systemic inflammation upon cervical tumorigenesis. Figure 35 illustrates the schematic work plan followed to investigate the same. Characterization process was initiated with comparative quantification of free radical titres and total antioxidant capacities of cervical tumor cells followed by assessment of inflammatory cytokine levels and expressions.

As shown in Figure 36 (A-D), a corroboration of systemic ROS, RNS and iNOS levels were detected among malignant cells isolated from cervical tissues or tumors collected intermittently. Cervical ROS (Figure 36A) increased exponentially from 12^{th} and 16^{th} weeks of 3MC treatment to reach sustained levels by 24^{th} and 30^{th} weeks. Similar trend was followed by RNS which peaked gradually with acceleration of 3MC exposure (Figure 36B). A hormesis in RNS levels were achieved by 30 weeks. This was confirmed to be facilitated by escalated iNOS activities within the cervical cells (Figure 36C). About 10.23 IU/L and 14.06 IU/L of iNOS enzyme yielded in RNS magnification through 12 and 16 weeks of 3MC exposure. Both iNOS and RNS levels equilibrated with significant escalation in the successive 24 and 30 weeks (Figure 36B & C). In accordance with these findings, the total antioxidant enzyme capacities were enumerated for all the three batches (Figure 36D). The free radical outburst in the cervical cells was found to be facilitated by unusual trends in the cellular antioxidant enzyme actions. The graphical overview of Figure 36D clearly depicted a stochastic rise in free radical scavenging activity up to 12^{th} and 16^{th} week of carcinogen treatment which subsequently declined by 24^{th} and 30^{th} week. In the vehicle control group, this free radical scavenging functioned properly even after 30

weeks of PET exposure and were thus comparable with untreated control. This subtly surging kinetics of anti-oxidant enzymes quenched the PET generated mild free radicals which otherwise went unchecked in the carcinogen treated groups especially after 16 weeks. Indeed, the definite impact of inflammation was apparent in the systemic as well as localized levels.

In conjugation with free radicals, quantitates of cytokines namely IL6, IL8, IL10 and TNF-α were also estimated to comprehend their role in intensifying inflammation within murine cervix (Figure 37A). Herein, 3MC treatment duration dependent gradual rise in IL6, IL8 and TNF-α titres was viewed. Their levels got detectable from 6^{th} week onwards unlike the vehicle and untreated controls. A surge in IL6 activity in the mice cervix by 81.2±0.7307 fold was noted during 24^{th} week of treatment. No significant alteration in IL6 and IL8 quantitates was however observed (IL-6:3.9±0.193; IL-8: 5.2 ±0.09) among untreated control mice. IL6 and IL8 activities were extremely high in the cervix of mice which received 30 weeks of 3MC treatment. TNF-α followed up with similar patterns while IL10 did not show any significant variation all this while. For further validation, western blot analysis was performed to study the expressions of these escalated cytokines in the isolated cervix tissues of all experimental batches (Figure 37B). In untreated control and vehicle control groups, expression profiles of these cytokines were poor while it increased considerably across the 3MC treatment group. Expression profiles of IL6, IL8 and TNF-α strongly corroborated with their activities. STRING Interactome results asserted that activation of these cytokines closely relates with that of NFκB (p65) subunit thereby hinting at inflammation mediated prosurvival upregulation (Figure 37C). All these findings collaboratively established that chronic 3MC treatment induced inflammogenesis of cervical cancer.

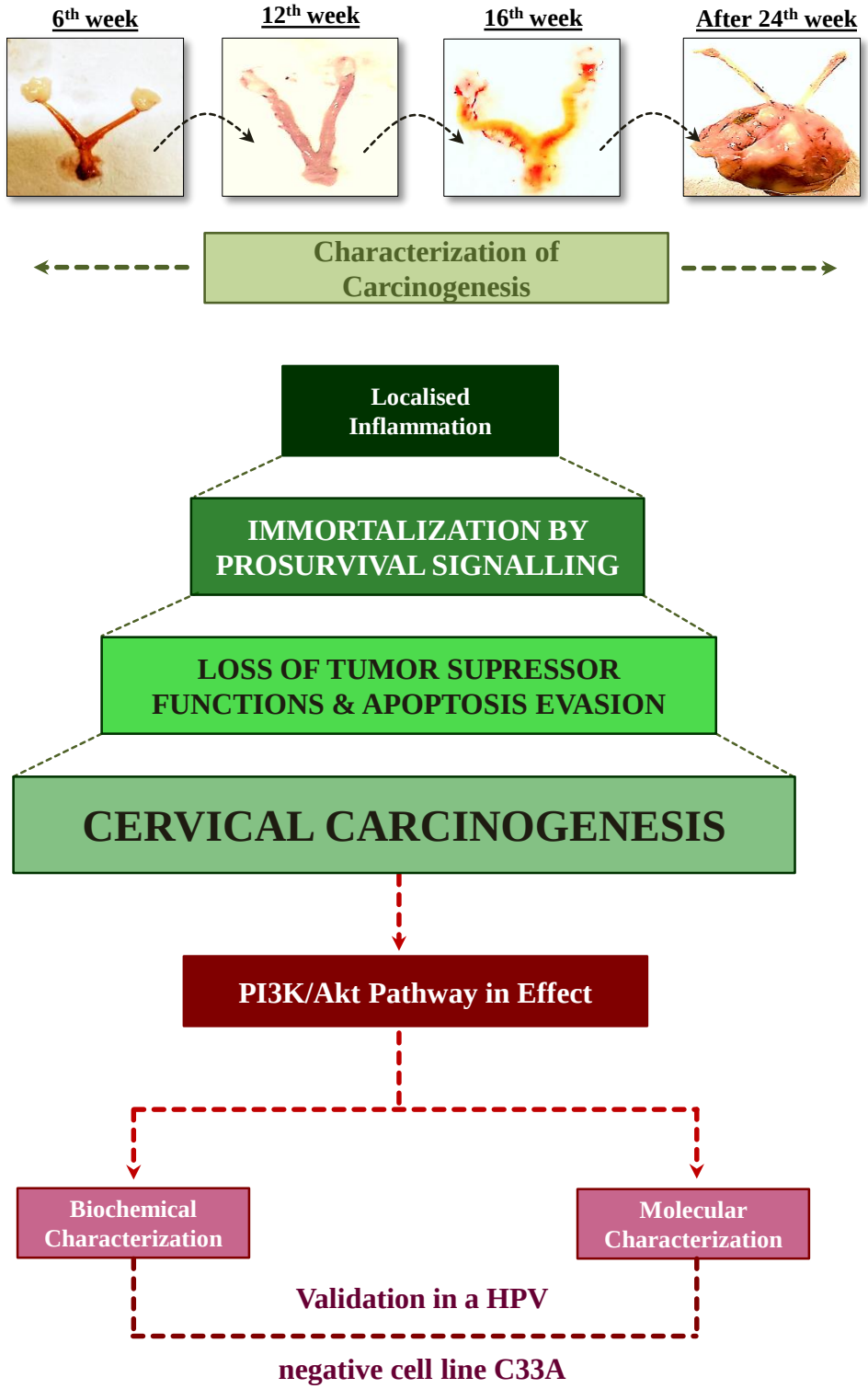

Figure 35: Elaborated Work Plan for Characterization and Validation of Cervical Carcinogenesis *in vivo*

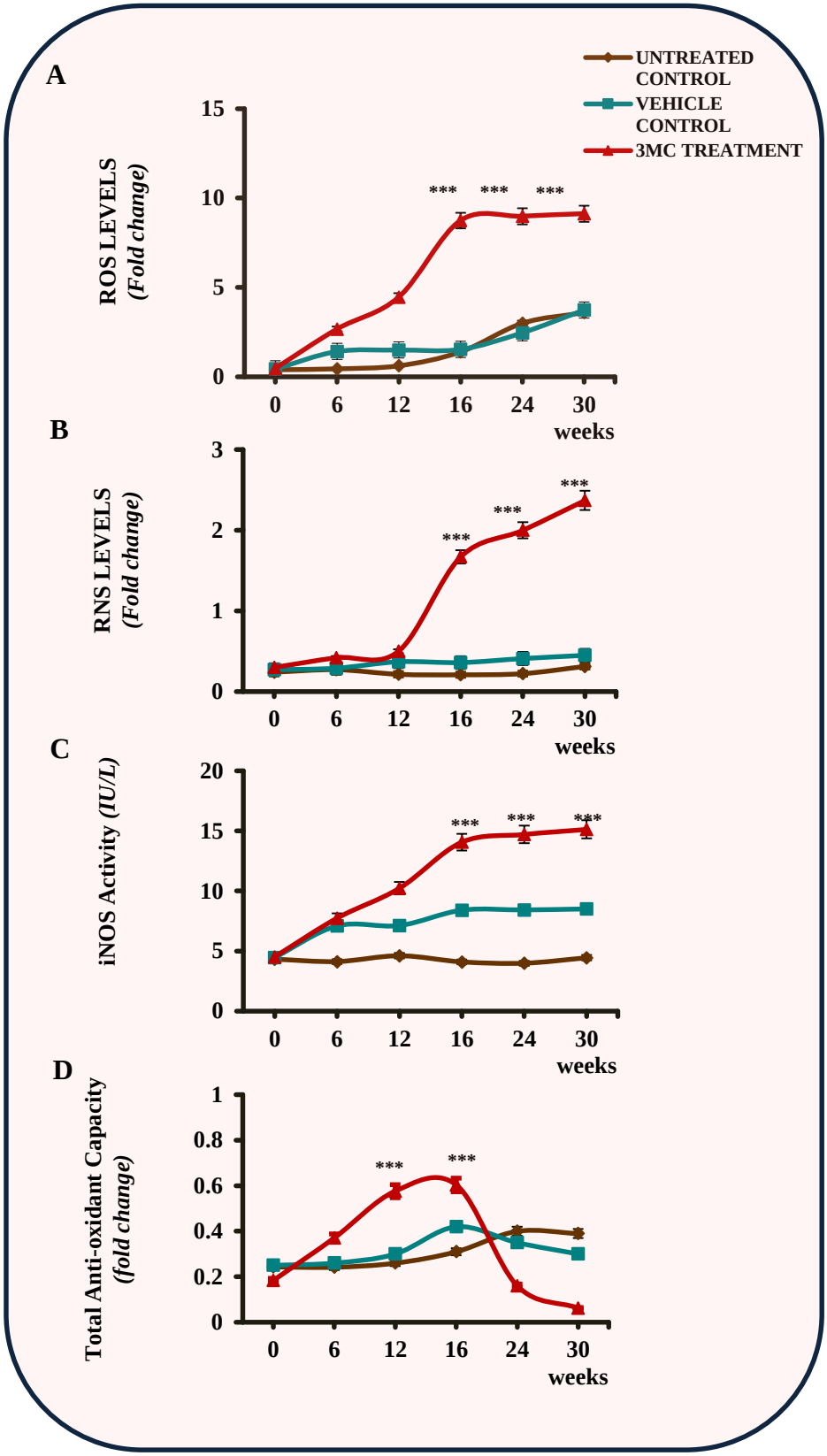

Figure 36: Stage wise Biochemical Characterization:(A) ROS levels (B) RNS levels (C) iNOS activity and (D) Total Antioxidant Capacity in the cervix of Group I, II and III mice. Fold change values were normalized with respect to untreated control and represented as Mean ±S.D (***p<0.0001)

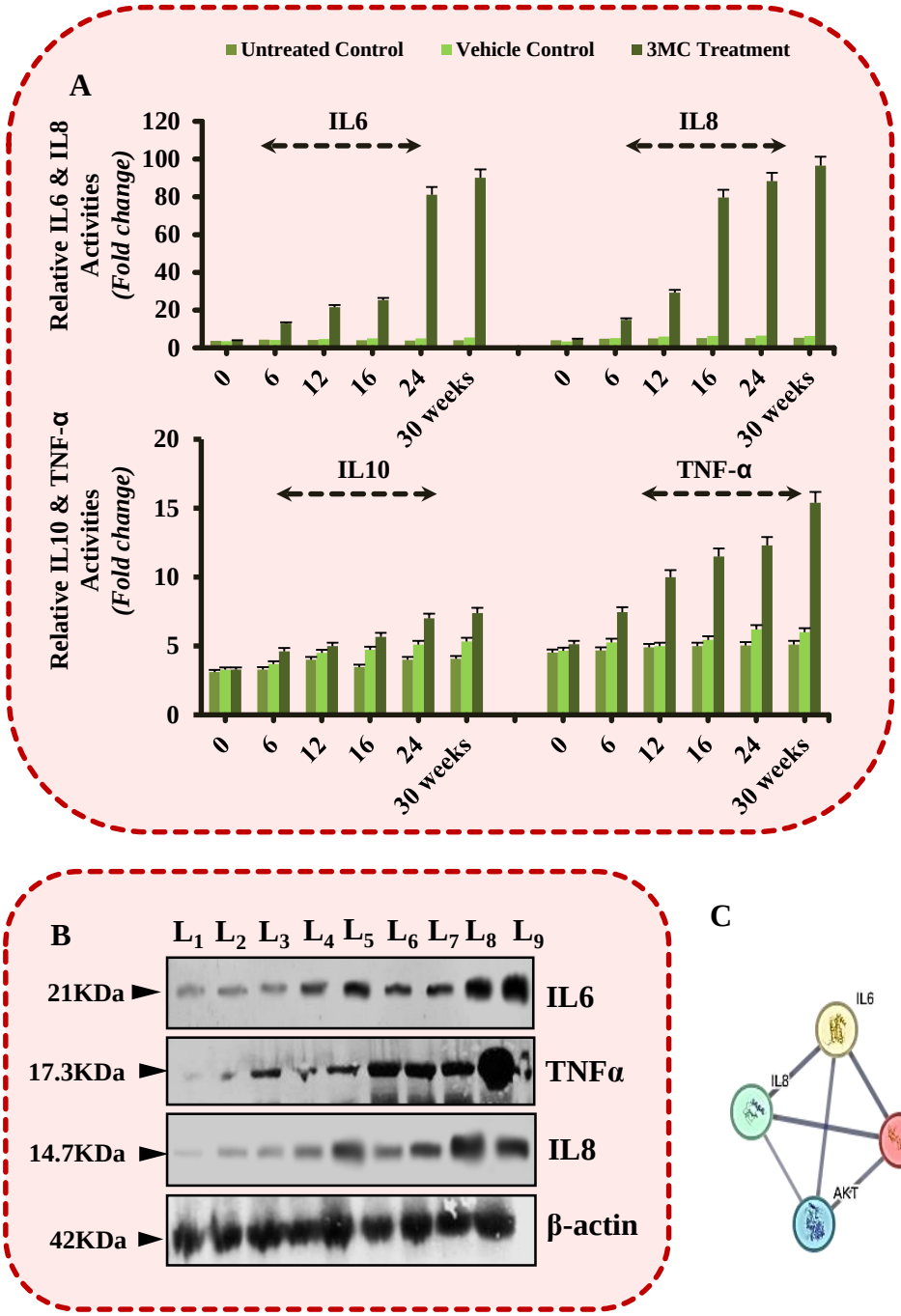

Figure 37: Characterization of Localized Inflammation: (A) Relative Activities of IL6, IL8, IL10 and TNFα. (B) Western Blot bands depicting the expression patterns of these cytokines [Lanes(L): L_1-Untreated Control; L_2-Vehicle Control; L_3-6 week 3MC Treatment; L_4- 12 week 3MC Treatment; L_5- 16 week 3MC Treatment; L_6- 24 week 3MC Treatment; L_7- 30 week 3MC induced tumour's cortex; L_8- 30 week 3MC induced tumour's cortico-medulla; L_9- 30 week 3MC induced tumour's medulla]. β-actin was used as loading control. (C) STRING Interactome delineating possible protein level interactions of cytokines, Akt and NFκB.

❖ **Pro-carcinogenic Cervical Inflammation Resulted from PI3K/Akt Pathway Upregulation**

As portrayed in Figure 38A, growth favouring inflammation is manifested as a cumulative effect of prosurvival upregulation, tumor supressor deregulation and uncontrolled cellular inflammation. Therefore, upregulation of PI3K/Akt pathway was assessed for its role in triggering cytokine surge within the carcinogen treated murine cervix. Ahead of molecular characterization, STRING Database was excavated for the possible interactions of PI3K/Akt pathway effectors, tumor supressors (Rb, p53, p21) and IAPs (XIAP, survivin). The interactome images showcased in Figure 38 (B-D) delineates the presence of close-knitted molecular interaction loops. The prosurvival molecules such as NFκB (p65/p50), Ku70, HIF-1α, VEGF and COX2 were sequentially linked to its master regulator Akt, either directly or indirectly (Figure 38B). Likewise, regulation of tumor supressors appeared to be in close control of Akt (Figure 38C). However, the XIAPs branched apart as the only Akt-interacting IAP whereas survivin emerged as an unrelated one (Figure 38D). This existent information served as a basis for further enquiry of their expression status at protein levels. Western blot bands as shown in Figure 38 (E-G) affirmed that PI3K/Akt upregulation led to unstable tumor supressor expressions and IAP escalation. Figure 38E shows that overexpression patterns of prosurvival molecules varied in close coherence with the 3MC treatment time. It was interesting to note that a gain in expression of $pAkt^{Thr308}$ resulted in recurrence of the same for NFκB (p65/p50), Ku70, HIF-1α, VEGF and COX2. Moreover, a decline in total Akt content among the 3MC treated cervical tissues especially after 6 weeks were evidential for PI3K/Akt activation which also evoked cytokine overproduction. Such an observation was absent among untreated control and vehicle control groups. Relative band intensities of prosurvival effectors

alongwith the inflammatory cytokines espoused an intertwining pattern in their expression profiles which furthermore strengthened this notion (Figure 39A).

Continual inflammation subsequently impaired tumor supressor actions as their expression profiles reduced following 16 weeks of 3MC exposure. As shown in Figure 38F, a gradual fall in protein expressions of p53, p21 and Rb, specifically at and after 16 weeks of 3MC treatment was noteworthy. Such a deregulation thereafter enabled evasion of apoptosis to favour cervical carcinogenic progression as well. Western blot results (Figure 38G) clearly showed a rising pattern for XIAP and survivin proteins in the mice cervical extracts through 30 weeks span of 3MC treatment. Their relative band intensities (Figure 39B) were imperative of inflammation mediated prosurvival upregulation which ultimately favoured malignant transformation of cervical epithelium.

As a confirmation, the expression of proliferative antigen Ki67 was studied by western blot to determine the extent of immortalization (Figure 40A). Results evinced an upregulation of Ki67 among the 3MC treated cervical tissues. On this basis, the spatial distribution of Ki67 was ascertained by IHC (Figure 40B). Herein, Ki67 positive cellular nucleus was discerned among the differential epithelial layers of mice cervix. This was characteristically observed among mice batches receiving 3MC treatment for 16 or 24 weeks or more. On the contrary, these patterns were delimited only to the proliferative basal epithelial cell layers of the untreated control and vehicle control groups. Clear manifestations of uniform staining for Ki67 among 3MC exposed mice were quantified by Allred's Scoring (Figure 41). Maximal cells with highest intensities of Ki67 were noticed among mice batches administered with 3MC for 24 and 30 weeks respectively. Conclusively, inflammation, prosurvival signalling

and tumor supressor ablation synergistically immortalized cervical cells to promote carcinogenic progression.

Validation of these *in vivo* findings was undertaken in a well-established *in vitro* set up using HPV negative C33A cell line (Figure 42). In order to achieve a tumor microenvironment, C33A was allowed to form large viable spheres over a period of 5days (Figure 42A). The conditioned medium collected intermittently was thereafter quantitated for the titres of inflammatory cytokines IL6, IL8, IL10 and TNF-α. The trend curves shown in Figure 42B clearly depicted an escalation in release of IL6, IL8 and TNF-α along the 5days of sphere formation. Cytokine levels heightened at the 3rd day followed by achievement of stasis by the 5th day. All this while, IL10 titres hardly underwent any remarkable change. These patterns were corroborative of *in vivo* findings which thereafter required its affirmation in relation to the expressions of few key effectors of PI3K/Akt pathway. Flow cytometry results shown in Figure 43 delineated detectable expressions of pAkt^{Thr308}, NFκB (p65/p50), XIAP, survivin and Ki67 inside the spheres. About 37.3% and 32.1% of sphere forming C33A cells expressed pAkt^{Thr308} with high and moderate intensities. These were suggestive of PI3K/Akt activation because only 15.4% (high) and 7.9% (moderate) of sphere forming cells were Akt positive. Again, 35.1% and 37.3% of these cells were also positive for NFκB subunits. XIAP got detected in 39.8% of C33A sphere cells whilst only 18.7% of them harboured survivin. A gain in proliferative potential was evident because 48.3% and 34.1% of C33A cells expressed Ki67 antigen with high and moderate intensities. These findings established that PI3K/Akt activation by any means could induce growth promoting inflammation for driving malignant transformations. In this case, a successful development of 3MC induced *in vivo* cervical cancer model with PI3K/Akt pathway upregulation was therefore confirmed.

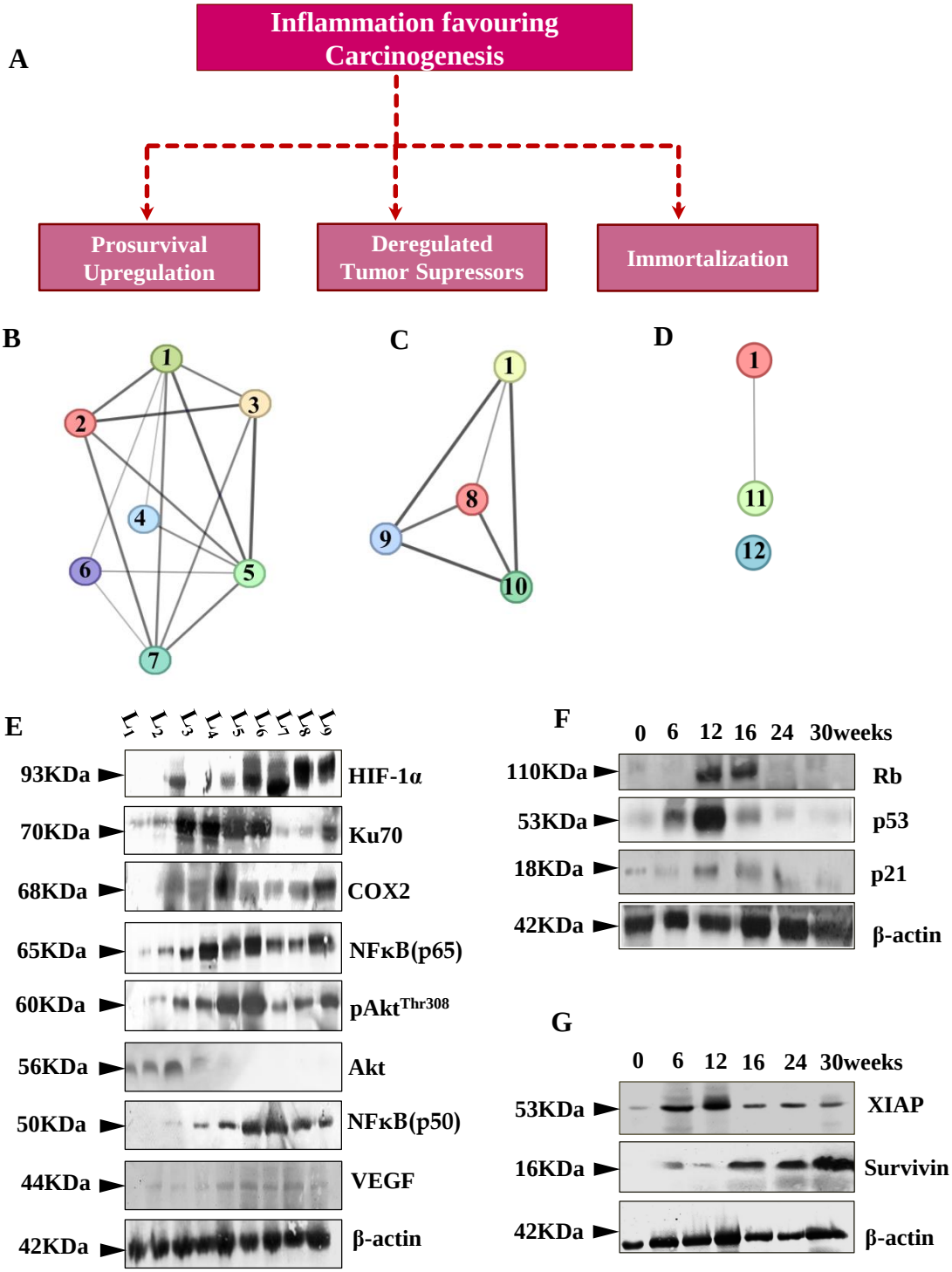

Figure 38: Characterization of Carcinogenic Progression: (A) Depiction of inflammogenic events responsible for cervical carcinogenesis. (B-D) STRING Interactome predicting interactions of Akt (1) with prosurvival effector [p65(2), p50(3), Ku70(4), HIF-1α (5), VEGF (6), COX2 (7)], tumor supressor [TP53 (8), p21 (9), Rb (10)] and IAP [XIAP (11), survivin (12)] proteins. (E-G) Western Blot bands depicting the expression patterns of (E) prosurvival effectors [Lanes: L_1-Untreated Control; L_2-Vehicle Control; L_3-6 week 3MC Treatment; L_4- 12 week 3MC Treatment; L_5- 16 week 3MC Treatment; L_6- 24 week 3MC Treatment; L_7- 30 week 3MC induced tumour's cortex; L_8- 30 week 3MC induced tumour's cortico-medulla; L_9- 30 week 3MC induced tumour's medulla], (F) tumor supressors and (G) IAPs. β-actin was used as loading control.

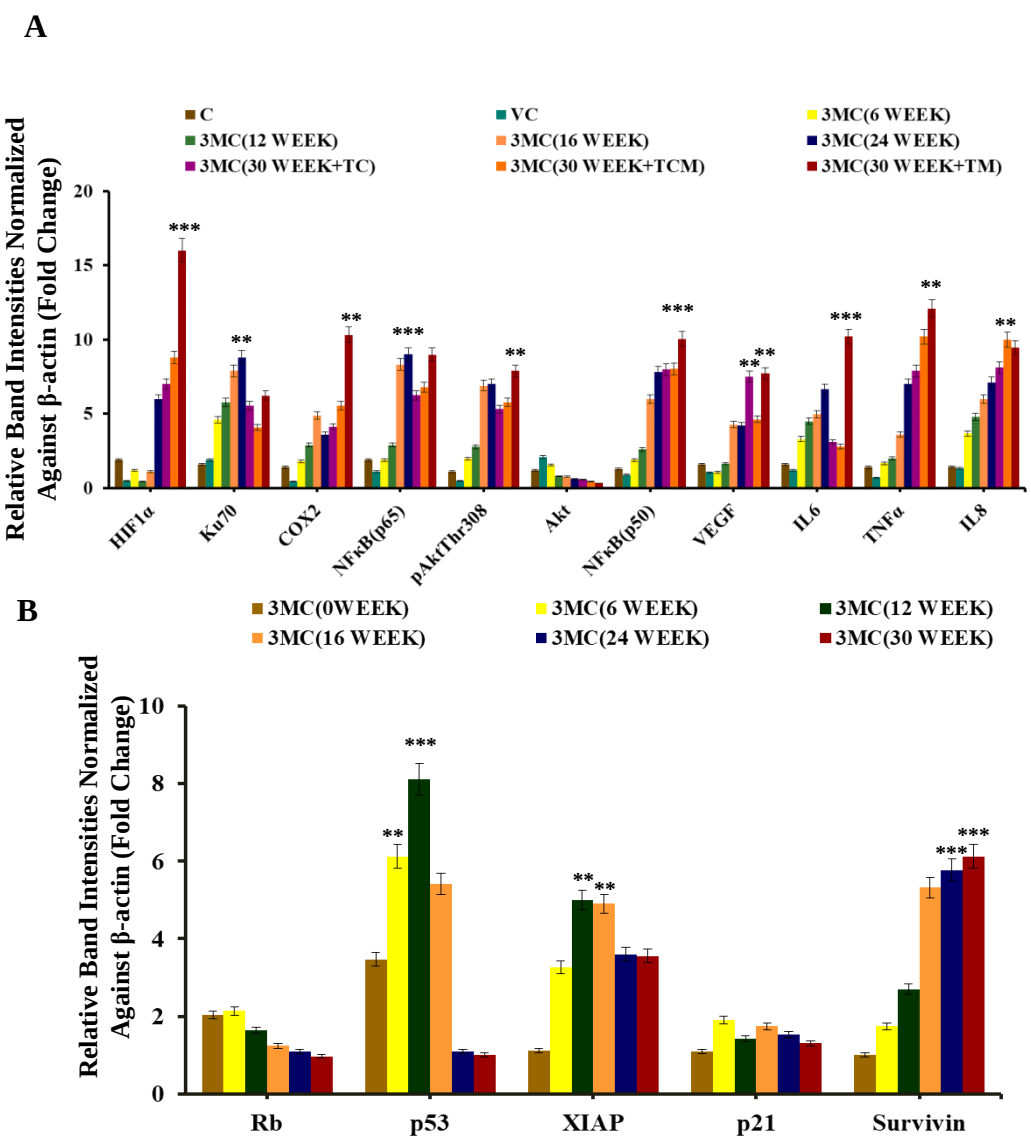

Figure 39: Semi-Quantitative Estimation of Protein Expressions: (A&B) Relative band intensities- (A) prosurvival effectors and inflammatory mediators alongwith (B) tumor supressors and IAPs after normalisation against β-actin. Values are expressed as Mean ±S.D ($^{***}p<0.0001$; $^{**}p<0.05$).

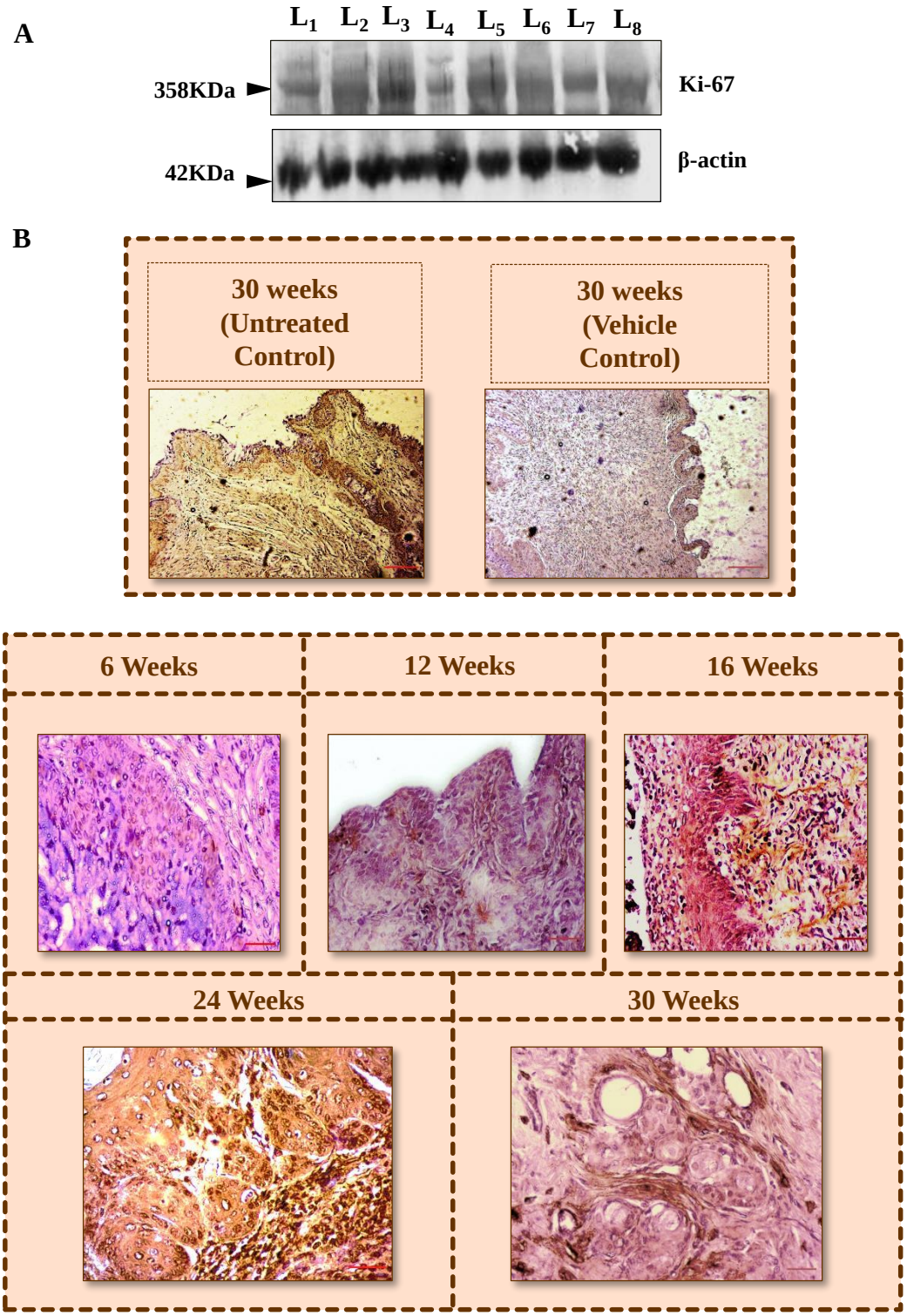

Figure 40: Tissue Specific Expression of Proliferative Antigen Ki67: (A) Western blot bands depicting the expression patterns of Ki67 in whole tissue lysates of mice cervix [Lanes: L_1-Untreated Control; L_2-Vehicle Control; L_3- 6 week 3MC Treatment; L_4- 12 week 3MC Treatment; L_5- 16 week 3MC Treatment; L_6- 24 week 3MC Treatment; L_7- 30 week 3MC induced tumour's cortex; L_8- 30 week 3MC induced tumour]. (B) IHC micrographs showing the tissue specific localization of Ki-67 in the mice cervix [Magnification: 400X; Scale bar: 20µm]. Brown stained nuclei or cytoplasm corresponds to Ki67 positive foci.

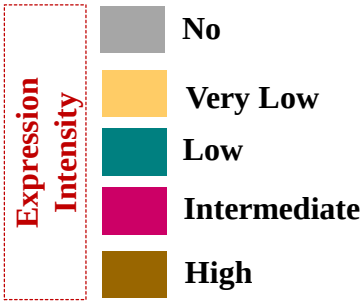

Cellular Layers	Positively Stained Cells (%)					Score				
	6 wk	12 wk	16 wk	24 wk	30 wk	6 wk	12 wk	16 wk	24 wk	30 wk
Basal Layer	5	40	68	91	92	1	2	3	4	4
Parabasal Layer	1	35	75	82	95	1	2	3	4	4
Intermediate Layer	1.5	25	60.1	70	84	1	2	3	3	3
Superficial Layer	0	5	15	65	77	0	1	1	3	3

Figure 41: IHC Scores for Ki-67

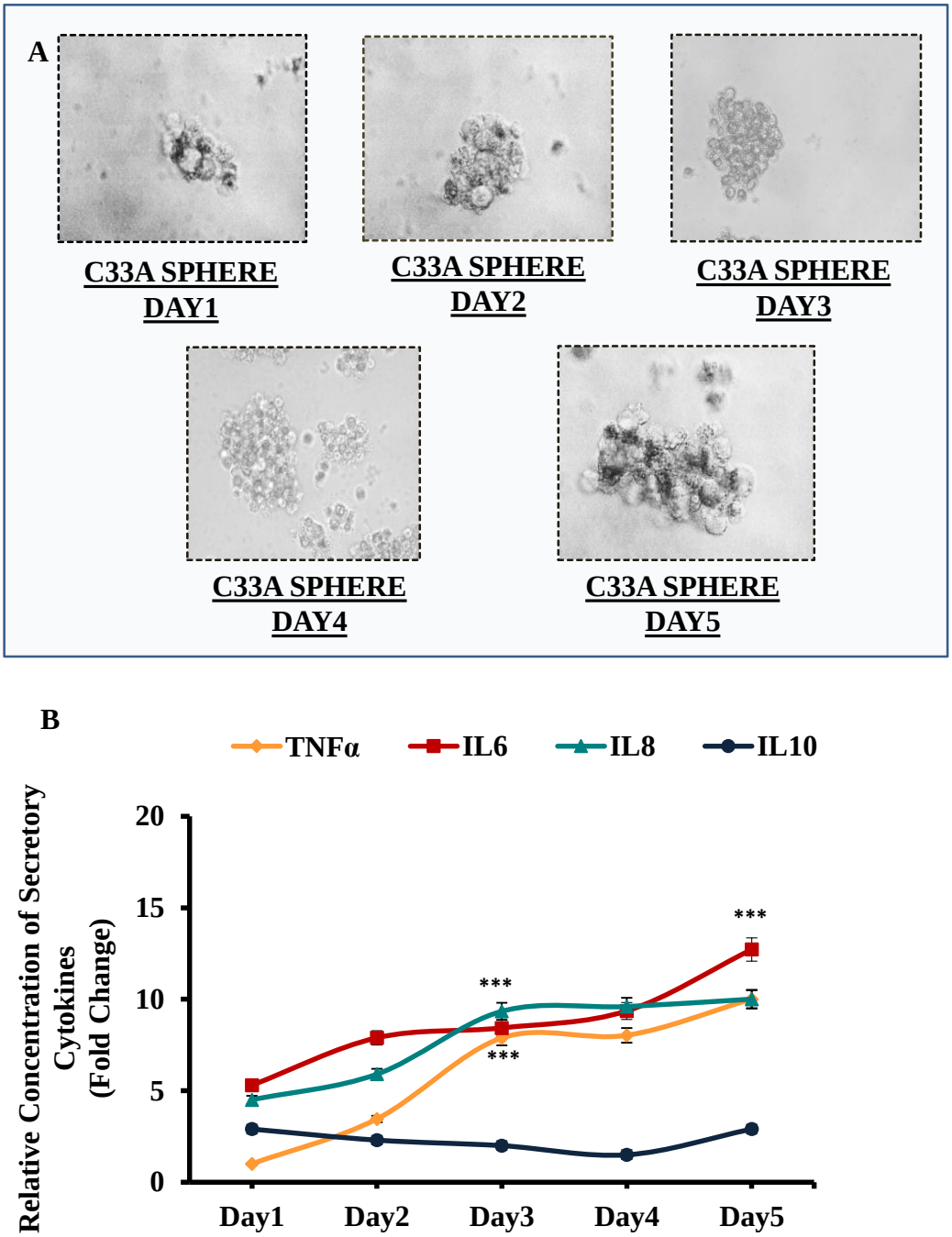

Figure 42: Validation of PI3K/Akt pathway's role in driving HPV negative cervical carcinogenesis *in vitro*: (A) Micrographs revealing Sphere forming ability of C33A cells over a period of 5 days (B) Time dependent quantification of secreted cytokines in the conditioned medium during the event of sphere formation. Relative concentrations were calculated against standard curve and represented as a fold change graph with respect to Day1. Evaluations are represented as Mean ± SD ($^{***}p<0.0001$).

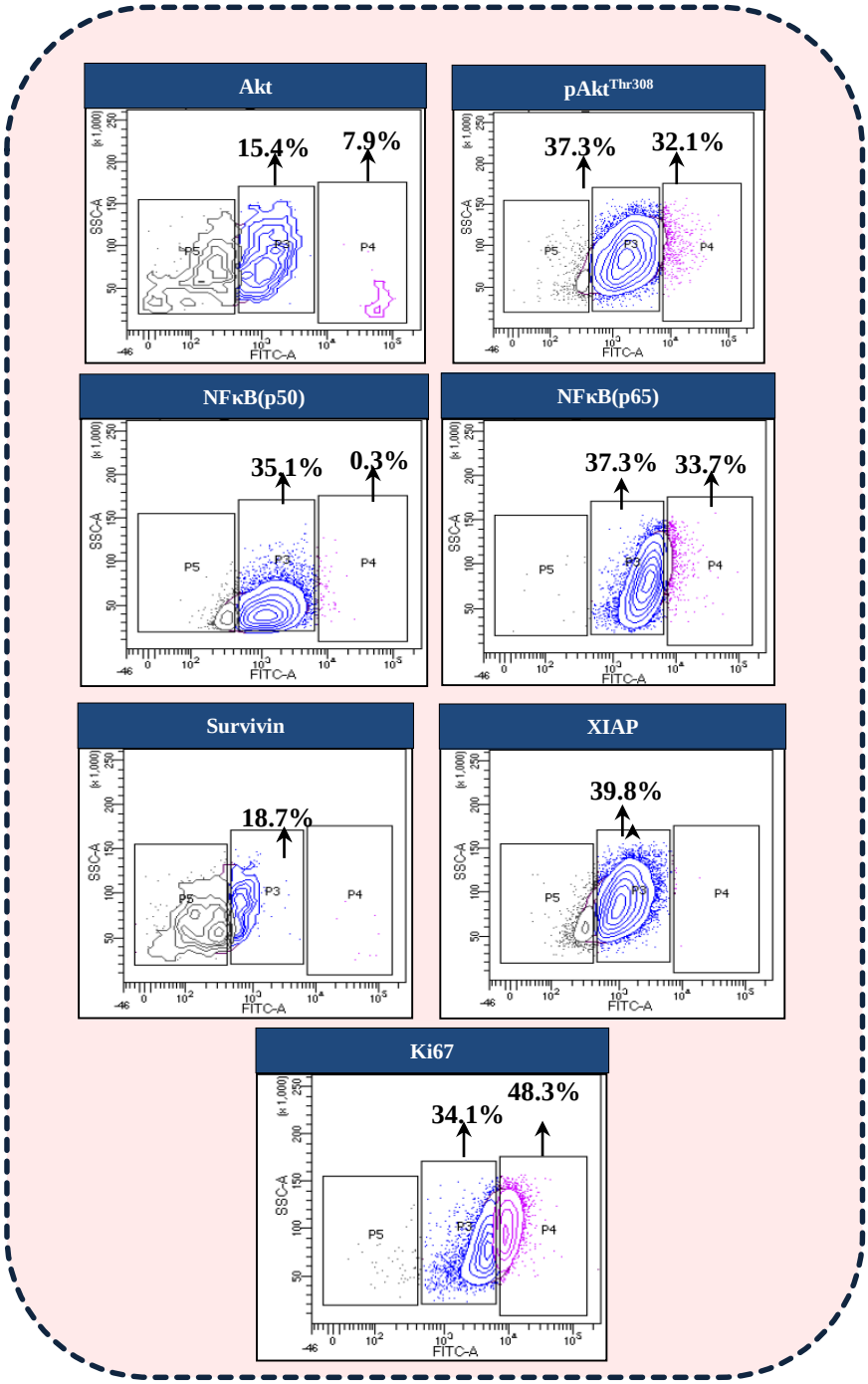

Figure 43: Cell Specific expression patterns of Key PI3K/Akt pathway effectors in C33A spheres obtained at 5th day: Flow cytometry contour plots depicting the expressions of Akt, pAkt^{Thr308}, NFκB (p65/p50), IAPs and Ki67.

❖ **Inflammation Enriched Cervical Tumor Microenvironment with PI3K/Akt Pathway Upregulation were CDDP Resistant**

Once the *in vivo* cervical cancer model was established, invasive cancer stages developed by the 16th week were directed for assessment of CDDP-responsiveness. Figure 44 upholds the overall work plan followed for determining the effect of the molecular underpinnings of a TME on CDDP response. Ahead of CDDP administration for this purpose, a dosimetry was undertaken for selection of the 'Maximum Tolerated Dose (MTD)' which was safe for treating the invasive cancer bearing mice. Thereafter, a 2 week CDDP chemocycle regimen was observed for characterization of drug responsiveness by estimating the altered profiles of biochemical parameters, PI3K/Akt effector and CDDP exporter expressions.

In the process of dosimetry, invasive cancer bearing mice were distributed among three separate batches receiving 1mg/kg body weight, 3mg/kg body weight and 5mg/kg body weight of CDDP respectively. Thereafter, these mice were profiled for their possible fluctuations in *in vivo* toxicity parameters, body weight and survivability. As shown in Figure 45, the CDDP dose of 3mg/kg bodyweight induced median and tolerable alterations in these factors compared to the other two doses. Herein, 3mg/kg body weight of CDDP was the MTD chosen to be the safest for treating mice henceforth.

Invasive cancer bearing mice were intraperitoneally injected with MTD of CDDP for 2 consecutive weeks followed by monitoring of the resultant molecular and biochemical variations within their cervix. As portrayed in Figure 46 (A-C), a concomitant upregulation in the protein expressions of PI3K/Akt effectors was apparent. These molecules were the decision makers for CDDP response to the cervical tissues. Western blot bands exhibited in Figure 46A, vividly confirmed that

the prosurvival effectors overexpressed with extended period of incoming chemotherapy in relation to their constitutive status associated with invasive cancer stages. As stated in the relative band intensities, expression profiles of $pAkt^{Thr308}$ increased eventually while that of total-Akt espoused a significant gradual decline. These findings were suggestive of PI3K/Akt pathway being in effect of a presumptive remodelling of the TME upon CDDP encounter. However, the downstream effectors of this pathway namely NFκB (p65) and NFκB (p50) showed an antagonising trend in their expression profiles (Figure 46A & B). The p65 subunit expressed in an intensity which was 3.78 fold higher among invasive cancer stages in the 2^{nd} week of CDDP treatment than those in 1^{st} week. Hereby, a reduced expression of p50 subunit was noted. Interestingly, the expression trends of p65 matched those of PXR protein which is further reported to partner with p65 for promoting the translation of CDDP exporter pumps (Figure 46A & B). In alliance with these findings, CDDP exporters such as MRP2, ATP7A and ATP7B surged by manifolds with progression of chemotherapy cycles to 2 weeks. All this while, XIAP and survivin protein titres kept on peaking significantly which were affirmative of the tumor being resilient to CDDP induced apoptosis. Possible prevalence of this signalling nexus got verified in the STRING Interactome study (Figure 46C). Results obtained clearly supported the possible interactions of the prosurvival molecules making up PI3K/Akt pathway and CDDP exporters alongwith PXR being the mediator. So, a revalidation of these western blot findings were done by performing IHC studies where the tissue specific expression profiles of PXR, NFκB (p65), NFκB (p50), XIAP and survivin was closely discerned. Micrographic exhibits of Figure 47 displayed that an intensified nuclear PXR localisation intertwined with the same for p65 subunit. A characteristic nuclear localization of these antigens became more prominent as CDDP administration time

progressed to 2 weeks. On the contrary, the nuclear presence of p50 diminished gradually as was evident from the clear and distinct cytoplasmic signals rising along the chemocycles. These observations were assertive of the combinatorial role of p65 and PXR in mediating CDDP exporter expressions. Again, XIAP and IAP presented cytoplasmic localization which positively allied with their function status. Table 4 enlisting the respective scores of these IHC results corroborated with the microscopic findings. All these observations were suggestive of a role played by incessant PI3K/Akt pathway upregulation in imparting CDDP unresponsiveness.

A measure of chemotherapeutic efficacy positively correlates with therapy response. To ensure biochemical basis of CDDP insensitivity, cellular drug response towards CDDP was quantified in terms of enumerating Total GSH content, ROS levels and Rhodamine accumulation (Figure 48). Interesting observations were attained in terms of basal GSH espousing an escalating trend even after CDDP challenge for 2 consecutive weeks. This pertained with an unchanged profile of ROS and Rhodamine accumulation which suggested that CDDP failed to perturb the mitochondrial membrane potentials for enabling ROS outburst. Taken together, these observations summarized the inhibitory effect of a basally upregulated PI3K/Akt pathway upon the chemotherapeutic efficacy of CDDP as well as the chemoresponsiveness of the cancer cells.

- **PEITC successfully restricted tumor growth in an *in vivo* model by augmenting CDDP responses**

Chemoenhancing effect of PEITC among *in vivo* invasive cervical cancer model was further explored by its intra-peritoneal administration either singularly or in combination with CDDP (Figure 49). Prior to ensuing treatment, MTD of PEITC was determined for its safe administration among mice only following exposure to

three separate doses (1.5mg/kg, 2.5mg/kg, 3mg/kg bodyweight) of the phytochemical. With reference to the alterations induced in profiles of *in vivo* toxicity parameters, body weight and survivability, 2.5mg/kg body weight of PEITC was considered safe for administration (Figure 50). Thereafter, invasive cancer bearing mice batches were individually subjected to 2 weeks of PEITC treatment either singly or in combination with CDDP. As depicted in Figure 51A, PEITC's efficacy as a RMA was ascertained on the basis of its potential to alter PI3K/Akt status, chemoenhance CDDP and reduce tumor size. Initial findings clearly stated that PEITC was successful in bringing about tumor attrition when administered alongwith CDDP. Pictorial and graphical depictions of Figure 51B successfully established that combinatorial treatment with PEITC and CDDP could efficiently induce tumor regression and subsequently decrease its weight. Sole CDDP treatment failed to reduce the tumor-size as was evident from the unaffected tumor weights. In fact, PEITC treatment successfully harmonized the fluctuating patterns of murine body weight (Figure 51C). In IHC study (Figure 52 & Table 5), PEITC was found to impart a negative impact upon the tissue specific expression profiles of PXR, NFκB (p65), NFκB (p50), XIAP and survivin. Again, reduced nuclear PXR and p65 expressions of intermediate intensities were deciphered at the end of 2 weeks treatment. PEITC treatment as a single agent led to diminished nuclear (low intensity) and cytoplasmic (intermediate intensity) expressions of p50 subunit. Addition of CDDP with PEITC further reduced this pattern of expression. Cytoplasmic localization of XIAP and survivin was also downregulated by PEITC administration. On the other hand, their presence in the nucleus became more prominent (intermediate intensity) which suggested a comparative loss of their function. All these observations indicated that PEITC restrained PI3K/Akt pathway to bring about change in cellular response to CDDP.

The potential of PEITC in chemoenhancing CDDP was thereafter investigated by quantifying total GSH content, ROS levels and Rhodamine accumulation (Figure 53). Herein, PEITC was found to aggravate ROS generation by reducing the free GSH content of the cervical cells. ROS level escalation was in alignment with Rhodamine accumulation patterns as well. These results were suggestive of the pro-oxidant role of PEITC which facilitated CDDP to relay better cytotoxicity. These findings prompted an investigation of the protein-expression status of CDDP exporter MRP2. For this purpose, the tumor cortex, stroma and cortico-medullary regions were differentially studied for the expression profiles of MRP2, both with and without PEITC interventions during CDDP chemocycles of 2weeks. Interestingly, MRP2 levels were characteristically high in all the tumor regions (Figure 54A). However, 2.5mg/kg body weight of PEITC brought down these increasing expression patterns of MRP2 which went unchecked in presence of sole CDDP intervention. Histopathology and cytopathology (Figure 54B) of these groups further supported these findings as administration of PEITC in individual or in combination with CDDP restricted the invasive basal cells from intruding stromal-region of cervical epithelium besides checking their extensive keratinization. Therefore, PEITC acted as a chemoenhancer of CDDP in the *in vivo* cancer model which allowed reversion of resistant behaviour.

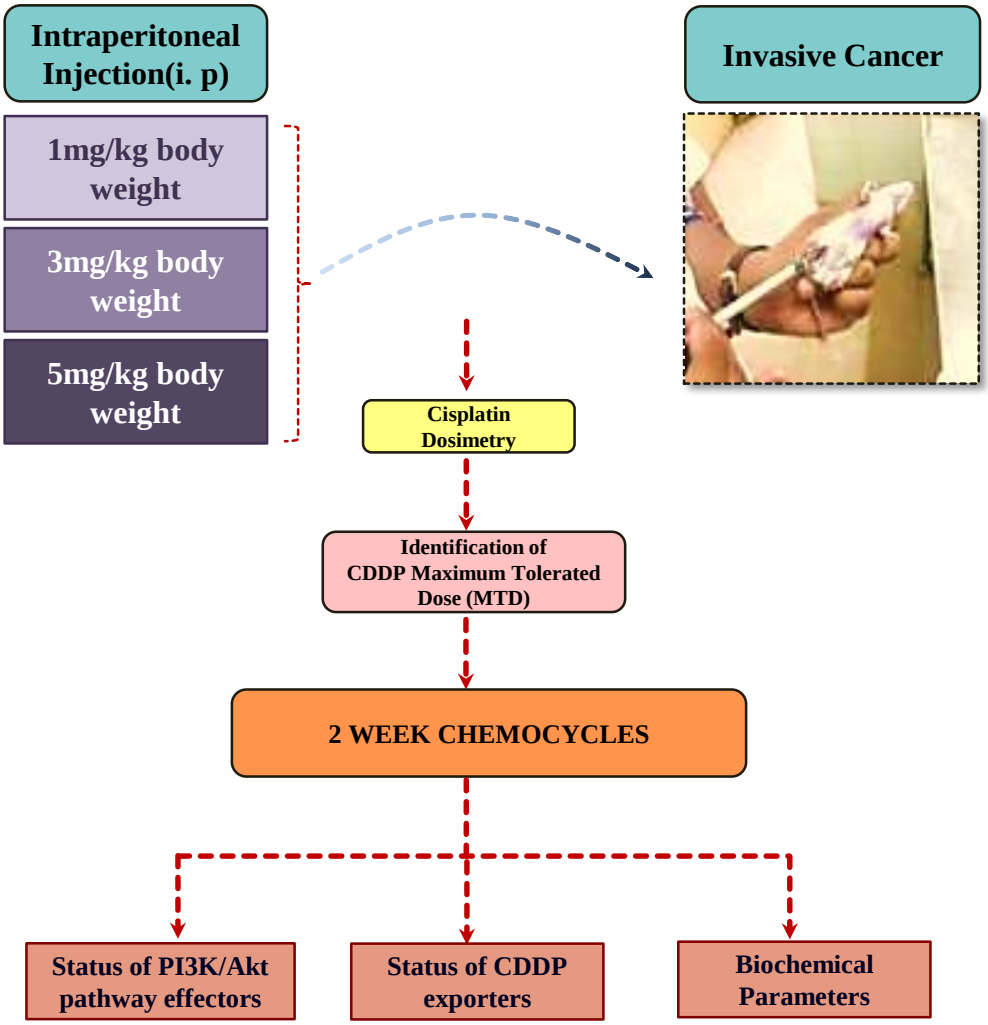

Figure 44: Demonstration of the Work Plan followed for assessment of cisplatin response *in vivo*

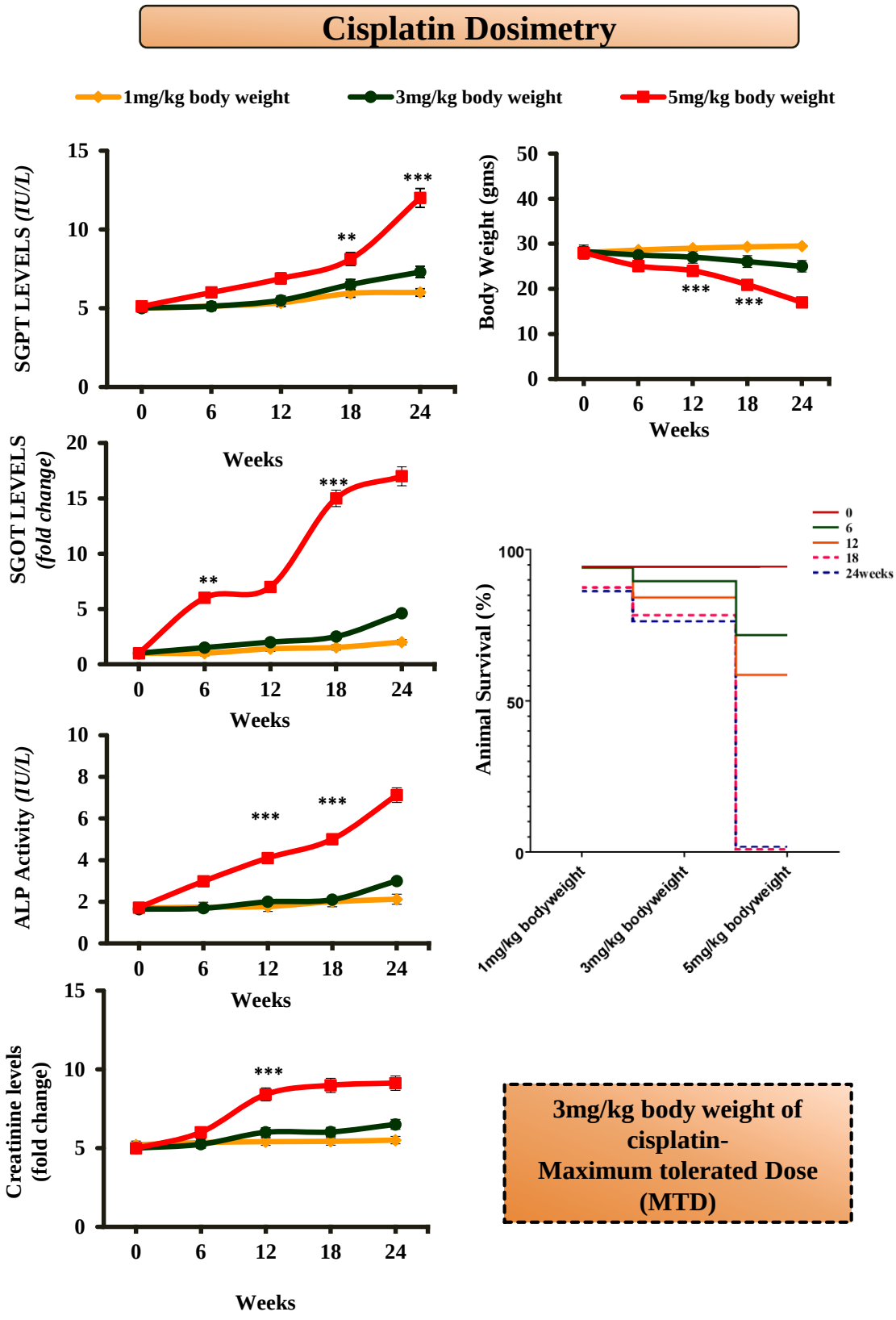

Figure 45: Ascertaining the Maximum Tolerated Dose (MTD) of CDDP for treating invasive cancer bearing mice with respect to altered profiles of *In vivo* toxicity parameters.

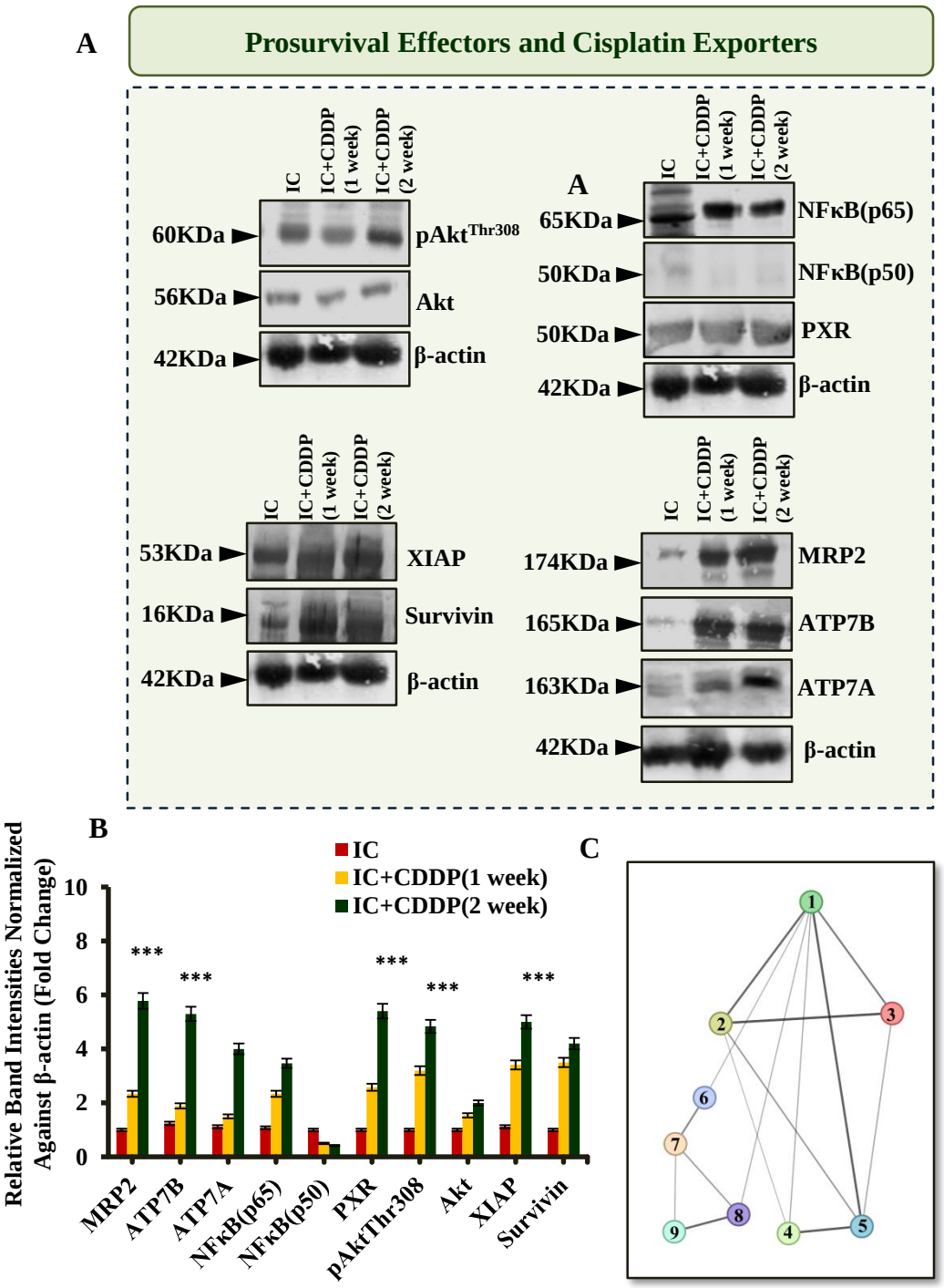

Figure 46: PI3K/Akt Pathway Alterations accompanying Cisplatin Treatment: (A) Western Blot Bands delineating altered protein expressions of Prosurvival effectors and Cisplatin Exporters related to PI3K/Akt Pathway. β-actin was used as loading control. (B) Relative Band Intensities of PI3K/Akt Pathway molecules represented as a fold change graph following normalization against β-actin. Values are represented as Mean ± SD ($^{***}p<0.0001$; $^{**}p< 0.05$). (C) STRING Interactome involving Akt (1), NFκB units [p65(2), p50(3)], XIAP (4), survivin (5), PXR (6), MRP2 (7), ATP7A (8) and ATP7B (9).

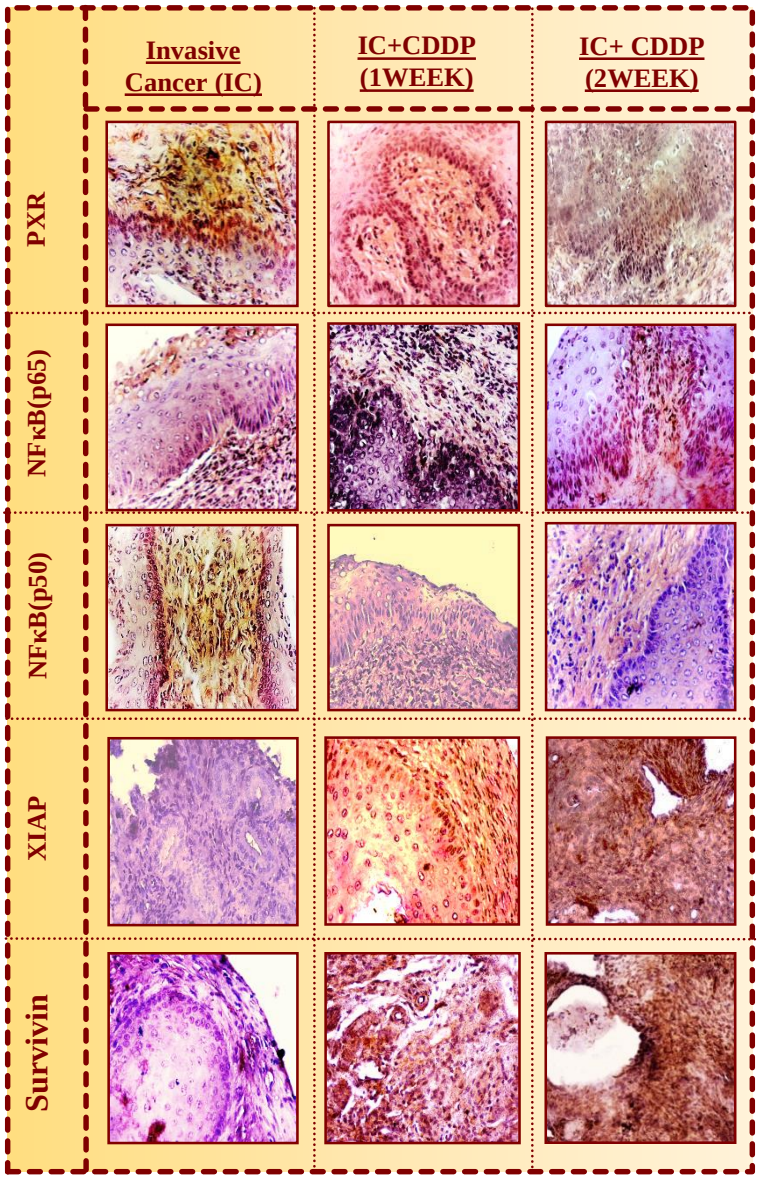

Figure 47: Tissue Specific Expression of PI3K/Akt Pathway Effectors: IHC Micrographs espousing the localization of PXR, NFκB (p65/p50), XIAP and survivin within cervical tissues. Brown Stained cytoplasm or nucleus corresponds to positive stains for the antigens.

TABLE 4: IHC SCORES FOR THE EXPRESSION OF PXR, NFκB(p65/p50), XIAP AND SURVIVIN AFTER CDDP TREATMENT

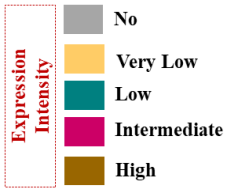

Antigens	Cellular Fraction	Positively Stained Cells (%)			Scores			Expression Intensity		
		IC	IC+CDDP (1 WK)	IC+CDDP (2 WK)	IC	IC+CDDP (1 WK)	IC+CDDP (2 WK)	IC	IC+CDDP (1 WK)	IC+CDDP (2 WK)
PXR	Nucleus	49.2	67.8	79.7	2	3	3	L	I	I
	Cytoplasm	50	32.2	20.3	2	2	2	L	L	L
NFκB (p65)	Nucleus	45	70.3	83	2	3	4	L	I	H
	Cytoplasm	55	29.7	17	3	2	1	I	L	VL
NFκB (p50)	Nucleus	67	43	16	3	2	1	I	L	VL
	Cytoplasm	33	57	84	2	3	4	L	I	H
XIAP	Nucleus	44.22	15.94	3	2	1	1	L	VL	VL
	Cytoplasm	55.78	84.06	97.1	3	4	4	I	H	H
Survivin	Nucleus	54.88	21	13	3	2	1	I	L	VL
	Cytoplasm	45.12	79	87	2	3	4	L	I	H

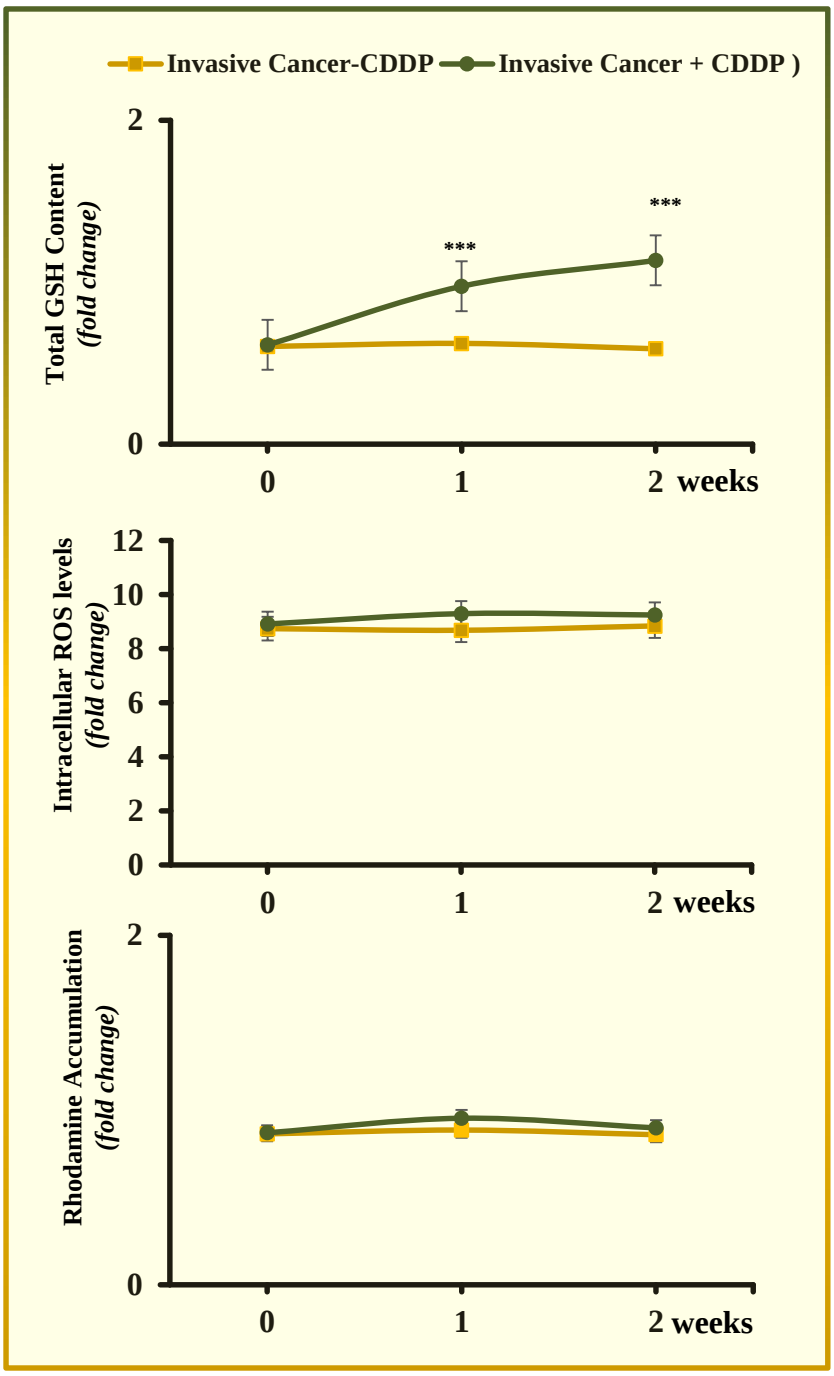

Figure 48: Biochemical Parameters: CDDP Induced changes in the *in vivo* biochemical parameters supporting its efficacy *in vivo*.

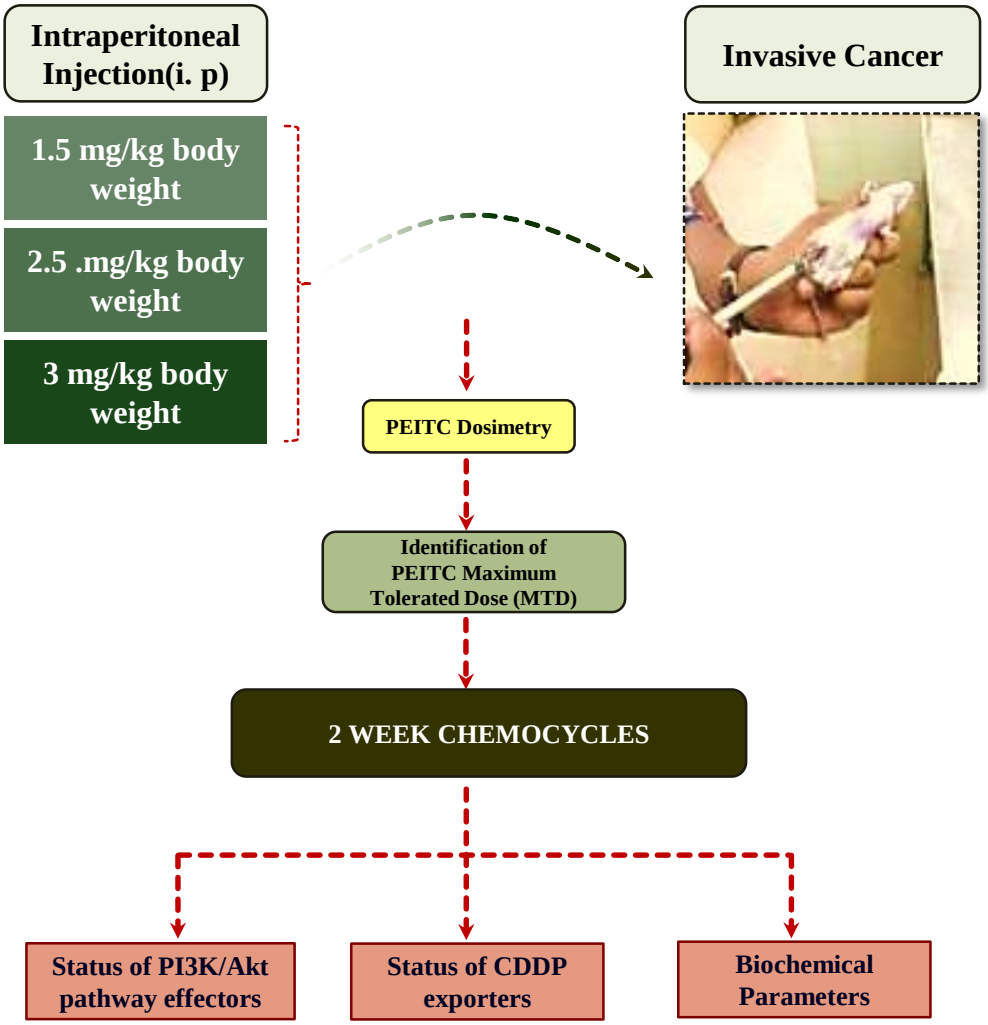

Figure 49: Demonstration of the Work Plan followed for selection of PEITC dose for *in vivo* treatment in combination with CDDP.

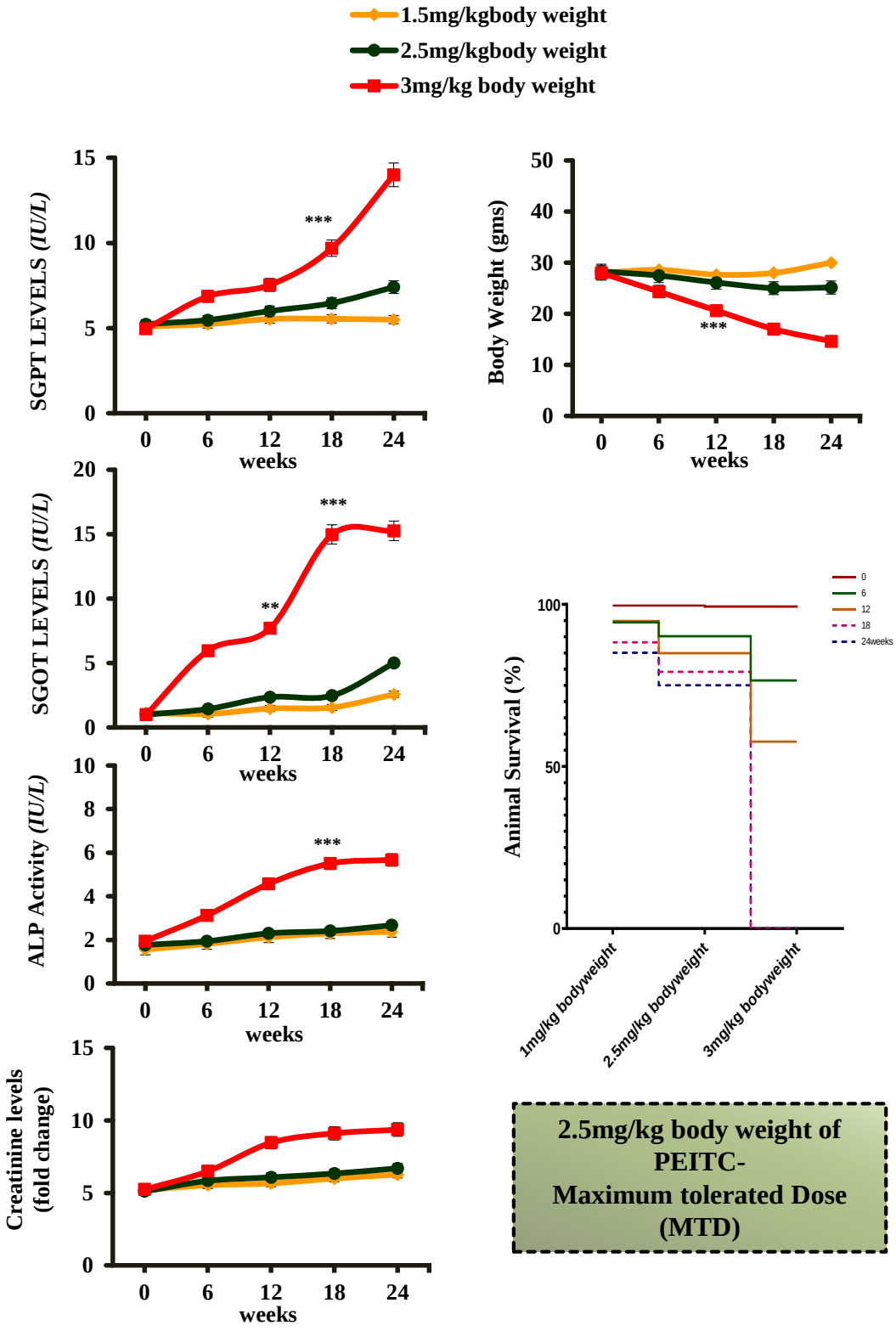

Figure 50: Ascertaining the Maximum Tolerated Dose (MTD) of PEITC for treating invasive cancer bearing mice in combination with CDDP based upon the alterations of *In vivo* toxicity parameters.

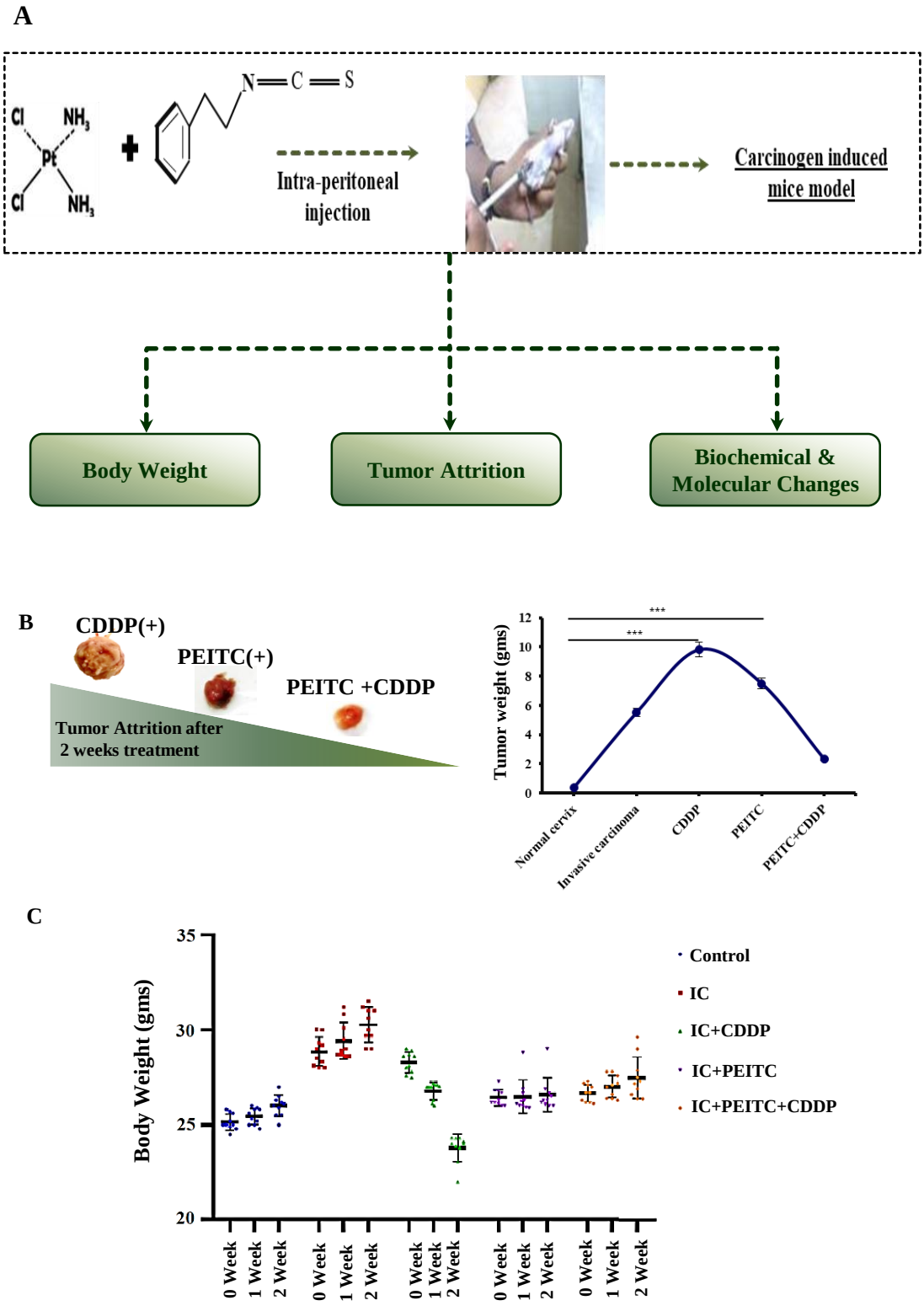

Figure 51: PEITC Induced changes of *In vivo* Parameters: (A) Pictorial Representation of Work Plan for monitoring PEITC's role as a RMA *in vivo.* (B) Snippets of tumors undergoing size reduction following PEITC treatment singly as well as in combination with CDDP in 2weeks duration alongwith a graphical corroboration of the same. (C) Body weight alterations in mice following PEITC and CDDP treatment ($^{***}p< 0.0001$).

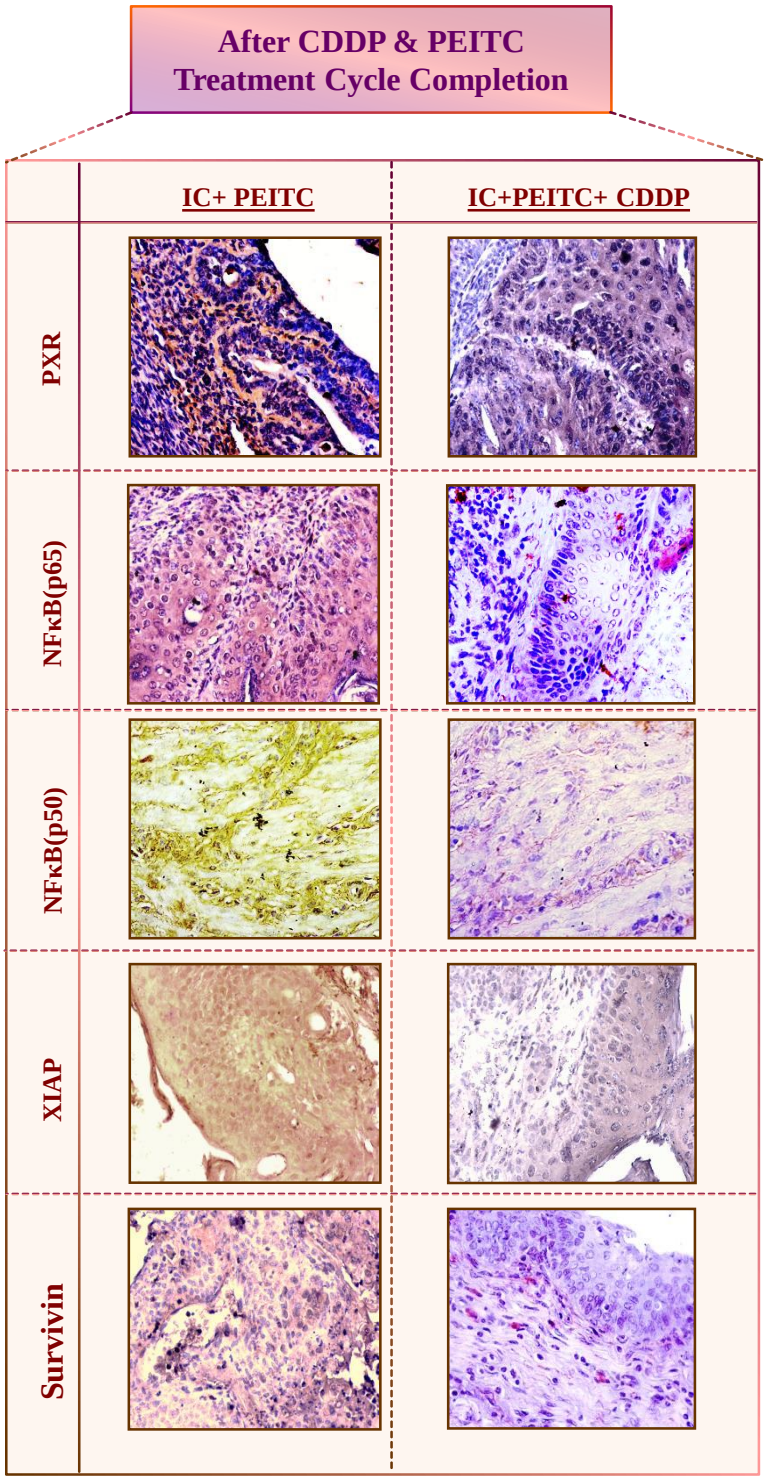

Figure 52: PEITC induced Tissue Specific Expression of PI3K/Akt Pathway Effectors: IHC Micrographs espousing the localization of PXR, NFκB (p65/p50), XIAP and survivin within cervical tissues after 2 weeks of concurrent treatment with PEITC as well as CDDP. Brown Stained cytoplasm or nucleus corresponds to positive stains for the antigens.

TABLE 5: IHC SCORES FOR THE EXPRESSION OF PXR, NFκB(p65/p50), XIAP AND SURVIVIN AFTER PEITC TREATMENT

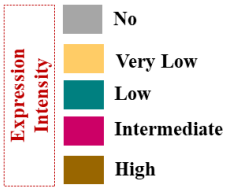

Antigens	Cellular Fraction	Positively Stained Cells (%)		Scores		Expression Intensity	
		IC +PEITC (2 WK)	IC+ PEITC+ CDDP (2 WK)	IC+ PEITC (2 WK)	IC+ PEITC +CDDP (2 WK)	IC+PEITC (2 WK)	IC+ PEITC +CDDP (2 WK)
PXR	Nucleus	41.5	35	2	2	L	L
	Cytoplasm	58.5	65	3	3	I	I
NFκB (p65)	Nucleus	42	33.3	2	2	L	L
	Cytoplasm	58	66.7	3	3	I	I
NFκB (p50)	Nucleus	45	35	2	2	L	L
	Cytoplasm	55	65	3	3	I	I
XIAP	Nucleus	62.5	78.2	3	3	I	I
	Cytoplasm	37.5	21.8	2	2	L	L
Survivin	Nucleus	55	62	3	3	I	I
	Cytoplasm	45	38	2	2	L	L

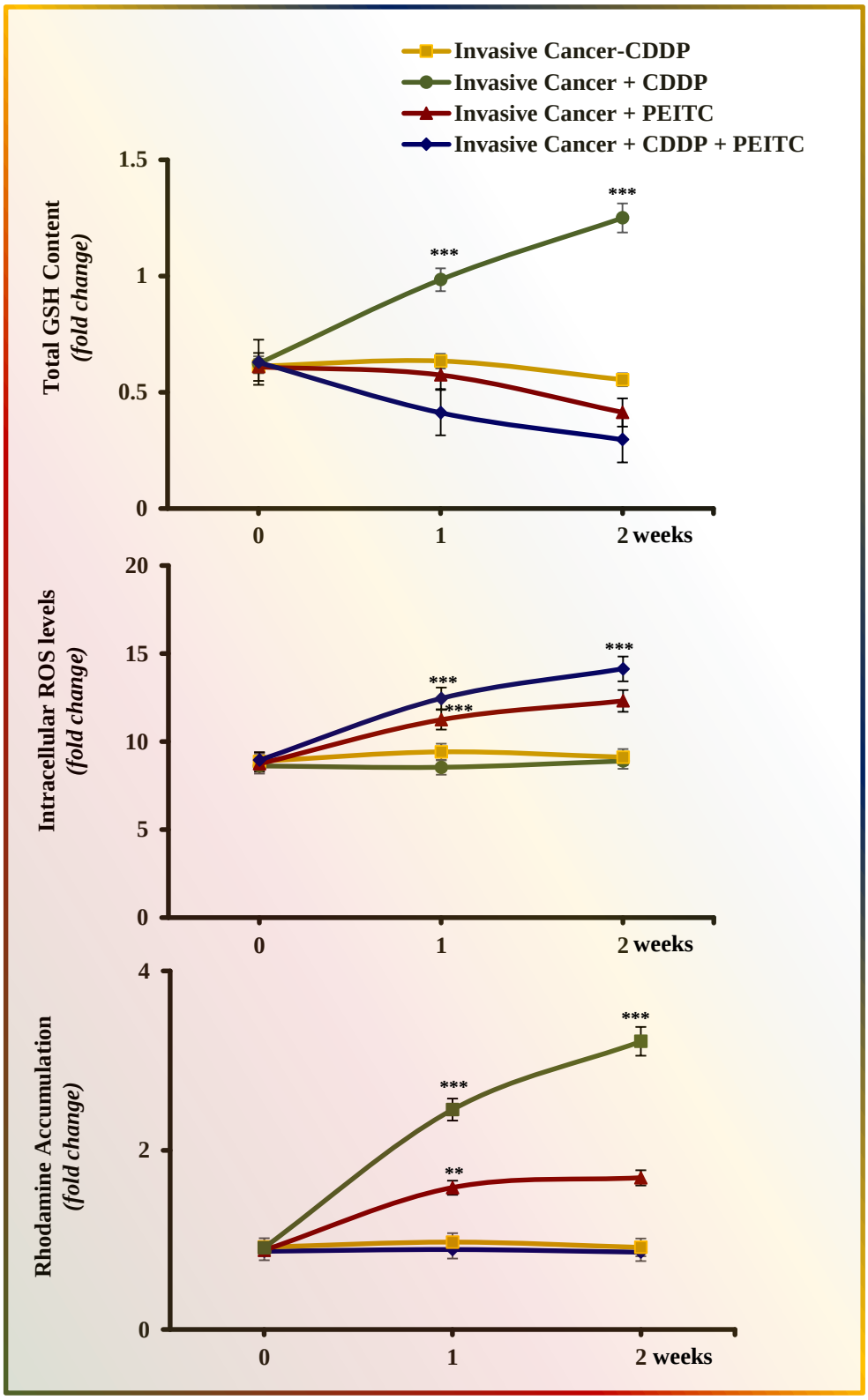

Figure 53: Biochemical Parameters: PEITC and CDDP Induced changes in the *in vivo* biochemical parameters delineating the potential of PEITC in improving CDDP's effect *in vivo.*

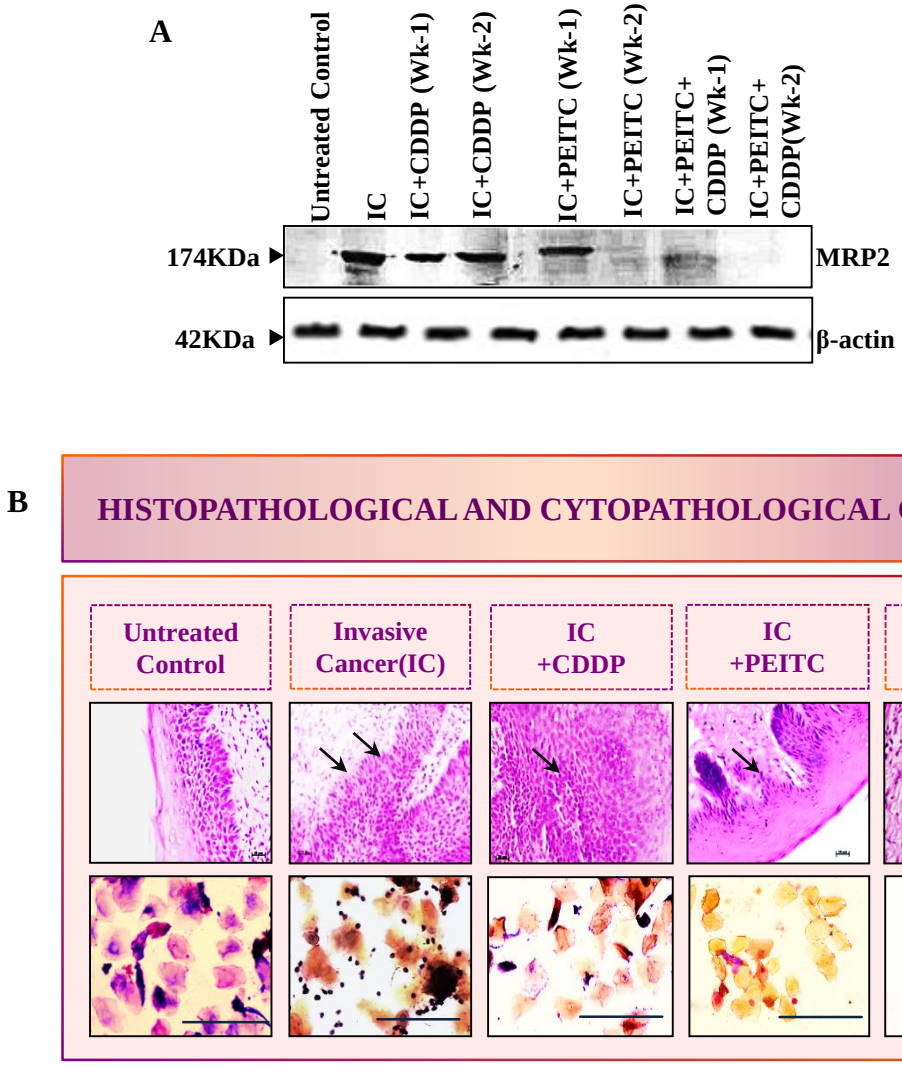

Figure 54: Combinatorial Effect of CDDP and PEITC upon cervical histopathology, cytopathology and MRP2 expressions: (A) Western Blot bands revealing the effect of PEITC and CDDP upon MRP2 expressions. (B) Light microscope glimpses of PEITC ameliorated histology and cytology of cervix.

In vitro findings

7.2. *In vitro* Findings

- **CDDP Pulse Treatment of SiHa led to development of a resistant subline SiHa^{R}**

With an aim to comprehend the complex pandemonium of 'acquired cisplatin resistance' in cervical cancer scenario, a drug-resistant *in vitro* model was developed using SiHa (HPV 16 positive) cell line. Figure 55 well describes the rationale supporting this idea for understanding the mechanism in which PI3K/Akt regulation allows a gradual transformation of a CDDP sensitive phenotype to a resistant one. Varied PI3K/Akt status of cellular clones in a heterogeneous TME bestows them with properties to respond differentially to CDDP. Accordingly, these are either CDDP-sensitive (responders) or CDDP-tolerant (intermediate responders) or CDDP-resistant (non-responders) cellular subtypes. In presence of the incumbent CDDP, the resistant and tolerant clones survive well while the sensitive ones get eliminated. As a result, the resistant cells undergo selection in presence of CDDP. Again, it induces tolerant cells in the tumor to express all the necessary factors which provide them with a survival advantage for reinforcement of a CDDP-resistant phenotype. Altogether, these resistant cells gradually overpopulate the tumor to mediate resistance and eventuate in therapy failure. Concoction of PI3K/Akt pathway modulators including the prosurvival effectors alongwith the CDDP exporters are deemed to accompany this phenomenon of 'neoplasm evolution'. Therefore, understanding this function of PI3K/Akt could aid in identification of its key contributors of CDDP resistance with properties to be targeted by RMAs like PEITC for its reversion.

In this regard, an attempt to recreate the canonical theory of 'clonal evolution of tumor' within a cell plate was made by observing the discourse of 'pulse treatment'. As aforementioned, 'pulse treatment' ensured gradual selection and establishment of the CDDP insensitive cellular cohort among the heterogeneous SiHa as a cisplatin-

resistant subline $SiHa^R$. A microscopic overview of the said process is displayed in Figure 56. To identify and better understand the status of PI3K/Akt pathway that encompassed the establishment of $SiHa^R$ subline from SiHa, flow cytometry analysis of the cell specific co-expressions of $pAkt^{Thr308}$ and CDDP exporters (MRP2, ATP7A, ATP7B) was undertaken (Figure 57 & 58). Dot plots of double stained cells suggested that 'clonal selection' had led to emergence of $SiHa^R$ from SiHa. As per the results, a certain proportion of CDDP sensitive SiHa already expressed pAkt (~8%) and MRP2 (~10.3%) antigens while about 15% of it were positive for both pAkt and MRP2. This subpopulation, although scanty, kept rising with exposure to escalated doses. In the finally isolated $SiHa^R$ (3µM) about 99% of cells were found to co-express pAkt and MRP2. Interestingly, a different pattern was observed for ATP7A and $pAkt^{Thr308}$. In the $SiHa^R$ subline, double positive cells came up with an escalated value of about 91.5% unlike SiHa which had only 9.2% $pAkt^{Thr308}$ positive, 0.6% ATP7A and 0.23% double positive subsets. The double positive population increased gradually along the transiting treatment isolates namely $SiHa^{R1\mu M}$ and $SiHa^{R1.5\mu M}$. A similar pattern was observed for ATP7B (98.9% double positive) expression as well. These findings indicated that $pAkt^{Thr308}$ and MRP2 positive SiHa cells underwent a 'CDDP-Selection' while the expression of $pAkt^{Thr308}$ alongwith ATP7A and ATP7B were 'CDDP-Induced'.

❖ **Acquirement of CDDP resistance by $SiHa^R$ resulted from PI3K/Akt Upregulation**

As a validation of the acquired resistant phenotype, SiHa and $SiHa^R$ sublines were characterized for their differences in morphology, doubling time, molecular profile, fold-resistance and drug retention capacities (Figure 59). As shown in Figure 60A, micrographs of SiHa and $SiHa^R$ recorded intermittently during pulse treatment portrayed the gradual transformative events. Apparently, both these cellular

counterparts varied remarkably in terms of morphology and appearance. With respect to sensitive SiHa, $SiHa^R$ was lesser elliptical and more spherical with dense and conspicuous nuclei. Interestingly, $SiHa^R$ was calculated to exhibit an increased nucleus-to-cytoplasmic ratio (666.81 μm^2) compared with that of SiHa (367.97 μm^2).

In fact, the resistant subline $SiHa^R$ doubled within 16h unlike SiHa which doubled in 32h (Figure 60B). These observations were suggestive of a gain in their proliferative potentials which warranted an investigation of the plausible alterations in the PI3K/Akt prosurvival signalling pathways that might be in effect. As per the western blot results shown in Figure 60 C&D, $SiHa^R$ expressed remarkably higher levels of MRP2 (2.1 fold) and $pAkt^{Thr308}$ (1.91 fold) unlike the parental SiHa. A significantly higher ratio of p-Akt/Akt (1.7 fold) in $SiHa^R$ cells indicated the contributory role of upregulated PI3K/Akt pathway in acquirement of CDDP-resistant phenotype.

Consequently, the surviving potentials of $SiHa^R$ was validated by MTT assay wherein it showed appreciable survival in the parental IC_{20} (2 µM), IC_{30} (3.5 µM) and IC_{50} (4 µM) CDDP concentrations for 24, 48 or even 72h (Figure 61A). Herein, killing of $SiHa^R$ cells in comparison to SiHa at IC_{70} (8 µM) and IC_{100} (11.5 µM) CDDP doses were notably less, (Figure 61B). Relatively, the calculated IC_{70} and IC_{100} dose of CDDP in SiHa turned out to be the IC_{30} and IC_{60} of $SiHa^R$ while the IC_{50} of CDDP for $SiHa^R$ was calculated to be around 11µM. Therefore, $SiHa^R$ was estimated to be 2.75 fold resistant to CDDP.

These findings were in corroboration with IF results (Figure 62A) which revealed the functional significance of such expression patterns of CDDP exporters. Mostly, the pumps were found to be localized in cell membrane as well as in the nuclear periphery. In all probability, these exporters being present in the membrane

were relaying the function of exit-ways for CDDP and might have catered to decrease intracellular drug accumulation. Such an exhilarated prosurvival signalling also leads to a shift in metabolic paradigm of the cells which facilitates hasty metabolism and egestion of cytotoxicants like CDDP. Hence, the results of FAAS delineated a decreasing trend of drug accumulation or retention capacities of $SiHa^R$ with respect to its sensitive counterpart SiHa in a time dependent manner (Figure 62B). Accordingly, the half-life of CDDP got reduced to 12h from 24h in $SiHa^R$. In fact, the mitochondrial membrane depolarization remained unaffected by CDDP treatment in $SiHa^R$ unlike the sensitive SiHa cells (Figure 62C). This confirmed the CDDP insensitive behaviour of $SiHa^R$ as a permanent chemoresistant phenotype.

Additionally, enhanced ability to repair away drug-DNA conjugates may also negate CDDP cytotoxicity. Ku70/XRCC6 is therefore highly implicated in the scenario of CDDP resistance. In this regard, the CDDP evasive nature of $SiHa^R$ could be detected in their patterns of cell cycle distribution following drug treatment. CDDP which is known to work in a cell cycle independent fashion would mediate an attack on DNA based upon its accessibility. Moreover, repair machinery always functions in a cell-cycle phase specific manner. Therefore, Ku70 expression was checked in a cell cycle phase specific manner by flow cytometry (Figure 63 A&B). As evident from these results, majority of SiHa cells got arrested in G0/G1 phase among which only 0.2% cells were found to be Ku70 positive. SiHa cells of S and G2/M phase did not exhibit any significant number of positively stained cells. On the other hand, $SiHa^R$ cells were found to be comprised of a significant cellular cohort which was Ku70 positive. In absence of CDDP treatment, 57% of $SiHa^R$ cells present in G0/G1 phase were Ku70 positive while 77.6% and 82% of those distributed in S and G2/M phases stained positive for the antigen. This percentage escalated vehemently when CDDP

treatment was administered. Such a pattern of result was found to be in alignment with the theory of clonal evolution wherein presumably Ku70 expressing cells were gaining a survival advantage over others. In case of SiHa cells, Ku70 exhibitants were sparse in S phase compared to those in the other two cell cycle phases. Probably, these cells eventually got selected with incremental drug dose exposure as a result of which their number was found be about 13-14 folds higher in $SiHa^R$ in absence of drug. Eventual escalation of this number with drug exposure further strengthened the notion. Additionally, decreased length of the S-phase for $SiHa^R$ cells in drug treated cases highlights a gain in their survival propensity owing to which they tend to escape drug induced arrest and complete cell cycle to proceed for division. As a result, $SiHa^R$ cells failed to retain drug-DNA conjugates with respect to SiHa (Figure 63C). Therefore, Ku70 expression was providing the $SiHa^R$ cells with an escape route to CDDP.

Upregulation of PI3K/Akt pathway was further evident at both protein and mRNA levels (Figure 64). A cumulative escalation in protein expression profiles of NFκB (p50/p65), XIAP, survivin and MRP2 in addition with $pAkt^{Thr308}$ and Akt was observed. Considering the linkage of Ku70 and MRP2 with Akt by means of PXR, its functional status was validated in immunofluorescence results (Figure 65A). Nuclear localization of PXR was witnessed in $SiHa^R$ cells unlike SiHa cells. Therefore, negative binding of p50 subunit was noted along with p65 at the promoter response element of MRP2 (Figure 65B). This pathway got further validated when a normal cell line HaCaT was transfected with wild-type Akt cloned plasmids. Originally devoid of Akt and MRP2 expressions, HaCaT cells began expressing the same upon transfection with overexpression plasmids (Figure 65C). This confirmed that deregulated PI3K/Akt pathway was responsible for rendering the cisplatin-sensitive cells unresponsive to the drug.

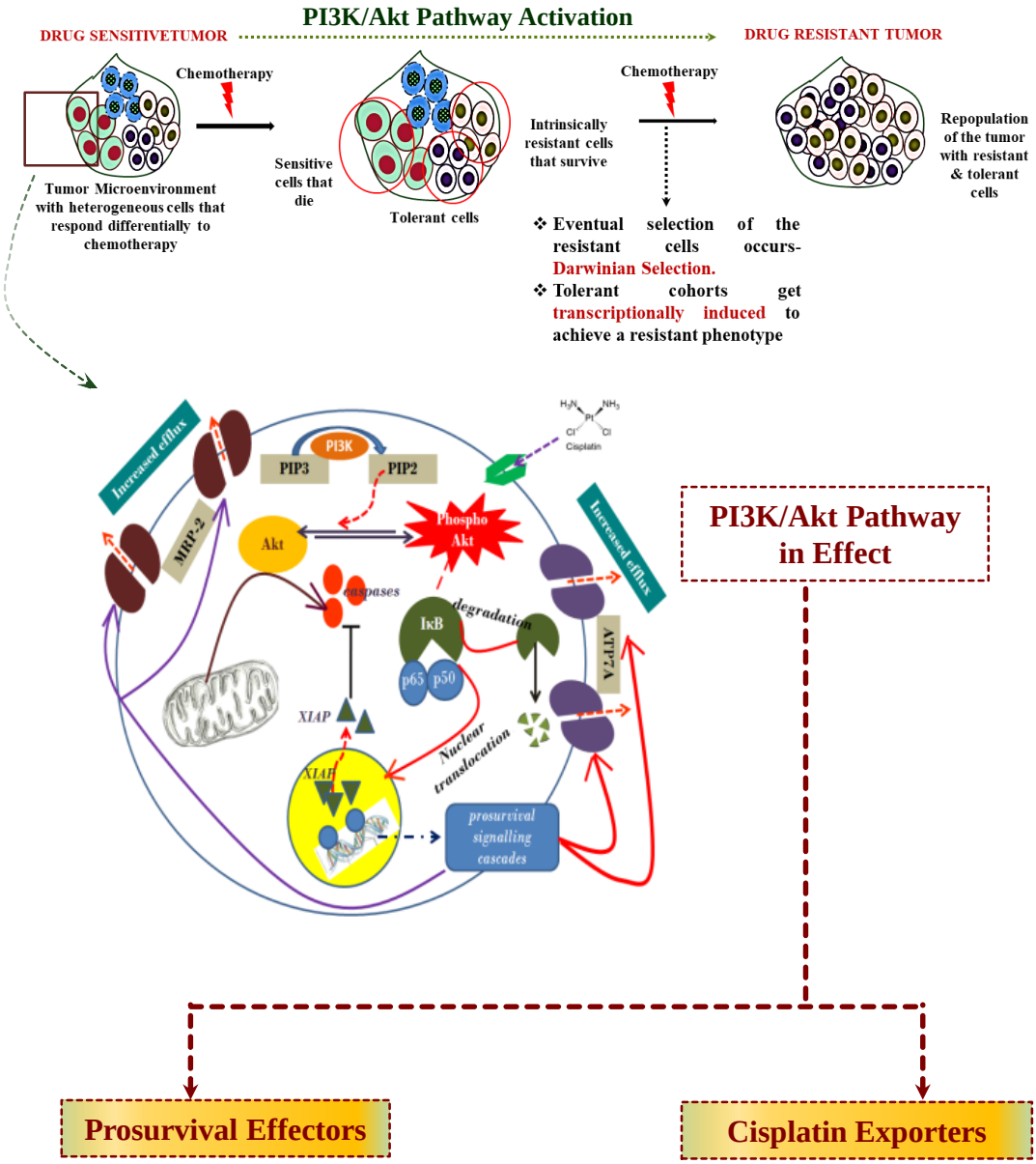

Figure 55: Overall Description of Work Rationale for *In vitro* study

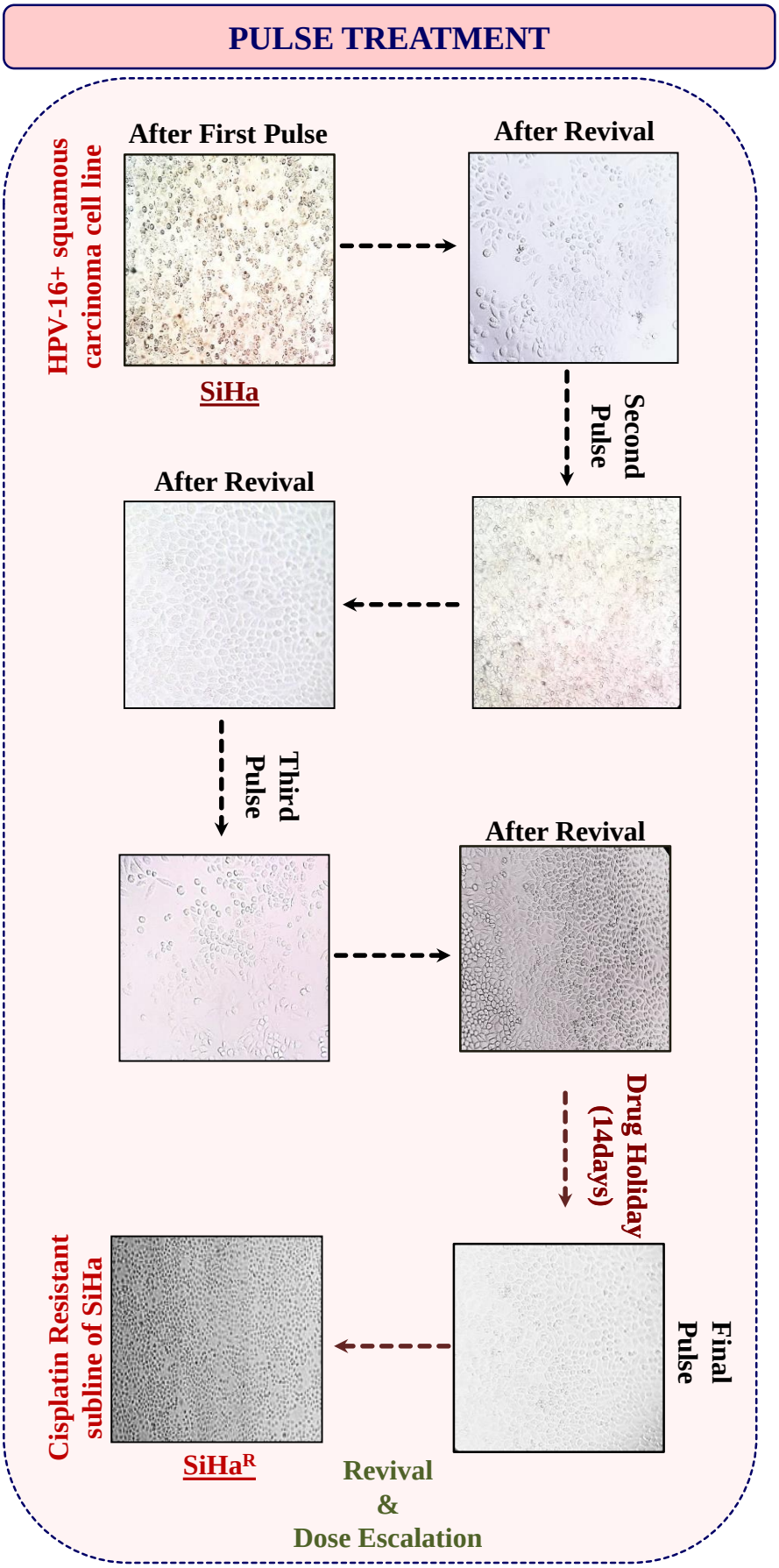

Figure 56: Pulse Treatment Scheme: Micrographic Snippets portraying the gradual transition of CDDP sensitive SiHa to the CDDP resistant SiHa^{R}.

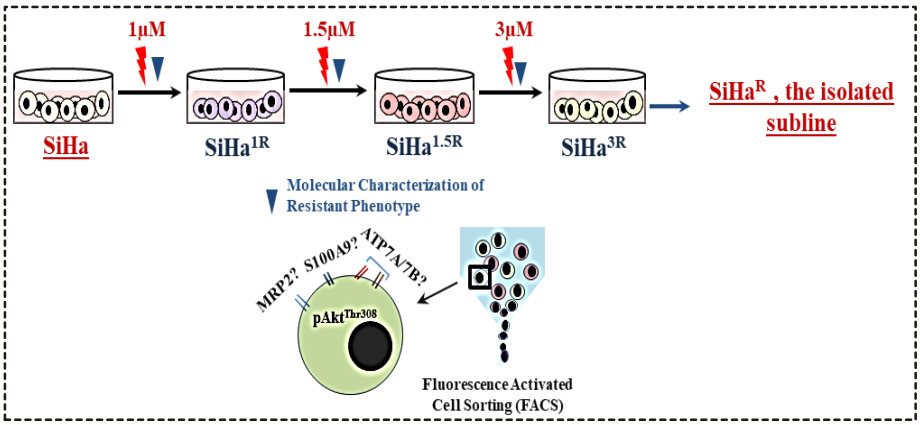

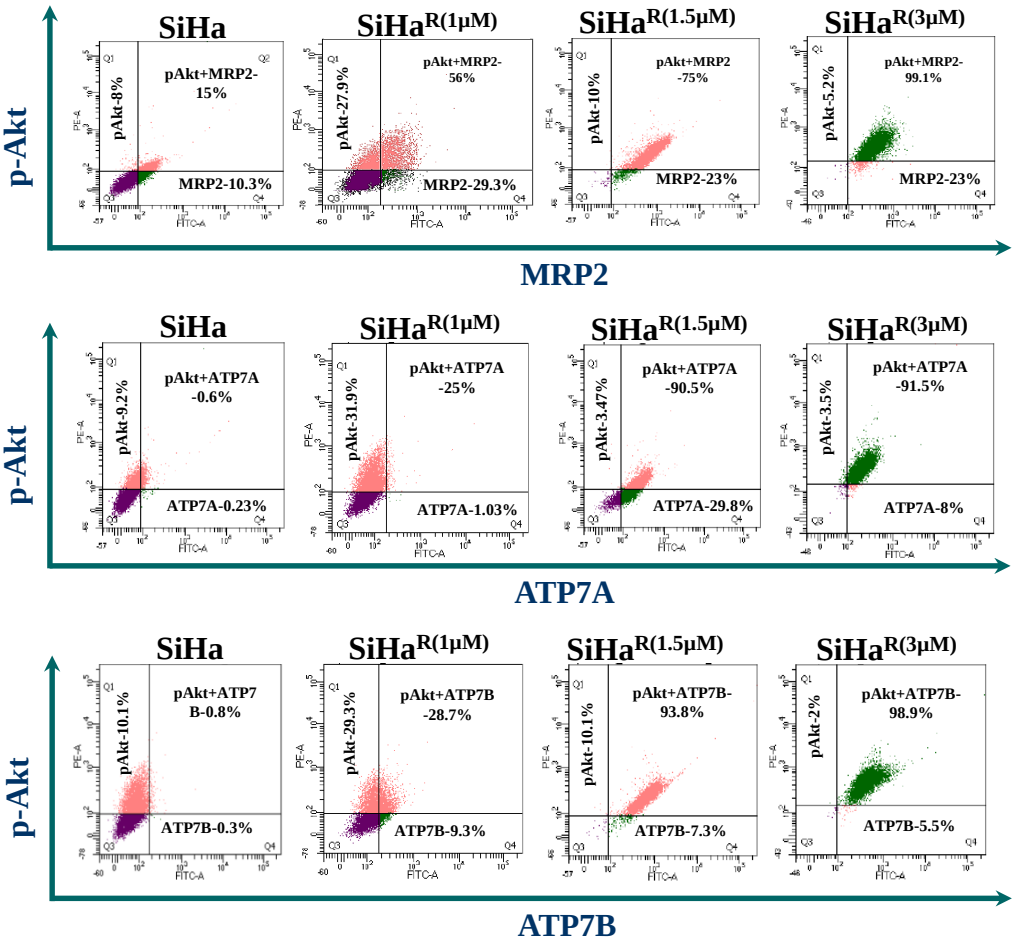

Figure 57: PI3K/Akt induced expressions of CDDP exporters enabled clonal selection of SiHa^{R} cells: Flow cytometry scatter plots delineating the pattern of co-expressions of CDDP exporters like MRP2, ATP7A/7B and its prosurvival inducer pAkt^{Thr308} during the process of Pulse treatment.

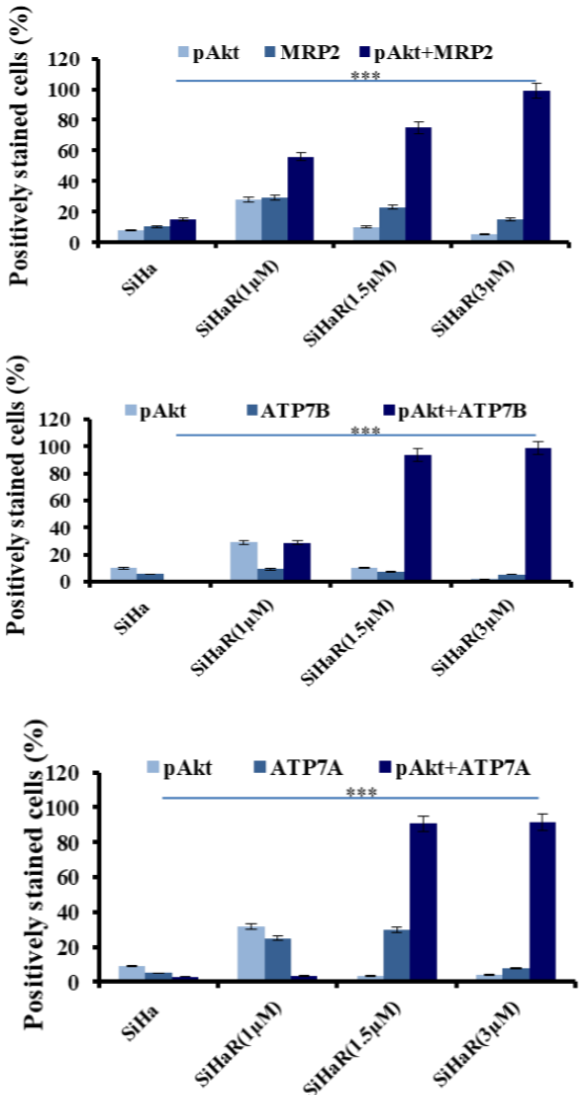

Figure 58: PI3K/Akt induced expressions of CDDP exporters enabled clonal selection of SiHa^{R} cells: Graphical Representations of flow cytometry results.

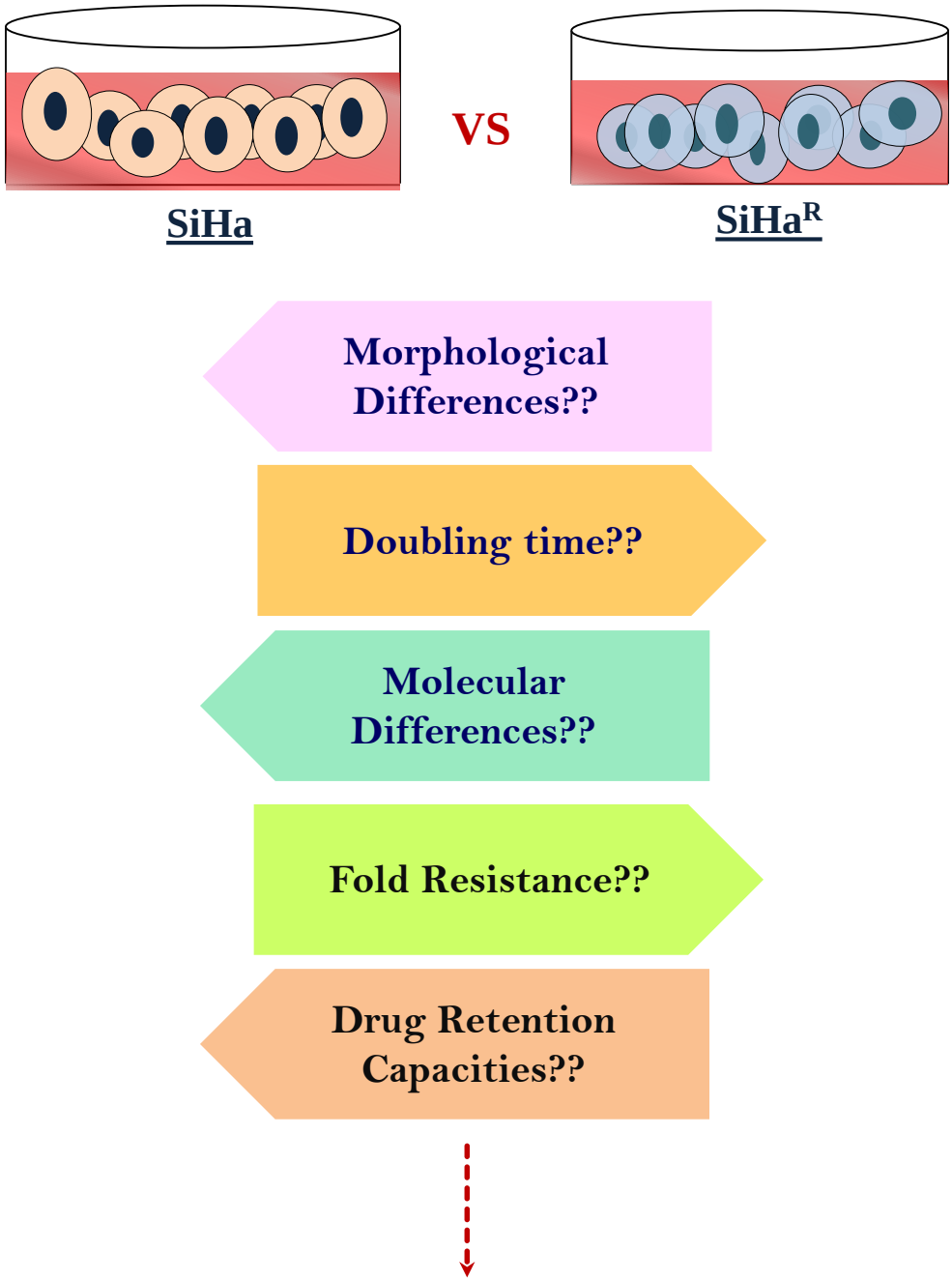

Figure 59: Plan of Work for characterization of acquired resistant phenotype of SiHa^R in comparison to SiHa.

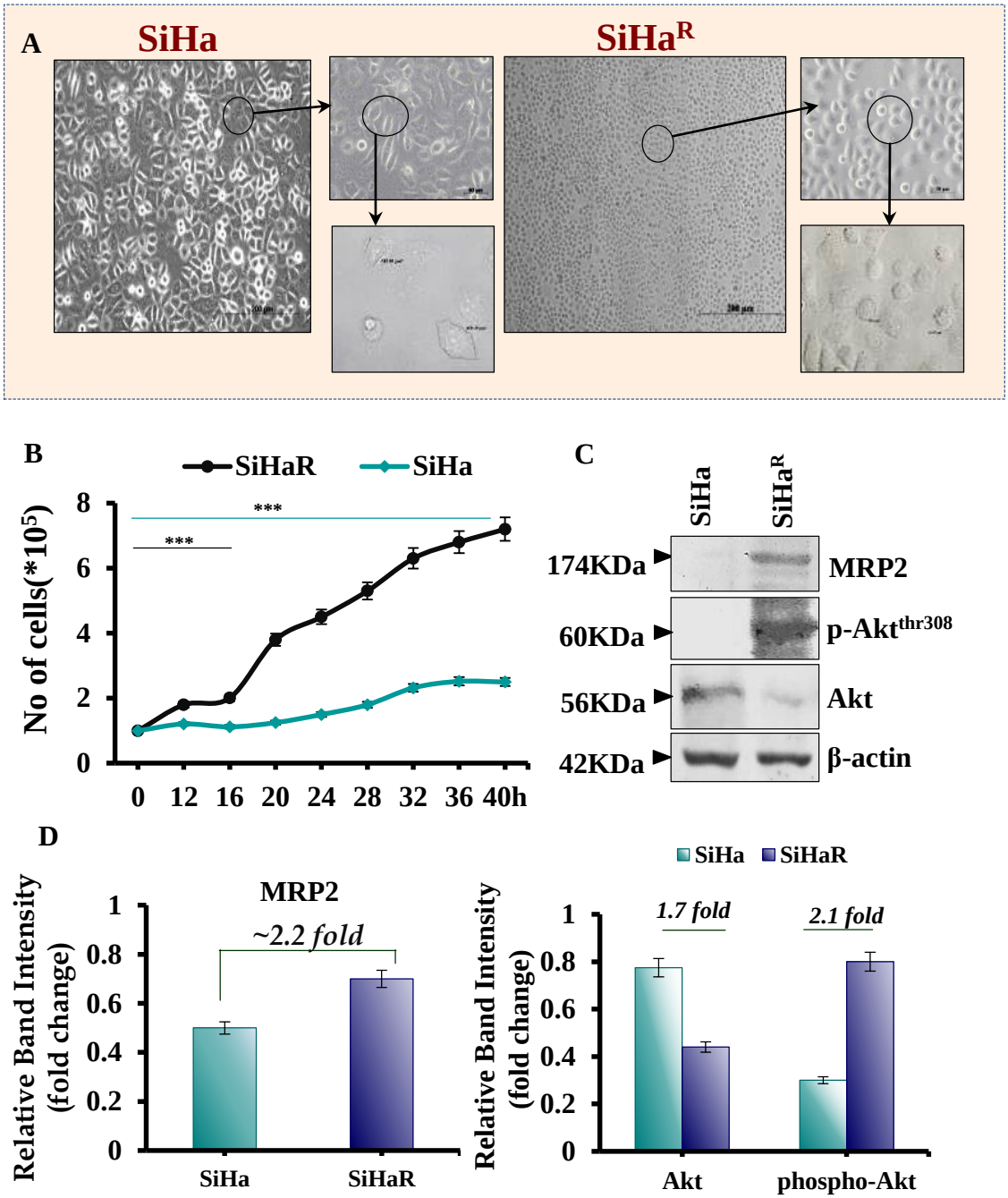

Figure 60: Morphological and Molecular Characterization of SiHa and SiHa^R: (A) Micrographs displaying morphological differences between SiHa and SiHa^R. (B) Doubling time of SiHa^R with respect to SiHa (C) Western blot bands for the expressions of Akt, pAkt^{Thr308} and MRP2 in SiHa and SiHa^R with β-actin being the loading control. (D) Relative Band Intensities of Akt, pAkt^{Thr308} and MRP2 represented graphically as a fold change graph after normalization against β-actin.

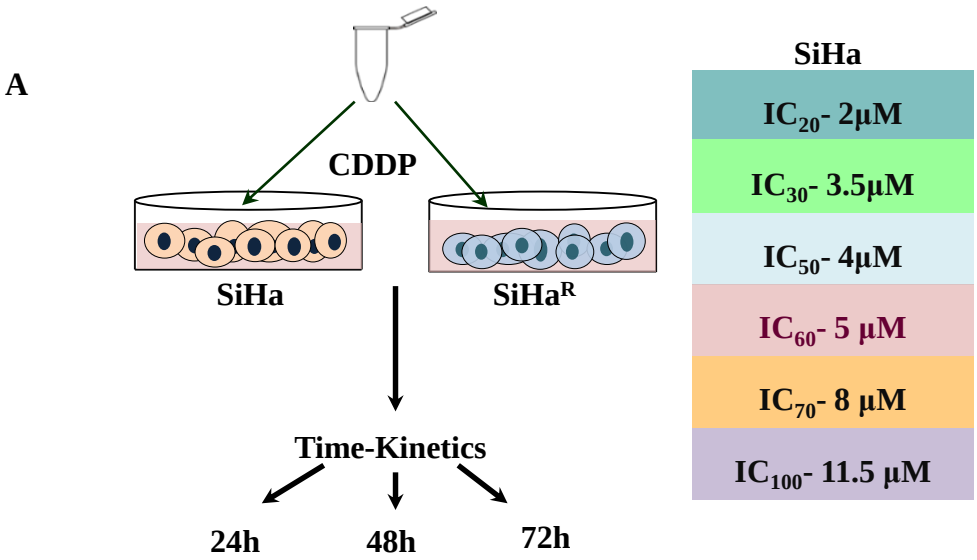

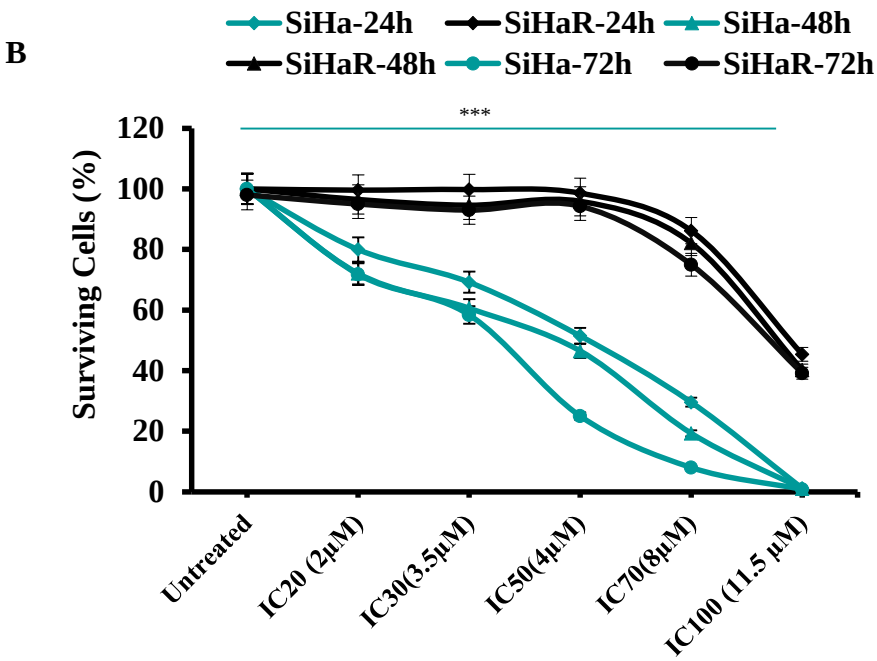

SiHa^R

IC_{30}- 8µM	2.285 fold high
IC_{50}- 11µM	2.75 fold high
IC_{60}- 11.5µM	2.765 fold high

Figure 61: Calculation of Fold Resistance: (A)Schematic overview of treatment process followed for calculation of fold resistance. (B) MTT Assay results showing the altered surviving potentials of $SiHa^R$ in the calculated IC_{20}, IC_{30}, IC_{50}, IC_{70} and IC_{100} doses for CDDP sensitive SiHa cells. Respective IC_{30}, IC_{50} and IC_{60} values of $SiHa^R$ displaying its grade of CDDP resistance in relation to SiHa.

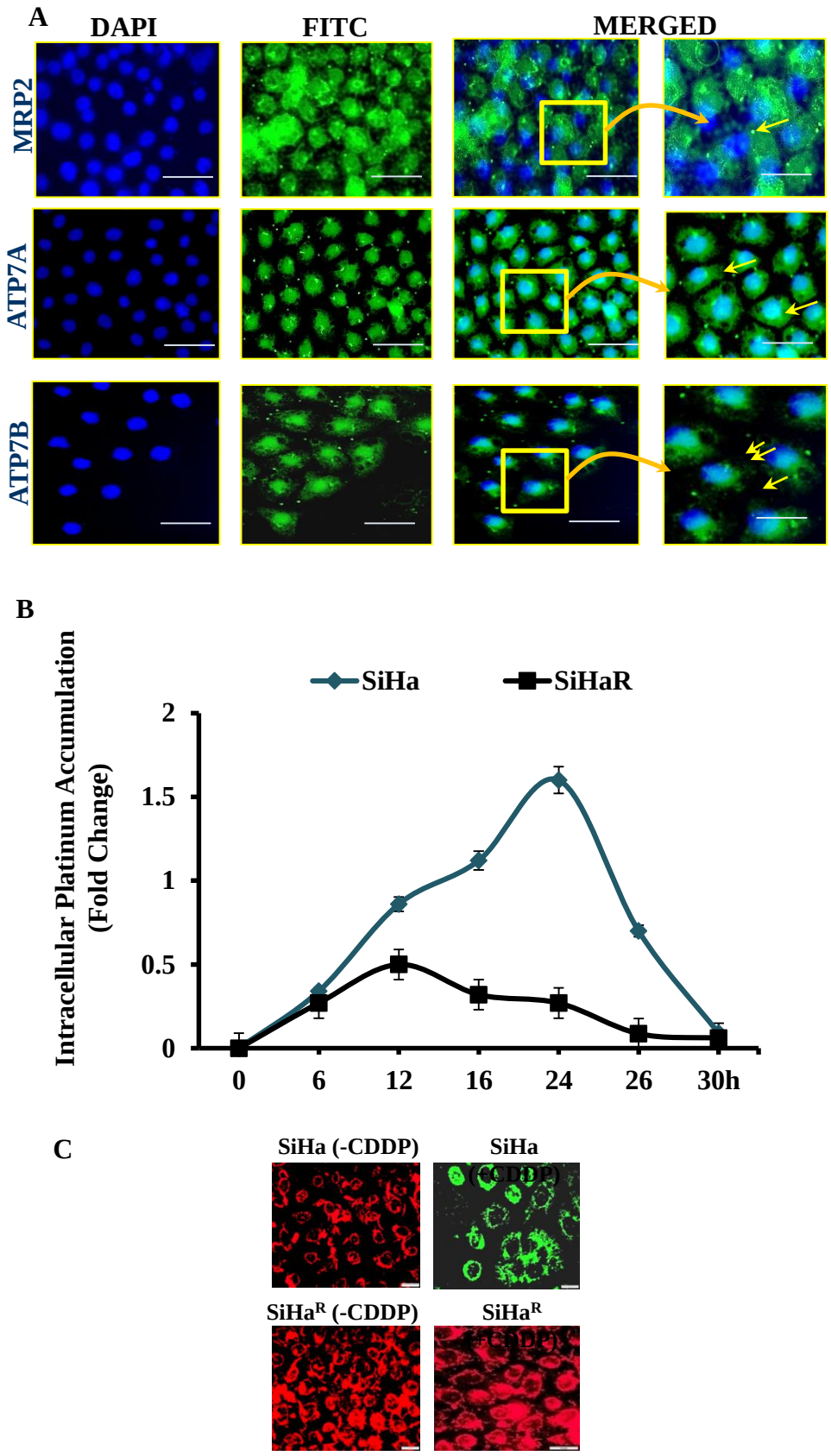

Figure 62: CDDP Retention by SiHa^R: (A) Fluorescent micrographs delineating cell specific localization of CDDP exporters. (B) Comparative CDDP retaining potentials of SiHa and SiHa^R as calculated in terms of cellular platinum retention levels. (C) Mitochondrial membrane depolarization assessment by JC-1 staining.

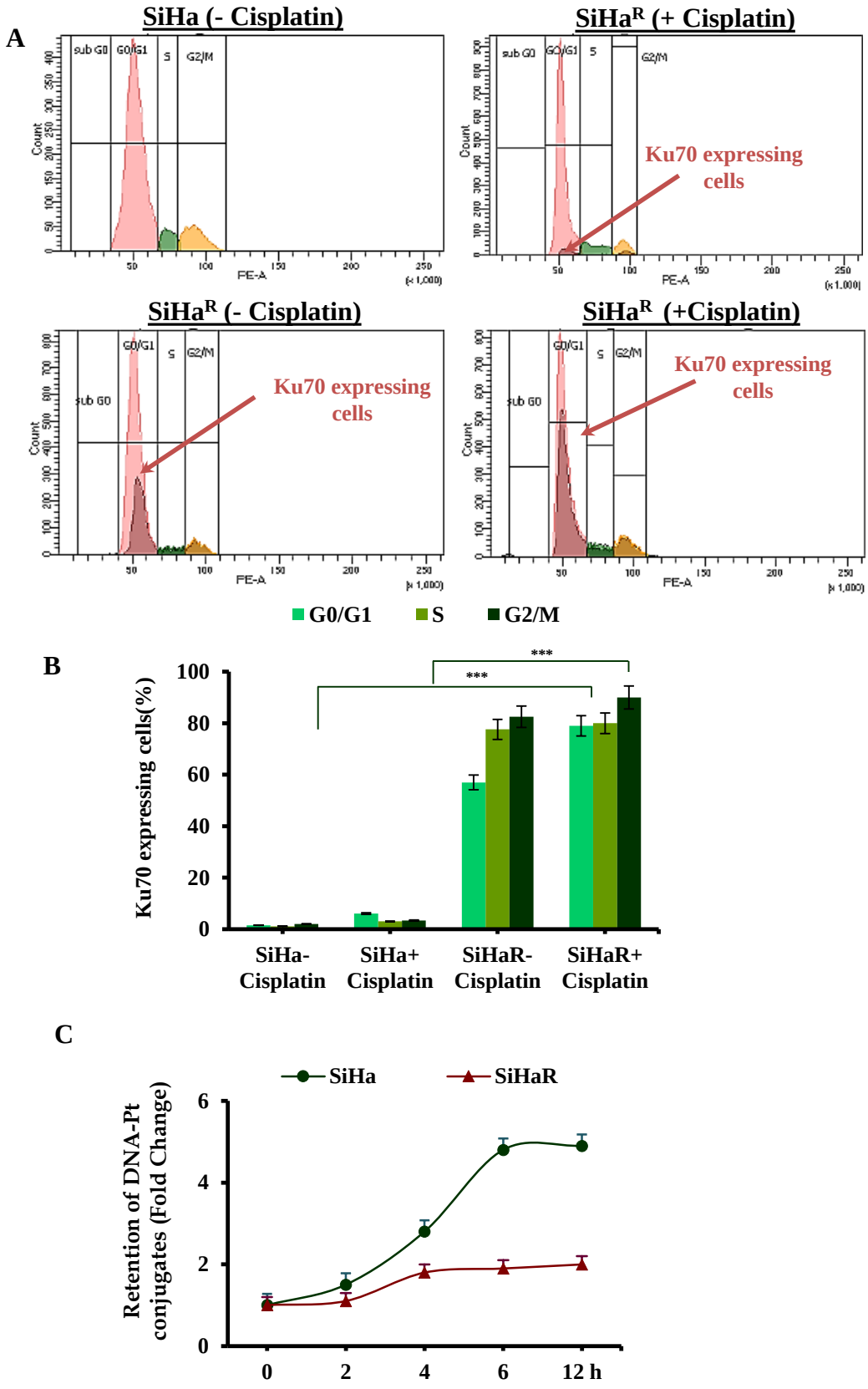

Figure 63: Impaired CDDP-DNA adduct Retention by SiHa^R: (A)Flow Cytometry results displaying the distribution of Ku70 positive cells in the different phases of cell cycle. (B) Stage specific frequencies of Ku70 positive cells. (C) Patterns of CDDP-DNA adduct retention by SiHa and SiHa^R cells.

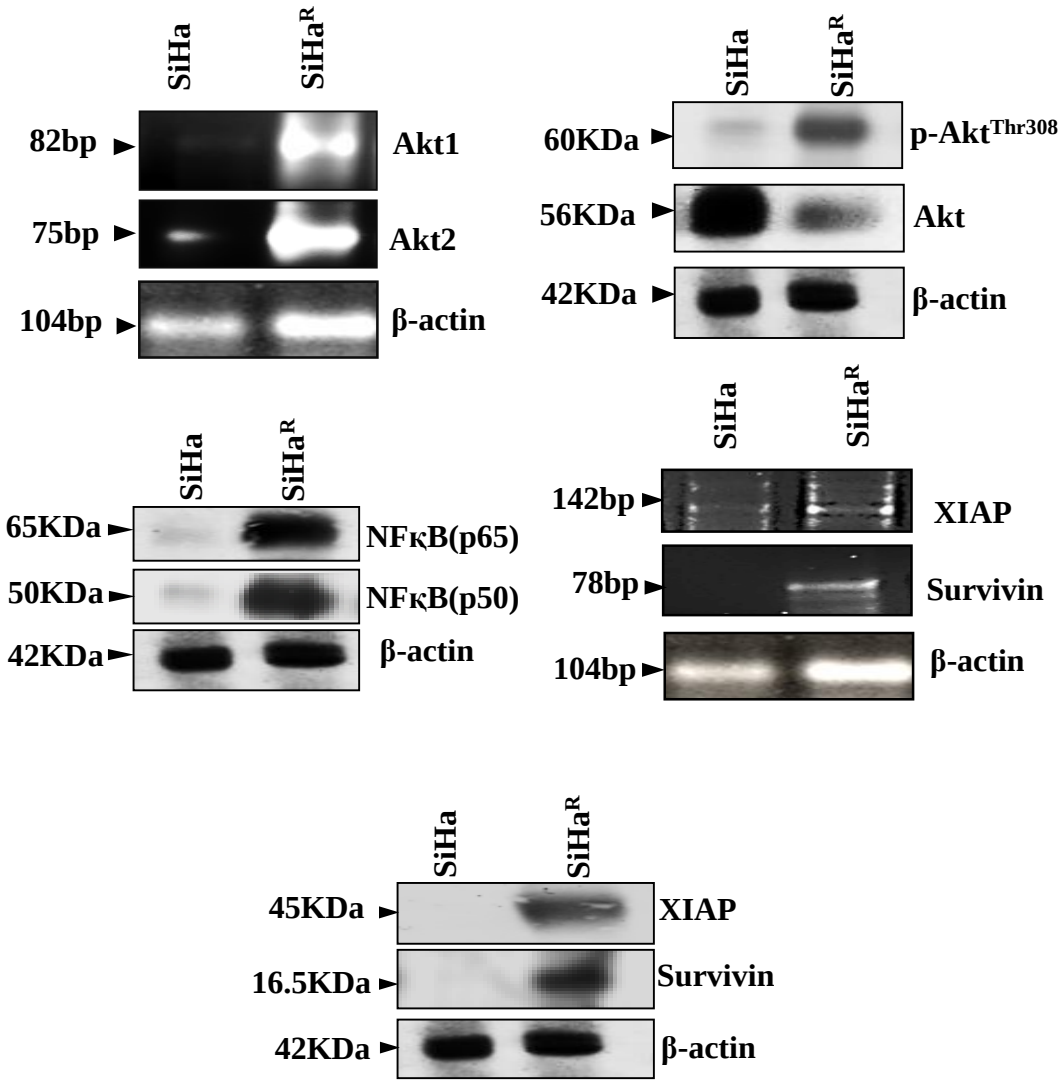

Figure 64: Molecular Differences between SiHa and SiHa^R: Western Blot and RT-PCR bands delineating differences in expressions of key prosurvival effectors of PI3/Akt pathway at protein and mRNA levels within SiHa and SiHa^R sublines. In each case, β-actin was used as loading control.

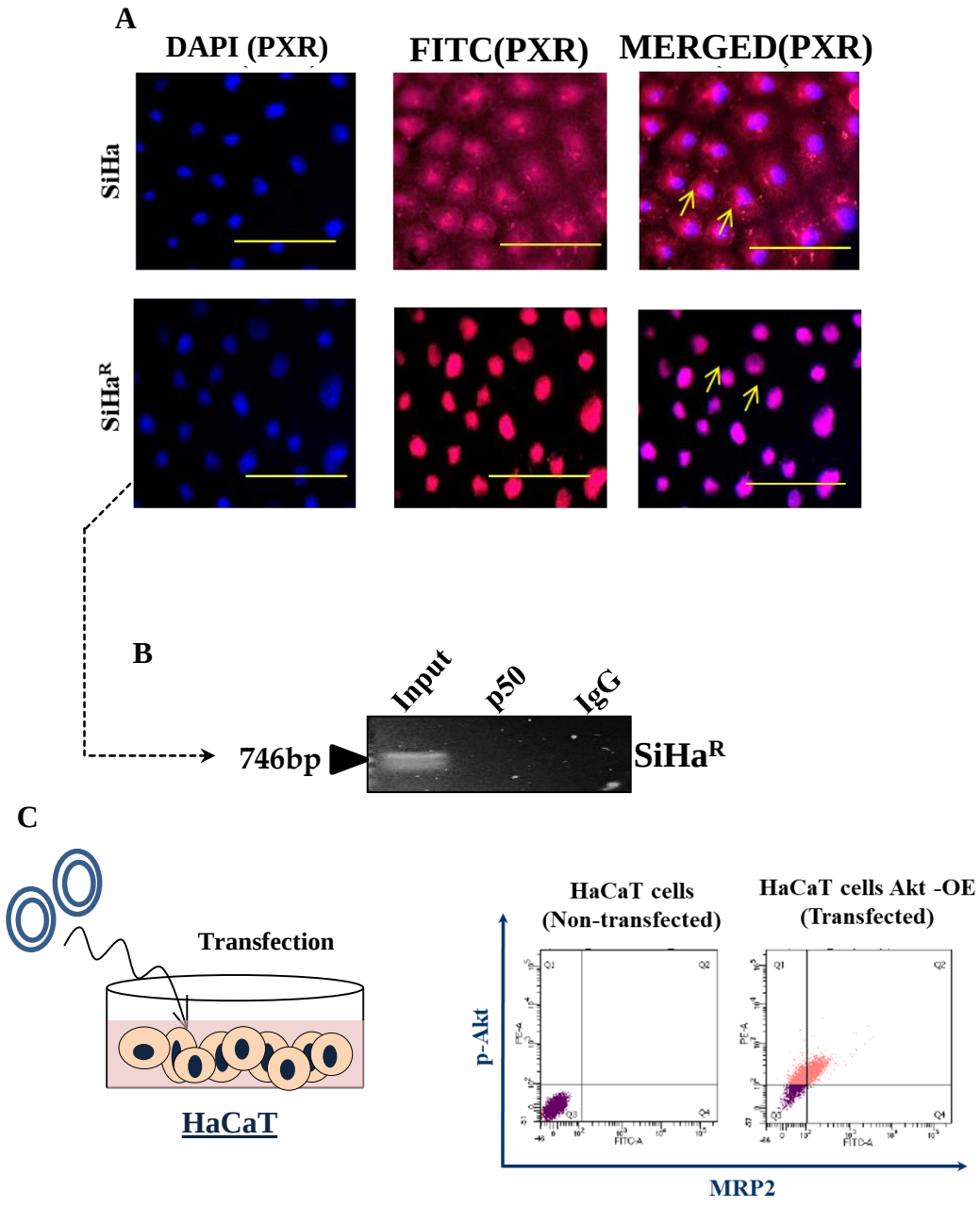

Figure 65: Cell Specific Expression of PXR and Validation of PI3K/Akt Pathway in conferring CDDP resistance: (A) Immunofluorescence Micrographs showing differential location of PXR in SiHa and $SiHa^R$ (B) DNA gel images for ChIP assay depicting negative binding of p50 upon the promoter response elements of MRP2 and Ku70. (C) Transfection of Normal Human Keratinocytes with wild-type Akt followed by investigation of CDDP exporter and $pAkt^{Thr308}$ expressions by flow cytometry.

❖ **Elevated expression of MRP2 in SiHa^R facilitates better intracellular uptake and accumulation of PEITC**

Owing to the deviant nature of SiHa and SiHa^R cells, PEITC was suspected to induce differential effects (Figure 66). Therefore, before exploring the mechanistic role of PEITC in overcoming acquired CDDP resistance, it was important to calculate the growth inhibitory dosage of PEITC in SiHa and SiHa^R cells (Figure 67A). MTT assay was undertaken following treatment of cells with PEITC doses ranging between 0.5-3µM for 3-12h respectively. Accordingly, the time-point of 3h was selected in which the IC_{50} dose of PEITC was calculated to be 1µM and 2µM for SiHa^R and SiHa respectively. This indicated that 50% killing in SiHa^R got mediated by exactly half of the PEITC IC_{50} dose of SiHa cells. This was supported by spectrophotometric results of cyclocondensation assay wherein SiHa^R was found to accumulate higher intracellular PEITC (0.3656±0.0026; 1µM) than SiHa (0.1601±0.00006; 0.09µM) for 3h and 4h respectively. Treatment extension till 5h yielded reduced absorbances of 0.2836±0.00021 (0.7µM) in SiHa^R cells. However, a subtle rise (0.2±0.0005; 0.5 µM) in PEITC level among SiHa cells was noted after 5h. Apparently, SiHa^R accumulated PEITC better than SiHa. In alignment with the spectrophotometric findings of cyclocondensation assay, mass spectroscopic analysis of PEITC-treated SiHa and SiHa^R for the same time-intervals was performed in order to identify the retention time for PEITC (Figure 67C). Respective mass-peak intensities of the cyclocondensed intracellular PEITC intermediate (1, 3-Benzodithiol 2 thione) was found to be maximum for SiHa^R in 3h which sustained till 4h followed by a decline. PEITC levels in SiHa could only be detected from 3h and onwards. Conclusively, the results permitted selection of 3h time-point as the ‘optimum treatment time’ in successive experiments.

When these experiments were repeated with $SiHa^R$ following treatment with MRP2 and Akt inhibitors, interesting observations were attained (Figure 68). Inhibition of Akt activation compromised PEITC accumulation by $SiHa^R$ unlike its usual nature. Conversely, upon MRP2 inhibition, the uptake reduced manifold. These findings affirmed that increased PEITC uptake in $SiHa^R$ was a result of higher MRP2 expression.

- **PEITC expedited CDDP retention and enabled CDDP mediated intracellular ROS generation to curb the growth of resistant cervical cancer cells**

SiHa and $SiHa^R$ were furthermore treated with 3.5µM of CDDP following a 3h pre-treatment with their respective IC_{30} PEITC doses (SiHa: 1µM; SiHaR: 0.5µM) for exploring the association between their PEITC accumulation and CDDP-retention capacities (Figure 69A). PEITC pre-treatment efficiently restrained $SiHa^R$ growth in even higher CDDP doses wherein it would normally grow in absence of the phytochemical. As evident from the graphical anecdote, 50% PEITC pre-treated $SiHa^R$ got killed by only 2 µM of CDDP while the same for SiHa cells was achievable with higher CDDP concentrations of about 3.7 µM (Figure 69B). These results highlighted the chemo sensitizing potentials of PEITC.

Intracellular platinum levels as quantified by flameless atomic absorption spectroscopy (FAAS) revealed an improved and increasing trend in the drug retention capacities of PEITC-enriched $SiHa^R$ cells with respect to PEITC-deficient SiHa for 24h (Figure 70A). Mechanistic insights of the chemoenhancing potentials of PEITC was further explored by checking the cell killing ability of retained-CDDP by generating ROS via disruption of mitochondrial-membrane potential followed by depletion of free-GSH levels. Depictions of flow cytometry results portrayed a clear peak shift for DCF generation in CDDP treated $SiHa^R$ cells in presence of PEITC pre-

treatment as compared to SiHa (Figure 70B). Frequency of DCF-bearing $SiHa^R$ cells was greater than that of SiHa for combinatorial treatment modalities (Figure 70C). Additionally, these findings were strengthened by the corroborating fluorescent microscopic results representing the ROS content of SiHa and $SiHa^R$ cells (Figure 70D). In fact, the relative mitochondrial-membrane potential was found to be highly disrupted in Rhodamine 123 staining assay because $SiHa^R$ cells accumulated rhodamine 16.7 times more than SiHa in combination treatment setup (Figure 70E). Interestingly, the free-GSH levels of $SiHa^R$ reduced by 0.39 folds upon CDDP treatment only in case of prior PEITC priming unlike SiHa, which showed no noteworthy alterations (Figure 71A). Finally, trypan blue dye exclusion methodology revealed a significant ROS-mediated reduction in $SiHa^R$ viability to 66 % ($p<0.0001$) from 98.5 % upon PEITC pre-treatment ahead of CDDP treatment (Figure 71B). All these results also entitled PEITC as a CDDP chemoenhancer in $SiHa^R$ cells.

- **PEITC increased the efficacy of CDDP by negatively regulating prosurvival markers and drug exporter MRP2**

In an effort to investigate the regulatory effect of PEITC over deregulated proteins (Akt, NFκB, MRP2, XIAP and survivin) for chemoenhancing CDDP, the $SiHa^R$ cells were treated with the respective pharmacological inhibitors alongside differential treatment with either CDDP or PEITC or both (Figure 72A). Proteins isolated thereafter were comparatively studied for deciphering the inhibitory role of PEITC. Western blot results depicted remarkable decrease in the expression patterns of $pAkt^{Thr308}$, total-Akt, XIAP, urviving, NFκB (p65), NFκB (p50) and MRP2 in combinatorial treatment modalities of PEITC and CDDP in comparison to single-agent treatments as well as untreated $SiHa^R$ (Figure 72A). Respective band intensities also revealed that the results were comparable with pharmacological inhibition of the

respective molecular markers (Figure 72A). This inhibition was not delimited at protein levels of these cells as the RT-PCR blots suggested a depleted expression of the relative mRNAs (Figure 72B). Moreover, PEITC was observed to directly affect the subcellular localization of MRP2 in $SiHa^R$. As portrayed in immunofluorescence micrographs of Figure 73, PEITC restricted MRP2 localization in the nuclear periphery of $SiHa^R$ cells which was originally found in their membrane in presence of sole CDDP treatment. On the contrary, neither the cell membranes nor the nuclear periphery harboured any MRP2 in $SiHa^R$ upon subjection to CDDP after PEITC pre-treatment.

PEITC was lastly screened for the top-ranked poses based upon docking score and non-bonded contact potential with the target protein conformations. Docking results (Figure 74), delineated highest affinity between PEITC and Akt2 (-5.9 kcal/mol) and XIAP (-5.9 kcal/mol). Specifically, Thr213 residue of Akt2 formed hydrogen bond while its Leu204 formed pi-pi electrostatic interaction with PEITC. XIAP exhibited one hydrogen bond (Gly306), three pi-pi- electrostatic and two electrostatic interactions with Gln319 and Trp323 residues. An overall strong affinity was also observed between NFκB and PEITC (-5kcal/mol). Detailed portrayal of considerable interactions between PEITC and other molecules also supported the notion. Therefore, PEITC relayed the role of RMA successfully by reverting CDDP resistance through downregulation of PI3K/Akt pathway and improvement of cellular drug retention capacities.

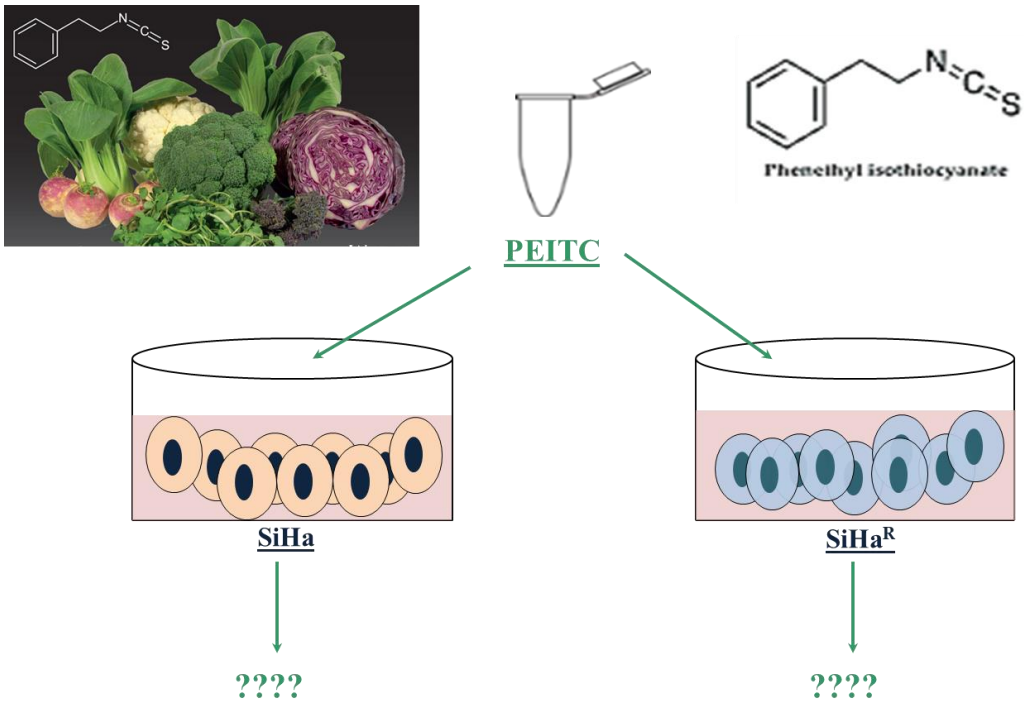

Figure 66: An overview of rationale followed for deciphering the differential effects of PEITC in SiHa and SiHa^R cells.

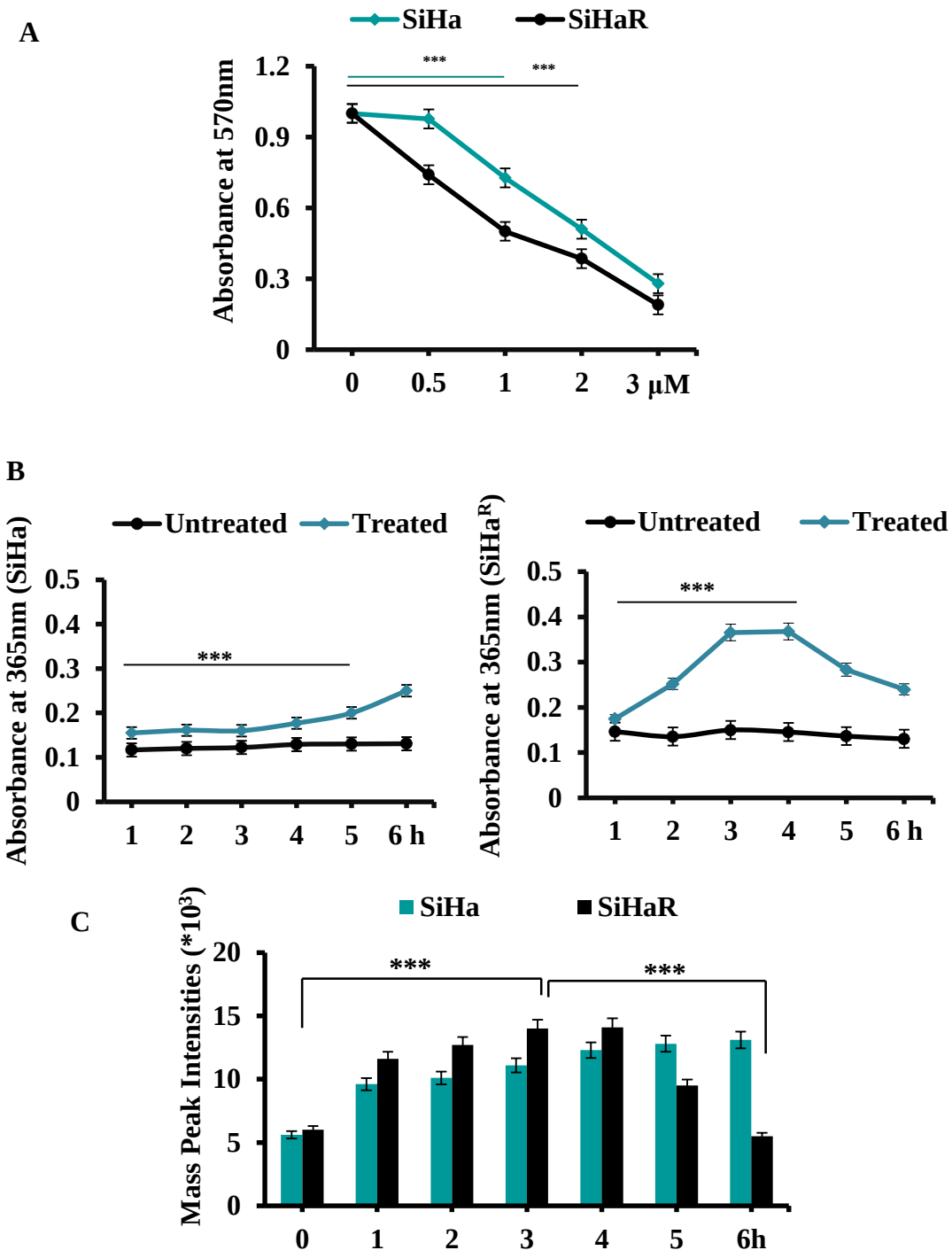

Figure 67: Cellular Accumulation of PEITC: (A) MTT Assay results confirming the differential response of SiHa and SiHa^R cells towards PEITC. (B) Cyclocondensation Assay results depicting better accumulation of PEITC by SiHa^R cells compared to SiHa. (C) Mass Peak Intensities corroborating with cyclocondensation assay findings.

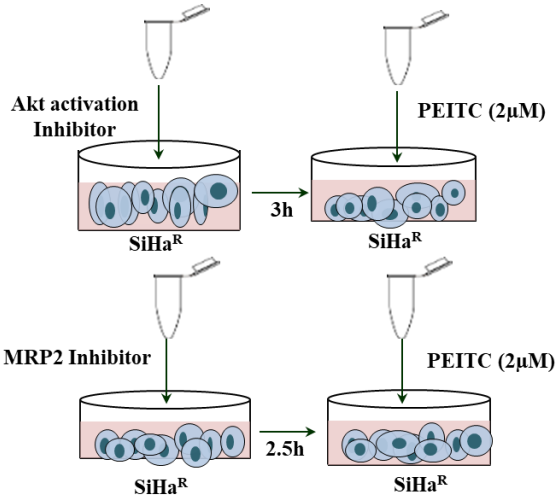

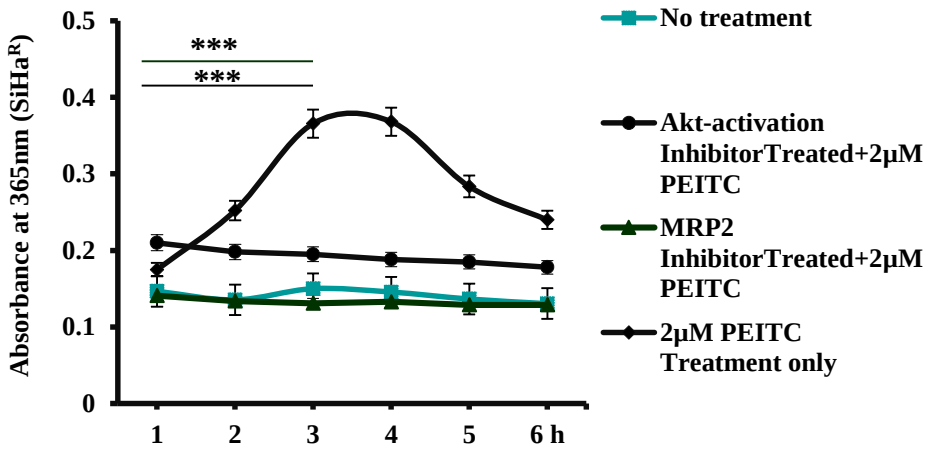

	MRP2 EXP	PEITC
MRP2 EXP	1.00	
PEITC	0.9876*	1.00
p<0.0001		

Figure 68: Importance of MRP2 in cellular PEITC uptake: Cyclocondensation Assay Results asserting the necessity of MRP2 for promoting PEITC uptake and accumulation.

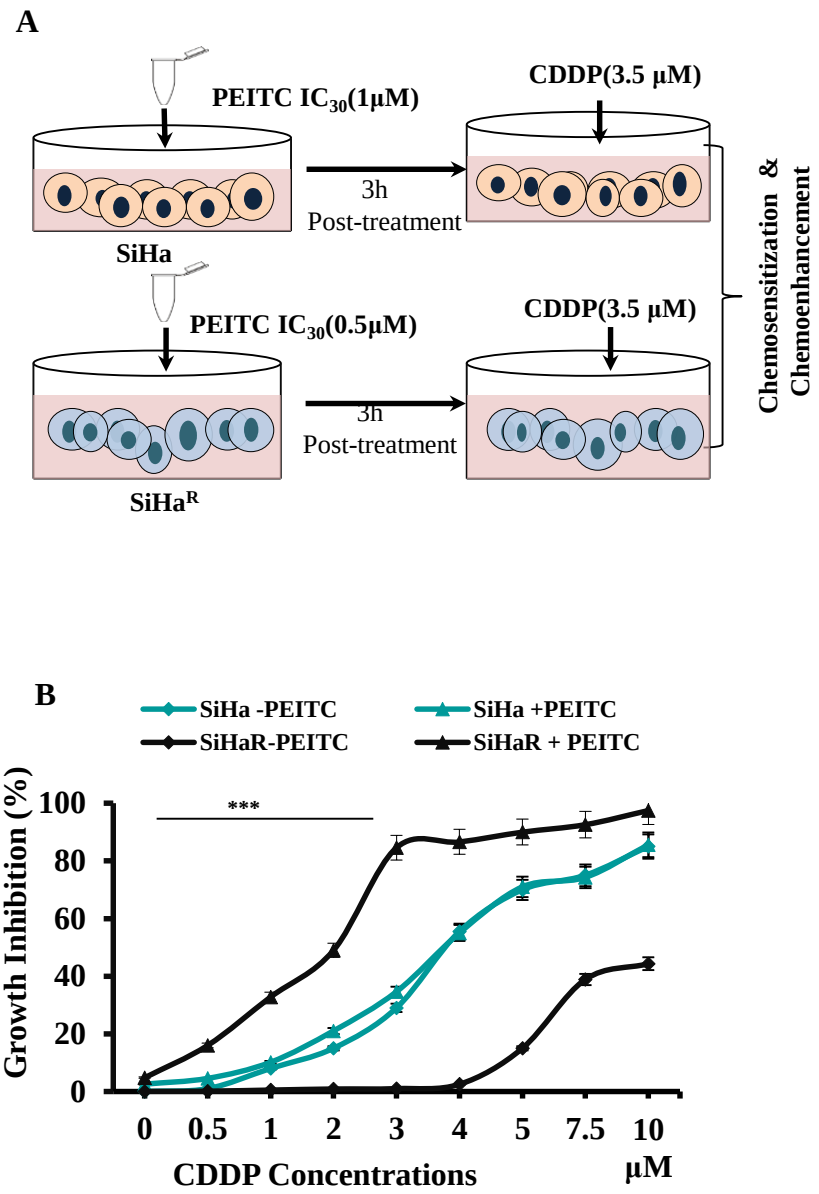

Figure 69: Role of PEITC as a RMA: (A) Pictorial Elaboration of the Work Plan followed for interpreting the role of PEITC as a CDDP chemosensitiser and chemoenhancer. (B) Growth Inhibition curves for SiHa and $SiHa^R$ representing extent (%) of cell growth restriction obtained on administration of their respective PEITC IC_{30} dose alongwith varied range of CDDP concentrations ($^{***}p<0.0001$).

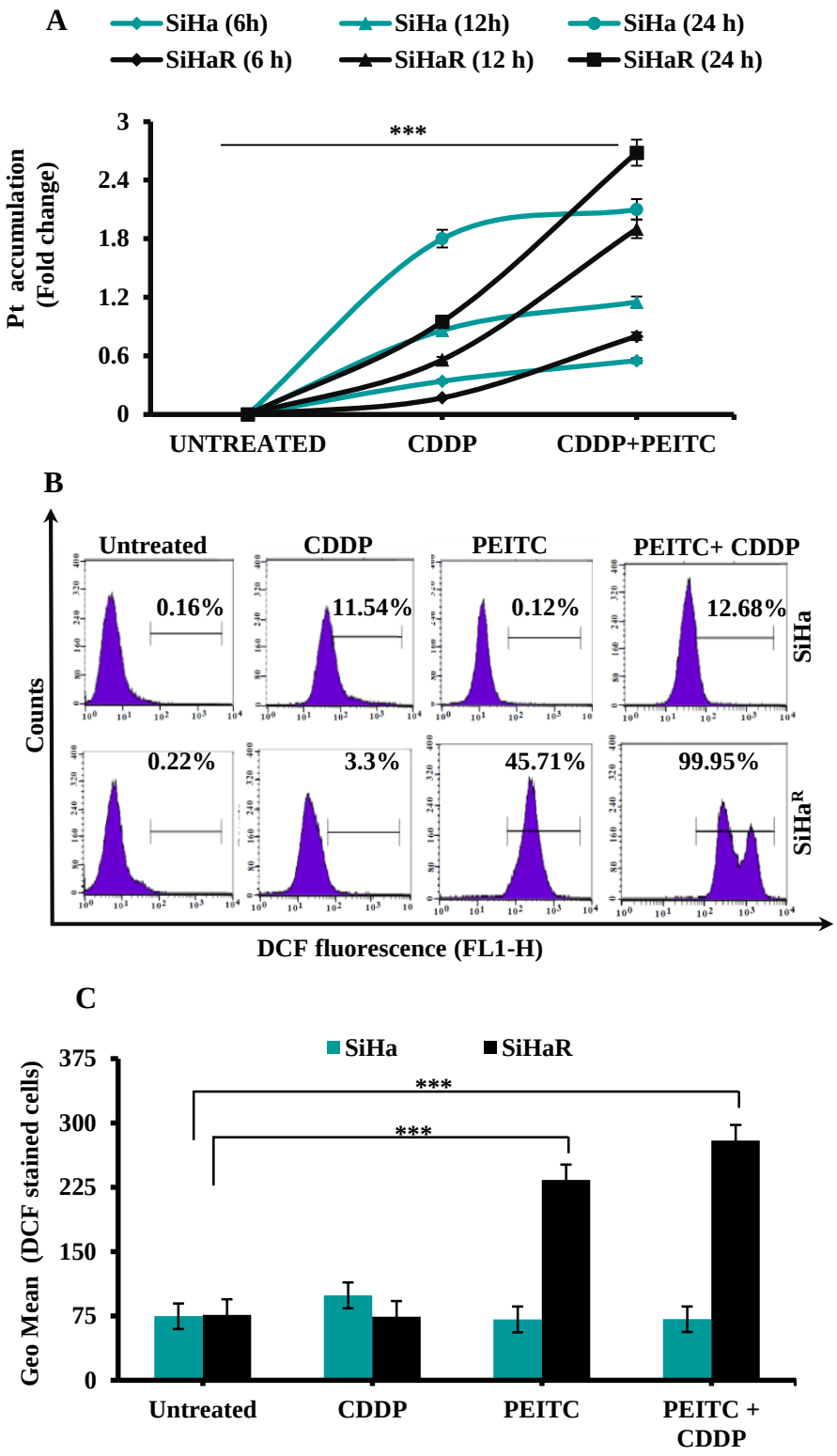

Figure 70: Efficacy of PEITC as a CDDP resistance reversing molecule: (A-C) Quantitative and Qualitative estimation of PEITC's potential as a CDDP sensitizer and enhancer in terms of– (A) Intracellular Platinum Retention. (B&C) Inducing ROS generation. All numerical values are represented as Mean ±S.D (***p<0.0001).

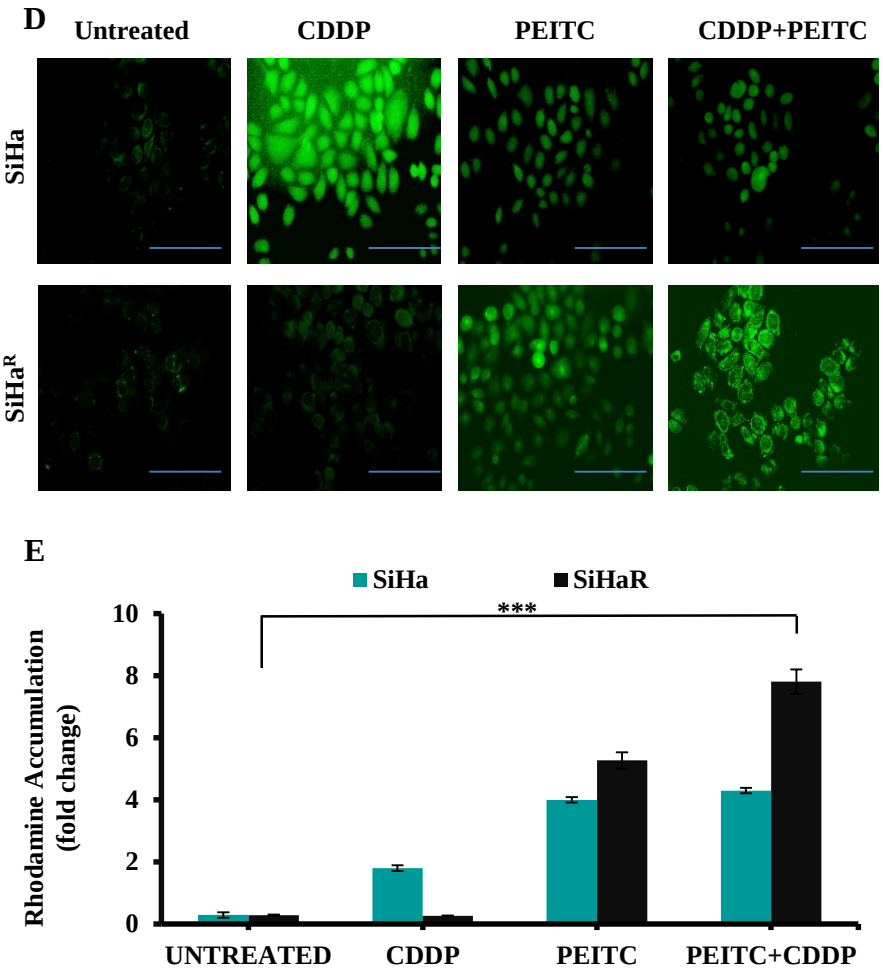

Figure 70: Efficacy of PEITC as a CDDP resistance reversing molecule: (D & E) Quantitative and Qualitative estimation of PEITC's potential as a CDDP sensitizer and enhancer in terms of– (D) Inducing ROS generation and (E) Disrupting Mitochondrial Membrane potential. All numerical values are represented as Mean ±S.D (***p<0.0001).

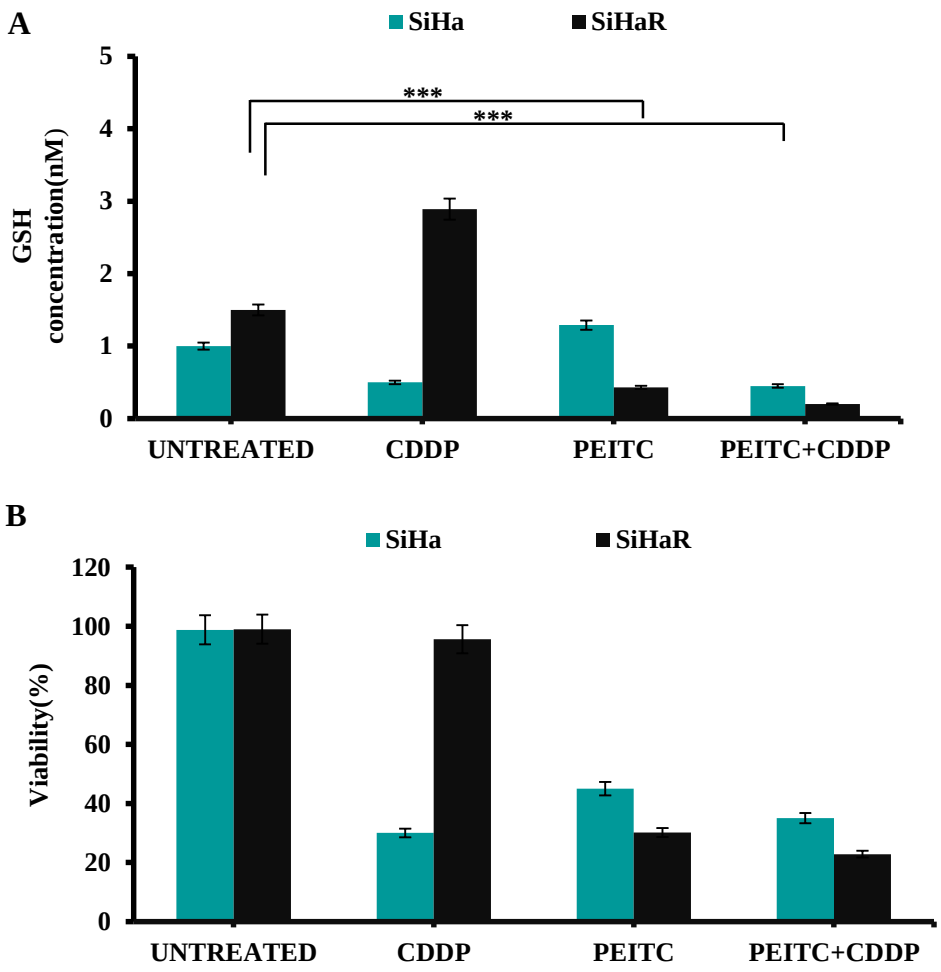

Figure 71: Role of PEITC as a pro-oxidant: (A) Graphical anecdote for the capacity of PEITC in reducing free-GSH levels among $SiHa^R$ for accelerating CDDP cytotoxicity. (B) Trends in cellular viability patterns for SiHa and $SiHa^R$ cells following treatment with PEITC either as single agents or alongside CDDP. Values are represented as Mean ±S.D (***$p<0.0001$).

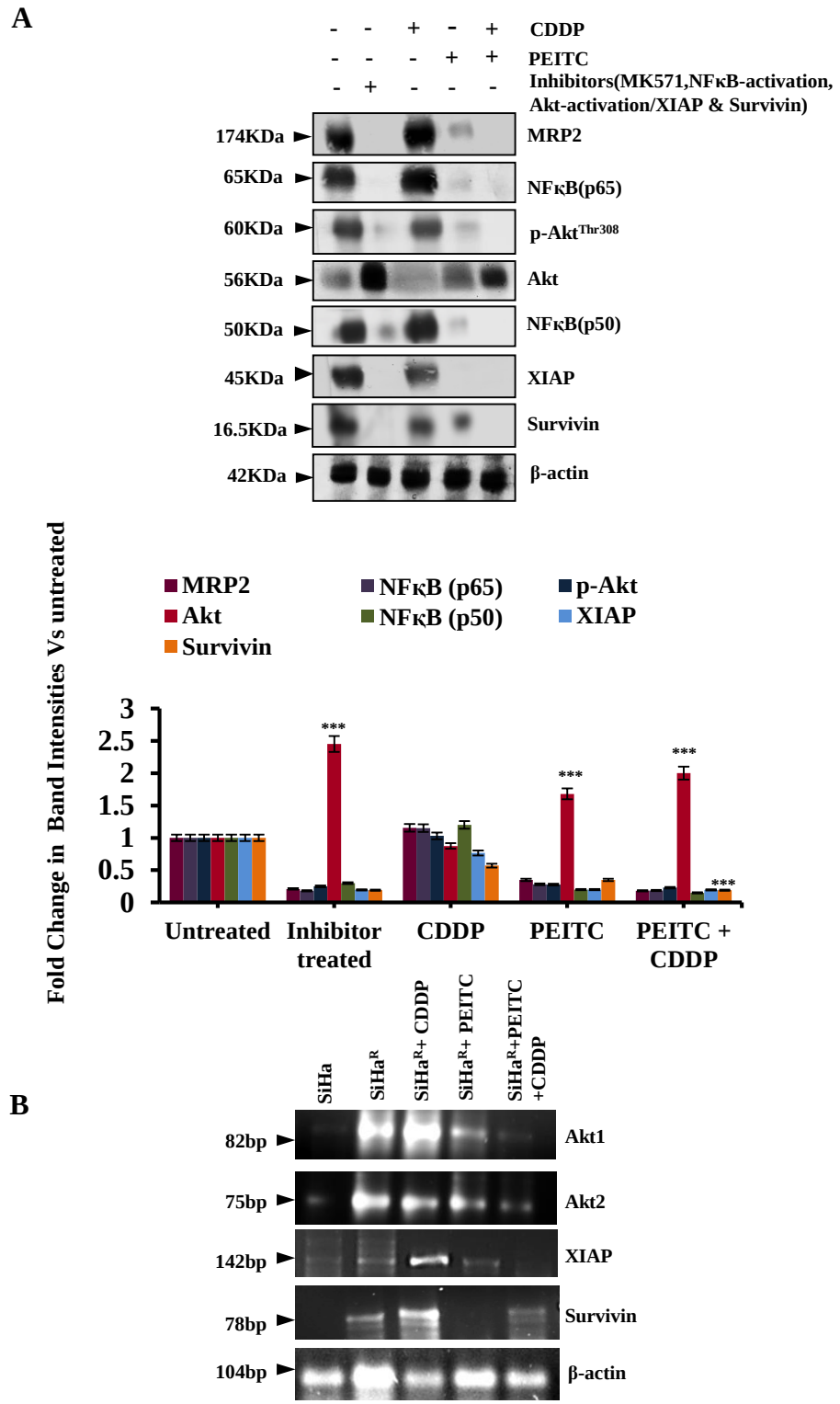

Figure 72: Role of PEITC in regulating PI3K/Akt pathway *in vitro*: (A)Western Blot Bands and their relative intensities showing the inhibitory effect of PEITC upon PI3K/Akt pathway effectors at protein levels. (B) RT-PCR bands confirming PEITC mediated inhibition of PI3K/Akt pathway at mRNA levels. β-actin was used as loading control for both cases. Protein Band Intensities were calculated after normalization with β-actin and were represented as Mean± S.D (***p<0.0001).

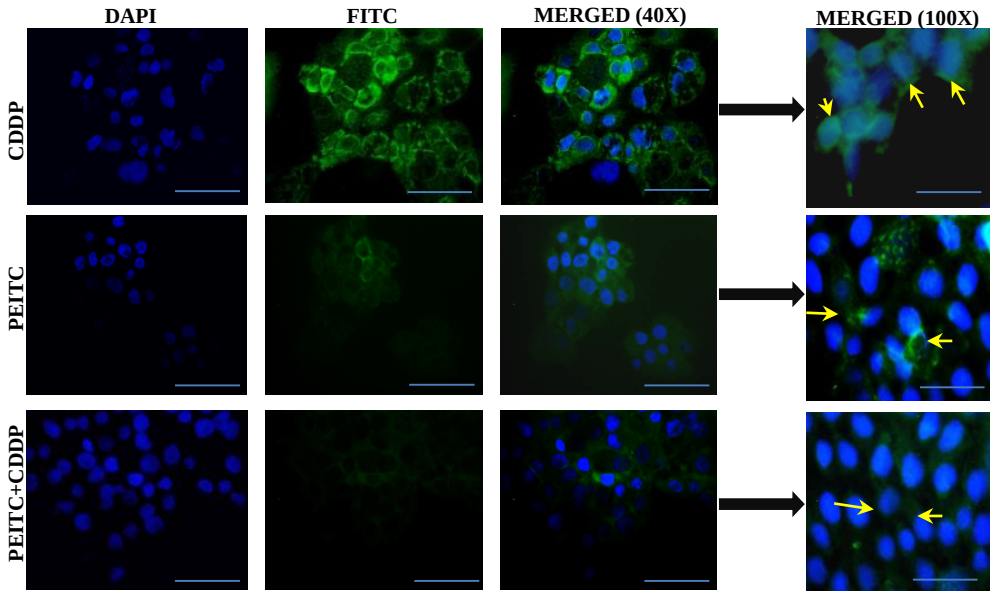

Figure 73: Immunofluorescence micrographs showcasing PEITC's ability to restrict membrane translocation of MRP2 for curtailing cellular CDDP export.

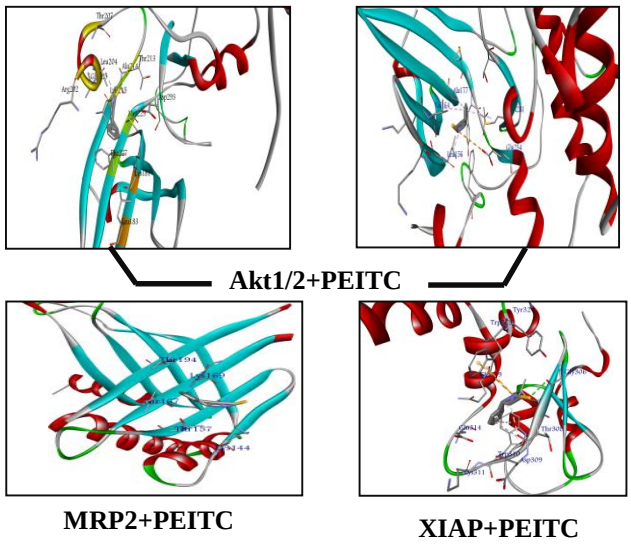

Protein	PDB ID	Affinity (kcal/mol)
Survivin	1FH3	-5.1
Akt1 pleckstrin homology domain	1H10	-4.7
Akt2	1MRY	-5.9
MRP2	2GIA	-3.6
XIAP	3CLX	-5.9
Akt1	3OCB	-5.3
NFκB	4Q3J	-5

Figure 74: Interaction of PEITC with PI3K/Akt pathway effectors: *In silico* analysis for finding out plausible interacting abilities of PEITC with key prosurvival effectors and CDDP exporter MRP2 of PI3K/Akt pathway.

Discussion

8. DISCUSSION

The rising incidences and mortalities of cervical cancer have made it a serious concern among the clinicians, scientists and patients. With ‘relapse’ and ‘recurrence’ frequenting the scenario, ‘therapy resistance’ to conventional platinum-ligated drugs like CDDP is regarded as the prime villain which has to be battled for proper disease management [Esmatabadi et al., 2016; Mitola et al., 2021]. The conundrum of resistance is complex, intricate and randomly-orchestrated within the TME as a mode to escape therapy [Gui and Bivona, 2022a]. Therefore, the solutions to it lie within the TME which needs to be explored well [Luan et al., 2021; Salemme et al., 2023]. Unearthing the molecular interplays of patient-specific cervical TMEs enable identification of druggable targets which might aid in reversal of resistance [Yuan et al., 2016; Henke et al., 2020]. However, this requires large scale studies to be conducted among significant size of patient samples with evidential supports from pre-clinical disease models. With this aim, the present study mainly focussed onto the mechanisms in which constitutive activation of oncogenic PI3K/Akt pathway within cervical cancers intensifies the cellular prosurvival instincts to ultimately render them CDDP insensitive.

For this purpose, two cervical cancer disease models within *in vivo* and *in vitro* set ups have been developed. Firstly, the study was initiated with development of an *in vivo* cervical cancer model in Swiss Albino mice by chronic treatment with 3MC over a period of 30 weeks [Mahapatra et al., 2020]. Use of 3MC as a carcinogen for development of carcinoma models is a well-studied fact in accordance to which it has been employed as an agent to induce cervical carcinogenesis [Murphy, 1961; Forsberg and Breistein, 1972; Graham, 2009; Jablonska et al., 2021]. In alliance with this fact, chronic 3MC exposure for 6, 12, 16, 24 and 30 weeks resulted in induction of mild dysplasia, moderate dysplasia, invasive carcinoma (carcinoma *in situ*) and severe full length dysplasia within the cervical epithelium. Especially,

at and after 24th week, poorly differentiated anaplastic tumors (~9gm weight) with large number of keratin pearls, giant tumor cells with aggressive features were attained. Interesting findings as noted in cytopathology studies showed that 3MC exposure led to extensive 'keratinization' of cervical exfoliated cells in addition to increasing their nuclear content and destroying their morphologies. These changes were reflected at histological levels as well; depicting 3MC mediated oncogenic remodelling of cervical epithelium. These first-hand findings cumulatively approved of the successful development of an *in vivo* cervical cancer model.

Traditionally, cervical cancer results from heavy infection burden of the oncogenic virus HPV [Pincock,2008; zur Hausen,2009]. Malignant transformative process as triggered by HPV priorly instils a CDDP evasive attribute among the cancer cells [Mahapatra et al., 2021]. When HPV infected cervical cancer cells encounter CDDP, a complex molecular interaction between deregulated tumor suppressors, DNA damage-repair enzymes and prosurvival molecules onsets. Such cells, by the virtue of their ambiguous molecular triggers develop a tendency of adapting to apoptotic inducers like CDDP so as to survive effortlessly [Mahapatra et al., 2021; Gui and Bivona, 2022]. The TME is therefore bestowed with a CDDP resistant phenotype wherein the neoplastic cells override the apoptotic cues generated during chemotherapy [Wan et al., 2021; Mann et al., 2023]. In this regard, the present study attempted to mimic these HPV induced carcinogenic remodelling by 3MC treatment which might serve as a presumptive driver of CDDP resistance. Therefore, 3MC treatment among mice was accompanied by methodical characterization of cervical tissues, tumors and murine systems for investigation of PI3K/Akt pathway deregulations which could predict CDDP response. Herein, characterization was initiated with trail of the immediate observations monitored in cervical cytopathology at 3MC treatment intermittence of 6th, 12th, 16th, 24th and 30th weeks. In this context, an important anecdote was high rate of leukocyte infiltrations in

the cervical region at the 16th week which was indicative of persistent inflammation. Cervix, being the uterine periphery is under constant immune surveillance [Carrero et al., 2021]. It is always patrolled by leukocytes, specifically eosinophils for its acidic nature. Any shift or drift in the cervical leukocyte subpopulation is therefore alarming. As observed in this study, large numbers of neutrophils were detected in mice cervical region due to chronic 3MC treatment [Mahapatra et al., 2020]. These neutrophils came up with altered morphologies and were eventually accompanied by monocytes. Cumulatively, they replaced the eosinophilic multitude of mice cervix at 16 weeks of 3MC treatment. High blood neutrophil count is always considered to be a vital marker for cancer prognosis [Wu et al., 2019]. Neutrophils are the major drivers of localized inflammation which releases cytokines as chemoattractants for other inflammatory cells [Liew and Kubes, 2019; Ng et al., 2019]. Herein, appearance of monocytes during the later phases of 3MC treatment justifies the role of neutrophil in maintaining a state of chronic cervical inflammation which potentiated neoplastic growth.

Another interesting observation of the present study was formation of enlarged spleen (splenomegaly) which was specifically observed in mice at 16th week of 3MC treatment and onwards. Documentation of the cumulative experimental findings had unveiled the treatment period of 16th week as a ‘crucial-interim’ for development of invasive cancer among these mice. Enlarged spleen showcased an altered histopathology which was characterized by the presence of eosinophil inflitrations and enhanced number of ‘germinal centres’ which are the nourishment and training hubs of the naive blood leukocytes for becoming immunologically competent [Aoufouchi et al., 2022]. These findings apparently bridged with the cytopathological observations. Cervical inflamogenic mediators therefore seemed to have drained into the cervix from an enlarged spleen wherein relentless leucopoiesis was existent. Besides spleen, mononuclear infiltrations and dysplasia was also evidenced in the murine livers owing to 3MC treatment in mice. This was a crucial finding with respect to 3MC which

is a carcinogen of PAH family. Metabolic transformation is a pre requisite for 3MC to mediate carcinogenesis in any organism [El-Bayoumy et al., 2016]. Like other PAHs, 3MC also gets metabolized by the liver CYP450 leading to generation of electrophilic moieties which eventually induces DNA damage for propelling carcinogenesis [El-Bayoumy et al., 2016]. Administration of 3MC in *in vivo* model of cervical cancer was although limited to the cervical region but its effect was discerned in the entire murine system. Excess of carcinogen induced stress lead to distorted liver function [Mahapatra et al., 2020]. In this study, it served as an important contributor in establishment of carcinoma. SGPT, SGOT and ALP activities in blood serve as the major determinants of liver function efficiency [Vinaykumar et al., 2020]. High serum SGPT and SGOT levels indicate despaired liver function which aids in assessing the impact of carcinogen induced stress upon the mice physiology [Vinaykumar et al., 2020; Altaf et al., 2022]. Here also, development of an *in vivo* carcinoma model was driven by a negatively impacted liver function profile. Escalated serum SGPT and SGOT levels, as evoked by 3MC were suggestive of systemic stress. This particular dosage of carcinogen when administered to mice in a chronic fashion induced necessary hepatic toxicity which became the prerequisite to keep carcinogenesis going. A similar trend in ALP kinetics within blood serum furthermore confirmed these findings. These biochemical changes allied with the transfigured histological architecture of murine livers of these animal batches. On the other hand, presence of median renal dysfunction was confirmed by high serum creatinine levels. A systemic fall out was therefore vivid and distinct in the entire process of 3MC treatment. With inflammation being the prime clue, the study further progressed with deciphering the impact of impaired hepatic and renal functions upon systemic ROS, RNS and iNOS titres. Yet again, a positive association was unravelled which clearly hinted towards a possibility of ‘inflammogenesis of cervical cancer’. A concurrent chronic surge in ROS and RNS levels allied with the rising activities of iNOS enzymes, particularly from 16^{th} week

onwards. Impact of multiple oxidative hits was apparent in the form of progressive genotoxic stress as observed from damage incurred upon the leukocyte DNA. As a result, 3MC got potentiated as a carcinogen only after biotransformation. Thus, its effect upon the systemic parameters in the long run was inevitably pro-carcinogenic.

The intricate association between inflammation and cancer dates back to 19th century [Balkwill and Mantovani, 2001]. Proposed to be one of the key factors responsible for initiating the malignant transformation, inflammation is rightly termed as the seventh hallmark of cancer [Colotta et al., 2009]. In this study, 'inflammogenesis of cervical cancer' became imperative when cervical ROS, RNS as well as iNOS were conjugatively escalated just like that of the murine systems. In fact, a compromised anti-oxidant capacity appeared to be allowing the free radical outburst to prevail within mice cervix. During the developmental stage of *in vivo model*, inflammation mediated carcinogenesis was found to be associated with higher expression and activity profiles of inflammatory cytokines as well. In HPV-16 mediated cervical carcinogenesis, IL6 titres are found to be comparatively higher in invasive cervical carcinoma stages than in the precursor lesions [Castle et al., 2001; Paradkar et al., 2014]. IL6 was reported to strengthen the scenario of inflammation by fostering monocyte chemoattractant protein-1 which recruits monocytes to the site of malignancy [Balode et al., 2018]. This signalling axis further activates IL8 which is also known as neutrophil activating factor [Matsushima et al., 2022]. A community signalling loop including IL6, IL8 and TNFα in the present findings, made the scenario of cervical inflammation fiercer. During development of this *in vivo* model, a long period of treatment with 3MC evoked a cytokine storm in the cervix which invited granulocytes and agranulocytes for orchestrating the episode of carcinogenesis.

Chronic inflammation plays a crucial role in enriching the TME with prosurvival signals that enable neoplastic cells to survive and proliferate by escaping the host immune

responses [Figueiredo, 2019; Andreeva et al., 2020]. So, next up the study delved deep into finding out whether this consistent inflammation resulted in upregulation of PI3K/Akt pathway or vice versa. An evident upregulation of prosurvival signalling surfaced with gaining expressions of $pAkt^{Thr308}$ vis-a-vis declining profiles of total Akt. Collaborating with an activated Akt, crucial prosurvival effectors like COX2, HIF-1α, Ku70, NFκB (p65/p50), VEGF, XIAP and survivin were severely upregulated. The cervical molecular interactome also involved erratically expressed tumor suppressor proteins (p53, p21 and Rb). This reinforced malignant transformation of the reproductive organ anatomy, cytopathology, histopathology and biochemistry of carcinogen treated mice. A built-up of growth favouring molecular crosstalk was very well discerned. For instance, COX2 and p53 are antagonistic in function because the later positively regulates 'thrombospondin-1' which reportedly inhibits VEGF to shut down angiogenesis [Janani. et al., 2021; Tong et al., 2014]. Hypoxia induced functional facilitation of p53 is a common occurrence within tumor lumps alongside activation of NFκB and COX2. However, during carcinogenic discourse, growth aiding cues received in terms of hiked iNOS activity reportedly encourages NFκB and COX2 for overriding p53 action so as to progress with neoplasia [Tong et al., 2014]. In agreement with these previously published reports, cervical tumors obtained after 24 weeks of carcinogen treatment in this study also exhibited a high COX2 and NFκB expressions in their core. Furthermore, a surged in cytokine allies with NFκB activation wherein IL6 is the upstream mediator while IL8 and TNF-α are the downstream effectors [Matsushima et al., 2022]. As a result, larger extent of immortalisation was thereafter found in terms of nuclear accumulation of proliferative antigen Ki67. As comprehensible from IHC results, Ki67 evenly disbursed from the proliferative basal layer to rest of the differentiated cervical epithelial layers. Conclusively, these findings pointed at successful promotion of inflammation mediated carcinogenesis.

The molecular intricacies of a TME also decide the chemotherapeutic response of tumors. For instance, hyperactivation of PI3K/Akt pathway negatively relates with CDDP sensitivity [Dong et al., 2021]. In this study, reiteration of similar findings was seen in the *in vivo* cervical cancer model. For the assessment of CDDP response, purposeful planning of a human-equivalent treatment regime with the animals was undertaken. On this basis, invasive cancer bearing mice were administered 3mg/kg bodyweight of CDDP dose in two consecutive chemocycles. Herein, a negative impact of constitutively upregulated PI3K/Akt pathway upon the drug action was evident in terms of compromised ROS and RNS generation in addition to maintenance of heightened GSH levels. Induction of excessive ROS generation is reported to be the ultimate way of cytotoxicity mediation [Mirzaei et al., 2021; Xin et al., 2022]. On the other hand, maintenance of sustained ROS levels is a must for proliferating cancer cells [Zhou et al., 2014; Xin et al., 2022]. CDDP challenge in repeated cycles of chemotherapy overtly induces a free-radical outburst to drive programmed cell death [Mirzaei et al., 2021]. Therefore, a cellular mechanism to prohibit CDDP from evoking extensive ROS generation could be the best way out for escaping the drug. Cervical cancer cells herein must have found an escape route to this chemotherapeutics by elevating its anti-oxidant capacities to quench therapy induced ROS.

In this context, an interesting molecular mechanism of cellular adaptation unfolded. An unusual observation in terms of NFκBp50 abrogation and p65 upregulation was noteworthy. Again, a collateral surge in PXR levels was also recorded. Popular as a nuclear orphan receptor, PXR plays an important role in aiding cells to overcome xenobiotic assault [Niu et al., 2022]. In absence of xenobiotics like CDDP, PXR subunits reside in the cytoplasm as a homodimer while in their presence, it heterodimerizes with various other factors including p65. This PXR-p65 heterodimer thereafter translocates to the nucleus to get recruited over the response elements of effectors like drug exporters and xenobiotic enzymes

which prepare cancer cells to adapt with chemotherapeutics by detoxifying them [Oladimeji and Chen, 2018; Lv et al., 2022].

PXR facilitates translation of cellular MRP2 which flushes CDDP out swiftly from the cellular interiors to promote resistance. In this study, PXR and p65 showed distinct nuclear accumulation whilst p50 subunits remained in the cytoplasm. These results asserted an interplay of PXR and p65 in remodelling the carcinogen induced TME towards gaining an inherent CDDP insensitive nature. It is because of this molecular crosstalk that CDDP administration for 2 consecutive weeks failed to invoke free-radical outburst and curtail free GSH levels to mediate tumor attrition.

These findings got further verified in an *in vitro* setup wherein a constitutive upregulation of the PI3K/Akt pathway provided survival advantage to SiHa cells which were isolated and grown separately as a CDDP-resistant subline named $SiHa^{R}$. This CDDP resistant counterpart was characterized by higher expressions of CDDP exporters like MRP2, ATP7A and ATP7B alongwith the repair enzyme Ku70 and prosurvival effectors like NFκB (p65/p50), XIAP and Survivin. Herein, PI3K/Akt upregulation allowed a gradual transformation of a CDDP sensitive phenotype to a resistant one. SiHa cells, in this study, were subjected to CDDP selection regime called ‘pulse treatment’ in which the resistant and tolerant clones survived while the sensitive ones got eliminated. Particularly, SiHa cells with heightened MRP2 expression managed to survive well with recurrent CDDP challenge during which ATP7A and ATP7B production got induced. Interesting observation was also seen in terms of Ku70 guiding SiHa cells to evade CDDP mediated cell cycle arrest. Patterns of cellular distribution among various phases of cell cycle clearly showed that with surged Ku70, the transformed $SiHa^{R}$ cells denounced the drug to keep progressing towards division. Herein, again PXR acted as a fulcrum of this episode where it maintained a balance between the

prosurvival and chemotherapy detoxification cues. In a nutshell, the phenomenon of 'clonal evolution of neoplasm' got orchestrated within a cell plate.

Resolving the problem of acquired CDDP resistance by finding specific chemosensitizers is the utmost need of this hour. In this regard, natural isothiocyanates can be considered as better options due to their ability to exploit drug-exporters for cellular entry. Paramount reports suggested that efflux-pumps (Pgp, MRP1/2 and BCRP) promotes intracellular import of isothiocyanates [Telang et al., 2009; Mi et al., 2011; Morris and Dave, 2014]. PEITC, in this study, was found to chemosensitize MRP2 overexpressing CDDP-resistant $SiHa^R$ cells which also promoted its intracellular uptake and retention. Hence, PEITC in this study was identified as a better cell growth inhibitor for $SiHa^R$ compared to SiHa. Previous experimental evidences have firmly established PEITC as an anticancer, chemopreventive [Chen et al., 2012; Ioannides and Konsue, 2015; Suvarna et al., 2017] and chemosensitizing agent [Yang et al., 2014]. Correlatively, $SiHa^R$ cells which grew prolifically in 3.5 µM of CDDP owing to acquired CDDP resistance; had surprisingly ceased to grow in the same as well as higher drug doses following PEITC pre-treatment for 3h. This permitted negation of relative toxicity of CDDP which often impedes therapy. This pre-treatment improved drug retention capacities of $SiHa^R$ and thereafter delivered adequate growth inhibition. However, PEITC-primed SiHa cells exhibited no enhancement in their platinum levels and their viability remained unaffected. This corroborated with the preferential PEITC accumulation in $SiHa^R$ over SiHa cells.

Chemosensitization is just not enough for reversal of acquired chemoresistance among aggressive cancers as their deregulated molecular signaling conveniently deteriorate the chemotherapeutic pharmacodynamicity. ROS overproduction in $SiHa^R$ cells upon PEITC treatment (sole/combinatorial) supported the above viewpoints and also aligned with pre-existing reports [Hong et al., 2015]. The present study recorded high free-GSH levels in

CDDP treated SiHa^{R} cells which went down manifold when 3h of PEITC pre-treatment was ensued. This abided with reports suggesting the prevalence of inverse correlation between increased cellular GSH levels and CDDP accumulation [Liu et al., 2021] as the drug also attacks GSH for allowing cellular cytotoxic death by free-radical outburst [Achkar et al., 2018]. Among SiHa cells, even tracer amounts of PEITC couldn't mediate pro-oxidant functions neither in presence nor in absence of CDDP. This gravitated the importance of 'exposure-time' and 'exposure-dose' of PEITC in relaying anti-oxidant or pro-oxidant functions in a cell-specific manner. Mitochondrial membrane-potential disruption furthermore confirmed that PEITC acted as a CDDP chemoenhancer in SiHa^{R} cells.

Considering the pioneering role of PI3K/Akt signalling cascade in orchestrating the scenario of acquired CDDP resistance in cervical cancer, it was intended to concentrate upon the ways in which PEITC modulated this cascade for altering MRP2 distribution in SiHa^{R} particularly. It was observed that phosphorylation status of Akt had remarkably reduced in SiHa^{R} with PEITC followed by CDDP treatment. Expression profiles (protein/mRNA) of downstream effectors of the signalling cascades aligned with that of p-Akt. The expression profiles of NFκB (p50/p65) decreased; resulting in cumulative inhibition of XIAP, survivin and MRP2. PI3K/Akt is reported to ubiquitously modulate the multi-drug resistant phenotype in cancer [Zhang et al., 2020; Liu et al., 2021]. Therefore, shutting down the activity of upstream effectors would concoct the acquired resistant phenotype of cancer cells. Accordingly, the spatio-temporal distribution of MRP2 proteins was apparently altered. PEITC pre-treatment for 3h among SiHa^{R} cells considerably reduced MRP2 accumulation in the membrane even upon CDDP treatment. This unveiled the root-cause of increasing CDDP levels within the resistant cells upon PEITC pre-treatment. A milieu of reference studies also reported that apparently PEITC reduces the expression of drug-exporters to promote reversal of acquired chemoresistance [Morris and Dave, 2014; Suvarna et al., 2017]. *In silico*

observations pin-pointing at specific-interactions of PEITC with Akt, XIAP and MRP2 proteins further established the role of PEITC as a chemosensitizer.

Upon validation in 3MC induced *in vivo* cervical cancer model, reiteration of similar results were attained. Mice group when treated with CDDP alone didn't restrict the tumor growth as evident from histopathological study and tumor images. However, prior PEITC administration alongside CDDP injection controlled tumor growth and improved the relative histology and cytology by permissibly surging systemic-ROS levels. These aggregated evidences were enough to confirm PEITC as a CDDP-sensitizer in cisplatin resistant cervical cancer. Although, detailed insights into PEITC mediated cisplatin-sensitization in *in vivo* set up is mandatory. The present study has laid down a foundation for the candidature of PEITC as a cisplatin sensitizer and enhancer in Phase I clinical trial.

Conclusion

9. CONCLUSION

This study majorly focuses on establishment of a better treatment rationale for cervical cancer using natural means. The models established here flaunt a microenvironment which has upregulated prosurvival molecules having referral values as prognostic and diagnostic markers for strategizing better therapy.

Cervical Cancers being the most lethal gynaecological cancer contributes to increasing mortalities among women worldwide due to higher relapse frequencies. Despite introduction of new therapeutic modalities, platinum therapy with cisplatin continues to be the 'first line of treatment'. However, onset of resistance during therapy eventuates in treatment failure and disease recurrence. Therefore, prior assessment of therapy response is critical for segregating cisplatin responders from non-responders ahead of prescribing CCRT. Screening strategies with reference to specific molecular markers intrinsic to cervical tumours are being designed in recent times for this purpose. Malignancy associated 'metabolic reprogramming' always results from deregulated PI3K/Akt/mTOR prosurvival signalling. Multiple studies have individually addressed these phenomena in light of cisplatin resistance. However, their concomitant credibility in designing new therapy strategies is yet to be deciphered.

The key molecular targets enlisted in our study are prospective with translational implications for future development of precision medicines in cervical cancer treatment. With this study, the fascinating role of PEITC, a natural phytochemical has come to the forefront. The capability of PEITC in making use of cellular MRP2 for further chemosensitizing it is indeed novel and requires extensive exploration. Twitching the phytochemical for mitigation purpose can help in feigning the enemy with its own sword. Such a holistic approach of therapy would prevent unnecessary dose exposure of patients and reduce therapy related toxicities to lengthen disease free survival periods.

Bibliography

10. BIBLIOGRAPHY

- Achkar, I.W., Abdulrahman, N., Al-Sulaiti, H., Joseph, J.M., Uddin, S., Mraiche, F., (2018). Cisplatin based therapy: the role of the mitogen activated protein kinase signaling pathway. J. Transl. Med. 16, 96. https://doi.org/10.1186/s12967-018-1471-1.

- Akhatova, A., Azizan, A., Atageldiyeva, K., Ashimkhanova, A., Marat, A., Iztleuov, Y., Suleimenova, A., Shamkeeva, S., Aimagambetova, G., (2022). Prophylactic Human Papillomavirus Vaccination: From the Origin to the Current State. Vaccines 10, 1912. https://doi.org/10.3390/vaccines10111912.

- Albadari, N., Li, W., (2023). Survivin Small Molecules Inhibitors: Recent Advances and Challenges. Molecules 28, 1376. https://doi.org/10.3390/molecules28031376.

- Altaf, I., Butt, M.A., Zaman, M., (2022). Disease Detection and Prediction Using the Liver Function Test Data: A Review of Machine Learning Algorithms, in: Khanna, A., Gupta, D., Bhattacharyya, S., Hassanien, A.E., Anand, S., Jaiswal, A. (Eds.), International Conference on Innovative Computing and Communications, Advances in Intelligent Systems and Computing. Springer, Singapore, pp. 785–800. https://doi.org/10.1007/978-981-16-2597-8_68.

- Andreeva, N.V., Gabbasova, R.R., Grivennikov, S.I., (2020). Microbiome in cancer progression and therapy. Curr. Opin. Microbiol., Microbe – Microbe Interactions • Microbiota 56, 118–126. https://doi.org/10.1016/j.mib.2020.09.001.

- Aoki, M., Fujishita, T., (2017). Oncogenic Roles of the PI3K/AKT/mTOR Axis. Curr. Top. Microbiol. Immunol. 407, 153–189. https://doi.org/10.1007/82_2017_6.

- Aoufouchi, S., Cogne, M., Fest, T., (2022). Germinal Centers in Lymphoid and Non-Lymphoid Tissues: Adaptive and Evolving Structures. Frontiers Media SA.

- Arbyn, M., Weiderpass, E., Bruni, L., de Sanjosé, S., Saraiya, M., Ferlay, J., Bray, F., (2020). Estimates of incidence and mortality of cervical cancer in 2018: a worldwide analysis. Lancet Glob. Health 8, e191–e203. https://doi.org/10.1016/S2214-109X(19)30482-6.

- Arnesano, F., Natile, G., (2009). Mechanistic insight into the cellular uptake and processing of cisplatin 30 years after its approval by FDA. Coord. Chem. Rev., 38th International Conference on Coordination Chemistry 253, 2070–2081. https://doi.org/10.1016/j.ccr.2009.01.028.

- Bai, D., Ueno, L., Vogt, P.K., (2009). Akt-mediated regulation of NFκB and the essentialness of NFκB for the oncogenicity of PI3K and Akt. Int. J. Cancer J. Int. Cancer 125, 2863–2870. https://doi.org/10.1002/ijc.24748.

- Baker, T.S., Newcomb, W.W., Olson, N.H., Cowsert, L.M., Olson, C., Brown, J.C., (1991). Structures of bovine and human papillomaviruses. Analysis by cryoelectron microscopy and three-dimensional image reconstruction. Biophys. J. 60, 1445–1456.

- Balkwill, F., Mantovani, A., (2001). Inflammation and cancer: back to Virchow? The Lancet 357, 539–545. https://doi.org/10.1016/S0140-6736(00)04046-0.

- Balode, E., Pilmane, M., Rezeberga, D., Jermakova, I., Kroica, J., (2018). Interleukin IL-1α, IL-6, IL-8, IL-10 Expression in Different Staging of Cervical Intraepithelial Neoplasia. Acta Chir. Latv. 17, 8–14. https://doi.org/10.1515/chilat-2017-0010.

- Barrington, D.A., Dilley, S.E., Landers, E.E., Thomas, E.D., Boone, J.D., Straughn, J.M., McGwin, G., Leath, C.A., (2016). Distance from a Comprehensive Cancer Center: A proxy for poor cervical cancer outcomes? Gynecol. Oncol. 143, 617–621. https://doi.org/10.1016/j.ygyno.2016.10.004.

- Basoya, S., Anjankar, A., (2022). Cervical Cancer: Early Detection and Prevention in Reproductive Age Group. Cureus 14, e31312. https://doi.org/10.7759/cureus.31312.

- Ben Ayed, W., Ben Said, A., Hamdi, A., Mokrani, A., Masmoudi, Y., Toukabri, I., Limayem, I., Yahyaoui, Y., (2020). Toxicity, risk factors and management of cisplatin-induced toxicity: A prospective study. J. Oncol. Pharm. Pract. Off. Publ. Int. Soc. Oncol. Pharm. Pract. 26, 1621–1629. https://doi.org/10.1177/1078155219901305.

- Bhatla, N., Meena, J., Kumari, S., Banerjee, D., Singh, P., Natarajan, J., (2021). Cervical Cancer Prevention Efforts in India. Indian J. Gynecol. Oncol. 19, 41. https://doi.org/10.1007/s40944-021-00526-8.

- Bhattacharjee, R., Dey, T., Kumar, L., Kar, S., Sarkar, R., Ghorai, M., Malik, S., Jha, N.K., Vellingiri, B., Kesari, K.K., Pérez de la Lastra, J.M., Dey, A., (2022). Cellular

landscaping of cisplatin resistance in cervical cancer. Biomed. Pharmacother. 153, 113345. https://doi.org/10.1016/j.biopha.2022.113345.

- Biswas, S., Mahapatra, E., Das, S., Roy, M., Mukherjee, S., (2022). PEITC: A resounding molecule averts metastasis in breast cancer cells in vitro by regulating PKCδ/Aurora A interplay. Heliyon 8. https://doi.org/10.1016/j.heliyon.2022.e11656.

- Biswas, S., Mahapatra, E., Das, S., Roy, M., Mukherjee, S., (2021). PEITC: A Resounding Molecule Averts Metastasis in Breast Cancer Cells *in vitro* by Targeting Serine/Threonine Kinase Interplay. https://doi.org/10.2139/ssrn.3923487.

- Bobdey, S., Sathwara, J., Jain, A., Balasubramaniam, G., (2016). Burden of cervical cancer and role of screening in India. Indian J. Med. Paediatr. Oncol. Off. J. Indian Soc. Med. Paediatr. Oncol. 37, 278–285. https://doi.org/10.4103/0971-5851.195751.

- Bourguignon, L.Y.W., (2019). Matrix Hyaluronan-CD44 Interaction Activates MicroRNA and LncRNA Signaling Associated With Chemoresistance, Invasion, and Tumor Progression. Front. Oncol. 9.

- Bragulla, H.H., Homberger, D.G., (2009). Structure and functions of keratin proteins in simple, stratified, keratinized and cornified epithelia. J. Anat. 214, 516–559. https://doi.org/10.1111/j.1469-7580.2009.01066.x.

- Bray, F., Ferlay, J., Soerjomataram, I., Siegel, R.L., Torre, L.A., Jemal, A., 2018. Global cancer statistics (2018): GLOBOCAN estimates of incidence and mortality

worldwide for 36 cancers in 185 countries. CA. Cancer J. Clin. 68, 394–424. https://doi.org/10.3322/caac.21492.

- Brisson, M., Kim, J.J., Canfell, K., Drolet, M., Gingras, G., Burger, E.A., Martin, D., Simms, K.T., Bénard, É., Boily, M.-C., Sy, S., Regan, C., Keane, A., Caruana, M., Nguyen, D.T.N., Smith, M.A., Laprise, J.-F., Jit, M., Alary, M., Bray, F., Fidarova, E., Elsheikh, F., Bloem, P.J.N., Broutet, N., Hutubessy, R., (2020). Impact of HPV vaccination and cervical screening on cervical cancer elimination: a comparative modelling analysis in 78 low-income and lower-middle-income countries. The Lancet 395, 575–590. https://doi.org/10.1016/S0140-6736(20)30068-4.

- Brouwers, E.E., Huitema, A.D., Beijnen, J.H., Schellens, J.H., (2008). Long-term platinum retention after treatment with cisplatin and oxaliplatin. BMC Clin. Pharmacol. 8, 7. https://doi.org/10.1186/1472-6904-8-7.

- Brown, A., Kumar, S., Tchounwou, P.B., (2019). Cisplatin-Based Chemotherapy of Human Cancers. J. Cancer Sci. Ther. 11, 97.

- Burd, E.M., (2003). Human papillomavirus and cervical cancer. Clin. Microbiol. Rev. 16, 1–17. https://doi.org/10.1128/CMR.16.1.1-17.2003.

- Burmeister, C.A., Khan, S.F., Schäfer, G., Mbatani, N., Adams, T., Moodley, J., Prince, S., (2022). Cervical cancer therapies: Current challenges and future perspectives.Tumour Virus Res. 13, 200238.https://doi.org/10.1016/j.tvr.2022.200238.

- Buskwofie, A., David-West, G., Clare, C.A., (2020). A Review of Cervical Cancer: Incidence and Disparities. J. Natl. Med. Assoc. 112, 229–232. https://doi.org/10.1016/j.jnma.2020.03.002.

- Buzdin, A., Sorokin, M., Garazha, A., Sekacheva, M., Kim, E., Zhukov, N., Wang, Y., Li, X., Kar, S., Hartmann, C., Samii, A., Giese, A., Borisov, N., (2018). Molecular pathway activation – New type of biomarkers for tumor morphology and personalized selection of target drugs. Semin. Cancer Biol., Cancer Stem Cells 53, 110–124. https://doi.org/10.1016/j.semcancer.2018.06.003.

- Cancer Statistics, 2020. . India Cancer. URL http://cancerindia.org.in/cancer-statistics/ (accessed 8.13.23).

- Carrero, Y.N., Callejas, D.E., Mosquera, J.A., (2021). In situ immunopathological events in human cervical intraepithelial neoplasia and cervical cancer: Review. Transl. Oncol. 14, 101058. https://doi.org/10.1016/j.tranon.2021.101058.

- Castle, P.E., Hillier, S.L., Rabe, L.K., Hildesheim, A., Herrero, R., Bratti, M.C., Sherman, M.E., Burk, R.D., Rodriguez, A.C., Alfaro, M., Hutchinson, M.L., Morales, J., Schiffman, M., (2001). An Association of Cervical Inflammation with High-Grade Cervical Neoplasia in Women Infected with Oncogenic Human Papillomavirus (HPV)1. Cancer Epidemiol. Biomarkers Prev. 10, 1021–1027.

- Chaudhary, A.K., Yadav, N., Bhat, T.A., O'Malley, J., Kumar, S., Chandra, D., (2016). A potential role of X-linked inhibitor of apoptosis protein in mitochondrial

membrane permeabilization and its implication in cancer therapy. Drug Discov. Today 21, 38–47. https://doi.org/10.1016/j.drudis.2015.07.014.

- Chen, L., Min, J., Wang, F., (2022). Copper homeostasis and cuproptosis in health and disease. Signal Transduct. Target. Ther. 7, 1–16. https://doi.org/10.1038/s41392-022-01229-y.

- Chen, P.-Y., Lin, K.-C., Lin, J.-P., Tang, N.-Y., Yang, J.-S., Lu, K.-W., Chung, J.-G., (2012). Phenethyl Isothiocyanate (PEITC) Inhibits the Growth of Human Oral Squamous Carcinoma HSC-3 Cells through G(0)/G(1) Phase Arrest and Mitochondria-Mediated Apoptotic Cell Death. Evid.-Based Complement. Altern. Med. ECAM 2012, 718320. https://doi.org/10.1155/2012/718320.

- Chen, R., Kim, O., Yang, J., Sato, K., Eisenmann, K.M., McCarthy, J., Chen, H., Qiu, Y., (2001). Regulation of Akt/PKB Activation by Tyrosine Phosphorylation*. J. Biol. Chem. 276, 31858–31862. https://doi.org/10.1074/jbc.C100271200.

- Chen, X., Chen, S., Yu, D., (2020). Metabolic Reprogramming of Chemoresistant Cancer Cells and the Potential Significance of Metabolic Regulation in the Reversal of Cancer Chemoresistance. Metabolites 10, 289. https://doi.org/10.3390/metabo10070289.

- Cheng, Y., Li, S., Gao, L., Zhi, K., Ren, W., (2021). The Molecular Basis and Therapeutic Aspects of Cisplatin Resistance in Oral Squamous Cell Carcinoma. Front. Oncol. 11, 761379. https://doi.org/10.3389/fonc.2021.761379.

- Choi, S.K., Hong, Y.O., Lee, W.M., Kim, E.K., Joo, J.E., Kim, D.W., Lee, H., (2015). Overexpression of PI3K-p110α in the progression of uterine cervical neoplasia and its correlation with pAkt and DJ-1. Eur. J. Gynaecol. Oncol. 36, 389–393.

- Choi, Y.-M., Kim, H.-K., Shim, W., Anwar, M.A., Kwon, J.-W., Kwon, H.-K., Kim, H.J., Jeong, H., Kim, H.M., Hwang, D., Kim, H.S., Choi, S., (2015). Mechanism of Cisplatin-Induced Cytotoxicity Is Correlated to Impaired Metabolism Due to Mitochondrial ROS Generation. PLOS ONE 10, e0135083. https://doi.org/10.1371/journal.pone.0135083.

- Colotta, F., Allavena, P., Sica, A., Garlanda, C., Mantovani, A., (2009). Cancer-related inflammation, the seventh hallmark of cancer: links to genetic instability. Carcinogenesis 30, 1073–1081. https://doi.org/10.1093/carcin/bgp127.

- Crowley, J.E., Treml, L.S., Stadanlick, J.E., Carpenter, E., Cancro, M.P., (2005). Homeostatic niche specification among naïve and activated B cells: a growing role for the BLyS family of receptors and ligands. Semin. Immunol. 17, 193–199. https://doi.org/10.1016/j.smim.2005.02.001.

- da Fonseca, L.M., da Silva, V.A., da Costa, K.M., dos Reis, J.S., Previato, J.O., Previato, L.M., Freire-de-Lima, L., (2022). Resistance to cisplatin in human lung adenocarcinoma cells: effects on the glycophenotype and epithelial to mesenchymal transition markers. Glycoconj. J. 39, 247–259. https://doi.org/10.1007/s10719-022-10042-2.

- da Silva, G.N., de Castro Marcondes, J.P., de Camargo, E.A., da Silva Passos Júnior, G.A., Sakamoto-Hojo, E.T., Salvadori, D.M.F., (2010). Cell cycle arrest and apoptosis in TP53 subtypes of bladder carcinoma cell lines treated with cisplatin and gemcitabine. Exp. Biol. Med. Maywood NJ 235, 814–824. https://doi.org/10.1258/ebm.2010.009322.

- Dai, M.-Y., Wang, Y., Chen, C., Li, F., Xiao, B.-K., Chen, S.-M., Tao, Z.-Z., (2016). Phenethyl isothiocyanate induces apoptosis and inhibits cell proliferation and invasion in Hep-2 laryngeal cancer cells. Oncol. Rep. 35, 2657–2664. https://doi.org/10.3892/or.2016.4689.

- Day, P.M., Schelhaas, M., (2014). Concepts of papillomavirus entry into host cells. Curr. Opin. Virol. 4, 24–31. https://doi.org/10.1016/j.coviro.2013.11.002.

- Dayalan Naidu, S., Suzuki, T., Yamamoto, M., Fahey, J.W., Dinkova-Kostova, A.T., (2018). Phenethyl Isothiocyanate, a Dual Activator of Transcription Factors NRF2 and HSF1. Mol. Nutr. Food Res. 62, 1700908. https://doi.org/10.1002/mnfr.201700908.

- De Brot, L., Pellegrini, B., Moretti, S.T., Carraro, D.M., Soares, F.A., Rocha, R.M., Baiocchi, G., da Cunha, I.W., de Andrade, V.P., (2017). Infections with multiple high-risk HPV types are associated with high-grade and persistent low-grade intraepithelial lesions of the cervix. Cancer Cytopathol. 125, 138–143. https://doi.org/10.1002/cncy.21789.

- Devi, G.R., Finetti, P., Morse, M.A., Lee, S., de Nonneville, A., Van Laere, S., Troy, J., Geradts, J., McCall, S., Bertucci, F., (2021). Expression of X-Linked Inhibitor of Apoptosis Protein (XIAP) in Breast Cancer Is Associated with Shorter Survival and Resistance to Chemotherapy. Cancers 13, 2807. https://doi.org/10.3390/cancers13112807.

- Dhillon, P.K., Mathur, P., Nandakumar, A., Fitzmaurice, C., Kumar, G.A., Mehrotra, R., Shukla, D.K., Rath, G.K., Gupta, P.C., Swaminathan, R., Thakur, J.S., Dey, S., Allen, C., Badwe, R.A., Dikshit, R., Dhaliwal, R.S., Kaur, T., Kataki, A.C., Visweswara, R.N., Gangadharan, P., Dutta, E., Furtado, M., Varghese, C.M., Bhardwaj, D., Muraleedharan, P., Odell, C.M., Glenn, S., Bal, M.S., Bapsy, P.P., Bennett, J., Bodal, V.K., Chakma, J.K., Chakravarty, S., Chaturvedi, M., Das, P., Deshmane, V., Gangane, N., Harvey, J., Jayalekshmi, P., Jerang, K., Johnson, S.C., Julka, P.K., Kaushik, D., Khamo, V., Koyande, S., Kutz, M., Langstieh, W.B., Lingegowda, K.B., Mahajan, R.C., Mahanta, J., Majumdar, G., Manoharan, N., Mathew, A., Nene, B.M., Pati, S., Pradhan, P.K., Raina, V., Rama, R., Ramesh, C., Sathishkumar, K., Schelonka, K., Sebastian, P., Shackelford, K., Shah, J., Shanta, V., Sharma, J.D., Shrivastava, A., Tawsik, S., Tyagi, B.B., Vaitheeswaran, K., Vallikad, E., Verma, Y., Zomawia, E., Lim, S.S., Vos, T., Dandona, R., Reddy, K.S., Naghavi, M., Murray, C.J.L., Swaminathan, S., Dandona, L., 2018. The burden of cancers and their variations across the states of India: the Global Burden of Disease Study 1990–(2016). Lancet Oncol. 19, 1289–1306. https://doi.org/10.1016/S1470-2045(18)30447-9.

- Dong, C., Wu, J., Chen, Y., Nie, J., Chen, C., (2021). Activation of PI3K/AKT/mTOR Pathway Causes Drug Resistance in Breast Cancer. Front. Pharmacol. 12.

- Dukaew, N., Chairatvit, K., Pitchakarn, P., Imsumran, A., Karinchai, J., Tuntiwechapikul, W., Wongnoppavich, A., (2020). Inactivation of AKT/NF-κB signaling by eurycomalactone decreases human NSCLC cell viability and improves the chemosensitivity to cisplatin. Oncol. Rep. 44, 1441–1454. https://doi.org/10.3892/or.2020.7710.

- El-Bayoumy, K., Chen, K.-M., Zhang, S.-M., Sun, Y.-W., Amin, S., Stoner, G., Guttenplan, J.B., (2016). Carcinogenesis of the Oral Cavity: Environmental Causes and Potential Prevention by Black Raspberry [WWW Document]. ACS Publ. https://doi.org/10.1021/acs.chemrestox.6b00306.

- Elmore, L.W., Greer, S.F., Daniels, E.C., Saxe, C.C., Melner, M.H., Krawiec, G.M., Cance, W.G., Phelps, W.C., (2021). Blueprint for cancer research: Critical gaps and opportunities. CA. Cancer J. Clin. 71, 107–139. https://doi.org/10.3322/caac.21652.

- Emran, T.B., Shahriar, A., Mahmud, A.R., Rahman, T., Abir, M.H., Siddiquee, Mohd.F.-R., Ahmed, H., Rahman, N., Nainu, F., Wahyudin, E., Mitra, S., Dhama, K., Habiballah, M.M., Haque, S., Islam, A., Hassan, M.M., (2022). Multidrug Resistance in Cancer: Understanding Molecular Mechanisms, Immunoprevention and Therapeutic Approaches. Front. Oncol. 12.

- Esmatabadi, M.J.D., Bakhshinejad, B., Motlagh, F.M., Babashah, S., Sadeghizadeh, M., (2016). Therapeutic resistance and cancer recurrence mechanisms: Unfolding the story of tumour coming back. J. Biosci. 41, 497–506. https://doi.org/10.1007/s12038-016-9624-y.

- Esteve, M., (2020). Mechanisms Underlying Biological Effects of Cruciferous Glucosinolate-Derived Isothiocyanates/Indoles: A Focus on Metabolic Syndrome. Front. Nutr. 7.

- Falzone, L., Salomone, S., Libra, M., (2018). Evolution of Cancer Pharmacological Treatments at the Turn of the Third Millennium. Front. Pharmacol. 9.

- Fares, J., Fares, M.Y., Khachfe, H.H., Salhab, H.A., Fares, Y., (2020). Molecular principles of metastasis: a hallmark of cancer revisited. Signal Transduct. Target. Ther. 5, 1–17. https://doi.org/10.1038/s41392-020-0134-x.

- Favre, M., (1975). Structural polypeptides of rabbit, bovine, and human papillomaviruses. J. Virol. 15, 1239–1247.

- Figueiredo, C.R.L.V., (2019). The unusual paradox of cancer-associated inflammation: an update. J. Bras. Patol. E Med. Lab. 55, 321–332. https://doi.org/10.5935/1676-2444.20190029.

- Fittall, M.W., Van Loo, P., (2019). Translating insights into tumor evolution to clinical practice: promises and challenges. Genome Med. 11, 20. https://doi.org/10.1186/s13073-019-0632-z.

- Forsberg, J.-G., Breistein, L.S., (1972). Carcinogenesis With 3-Methylcholanthrene in Uterine Cervix of Mice Treated Neonatally With Estrogen2. JNCI J. Natl. Cancer Inst. 49, 155–172. https://doi.org/10.1093/jnci/49.1.155.

- Fortes, H.R., von Ranke, F.M., Escuissato, D.L., Araujo Neto, C.A., Zanetti, G., Hochhegger, B., Souza, C.A., Marchiori, E., (2017). Recurrent respiratory papillomatosis: A state-of-the-art review. Respir. Med. 126, 116–121. https://doi.org/10.1016/j.rmed.2017.03.030.

- Gadducci, A., Cosio, S., (2020). Neoadjuvant Chemotherapy in Locally Advanced Cervical Cancer: Review of the Literature and Perspectives of Clinical Research. Anticancer Res. 40, 4819–4828. https://doi.org/10.21873/anticanres.14485.

- Galluzzi, L., Vitale, I., Michels, J., Brenner, C., Szabadkai, G., Harel-Bellan, A., Castedo, M., Kroemer, G., (2014). Systems biology of cisplatin resistance: past, present and future. Cell Death Dis. 5, e1257–e1257. https://doi.org/10.1038/cddis.2013.428.

- Ghoneum, A., Said, N., (2019). PI3K-AKT-mTOR and NFκB Pathways in Ovarian Cancer: Implications for Targeted Therapeutics. Cancers 11, 949. https://doi.org/10.3390/cancers11070949.

- Gierisch, J.M., Coeytaux, R.R., Urrutia, R.P., Havrilesky, L.J., Moorman, P.G., Lowery, W.J., Dinan, M., McBroom, A.J., Hasselblad, V., Sanders, G.D., Myers, E.R., (2013). Oral Contraceptive Use and Risk of Breast, Cervical, Colorectal, and

Endometrial Cancers: A Systematic Review. Cancer Epidemiol. Biomarkers Prev. 22, 1931–1943. https://doi.org/10.1158/1055-9965.EPI-13-0298.

- Graham, C.E., (2009). Histogenesis of Methylcholanthrene-Induced Murine Cervical Cancer. Oncology 25, 269–282. https://doi.org/10.1159/000224577.

- Gui, P., Bivona, T.G., (2022). Evolution of metastasis: new tools and insights. Trends Cancer 8, 98–109. https://doi.org/10.1016/j.trecan.2021.11.002.

- Gupta, P., Wright, S.E., Kim, S.-H., Srivastava, S.K., (2014). Phenethyl isothiocyanate: A comprehensive review of anti-cancer mechanisms. Biochim. Biophys. Acta BBA - Rev. Cancer 1846, 405–424. https://doi.org/10.1016/j.bbcan.2014.08.003.

- He, C., Xu, K., Zhu, X., Dunphy, P.S., Gudenas, B., Lin, W., Twarog, N., Hover, L.D., Kwon, C.-H., Kasper, L.H., Zhang, Junyuan, Li, X., Dalton, J., Jonchere, B., Mercer, K.S., Currier, D.G., Caufield, W., Wang, Y., Xie, J., Broniscer, A., Wetmore, C., Upadhyaya, S.A., Qaddoumi, I., Klimo, P., Boop, F., Gajjar, A., Zhang, Jinghui, Orr, B.A., Robinson, G.W., Monje, M., Freeman III, B.B., Roussel, M.F., Northcott, P.A., Chen, T., Rankovic, Z., Wu, G., Chiang, J., Tinkle, C.L., Shelat, A.A., Baker, S.J., (2021). Patient-derived models recapitulate heterogeneity of molecular signatures and drug response in pediatric high-grade glioma. Nat. Commun. 12, 4089. https://doi.org/10.1038/s41467-021-24168-8.

- He, S., Wang, Y., Lai, Y., Cao, X., Ren, Y., Chen, Y., (2022). Concurrent Chemoradiotherapy With Nedaplatin Versus Cisplatin in Patients With Stage IIB-IVA Cervical Cancer: A Randomized Phase III Trial. Front. Oncol. 11.

- Henke, E., Nandigama, R., Ergün, S., (2020). Extracellular Matrix in the Tumor Microenvironment and Its Impact on Cancer Therapy. Front. Mol. Biosci. 6.

- Hernandez, C., Glidden, A., Sandhu, M., Agrawal, K., Caicedo Murillo, M., Heritage, C., Ramovic, M., Akhtar, K., (2022). A Rare Case of Aggressive Atypical Cervical Cancer With Multi-Organ Involvement. Cureus 14, e32968. https://doi.org/10.7759/cureus.32968.

- Hodeify, R., Siddiqui, S.S., Matar, R., Vazhappilly, C.G., Merheb, M., Al Zouabi, H., Marton, J., (2021). Modulation of calcium-binding proteins expression and cisplatin chemosensitivity by calcium chelation in human breast cancer MCF-7 cells. Heliyon 7, e06041. https://doi.org/10.1016/j.heliyon.2021.e06041.

- Hoeschele, J.D., (2016). Dr Barnett Rosenberg – a Personal Perspective. Dalton Trans. 45, 12966–12969. https://doi.org/10.1039/C6DT02152B.

- Hong, Y.-H., Uddin, Md.H., Jo, U., Kim, B., Song, J., Suh, D.H., Kim, H.S., Song, Y.S., (2015). ROS Accumulation by PEITC Selectively Kills Ovarian Cancer Cells via UPR-Mediated Apoptosis. Front. Oncol. 5, 167. https://doi.org/10.3389/fonc.2015.00167.

- Housman, G., Byler, S., Heerboth, S., Lapinska, K., Longacre, M., Snyder, N., Sarkar, S., (2014). Drug Resistance in Cancer: An Overview. Cancers 6, 1769–1792. https://doi.org/10.3390/cancers6031769.

- Huang, S., Liang, S., Chen, G., Chen, J., You, K., Ye, H., Li, Z., He, S., (2021). Overexpression of glycosyltransferase 8 domain containing 2 confers ovarian cancer to CDDP resistance by activating FGFR/PI3K signalling axis. Oncogenesis 10, 1–9. https://doi.org/10.1038/s41389-021-00343-w.

- Ibragimova, M.K., Tsyganov, M.M., Litviakov, N.V., (2017). Natural and chemotherapy-induced clonal evolution of tumors. Biochem. Mosc. 82, 413–425. https://doi.org/10.1134/S0006297917040022.

- Iida, M., Harari, P.M., Wheeler, D.L., Toulany, M., (2020). Targeting AKT/PKB to improve treatment outcomes for solid tumors. Mutat. Res. Mol. Mech. Mutagen. 819–820, 111690. https://doi.org/10.1016/j.mrfmmm.2020.111690.

- Ioannides, C., Konsue, N., (2015). A principal mechanism for the cancer chemopreventive activity of phenethyl isothiocyanate is modulation of carcinogen metabolism.Drug Met. 47, 356–373. https://doi.org/10.3109/03602532.2015.1058819.

- Jablonska, E., Li, Q., Reszka, E., Wieczorek, E., Tarhonska, K., Wang, T., (2021). Therapeutic Potential of Selenium and Selenium Compounds in Cervical Cancer. CancerControl. 28,10732748211001808.https://doi.org/10.1177/10732748211001808.

- Jedy-Agba, E., Joko, W.Y., Liu, B., Buziba, N.G., Borok, M., Korir, A., Masamba, L., Manraj, S.S., Finesse, A., Wabinga, H., Somdyala, N., Parkin, D.M., (2020). Trends in cervical cancer incidence in sub-Saharan Africa. Br. J. Cancer 123, 148–154. https://doi.org/10.1038/s41416-020-0831-9.

- Jiang, B.-H., Liu, L.-Z., (2009). PI3K/PTEN Signaling in Angiogenesis and Tumorigenesis. Adv. Cancer Res. 102, 19–65. https://doi.org/10.1016/S0065-230X(09)02002-8.

- Kaarthigeyan, K., (2012). Cervical cancer in India and HPV vaccination. Indian J. Med. Paediatr. Oncol. Off. J. Indian Soc. Med. Paediatr. Oncol. 33, 7–12. https://doi.org/10.4103/0971-5851.96961.

- Karar, J., Maity, A., (2011). PI3K/AKT/mTOR Pathway in Angiogenesis. Front. Mol. Neurosci. 4, 51. https://doi.org/10.3389/fnmol.2011.00051.

- Keetile, M., Ndlovu, K., Letamo, G., Disang, M., Yaya, S., Navaneetham, K., (2021). Factors associated with and socioeconomic inequalities in breast and cervical cancer screening among women aged 15–64 years in Botswana. PLOS ONE 16, e0255581. https://doi.org/10.1371/journal.pone.0255581.

- Keysar, S.B., Astling, D.P., Anderson, R.T., Vogler, B.W., Bowles, D.W., Morton, J.J., Paylor, J.J., Glogowska, M.J., Le, P.N., Eagles-Soukup, J.R., Kako, S.L., Takimoto, S.M., Sehrt, D.B., Umpierrez, A., Pittman, M.A., Macfadden, S.M., Helber, R.M., Peterson, S., Hausman, D.F., Said, S., Leem, T.H., Goddard, J.A., Arcaroli, J.J.,

Messersmith, W.A., Robinson, W.A., Hirsch, F.R., Varella-Garcia, M., Raben, D., Wang, X.-J., Song, J.I., Tan, A.-C., Jimeno, A., (2013). A patient tumor transplant model of squamous cell cancer identifies PI3K inhibitors as candidate therapeutics in defined molecular bins. Mol. Oncol. 7, 776–790. https://doi.org/10.1016/j.molonc.2013.03.004.

- Kiss, R.C., Xia, F., Acklin, S., (2021). Targeting DNA Damage Response and Repair to Enhance Therapeutic Index in Cisplatin-Based Cancer Treatment. Int. J. Mol. Sci. 22, 8199. https://doi.org/10.3390/ijms22158199.

- Kokka, F., Bryant, A., Brockbank, E., Jeyarajah, A., (2014). Surgical treatment of stage IA2 cervical cancer. Cochrane Database Syst. Rev. 2014, CD010870. https://doi.org/10.1002/14651858.CD010870.pub2.

- Kuang, C., Fu, X., Hua, Y., Shuai, W., Ye, Z., Li, Yingchang, Peng, Q., Li, Yi-zhuo, Chen, S., Qian, C., Huang, W., Liu, R., (2017). BST2 confers cisplatin resistance via NF-κB signaling in nasopharyngeal cancer. Cell Death Dis. 8, e2874–e2874. https://doi.org/10.1038/cddis.2017.271.

- Lechner, M., Frampton, G.M., Fenton, T., Feber, A., Palmer, G., Jay, A., Pillay, N., Forster, M., Cronin, M.T., Lipson, D., Miller, V.A., Brennan, T.A., Henderson, S., Vaz, F., O'Flynn, P., Kalavrezos, N., Yelensky, R., Beck, S., Stephens, P.J., Boshoff, C., (2013). Targeted next-generation sequencing of head and neck squamous cell carcinoma identifies novel genetic alterations in HPV+ and HPV- tumors. Genome Med. 5, 49. https://doi.org/10.1186/gm453.

- Lee, C.M., Fuhrman, C.B., Planelles, V., Peltier, M.R., Gaffney, D.K., Soisson, A.P., Dodson, M.K., Tolley, H.D., Green, C.L., Zempolich, K.A., (2006). Phosphatidylinositol 3-kinase inhibition by LY294002 radiosensitizes human cervical cancer cell lines. Clin. Cancer Res. Off. J. Am. Assoc. Cancer Res. 12, 250–256. https://doi.org/10.1158/1078-0432.CCR-05-1084.

- Lei, Z.-N., Tian, Q., Teng, Q.-X., Wurpel, J.N.D., Zeng, L., Pan, Y., Chen, Z.-S., (2023). Understanding and targeting resistance mechanisms in cancer. MedComm 4, e265. https://doi.org/10.1002/mco2.265.

- Lemmon, M.A., Schlessinger, J., (2010). Cell signaling by receptor-tyrosine kinases. Cell 141, 1117–1134. https://doi.org/10.1016/j.cell.2010.06.011.

- Lewis, K.A., Lilly, K.K., Reynolds, E.A., Sullivan, W.P., Kaufmann, S.H., Cliby, W.A., (2009). Ataxia telangiectasia and rad3-related kinase contributes to cell cycle arrest and survival after cisplatin but not oxaliplatin. Mol. Cancer Ther. 8, 855–863. https://doi.org/10.1158/1535-7163.MCT-08-1135.

- Li, Q., Zhan, M., Chen, W., Zhao, B., Yang, K., Yang, J., Yi, J., Huang, Q., Mohan, M., Hou, Z., Wang, J., (2016). Phenylethyl isothiocyanate reverses cisplatin resistance in biliary tract cancer cells via glutathionylation-dependent degradation of Mcl-1. Oncotarget 7, 10271–10282. https://doi.org/10.18632/oncotarget.7171.

- Liew, P.X., Kubes, P., (2019). The Neutrophil's Role During Health and Disease. Physiol. Rev. 99, 1223–1248. https://doi.org/10.1152/physrev.00012.2018.

- Lillo, F.B., Lodini, S., Ferrari, D., Stayton, C., Taccagni, G., Galli, L., Lazzarin, A., Uberti-Foppa, C., (2005). Determination of human papillomavirus (HPV) load and type in high-grade cervical lesions surgically resected from HIV-infected women during follow-up of HPV infection. Clin. Infect. Dis. Off. Publ. Infect. Dis. Soc. Am. 40, 451–457. https://doi.org/10.1086/427032.

- Lippert, T.H., Ruoff, H.-J., Volm, M., (2008). Intrinsic and acquired drug resistance in malignant tumors. The main reason for therapeutic failure. Arzneimittelforschung. 58, 261–264. https://doi.org/10.1055/s-0031-1296504.

- Liu, Z., Zhu, G., Getzenberg, R.H., Veltri, R.W., (2015). The Upregulation of PI3K/Akt and MAP Kinase Pathways is Associated with Resistance of Microtubule-Targeting Drugs in Prostate Cancer. J. Cell. Biochem. 116, 1341–1349. https://doi.org/10.1002/jcb.25091.

- Lorusso, D., Petrelli, F., Coinu, A., Raspagliesi, F., Barni, S., (2014). A systematic review comparing cisplatin and carboplatin plus paclitaxel-based chemotherapy for recurrent or metastatic cervical cancer. Gynecol. Oncol. 133, 117–123. https://doi.org/10.1016/j.ygyno.2014.01.042.

- Luan, S., Zeng, X., Zhang, C., Qiu, J., Yang, Y., Mao, C., Xiao, X., Zhou, J., Zhang, Y., Yuan, Y., (2021). Advances in Drug Resistance of Esophageal Cancer: From the Perspective of Tumor Microenvironment. Front. Cell Dev. Biol. 9.

- Lv, Y., Luo, Y.-Y., Ren, H.-W., Li, C.-J., Xiang, Z.-X., Luan, Z.-L.,(2022). The role of pregnane X receptor (PXR) in substance metabolism. Front. Endocrinol. 13.

- Machida, K., McNamara, G., Cheng, K.T.-H., Huang, J., Wang, C.-H., Comai, L., Ou, J.-H.J., Lai, M.M.C., (2010). Hepatitis C Virus Inhibits DNA Damage-Repair through Reactive Oxygen and Nitrogen Species and by Interfering with the ATM-NBS1/Mre11/Rad50 DNA Repair Pathway in Monocytes and Hepatocytes. J. Immunol. Baltim. Md 1950 185, 6985–6998. https://doi.org/10.4049/jimmunol.1000618.

- Mahapatra, E., Biswas, S., Roy, M., Chakraborty Mukherjee, S., (2020). Inflammation: A protagonist in development of carcinogen induced cervical cancer in mice. Indian J. Biochem. Biophys. 57, 158–166.

- Mahapatra, E., Das, S., Biswas, S., Ghosh, A., Sengupta, D., Roy, M., Mukherjee, S., (2021). Insights of Cisplatin Resistance in Cervical Cancer: A Decision Making for Cellular Survival, in: Cervical Cancer - A Global Public Health Treatise. IntechOpen. https://doi.org/10.5772/intechopen.98489

- Mahapatra, E., Sengupta, D., Kumar, R., Dehury, B., Das, S., Roy, M., Mukherjee, S., (2022). Phenethylisothiocyanate Potentiates Platinum Therapy by Reversing Cisplatin Resistance in Cervical Cancer. Front. Pharmacol. 13, 803114. https://doi.org/10.3389/fphar.2022.803114.

- Maheshwari, A., Kumar, N., Mahantshetty, U., (2016). Gynecological cancers: A summary of published Indian data. South Asian J. Cancer 5, 112–120. https://doi.org/10.4103/2278-330X.187575.

- Mann, M., Singh, V.P., Kumar, L., (2023). Cervical cancer: a tale from HPV infection to PARP inhibitors. Genes Dis. 10, 1445–1456. https://doi.org/10.1016/j.gendis.2022.09.014.

- Manning, B.D., Toker, A., (2017). AKT/PKB Signaling: Navigating the Network. Cell 169, 381–405. https://doi.org/10.1016/j.cell.2017.04.001.

- Mansoori, B., Mohammadi, A., Davudian, S., Shirjang, S., Baradaran, B., (2017). The Different Mechanisms of Cancer Drug Resistance: A Brief Review. Adv. Pharm. Bull. 7, 339–348. https://doi.org/10.15171/apb.2017.041.

- Matsushima, K., Yang, D., Oppenheim, J.J., (2022). Interleukin-8: An evolving chemokine. Cytokine 153, 155828. https://doi.org/10.1016/j.cyto.2022.155828.

- Mazengenya, P., Bhikha, R., (2020). The genitourinary and reproductive systems: Interpretation of Avicenna's (980–1037 AD) treatise in the Canon of Medicine. Morphologie 104, 196–201. https://doi.org/10.1016/j.morpho.2019.12.002.

- McCann, C., Kerr, E.M., (2021). Metabolic Reprogramming: A Friend or Foe to Cancer Therapy? Cancers 13, 3351. https://doi.org/10.3390/cancers13133351.

- Mcclintock, M.K., (1971). Menstrual Synchrony and Suppression. Nature 229, 244–245. https://doi.org/10.1038/229244a0.

- McGranahan, N., Swanton, C., (2017). Clonal Heterogeneity and Tumor Evolution: Past, Present, and the Future. Cell 168, 613–628. https://doi.org/10.1016/j.cell.2017.01.018.

- Menges, C.W., Baglia, L.A., Lapoint, R., McCance, D.J., (2006). Human Papillomavirus Type 16 E7 Up-regulates AKT Activity through the Retinoblastoma Protein. Cancer Res. 66, 5555–5559. https://doi.org/10.1158/0008-5472.CAN-06-0499.

- Mi, L., Di Pasqua, A.J., Chung, F.-L., (2011). Proteins as binding targets of isothiocyanates in cancer prevention. Carcinogenesis 32, 1405–1413. https://doi.org/10.1093/carcin/bgr111.

- Mirzaei, S., Hushmandi, K., Zabolian, A., Saleki, H., Torabi, S.M.R., Ranjbar, A., SeyedSaleh, S., Sharifzadeh, S.O., Khan, H., Ashrafizadeh, M., Zarrabi, A., Ahn, K., (2021). Elucidating Role of Reactive Oxygen Species (ROS) in Cisplatin Chemotherapy: A Focus on Molecular Pathways and Possible Therapeutic Strategies. Molecules 26, 2382. https://doi.org/10.3390/molecules26082382.

- Mishra, G.A., Pimple, S.A., Shastri, S.S., (2015). HPV vaccine: One, two, or three doses for cervical cancer prevention? Indian J. Med. Paediatr. Oncol. Off. J. Indian Soc. Med. Paediatr. Oncol. 36, 201–206. https://doi.org/10.4103/0971-5851.171534.

- Mitola, G., Falvo, P., Bertolini, F., (2021). New Insight to Overcome Tumor Resistance: An Overview from Cellular to Clinical Therapies. Life 11, 1131. https://doi.org/10.3390/life11111131

- Mole, S., Faizo, A.A.A., Hernandez-Lopez, H., Griffiths, M., Stevenson, A., Roberts, S., Graham, S.V., (2020). Human papillomavirus type 16 infection activates the host serine arginine protein kinase 1 (SRPK1) – splicing factor axis. J. Gen. Virol. 101, 523. https://doi.org/10.1099/jgv.0.001402.

- Morandi, A., Indraccolo, S., (2017). Linking metabolic reprogramming to therapy resistance in cancer. Biochim. Biophys. Acta BBA - Rev. Cancer 1868, 1–6. https://doi.org/10.1016/j.bbcan.2016.12.004.

- Morris, M.E., Dave, R.A., (2014). Pharmacokinetics and pharmacodynamics of phenethyl isothiocyanate: implications in breast cancer prevention. AAPS J. 16, 705–713. https://doi.org/10.1208/s12248-014-9610-y.

- Mortensen, A.C.L., Mohajershojai, T., Hariri, M., Pettersson, M., Spiegelberg, D., (2020). Overcoming Limitations of Cisplatin Therapy by Additional Treatment With the HSP90 Inhibitor Onalespib. Front. Oncol. 10.

- Mu, Q., Lv, Y., Luo, C., Liu, X., Huang, C., Xiu, Y., Tang, L., (2021). Research Progress on the Functions and Mechanism of circRNA in Cisplatin Resistance in Tumors. Front. Pharmacol. 12.

- Murillo, R., Herrero, R., Sierra, M.S., Forman, D., (2016). Cervical cancer in Central and South America: Burden of disease and status of disease control. Cancer Epidemiol., Supplement: Cancer in Central and South America 44, S121–S130. https://doi.org/10.1016/j.canep.2016.07.015.

- Ng, L.G., Ostuni, R., Hidalgo, A., (2019). Heterogeneity of neutrophils. Nat. Rev. Immunol. 19, 255–265. https://doi.org/10.1038/s41577-019-0141-8.

- Niu, X., Wu, T., Li, G., Gu, X., Tian, Y., Cui, H., (2022). Insights into the critical role of the PXR in preventing carcinogenesis and chemotherapeutic drug resistance. Int. J. Biol. Sci. 18, 742–759. https://doi.org/10.7150/ijbs.68724.

- Obexer, P., Ausserlechner, M.J., (2014). X-Linked Inhibitor of Apoptosis Protein – A Critical Death Resistance Regulator and Therapeutic Target for Personalized Cancer Therapy. Front. Oncol. 4.

- Oeckinghaus, A., Ghosh, S., (2009). The NF-κB Family of Transcription Factors and Its Regulation. Cold Spring Harb. Perspect. Biol. 1, a000034. https://doi.org/10.1101/cshperspect.a000034.

- Okamura, M., Shizu, R., Abe, T., Kodama, S., Hosaka, T., Sasaki, T., Yoshinari, K., (2020). PXR Functionally Interacts with NF-κB and AP-1 to Downregulate the Inflammation-Induced Expression of Chemokine CXCL2 in Mice. Cells 9, 2296. https://doi.org/10.3390/cells9102296.

- Paradkar, P., Joshi, J., Mertia, P., Agashe, S., Vaidya, A., (2014). Role of Cytokines in Genesis, Progression and Prognosis of Cervical Cancer. Asian Pac. J. Cancer Prev. APJCP 15, 3851–3864. https://doi.org/10.7314/APJCP.2014.15.9.3851.

- Peng, F., Liao, M., Qin, R., Zhu, S., Peng, C., Fu, L., Chen, Y., Han, B., (2022). Regulated cell death (RCD) in cancer: key pathways and targeted therapies. Signal Transduct. Target. Ther. 7, 1–66. https://doi.org/10.1038/s41392-022-01110-y.

- Petignat, P., Roy, M., (2007). Diagnosis and management of cervical cancer. BMJ 335, 765–768. https://doi.org/10.1136/bmj.39337.615197.80.

- Pincock, S., (2008). Virologist wins Nobel for cervical cancer discovery. The Lancet 372, 1374. https://doi.org/10.1016/S0140-6736(08)61572-X.

- Pisa, R., Kapoor, T.M., (2020). Chemical strategies to overcome resistance against targeted anticancer therapeutics. Nat. Chem. Biol. 16, 817–825. https://doi.org/10.1038/s41589-020-0596-8.

- Podratz, J.L., Knight, A.M., Ta, L.E., Staff, N.P., Gass, J.M., Genelin, K., Schlattau, A., Lathroum, L., Windebank, A.J., (2011). Cisplatin induced mitochondrial DNA damage in dorsal root ganglion neurons. Neurobiol. Dis. 41, 661–668. https://doi.org/10.1016/j.nbd.2010.11.017.

- Ponnusamy, L., Mahalingaiah, P.K.S., Chang, Y.-W., Singh, K.P., (2019). Role of cellular reprogramming and epigenetic dysregulation in acquired chemoresistance in breast cancer. Cancer Drug Resist. 2, 297–312. https://doi.org/10.20517/cdr.2018.11.

- Puleo, G.E., Borger, T.N., Montgomery, D., Rivera Rivera, J.N., Burris, J.L., (2020). A Qualitative Study of Smoking-Related Causal Attributions and Risk Perceptions in Cervical Cancer Survivors. Psychooncology. 29, 500–506. https://doi.org/10.1002/pon.5291.

- Ramos, A., Sadeghi, S., Tabatabaeian, H., (2021). Battling Chemoresistance in Cancer: Root Causes and Strategies to Uproot Them. Int. J. Mol. Sci. 22, 9451. https://doi.org/10.3390/ijms22179451.

- Rascio, F., Spadaccino, F., Rocchetti, M.T., Castellano, G., Stallone, G., Netti, G.S., Ranieri, E., (2021). The Pathogenic Role of PI3K/AKT Pathway in Cancer Onset and Drug Resistance: An Updated Review. Cancers 13, 3949. https://doi.org/10.3390/cancers13163949.

- Reinson, T., Toots, M., Kadaja, M., Pipitch, R., Allik, M., Ustav, E., Ustav, M., (2013). Engagement of the ATR-dependent DNA damage response at the human papillomavirus 18 replication centers during the initial amplification. J. Virol. 87, 951–964. https://doi.org/10.1128/JVI.01943-12.

- Rocha, C.R.R., Silva, M.M., Quinet, A., Cabral-Neto, J.B., Menck, C.F.M., (2018). DNA repair pathways and cisplatin resistance: an intimate relationship. Clinics 73, e478s. https://doi.org/10.6061/clinics/2018/e478s.

- Salemme, V., Centonze, G., Avalle, L., Natalini, D., Piccolantonio, A., Arina, P., Morellato, A., Ala, U., Taverna, D., Turco, E., Defilippi, P., (2023). The role of tumor

microenvironment in drug resistance: emerging technologies to unravel breast cancer heterogeneity. Front. Oncol. 13.

- Sanaei, M.-J., Razi, S., Pourbagheri-Sigaroodi, A., Bashash, D., (2022). The PI3K/Akt/mTOR pathway in lung cancer; oncogenic alterations, therapeutic opportunities, challenges, and a glance at the application of nanoparticles. Transl. Oncol. 18, 101364. https://doi.org/10.1016/j.tranon.2022.101364.

- Sarkar, R., Mukherjee, S., Biswas, J., Roy, M., (2012). Sulphoraphane, a naturally occurring isothiocyanate induces apoptosis in breast cancer cells by targeting heat shock proteins. Biochem. Biophys. Res. Commun. 427, 80–85. https://doi.org/10.1016/j.bbrc.2012.09.006.

- Saunier, M., Monnier-Benoit, S., Mauny, F., Dalstein, V., Briolat, J., Riethmuller, D., Kantelip, B., Schwarz, E., Mougin, C., Prétet, J.-L., (2008). Analysis of Human Papillomavirus Type 16 (HPV16) DNA Load and Physical State for Identification of HPV16-Infected Women with High-Grade Lesions or Cervical Carcinoma. J. Clin. Microbiol. 46, 3678–3685. https://doi.org/10.1128/jcm.01212-08.

- Schiliro, C., Firestein, B.L., (2021). Mechanisms of Metabolic Reprogramming in Cancer Cells Supporting Enhanced Growth and Proliferation. Cells 10, 1056. https://doi.org/10.3390/cells10051056.

- Shakour, Z.T., Shehab, N.G., Gomaa, A.S., Wessjohann, L.A., Farag, M.A., (2022). Metabolic and biotransformation effects on dietary glucosinolates, their

bioavailability, catabolism and biological effects in different organisms. Biotechnol. Adv. 54, 107784. https://doi.org/10.1016/j.biotechadv.2021.107784.

- Shi, L., Zhu, W., Huang, Y., Zhuo, L., Wang, S., Chen, S., Zhang, B., Ke, B., (2022). Cancer-associated fibroblast-derived exosomal microRNA-20a suppresses the PTEN/PI3K-AKT pathway to promote the progression and chemoresistance of non-small cell lung cancer. Clin. Transl. Med. 12, e989. https://doi.org/10.1002/ctm2.989.

- Shizu, R., Abe, T., Benoki, S., Takahashi, M., Kodama, S., Miayata, M., Matsuzawa, A., Yoshinari, K., (2016). PXR stimulates growth factor-mediated hepatocyte proliferation by cross-talk with the FOXO transcription factor. Biochem. J. 473, 257–266. https://doi.org/10.1042/BJ20150734.

- Siddik, Z.H., (2003). Cisplatin: mode of cytotoxic action and molecular basis of resistance. Oncogene 22, 7265–7279. https://doi.org/10.1038/sj.onc.1206933.

- Singh, D., Vignat, J., Lorenzoni, V., Eslahi, M., Ginsburg, O., Lauby-Secretan, B., Arbyn, M., Basu, P., Bray, F., Vaccarella, S., (2023). Global estimates of incidence and mortality of cervical cancer in 2020: a baseline analysis of the WHO Global Cervical Cancer Elimination Initiative. Lancet Glob. Health 11, e197–e206. https://doi.org/10.1016/S2214-109X(22)00501-0.

- S.k., J., S.p., D., R., S., Sai Surya, N.U., Chenmala, K., (2021). Guardian of genome on the tract: Wild type p53-mdm2 complex inhibition in healing the breast cancer. Gene 786, 145616. https://doi.org/10.1016/j.gene.2021.145616.

- Song, M., Cui, M., Liu, K., (2022). Therapeutic strategies to overcome cisplatin resistance in ovarian cancer. Eur. J. Med. Chem. 232, 114205. https://doi.org/10.1016/j.ejmech.2022.114205.

- Soundararajan, P., Kim, J.S., (2018). Anti-Carcinogenic Glucosinolates in Cruciferous Vegetables and Their Antagonistic Effects on Prevention of Cancers. Molecules 23, 2983. https://doi.org/10.3390/molecules23112983.

- Sreedevi, A., Javed, R., Dinesh, A., (2015). Epidemiology of cervical cancer with special focus on India. Int. J. Womens Health 7, 405–414. https://doi.org/10.2147/IJWH.S50001.

- Srivastava, A.N., Misra, J.S., Srivastava, S., Das, B.C., Gupta, S., (2018). Cervical cancer screening in rural India: Status & current concepts. Indian J. Med. Res. 148, 687–696. https://doi.org/10.4103/ijmr.IJMR_5_17.

- Su, Y., Zhang, X., Li, S., Xie, W., Guo, J., (2022). Emerging Roles of the Copper–CTR1 Axis in Tumorigenesis. Mol. Cancer Res. 20, 1339–1353. https://doi.org/10.1158/1541-7786.MCR-22-0056.

- Suvarna, V., Murahari, M., Khan, T., Chaubey, P., Sangave, P., (2017). Phytochemicals and PI3K Inhibitors in Cancer-An Insight. Front. Pharmacol. 8, 916. https://doi.org/10.3389/fphar.2017.00916.

- Taneja, N., Chawla, B., Awasthi, A.A., Shrivastav, K.D., Jaggi, V.K., Janardhanan, R., (2021). Knowledge, Attitude, and Practice on Cervical Cancer and Screening

Among Women in India: A Review. Cancer Control J. Moffitt Cancer Cent. 28, 10732748211010799. https://doi.org/10.1177/10732748211010799.

- Tang, T., Song, X., Liu, Y.-F., Wang, W.-Y., (2014). PEITC reverse multi-drug resistance of human gastric cancer SGC7901/DDP cell line. Cell Biol. Int. 38, 502–510. https://doi.org/10.1002/cbin.10169.

- Tchounwou, P.B., Dasari, S., Noubissi, F.K., Ray, P., Kumar, S., (2021). Advances in Our Understanding of the Molecular Mechanisms of Action of Cisplatin in Cancer Therapy. J. Exp. Pharmacol. 13, 303–328. https://doi.org/10.2147/JEP.S267383.

- Telang, U., Ji, Y., Morris, M.E., (2009). ABC Transporters and Isothiocyanates: Potential for Pharmacokinetic Diet–Drug Interactions. Biopharm. Drug Dispos. 30, 335–344. https://doi.org/10.1002/bdd.668.

- Tiwari, A., Kishore, J., Tiwari, A., (2011). Perceptions and concerns of women undergoing Pap smear examination in a tertiary care hospital of India. Indian J. Cancer 48, 477–482. https://doi.org/10.4103/0019-509X.92261.

- Tong, X., Mirzoeva, S., Veliceasa, D., Bridgeman, B.B., Fitchev, P., Cornwell, M.L., Crawford, S.E., Pelling, J.C., Volpert, O.V., (2014). Chemopreventive apigenin controls UVB-induced cutaneous proliferation and angiogenesis through HuR and thrombospondin-1. Oncotarget 5, 11413–11427.

- Tuncer, H.A., Tuncer, S.F., (2020). The effect of age On cervical cancer screening in women aged 20-29. Acta Clin. Croat. 59, 277–284. https://doi.org/10.20471/acc.2020.59.02.11.

- Vaidya, A., Jain, S., Sahu, S., Jain, P.K., Pathak, K., Pathak, D., Kumar, R., Jain, S.K., (2020). Anticancer Agents Based on Vulnerable Components in a Signalling Pathway. Mini Rev. Med. Chem. 20, 886–907. https://doi.org/10.2174/1389557520666200212105417.

- Vaidya, F.U., Sufiyan Chhipa, A., Mishra, V., Gupta, V.K., Rawat, S.G., Kumar, A., Pathak, C., (2022). Molecular and cellular paradigms of multidrug resistance in cancer. Cancer Rep. 5, e1291. https://doi.org/10.1002/cnr2.1291.

- Veldman, T., Liu, X., Yuan, H., Schlegel, R., (2003). Human papillomavirus E6 and Myc proteins associate in vivo and bind to and cooperatively activate the telomerase reverse transcriptase promoter. Proc. Natl. Acad. Sci. U. S. A. 100, 8211–8216. https://doi.org/10.1073/pnas.1435900100.

- Venkatesan, S., Swanton, C., (2016). Tumor Evolutionary Principles: How Intratumor Heterogeneity Influences Cancer Treatment and Outcome. Am. Soc. Clin. Oncol. Educ. Book e141–e149. https://doi.org/10.1200/EDBK_158930.

- Wan, P.K.-T., Leung, T.H.-Y., Siu, M.K.-Y., Mo, X.-T., Tang, H.W.-M., Chan, K.K.-L., Cheung, A.N.-Y., Ngan, H.Y.-S., (2021). HPV-induced Nurr1 promotes cancer

aggressiveness, self-renewal, and radioresistance via ERK and AKT signaling in cervical cancer. Cancer Lett. 497, 14–27. https://doi.org/10.1016/j.canlet.2020.09.025.

- Wang, K., Lu, J., Li, R., (1996). The events that occur when cisplatin encounters cells. Coord. Chem. Rev. 151, 53–88. https://doi.org/10.1016/S0010-8545(96)90195-2.

- Wang, L., Zhao, X., Fu, J., Xu, W., Yuan, J., (2021). The Role of Tumour Metabolism in Cisplatin Resistance. Front. Mol. Biosci. 8.

- Wang, R., Pan, W., Jin, L., Huang, W., Li, Y., Wu, D., Gao, C., Ma, D., Liao, S., (2020). Human papillomavirus vaccine against cervical cancer: Opportunity and challenge. Cancer Lett. 471, 88–102. https://doi.org/10.1016/j.canlet.2019.11.039.

- Wang, S., Higgins, V.J., Aldrich-Wright, J.R., Wu, M.J., (2012). Identification of the molecular mechanisms underlying the cytotoxic action of a potent platinum metallointercalator. J. Chem. Biol. 5, 51–61. https://doi.org/10.1007/s12154-011-0070-x.

- Wang, X., Govind, S., Sajankila, S.P., Mi, L., Roy, R., Chung, F.-L., (2011). Phenethyl isothiocyanate sensitizes human cervical cancer cells to apoptosis induced by cisplatin. Mol. Nutr. Food Res. 55, 1572–1581. https://doi.org/10.1002/mnfr.201000560.

- Wang, X., Zhang, H., Chen, X., (2019). Drug resistance and combating drug resistance in cancer. Cancer Drug Resist. 2, 141–160. https://doi.org/10.20517/cdr.2019.10.

- Wiebe, E., Denny, L., Thomas, G., (2012). Cancer of the cervix uteri. Int. J. Gynaecol. Obstet. Off. Organ Int. Fed. Gynaecol. Obstet. 119 Suppl 2, S100-109. https://doi.org/10.1016/S0020-7292(12)60023-X.

- Wilailak, S., Kengsakul, M., Kehoe, S., (2021). Worldwide initiatives to eliminate cervical cancer. Int. J. Gynaecol. Obstet. 155, 102–106. https://doi.org/10.1002/ijgo.13879.

- Wiltshaw, E., (1979). Cisplatin in the Treatment of Cancer. Platin. Met. Rev. 23, 90–98.

- Wu, F., Yang, J., Liu, J., Wang, Y., Mu, J., Zeng, Q., Deng, S., Zhou, H., (2021). Signaling pathways in cancer-associated fibroblasts and targeted therapy for cancer. Signal Transduct. Target. Ther. 6, 1–35. https://doi.org/10.1038/s41392-021-00641-0.

- Wu, J., Chen, J., Zhang, L., Masci, P.P., Zhao, K.-N., (2014). Four major factors regulate phosphatidylinositol 3-kinase signaling pathway in cancers induced by infection of human papillomaviruses. Curr. Med. Chem. 21, 3057–3069. https://doi.org/10.2174/09298673216661404141015 28.

- Wu, J., Cui, S., Liu, J., Tang, X., Zhao, J., Zhang, H., Mao, B., Chen, W., (2023). The recent advances of glucosinolates and their metabolites: Metabolism, physiological functions and potential application strategies. Crit. Rev. Food Sci. Nutr. 63, 4217–4234. https://doi.org/10.1080/10408398.2022.2059441.

- Wu, L., Cai, S., Deng, Y., Zhang, Z., Zhou, X., Su, Y., Xu, D., 2021. PD-1/PD-L1 enhanced cisplatin resistance in gastric cancer through PI3K/AKT mediated P-gp expression. Int. Immunopharmacol. 94, 107443. https://doi.org/10.1016/j.intimp.2021.107443.

- Wu, L., Saxena, S., Awaji, M., Singh, R.K., 2019. Tumor-Associated Neutrophils in Cancer: Going Pro. Cancers 11, 564. https://doi.org/10.3390/cancers11040564.

- Xia, P., Xu, X.-Y., (2015). PI3K/Akt/mTOR signaling pathway in cancer stem cells: from basic research to clinical application. Am. J. Cancer Res. 5, 1602–1609.

- Yang, Y.-T., Shi, Y., Jay, M., Di Pasqua, A.J., (2014). Enhanced toxicity of cisplatin with chemosensitizer phenethyl isothiocyanate toward non-small cell lung cancer cells when delivered in liposomal nanoparticles. Chem. Res. Toxicol. 27, 946–948. https://doi.org/10.1021/tx5001128.

- Yu, Y., Wan, Y., Huang, C., (2009). The Biological Functions of NF-κB1 (p50) and its Potential as an Anti-Cancer Target. Curr. Cancer Drug Targets 9, 566–571.

- Yuan, Y., Jiang, Y.-C., Sun, C.-K., Chen, Q.-M., (2016). Role of the tumor microenvironment in tumor progression and the clinical applications. Oncol. Rep. 35, 2499–2515. https://doi.org/10.3892/or.2016.4660.

- Zhang, L., Wu, J., Ling, M.T., Zhao, L., Zhao, K.-N., (2015). The role of the PI3K/Akt/mTOR signalling pathway in human cancers induced by infection with

human papillomaviruses. Mol. Cancer 14, 87. https://doi.org/10.1186/s12943-015-0361-x.

- Zhang, X., Zeng, Q., Cai, W., Ruan, W., (2021). Trends of cervical cancer at global, regional, and national level: data from the Global Burden of Disease study 2019. BMC Public Health 21, 894. https://doi.org/10.1186/s12889-021-10907-5.

- Zhou, D., Shao, L., Spitz, D.R., (2014). Reactive Oxygen Species in Normal and Tumor Stem Cells. Adv. Cancer Res. 122, 1–67. https://doi.org/10.1016/B978-0-12-420117-0.00001-3

- Zhu, H., Shen, Z., Luo, H., Zhang, W., Zhu, X., (2016). Chlamydia Trachomatis Infection-Associated Risk of Cervical Cancer: A Meta-Analysis. Medicine (Baltimore) 95, e3077. https://doi.org/10.1097/MD.0000000000003077

- zur Hausen, H., (2009). Papillomaviruses in the causation of human cancers — a brief historical account. Virology, Small Viruses, Big Discoveries: The Interwoven Story of the Small DNA Tumor Viruses 384, 260–265. https://doi.org/10.1016/j.virol.2008.11.046.

Publications

15. List of Publications

❖ ***First Author Publications***

1. ***Mahapatra E***, Sengupta D, Kumar R, Dehury B, Das S, Roy M, Mukherjee S (2022). Phenethylisothiocyanate Potentiates Platinum Therapy by Reversing Cisplatin Resistance in Cervical Cancer. ***Frontiers in Pharmacology***; 2022 Apr 25;13:803114. doi: 10.3389/fphar.2022.803114.

2. ***Mahapatra E***, Das S, Biswas S, Ghosh A, Sengupta D, Roy M, Mukherjee S (2021) Insights of Cisplatin Resistance in Cervical Cancer: A Decision Making for Cellular Survival. Cervical Cancer - A Global Public Health Treatise. ***IntechOpen***; 2021. doi: http://dx.doi.org/10.5772/intechopen.98489.

3. ***Mahapatra E***, Biswas S, Roy M, Mukherjee S (2020). Inflammation: A protagonist in development of carcinogen induced cervical cancer in mice. ***Indian Journal of Biochemistry & Biophysics***, 57(2020)158-166.

❖ ***Co-Author Publications***

1. Biswas S, ***Mahapatra E***, Das S, Roy M, Mukherjee S. PEITC: A resounding molecule averts metastasis in breast cancer cells in vitro by regulating PKCδ/Aurora A interplay. ***Heliyon***. 2022 Nov 15;8(11):e11656. doi: 10.1016/j.heliyon.2022.e11656.

2. Das, S, Ray DK, Sengupta D, ***Mahapatra E***, Biswas S, Roy M, Mukherjee S (2022). Aspirin restores radiosensitivity in cervical cancer cells by inducing mitotic catastrophe through downregulating G2/M effectors. ***Asian Pacific Journal of Cancer Prevention***. 23(11): 3801-3813. doi: 10.31557/APJCP.2022.23.11.3801.

3. Das S, Ray DK, ***Mahapatra E***, Biswas S, Sengupta D, Roy M, Mukherjee S (2022). AURKA/NFκB Axis: A Key Determinant of Radioresistance in Cervical Squamous Carcinoma Cells. ***Archives of Clinical and Biomedical Research*** 6: 707-721.

4. Das S, ***Mahapatra E***, Biswas S, Roy M, Mukherjee S (2021). Emerging Role of Aurora A in Radioresistance: A Comprehensive Review. ***European Medical Journal***. 2021 Nov; 9(1):81-90. https://doi.org/10.33590/emjoncol/20-00251.

5. Biswas S, ***Mahapatra E***, Ghosh A, Das S, Roy M, Mukherjee S (2021). Curcumin Rescues Doxorubicin Responsiveness via Regulating Aurora a Signaling Network in Breast Cancer Cells. ***Asian Pacific Journal of Cancer Prevention***. 2021 Mar 1; 22(3):957-970. doi: 10.31557/APJCP.2021.22.3.957.

6. Biswas S, ***Mahapatra E,*** Roy M, Mukherjee S (2020). PEITC by regulating Aurora Kinase A reverses chemoresistance in breast cancer cells. ***Indian Journal of Biochemistry & Biophysics***, 57(2020)167-177.

frontiers | Frontiers in Pharmacology

BRIEF RESEARCH REPORT
published: 25 April 2022
doi: 10.3389/fphar.2022.803114

Phenethylisothiocyanate Potentiates Platinum Therapy by Reversing Cisplatin Resistance in Cervical Cancer

*Elizabeth Mahapatra[1], Debomita Sengupta[1], Ravindra Kumar[2], Budheswar Dehury[3], Salini Das[1], Madhumita Roy[1] and Sutapa Mukherjee[1]**

[1]Department of Environmental Carcinogenesis and Toxicology, Chittaranjan National Cancer Institute, Kolkata, India, [2]School of Biotechnology, National Institute of Technology Calicut, Kozhikode, India, [3]ICMR-Regional Medical Research Centre, Chandrasekharpur, Bhubaneswar, India

Acquired cisplatin resistance in cervical cancer therapy is principally caused by reduction in intracellular drug accumulation, which is exerted by hyperactivation of the oncogenic PI3K/Akt signaling axis and overexpression of cisplatin-exporter MRP2 along with prosurvival effectors NF-κB and IAPs in cervical cancer cells. These activated prosurvival signaling cascades drive drug efflux and evasion of apoptosis for rendering drug-resistant phenotypes. Our study challenges the PI3K/Akt axis in a cisplatin-resistant cervical cancer scenario with phenethylisothiocyanate (PEITC) for chemosensitization of SiHa^{R}, a cisplatin-resistant subline of SiHa and 3-methylcholanthrene–induced cervical cancer mice models. SiHa^{R} exhibited higher MRP2, p-Akt^{Thr308}, NF-κB, XIAP, and survivin expressions which cumulatively compromised cisplatin retention capacity and accumulated PEITC better than SiHa. SiHa^{R} appeared to favor PEITC uptake as its accumulation rates were found to be positively correlated with MRP2 expressions. PEITC treatment in SiHa^{R} for 3 h prior to cisplatin exposure revived intracellular platinum levels, reduced free GSH levels, generated greater ROS, and altered mitochondrial membrane potential compared to SiHa. Western blot and immunofluorescence results indicated that PEITC successfully downregulated MRP2 in addition to suppressing p-Akt^{Thr308}, XIAP, survivin, and NF-κB expressions. In mice models, administration of 5 mg/kg body-weight PEITC priming dosage prior to treatment with 3 mg/kg body-weight of cisplatin remediated cervical histology and induced tumor regression in contrast to the group receiving the same dosage of cisplatin only. This suggested PEITC as a potential chemosensitizing agent in light of acquired cisplatin resistance in cervical cancer and established its candidature for Phase I clinical trial.

Keywords: PEITC, chemosensitization, cisplatin resistance, MRP2, PI3K/AKT

OPEN ACCESS

Edited by:
Hardeep Singh Tuli, Maharishi Markandeshwar University, Mullana, India

Reviewed by:
Kaikai Gong, Binzhou Medical University Hospital, China
Sze Kwan Lam, The University of Hong Kong, Hong Kong SAR, China

****Correspondence:***
Sutapa Mukherjee
sutapa_c_in@yahoo.com
orcid.org/0000-0002-4411-7257

Specialty section:
This article was submitted to Pharmacology of Anti-Cancer Drugs, a section of the journal Frontiers in Pharmacology

Received: *27 October 2021*
Accepted: *22 March 2022*
Published: *25 April 2022*

Citation:
Mahapatra E, Sengupta D, Kumar R, Dehury B, Das S, Roy M and Mukherjee S (2022) Phenethylisothiocyanate Potentiates Platinum Therapy by Reversing Cisplatin Resistance in Cervical Cancer. Front. Pharmacol. 13:803114. doi: 10.3389/fphar.2022.803114

INTRODUCTION

Cervical cancer, the fourth-leading cause of morbidity among women worldwide (Globocan, 2018), is reported to cause maximum deaths among Indian women (NICPR, 2018). Relapse and recurrence catered by failure in treatment owing to acquirement of resistance to chemo/radiotherapy is a common occurrence (Dasari and Tchounwou, 2014; D'Alterio et al., 2020). Conventionally, chemotherapy with platinum-based drugs such as cisplatin, alongside other chemotherapeutics or radiation (Concurrent

Chapter

Insights of Cisplatin Resistance in Cervical Cancer: A Decision Making for Cellular Survival

Elizabeth Mahapatra, Salini Das, Souvick Biswas, Archismaan Ghosh, Debomita Sengupta, Madhumita Roy and Sutapa Mukherjee

Abstract

The clinical scenario of acquired cisplatin resistance is considered as a major impediment in cervical cancer treatment. Bulky drug-DNA adducts formed by cisplatin elicits *DNA damage response (DDR)* which either subsequently induces apoptosis in the cervical cancer cells or enables them to adapt with drug assault by invigorating pro-survival molecular cascades. When HPV infected cervical cancer cells encounter cisplatin, a complex molecular interaction between *deregulated tumor suppressors*, *DNA damage-repair enzymes*, and *prosurvival molecules* get initiated. Ambiguous molecular triggers allow cancer cells to cull apoptosis by opting for a survival fate. Overriding of the apoptotic cues by the pro-survival cues renders a *cisplatin resistant phenotype* in the tumor microenvironment. The present review undrapes the impact of deregulated signaling nexus formed due to crosstalk of the key molecules related to cell survival and apoptosis in orchestrating platinum resistance in cervical cancer.

Keywords: HPV, Cervical cancer, Cisplatin resistance, tumor suppressors, DNA-damage repair, prosurvival signaling

1. Introduction

Cervical cancer, one of the widespread gynecological cancers, accounts for the maximum deaths amongst women across the globe. As per GLOBOCAN 2018, cervical cancer is helmed as the fourth leading cause of mortality and morbidity in women after breast and ovarian cancers [1]. As revealed from the data collated by World Health Organization (WHO) in 2013, over 85% of the cervical cancer cases had surfaced mostly from developing countries with a poor socio-economic backdrop [2]. Women, owing to lack of awareness, often arrive for seeking medical help when the malignant growth of cervix has attained advancement [3].

Infections with a special class of oncogenic DNA viruses called *Human Papilloma Viruses (HPVs)*, hailing from the viral family *Papillomaviridae,* are highly accredited for the malignant transformation of cervix. Principally, HPVs are sexually transmitted [4]. On the basis of its carcinogenic potentials, HPVs can be categorized as –*(i) low-risk HPVs (lr-HPVs)* like *HPV 6, 11, 42, 43* and *44*, and *(ii) high-risk*

Indian Journal of Biochemistry & Biophysics
Vol. 57, April 2020, pp. 158-166

Inflammation: A protagonist in development of carcinogen induced cervical cancer in mice

Elizabeth Mahapatra, Souvick Biswas, Madhumita Roy & Sutapa Mukherjee*

Department of Environmental Carcinogenesis & Toxicology, Chittaranjan National Cancer Institute, Kolkata-700 026, West Bengal, India

Received 14 September 2019; *revised 1 November 2019*

Inflammation– induced systemic stress plays an essential role in neoplastic progression. Chronic exposure to chemical carcinogens can induce persistent inflammatory changes which further augment loss in physiological hormesis of an organism thereby favouring carcinogenesis. The present study investigated the role of inflammation and associated systemic stress in the development of cervical carcinoma in a 3-methylcholanthrene (3-MC; a chemical carcinogen) induced *in vivo* cervical cancer model. When the cervix of 5-6 weeks old virgin female Swiss Albino mice (*Mus musculus*) was treated with 3-MC (0.6 mg/mL), remarkable alteration in its cervical cytopathology was observed. An increase in duration of 3-MC treatment caused an outburst in the number and variety of infiltrating granulocytes and agranulocytes in mice cervix. Thus, a high leukocyte index was indicative of prevalent cervical inflammatory changes. Elevated activities of SGPT, SGOT, serum alkaline phosphatase enzymes along with the presence of elevated serum creatinine levels suggested liver and renal dysfunctions. These observations were supported by alterations in hepatic histopathology of 3-MC treated mice. Surged activities and expression profiles of inflammatory cytokines (IL-6 and IL-8) in cervix tissue had conclusively established the crucial role played by inflammation– mediated systemic stress in favouring the development of cervical cancer in a carcinogen-induced *in vivo* model.

Keywords: Cervical cancer, Chronic inflammation, Cytokines, Dysplasia, *Helicobacter pylori*, Methylcholanthrene, Systemic stress

The concept of an intricate association between inflammation and cancer dates back to 19th century as chronic inflammation triggers mechanisms underlying the progression of cancer[1]. Proposed to be one of the key factors responsible for initiating the malignant transformation, inflammation is also termed as the seventh hallmark of cancer[2]. Chronic inflammation plays a crucial role in enriching the tumour microenvironment with prosurvival signals which enables the neoplastic cells to survive and proliferate by evading the adaptive immune response of the host and by developing chemoresistance[3,4]. Sometimes localized inflammation mediated by a persistent bacterial and viral infection can lead to increased cancer risk. Unremitted *Helicobacter pylori* infections of the stomach may result in gastric adenocarcinoma along with lymphoma of the MALT (mucosa-associated lymphoid tissue)[5,6]. Although, inflammation can act as a "two-edged sword" because, in some diseases like psoriasis, the presence of a steady–state of inflammation helps in reducing the disease[7,8]. Conversely, carcinogens like polycyclic aromatic hydrocarbons (PAHs) or various aromatic amines render their carcinogenicity by triggering chronic inflammation which furthers tumorigenesis[8,9]. The whole episode of cancer– related inflammation is dictated over by the transcription factor NF-κB and its relative signal transducers such as COX2, IL-6, and IL-8[10-12]. These inducers of malignant transformation drive the process of neoplasia by bringing about subsequent deregulation of tumour suppressor genes (p53, p21, and Rb) followed by upregulation of proliferative markers (Ki-67 and PCNA)[13,14].

3-methylcholanthrene (3-MC), a carcinogen belonging to the family of PAHs is known to cause

*Correspondence:
Phone: +91-332476-5101
E-mail: sutapa_c_in@yahoo.com

Abbreviations: 3-MC, 3- methylcholanthrene; HH, Harris Haematoxylin; IL-6, interleukin-6; IL-8, interleukin-8; LI, leukocyte index; MALT, Mucosa-associated lymphoid tissue; NBF, Neutral Buffered Formalin; PAH, polycyclic aromatic hydrocarbon; PCNA, Proliferating cell nuclear antigen; RNS, Reactive nitrogen species; ROS, Reactive oxygen species

Heliyon 8 (2022) e11656

Contents lists available at ScienceDirect

Heliyon

journal homepage: www.cell.com/heliyon

Research article

PEITC: A resounding molecule averts metastasis in breast cancer cells *in vitro* by regulating PKCδ/Aurora A interplay

Souvick Biswas, Elizabeth Mahapatra, Salini Das, Madhumita Roy, Sutapa Mukherjee *

Dept of Environmental Carcinogenesis & Toxicology, Chittaranjan National Cancer Institute, 37, S. P. Mukherjee Road, Kolkata 700 026, India

HIGHLIGHTS

- PEITC-mediated PKCδ activation disrupts nuclear lamin expression
- Activated PKCδ facilitates nuclear accumulation of phospho-Nrf2 (Ser-40).
- PKCδ imparted a negative impact on functional expression of Aurora A.
- Consequentially, repression of Aurora A effectuated in suppression of PLK1.
- Altered STKs begat apoptosis & suppressed metastasis in breast-cancer cells.

ARTICLE INFO

Keywords:
Serine/threonine kinases
PEITC
Cell cycle
Apoptosis
Invasion
Migration

ABSTRACT

Background/aim: Intricate association and aberrant activation of serine/threonine kinase (STK) family proteins like Polo-like kinase (PLK1) and Aurora kinase (Aurora A abruptly regulate mitotic entry whereas activation of PKCδ), another important member of STK family conversely induces apoptosis which is preceded by cell cycle arrest. These STKs are considered as major determinant of oncogenicity. Therefore, the contributory role of Aurora A/PLK-1 axis in mitotic control and PKCδ in apoptosis control and their reciprocity in cancer research is an emerging area to explore. The present study investigated the intricate involvement of STKs in breast cancer cells (MCF-7 and MDA-MB-231) and their disruption by PEITC.

Methods: Both MCF-7 and MDA-MB-231 cells were checked for clonogenic assay, cell-cycle analysis and the results were compared with normal MCF-10A, Western blotting, TUNEL & DNA-fragmentation assay, wound healing, transwell migration assays in presence and absence of PEITC.

Results: PEITC was found to increase the expression of PKCδ with subsequent nuclear translocation. Nuclear translocation of PKCδ was accompanied by inhibition of nuclear lamin vis a vis phosphorylation of Nrf2 at Ser 40 alongside nuclear accumulation of phospho-Nrf2. Activated PKCδ furthermore exerted its apoptotic effect by negatively regulating Aurora A and consequentially PLK1; indicating activation of PLK1 by Aurora A. Involvement of PEITC induced PKCδ activation and Aurora A inhibition was ascertained by using Rottlerin/Aurora A Inhibitor.

Discussion & conclusion: Natural isothiocyanates like PEITC efficiently altered the functional abilities of STKs concerning their entangled functional interplay. Such alterations in protein expression by PEITC was chaperoned with inhibition of the aggressiveness of breast cancer cells and ultimately induction of apoptosis.

1. Introduction

Several serine/threonine kinases are reported to be aberrantly expressed in many cell types and ultimately pre-disposed to cancer in most of the cases [1, 2]. Mitosis, a highly orchestrated self-reproducing process of somatic cells, involves several serine/threonine kinases of which Aurora Kinase A (Aurora A) and Polo-like kinase-1 (PLK1) are noteworthy [3]. Spatio-temporal distribution of these serine/threonine kinases regulate cell cycle checkpoint, centrosome duplication & maturation, mitotic entry & exit, cytokinesis, and programmed cell death [4]. Protein Kinase C delta or PKCδ, a member of the novel PKC family functions as a double edged sword, and balances cell death and cell survival [5]. Functional behaviour of PKCδ depends on differential phosphorylation status of the protein [6]. Depending on the stimuli and/or cell type, PKCδ has several phosphorylable

* Corresponding author.
E-mail address: sutapa_c_in@yahoo.com (S. Mukherjee).

https://doi.org/10.1016/j.heliyon.2022.e11656
Received 26 July 2021; Received in revised form 3 January 2022; Accepted 7 November 2022

RESEARCH ARTICLE

Editorial Process: Submission:06/06/2022 Acceptance:11/01/2022

Aspirin Restores Radiosensitivity in Cervical Cancer Cells by Inducing Mitotic Catastrophe through Downregulating G2/M Effectors

Salini Das[1], Dilip Kumar Ray[2], Debomita Sengupta[1], Elizabeth Mahapatra[1], Souvick Biswas[1], Madhumita Roy[1], Sutapa Mukherjee[1]*

Abstract

Background/Aim: Compromised cell-cycle checkpoint is a major obstacle for rendering radiotherapeutic success of radioresistant cells. Aspirin (ASA), an anti-inflammatory agent was repurposed previously for improving radiotherapy by limiting radiation toxicity. However, the underlying mechanism was unclear. The present study aimed to identify the mechanism of ASA mediated reversal of radioresistance in cervical cancer cells. **Methods:** Radioresistant subline SiHa/RR was developed from parental cervical squamous carcinoma cell line SiHa by chronic fractionated irradiation (IR). The radioresistance property of SiHa/RR was confirmed by clonogenic assay. Alteration in cell-cycle by ASA was determined by flow cytometry. ASA induced nuclear damage as consequence of mitotic catastrophe was confirmed by microscopic observation. The interaction between ASA and G2/M regulators was explored through *in silico* docking analysis and expressional change of them was affirmed by western blotting. Immunofluorescence study to examine Aurora Kinase A localization in presence and absence of ASA treatment was conducted. Finally the radiosensitizing ability of ASA was verified by apoptotic parameters (flow cytometrically and by western blotting). **Result:** Higher colony forming ability of SiHa/RR compared to SiHa became restrained upon ASA (5μM) treatment prior to IR. Flow cytometric analysis of ASA treated cells showed increased G2/M population followed by enlargement of cells displaying giant multinucleated morphology; typical characteristics of mitotic catastrophe. Underlying noteworthy mechanisms involved decreased expressions of G2/M regulatory proteins (Cyclin B1, CDK1, Aurora A Kinase, pAurora A Kinase) in IR/ASA along with inhibiting nuclear localization of Aurora Kinase A in SiHa/RR. Docking results also supported the findings. Prolonged treatment (12 h) with ASA led to apoptosis by altering expressions of Bcl2, Bax and Cytochrome C; which was achieved through the event of mitotic catastrophe. **Conclusion:** This work established that G2/M arrest and mitotic catastrophe can be considered as the principle mechanism of restoration of radiosensitivity in SiHa/RR by ASA pretreatment.

Keywords: AURKA- ASA- Radioresistance- Mitotic Catastrophe

Asian Pac J Cancer Prev, **23 (11)**, 3801-3813

Introduction

Cervical cancer being the fourth common cancer in women is posing a major threat due to its increasing events of recurrence (Sung et al., 2021). Radiotherapy, the primary treatment modality of cervical cancer, executes its action by instigating DNA damage, cell-cycle arrest and oxidative stress (Bader et al.,2021; Mavragani et al., 2019; Marill et al., 2019). However, development of acquired radioresistance is the principal hindrance behind the reduced efficacy of radiotherapy (Galeaz et al., 2021; Schulz et al., 2019). Acquired radioresistance is manifested at the molecular level by sequestering adaptive alterations within the cells, tissues and finally to tumor. These transformations include development and persistence of efficient repair system, degradation of DNA damage sensors subsequently leading to cell-cycle progression and proliferation (Domogaur et al., 2021; Huang et al., 2020; Alsubhi et al., 2016; Lim et al., 2012; Zhao et al., 2012). Mitotic progression being one of the prevalent radioresistant properties raises attention of the researchers. Mitotic serine threonine kinases which are the effective regulators of sequential mitotic events, act as prospective players to achieve such alterations in cells (Hauge et al., 2021). Aurora Kinase A is such a well characterized mitotic serine threonine kinase, predominantly accountable for G2/M progression of cell-cycle (Shen et al., 2019; Liu et al., 2019; Woo et al.,

*[1]Department of Environmental Carcinogenesis & Toxicology, Chittaranjan National Cancer Institute, Kolkata, India. [2]Department of Medical Physics, Chittaranjan National Cancer Institute, Kolkata, India. *For Correspondence: sutapa_c_in@yahoo.com*

fortune Journals

Research Article

ARCHIVES OF
CLINICAL AND
BIOMEDICAL RESEARCH

ISSN: 2572-5017

AURKA/NFκB Axis: A Key Determinant of Radioresistance in Cervical Squamous Carcinoma Cells

Salini Das[1], Dilip Kumar Ray[2], Elizabeth Mahapatra[1], Souvick Biswas[1], Debomita Sengupta[1], Madhumita Roy[1], Sutapa Mukherjee[1*]

Abstract

Cervical cancer being one of the leading gynecological cancers, poses a major threat by its ever-increasing trend of global recurrence. Radioresistance, one of the major challenges confronted during the treatment of cervical cancer is manifested by increased rate of cellular proliferation, migration, invasion and alterations in cell cycle. Aurora Kinase A (AURKA), a mitotic serine/threonine kinase was found to be overexpressed in cancers and is associated with development of acquired therapy resistance. The principal objective of this study was to explore the mechanisms by which AURKA confers radioadaptive response in cervical cancer cells. Parental cervical squamous carcinoma cell line SiHa was subjected to recurrent challenge towards fractionated dose of X-irradiation. Finally, a resistant subline (SiHa/RR) was isolated at 40Gy. SiHa/RR exhibited higher expression of AURKA/ pAURKA along with activation of the signaling pathways (HIF1α, pAkt, NFκB) vis-à-vis lower expressions of the proteins (p53, Gadd45a), which are generally suppressed by AURKA. Interestingly, inhibition of AURKA in SiHa/RR showed improved radiosensitivity by reducing cell viability, restrained wound healing capacity as well as sphere forming ability and accelerated radiation induced apoptosis. Ectopic overexpression of AURKA gave rise to radioresistant phenotype in parental SiHa by stimulating nuclear translocation of NFκB. This pattern of increased nuclear localization of NFκB was also observed in resistant subline as a consequence of activation and overexpression of AURKA. These findings strengthened the active involvement of AURKA in radioresistance via driving NFκB mediated signaling pathway to deliver radioresistant associated adaptive complexities.

Keywords: Acquired Radioresistance; AURKA; Cervical Squamous Carcinoma Cells; Prosurvival Signaling; Radioadaptive Response

Introduction

Cervical cancer prevails as one of the leading gynecological cancers for its higher incidences and mortality [1-3]. Therapeutic success might be achieved against cervical cancer at early stage of diagnosis, primarily by surgery or radiation [4, 5]. The metastatic form of carcinoma is yet a challenging regimen that seeks urgent attention to explore novel therapeutic approaches. Globally, cervical cancer has a moderate to high recurrence rate throughout the stages after the initial treatment because of survival of cancer cells which escapes radiation therapy and causes disease relapse [6, 7, 8]. Understanding the underlying strategies of these surviving cells is an urgent need of the hour. Most of the time, the efficacy of radiation therapy depends on the phases

Affiliation:

[1]Department of Environmental Carcinogenesis & Toxicology, Chittaranjan National Cancer Institute, 37, S. P. Mukherjee Road, Kolkata 700 026, India

[2]Department of Medical Physics, Chittaranjan National Cancer Institute, 37, S. P. Mukherjee Road, Kolkata 700 026, India

***Corresponding author:**
Sutapa Mukherjee, Department of Environmental Carcinogenesis & Toxicology, Chittaranjan National Cancer Institute, 37, S. P. Mukherjee Road, Kolkata 700 026, India.

Citation: Salini Das, Dilip Kumar Ray, Elizabeth Mahapatra, Souvick Biswas, Debomita Sengupta, Madhumita Roy, Sutapa Mukherjee. AURKA/NFκB Axis: A Key Determinant of Radioresistance in Cervical Squamous Carcinoma Cells. Archives of Clinical and Biomedical Research 6 (2022): 707-721.

Received: August 13, 2022
Accepted: August 22, 2022
Published: September 16, 2022

Emerging Role of Aurora A in Radioresistance: A Comprehensive Review

Authors: Salini Das, Elizabeth Mahapatra, Souvick Biswas, Madhumita Roy, *Sutapa Mukherjee

Department of Environmental Carcinogenesis and Toxicology, Chittaranjan National Cancer Institute, Kolkata, India

*Correspondence to sutapa_c_in@yahoo.com

Disclosure: The authors have declared no conflicts of interest.

Received: 17.10.20

Accepted: 10.05.21

Keywords: Aurora A, cancer, radioresistance.

Citation: EMJ Oncol. 2021;9[1]:81-90.

Abstract

Radiotherapy is one of the most conventional modes of treatment in several cancers. Failure of radiotherapy followed by acquisition of radioresistance is one of the emerging challenges faced by clinical experts. Unusual expression and functional implications of several molecules are observed to facilitate radioresistance. Aurora A, a member of the Aurora kinase (serine/threonine kinase) family, is one such molecule that shows significantly altered expression as well as non-canonical functional crosstalk with other associated factors (cell cycle regulators, signaling molecules, stemness markers, etc.) to favour the adaptations for the acquirement of radioresistance. These mechanisms include progression of cell cycle, stimulatory activation of factors by phosphorylation for enhancing the chance of cellular survivability, and prevention of apoptosis. This review article summarises how Aurora A is responsible for radioresistance in cancer and why this kinase should be considered a negative biomarker of radiosensitivity. This review discloses a wider opportunity in the field of research to find the mechanistic key regulatory pathway of Aurora A, which can be a potential target for enhancing the efficiency of treatment. Further investigations are required to explore the potential of Aurora A inhibitors as reliable radiosensitisers.

INTRODUCTION

Radioresistance is known to create complications in the treatment of cancer.[1] Radiation-induced altered adaptive responses by tumour cells or tissues are considered to be primary reasons behind the failure of radiotherapy.[2] Acquirement of radioresistance followed by treatment failure and locoregional recurrence is a multifaceted process. Emerging data have suggested various molecular biomarkers necessitate radioresistance in cancer.[3,4] It is well established that the level of radioresistance alters in different phases of the cell cycle. Several researchers have experimentally proven that most cells are resistant in the G0 phase, early G1 phase, and late S phase of the cell cycle. In contrast, most cells are radiosensitive in the late G1 phase, G2 phase, and throughout the M phase of the cell cycle.[5] In the S phase, radiation resistance is thought to be due to an increased amount of DNA synthesis and repair enzymes, as well as a rise in the intracellular levels of glutathione (a free radical scavenger). In response to ionising radiation, the G1 phase of

RESEARCH ARTICLE

Editorial Process: Submission:12/02/2020 Acceptance:03/24/2021

Curcumin Rescues Doxorubicin Responsiveness via Regulating Aurora a Signaling Network in Breast Cancer Cells

Souvick Biswas, Elizabeth Mahapatra, Archismaan Ghosh, Salini Das, Madhumita Roy, Sutapa Mukherjee*

Abstract

Background: Insensitivity towards anthracycline drugs like doxorubicin poses a significant challenge in the treatment of breast cancer. Among several factors, Aurora A (a mitotic serine threonine kinase) plays crucial roles in acquiring non-responsiveness towards doxorubicin. However, the mechanisms underlying need to be elucidated. The present study was therefore designed to evaluate the underlying mechanisms of Aurora A mediated doxorubicin insensitivity in MCF-7Dox/R, an isolated resistant-subline of MCF-7 (breast adenocarcinoma cell line). Effect of curcumin, a natural phytochemical in restoring doxorubicin sensitivity by targeting Aurora A was assessed furthermore. **Methods:** A doxorubicin resistant subline (MCF-7Dox/R) was isolated from the parental MCF-7 cells by treating the cell with gradual step-wise increasing concentration of the drug. Expressions of Aurora A and its target proteins (Akt, IκBα and NFκB) were assessed in both parental and MCF-7Dox/R cells. Both the cell lines were pretreated with curcumin prior to doxorubicin treatment. Cellular proliferation rate was measured using BrdU (5-bromo-2'-deoxyuridine) assay kit. Intracellular doxorubicin accumulation was estimated spectrofluorimetrically. Cellular uptake of curcumin (spectrophotometric and spectrofluorimetric method) and its nuclear localization was confirmed by confocal microscopic study. Protein expressions were determined by western blot analysis. Localization of Aurora A was ascertained by immunofluorescence assay. To explore the possible outcome of impact of curcumin on Aurora A, cell-cycle distribution and apoptosis were performed subsequently. **Results:** Higher expressions of Aurora A in MCF-7Dox/R cells led to phosphorylation of Akt as well as IκBα. Phosphorylated IκBα preceded release of NFκB. Phospho-Akt, NFκB consequentially decreased doxorubicin accumulation by enhancing the expressions of ABCG2 and Pgp1 respectively. Curcumin by regulating Aurora A and its target molecules sensitized resistant subline towards doxorubicin mediated G2/M-arrest and apoptosis. **Conclusion:** Molecular targeting of Aurora A by curcumin restores chemosensitivity by increasing the efficacy of doxorubicin in breast cancer.

Keywords: Aurora A- doxorubicin insensitivity- breast cancer- curcumin

Asian Pac J Cancer Prev, **22 (3)**, 957-970

Introduction

Doxorubicin, conventionally used as chemotherapeutic agent against breast cancer limits its therapeutic benefits due to development of acquired insensitivity following long-term therapy (Christowitz et al., 2019). Therefore, understanding the molecular factors hindering the responsiveness of breast cancer cells towards doxorubicin is crucial to unravel and prevent therapeutic insensitivity.

Human Aurora A protein belonging to the family of serine/threonine kinases is expressed within the centrosome during the early S phase and helps in centrosome duplication and maturation. During G2/M transition Aurora A facilitates mitotic entry by triggering duplicated centrosomes to be separated (Tang et al., 2017). Aurora A undergoes autophosphorylation at Threonine 288 residue to become functionally active. In a wide variety of cancers including breast cancer, aberrant expressions or gene amplification of Aurora A has been documented; indicating its involvement in prosurvival activity and tumorigenesis (D'Assoro et al., 2013; Ferchichi et al., 2013; Zardavas et al., 2014; Cirak et al., 2015). Emerging evidences have documented an association between Aurora A overexpression and decreased chemosensitivity in cancer (He et al., 2014; Kuang et al., 2017; Wang et al., 2017). In triple negative breast cancer cells, response towards doxorubicin was reported to be restored by administration of Aurora A inhibitor (Romanelli et al., 2012). Apart from mitotic involvement, aberrant activation of the non-canonical Aurora A/SMAD5 oncogenic axis in breast cancer has been documented, which eventually led to chemoinsensitivity (Opyrchal et al., 2017). However,

*Department of Environmental Carcinogenesis & Toxicology, Chittaranjan National Cancer Institute, 37, S. P. Mukherjee Road, Kolkata, India. *For Correspondence: sutapa_c_in@yahoo.com*

Indian Journal of Biochemistry & Biophysics
Vol. 57, April 2020, pp. 167-177

PEITC by regulating Aurora Kinase A reverses chemoresistance in breast cancer cells

Souvick Biswas, Elizabeth Mahapatra, Madhumita Roy & Sutapa Mukherjee*

Department of Environmental Carcinogenesis & Toxicology, Chittaranjan National Cancer Institute, Kolkata-700 026, West Bengal, India

Received 23 September 2019; *revised 02 November 2019*

Development of acquired chemoresistance renders a challenge in breast cancer therapy. Aurora kinases, a family of serine/threonine mitotic kinases play pivotal roles in the acquirement of chemoresistance. Aurora A is intricately associated with mitotic events and is overexpressed in different cancers including breast cancer. Amplification or overexpression Aurora A confers chemoresistance and are considered as a promising therapeutic target in cancers. Therefore, targeting Aurora A by natural means particularly by using Phenethyl isothiocyanate (PEITC), a natural isothiocyanate might be an effective strategy for reversing resistance towards chemotherapeutics. The present study investigated the modulatory role of PEITC on Aurora A and their downstream target proteins in breast adenocarcinoma cell line (MCF-7) and its paclitaxel-resistant counterpart; designated as MCF-$7^{Pacli/R}$. Paclitaxel resistance was warranted by P-gp1, MRP1, Ki-67 overexpression, rhodamine 123 accumulations and upregulation of Aurora-A along with phospho-IκBα. Multidrug resistance was confirmed by MTT assay. Western blotting, RT-PCR analysis revealed overexpression of Aurora-A in MCF-$7^{Pacli/R}$ cells; which was eventually diminished by PEITC. PEITC by targeting Aurora A and their downstream proteins (phospho-p53, phospho-IκBα) acted as a resistance-modifying agent and ultimately led to paclitaxel- induced apoptosis. These findings demonstrated that PEITC reverses chemoresistance by regulating Aurora A and restores chemosensitivity towards paclitaxel.

Keywords: Aurora-A, Chemoresistance, Paclitaxel, Phenethyl isothiocyanate, Threonine

The development of acquired chemoresistance is a major challenge to combat the recurrence of breast cancer in spite of the recent advancement in the treatment modality. Many molecular markers have been identified to date that is responsible for the multidrug resistance in cancer cells and its relapse[1-3]. Apart from the known molecular markers like P-glycoprotein 1 (P-gp1), Multidrug resistance-associated protein 1 (MRP1), ATP-binding cassette sub-family G member 2 (ABCG2) (drug efflux markers) responsible for decreasing efficacy of the drug, organic anion transporter (OAT), organic cation transporter (OCT) (SLC family of drug influx markers) and certain other markers belonging to the family of mitotic kinases like Aurora A and Aurora B (cell cycle regulatory kinase protein) are also contributing a major role in acquirement of chemoresistance[4-10]. Several mitotic and non-mitotic roles of Aurora- A have been identified that are directly associated with the resistance to chemotherapy[11-17]. In human, evolutionary conserved three members of Aurora family (Aurora A, B, and C) have been identified and interestingly they almost share the conserved catalytic domain, indicating their origin from a common ancestor gene[10,18]. Aurora-A, located on chromosome 20q13.2 is reported to be aberrantly expressed in breast cancer[19]. Majorly being

*Correspondence:
E-mail : sutapa_c_in@yahoo.com

*Abbreviation:*Aurora A, Aurora Kinase A; PEITC, Phenethyl isothiocyanate; P-gp1, P-glycoprotein 1; MRP1, Multidrug resistance- associated protein 1; ABCG2, ATP-binding cassette sub-family G member 2; OAT, Organic anion transporter; OCT, Organic cation transporter; SLC, Solute Carrier; Ki-67, Kiel-clone 67; BRCA1, Breast cancer type 1 Susceptibility protein; MDM2, Mouse double minute 2 homolog; NF-κB, Nuclear Factor kappa-light-chain-enhancer of activated B cells; IκBα, Nuclear Factor of kappa light polypeptide gene enhancer in B-cells inhibitor, alpha; MCF-7, Michigan Cancer Foundation-7; MCF-7Pacli/R, Paclitaxel resistant MCF-7; MEM, Minimum Essential Medium Eagle; FBS, Fetal Bovine Serum; 5-FU, 5-fluorouracil; MTT, 4,5-Dimethylthiazol-2-yl)-2,5-Diphenyltet razolium Bromide; PBS, Phosphate Buffered Saline; DMSO, Dimethyl sulfoxide; ELISA, Enzyme-linked Immune Sorbent Assay; IC50, half maximal Inhibitory Concentration; PCR, Polymerase Chain Reaction; EtBr, ethidium bromide; PI, Propidium Iodide; BCIP/NBT, 5-bromo-4-chloro-3-indolyl phosphate/nitro blue tetrazolium; TUNEL, Terminal deoxynucleotidyl transferase-mediated dUTP Nick-End Labeling.

Achievements

16. ACHIEVEMENTS

❖ ***Work Presentations***

- Presented poster on "**3-methylcholanthrene, a potent initiator of cervical carcinogenesis in *in vivo* model"** at the three days national seminar on "Environmental Mutagenesis: Integration of Basic Biology & Omics to improve human health" organized by the Environmental Mutagen Society of India (EMSI), Bhabha Atomic Research Centre (BARC), Mumbai, held from 25.01.2018 to 27.08.2018.
- Presented Oral presentation on **"Interplay of stress induced inflammatory mediators: Role in progression of carcinogen induced cervical cancer *in vivo*"** two days Symposia on "Molecular Diagonistics and Therapeutics" organized by the Department of Biochemistry, College of Medicine & JNM hospital, WBUHS, Kalyani held from 21.06.2019 to 22.06.2019.
- Presented poster on **"Stress induced inflammatory mediators favour progression of cervical cancer *in vivo*."** National Symposia on "Air Pollution and its Impact on human Health" organized jointly by the CSIR- Indian Institute of Chemical Biology" and Archana Sharma foundation of Calcutta, held from 2.12.2019 to 4.12.2019.
- Presented poster on **"Interplay of stress-induced inflammatory mediators: A prerequisite for progression of cervical cancer *in vivo*"** at one day National Symposia and IACR WB Chapter meet on **"Cancer Research: Bench to Bedside"** organized by ***Chittaranjan National Cancer Institute (CNCI), Kolkata on*** 11.01.2020.
- Presented poster on **"Upregulated IAPS: An escape route for evading platinum based chemotherapy in cervical cancer"** at the International Symposium on

"**Present and future challenges of Xenobiotic Mediated Mutagenesis: Impact on Human health & Environmental Safety"** organized jointly by the ***Environmental Mutagen Society of India (EMSI)*** & CSIR-Indian Institute of Toxicology Research, held from 18.02.2020 to 20.02.2020.

- Delivered an oral presentation on "**Reversal effect of PEITC on PI3K/Akt signalling mediated Cisplatin Resistance in Cervical Cance**r" in the 47th Annual Conference of Association of Clinical Biochemists of India (ACBICON 2021) held during the period of December 12-15, 2021.

- Presented a poster on **"Reversal effect of PEITC on PI3K/Akt signalling mediated Cisplatin Resistance in Cervical Cancer"** at the 42nd Annual Meeting of Indian Association for Cancer Research (IACR) organized by ACTREC, Tata Memorial Center, Khargar, Navi Mumbai during the period of January 12 – 16, 2023.

❖ ***Achievements***

- Qualified State Eligibility Test (SET) organised by West Bengal College Service Commission (WBCSC) in 2022.

- Qualified Life Science GATE in 2016.

- Awarded with "Best Poster Award" on "3-methylcholanthrene, a potent initiator of cervical carcinogenesis in in vivo model" at 42nd Annual Conference of Environmental Mutagen Society of India (EMSI) organized by the Environmental Mutagen Society of India (EMSI), Bhabha Atomic Research Centre (BARC), Mumbai, held from 25.01.2018 to 27.08.2018.

- Awarded with “Student Award” from Mutation Research-Genetic Toxicology and Environmental Mutagenesis Section of Elsevier Publications for best poster presentation at 42nd Annual Conference of Environmental Mutagen Society of India (EMSI) organized by the Environmental Mutagen Society of India (EMSI), Bhabha Atomic Research Centre (BARC), Mumbai, held from 25.01.2018 to 27.08.2018.

- Awarded with second prize for best poster presentation one day National Symposia and IACR WB Chapter meet on “Cancer Research: Bench to Bedside” organized by Chittaranjan National Cancer Institute (CNCI), Kolkata on 11.01.2020.